

**INTERRUPTING THE FORMATION OF
HARMFUL AMYLOID FIBRILS OF HUMAN
INSULIN WITH DIFFERENT CO-SOLVENTS
AND SMALL MOLECULES**



Thesis Submitted by

SWARNALI PAUL

INDEX No.168/18/LIFE SC./26

Department of Life Science and Biotechnology, Jadavpur University

For the award of the degree of

DOCTOR OF PHILOSOPHY (SCIENCE)

2024

UNDER THE SUPERVISION OF

PROF. (DR.) UMESH CHANDRA HALDER,

Professor, Department of Chemistry

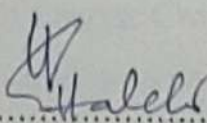
JADAVPUR UNIVERSITY

KOLKATA-700 032, WEST BENGAL, INDIA



CERTIFICATE FROM THE SUPERVISOR

This is to certify that the thesis entitled "*Interrupting the formation of harmful amyloid fibrils of human insulin with different co-solvents and small molecules*" Submitted by Swarnali Paul who got her name registered on 12.09.2018 for the award of Ph. D. (Science) Degree of Jadavpur University, is absolutely based upon her own work under the supervision of Prof. (Dr.) Umesh Chandra Halder and that neither this thesis nor any part of it has been submitted for either any degree / diploma or any other academic award anywhere before.

 15/07/2024

(Signature of the Supervisor with date and official seal)



DR. UMESH CHANDRA HALDER
Professor of Chemistry
Department of Chemistry
Jadavpur University
Kolkata-700032

JADAVPUR UNIVERSITY
KOLKATA – 700 032, INDIA

INDEX No.168/18/Life Sc./26

1. Title of the thesis:

Interrupting the formation of harmful amyloid fibrils of human insulin with different co-solvents and small molecules

2. Name, Designation, and institution of supervisor:

Professor (Dr.) Umesh Chandra Halder

Professor,

Department of Chemistry,

Jadavpur University, Kolkata - 700032, India.

3. List of publications (related to thesis):

- i. **Swarnali Paul**, Shahnaz Begum, Hasan Parvej, Ramkrishna Dalui, Subrata Sardar, Falguni Mondal, Nayim Sepay and Umesh Chandra Halder. 2024. In vitro retardation and modulation of human insulin amyloid fibrillation by Fe³⁺ and Cu²⁺ ions, New J. Chem., 48: 3120–3135, <https://doi.org/10.1039/D3NJ04431A>.

Other Publications

- ii. Shahnaz Begum, **Swarnali Paul**, Hasan Parvej, Falguni Mondal, Ramkrishna Dalui, Anirban Pradhan, Nayim Sepay and Umesh Chandra Halder. 2024. Anion–Induced Amyloid Fibrillation of Human Insulin In vitro, ChemistrySelect, 9: e202303699, <https://doi.org/10.1002/slct.202303699>.
- iii. Hasan Parvej, Ramkrishna Dalui, Shahnaz Begum, **Swarnali Paul**, Falguni Mondal, Sanhita Maity, Nayim Sepay, Umesh Chandra Halder. 2024. Promotion and modulation of amyloid fibrillation of bovine beta-lactoglobulin by hydroxychalcones, J. Mol. Struct., 1318 (2024) 139164, <https://doi.org/10.1016/j.molstruc.2024.139164>.
- iv. Shahnaz Begum, Hasan Parvej, Ramkrishna Dalui, **Swarnali Paul**, Sanhita Maity, Nayim Sepay, Mohd Afzal and Umesh Chandra Halder. 2023. Structural modulation of insulin by hydrophobic and hydrophilic molecules, RSC Adv., 13: 34097–34106, <https://doi.org/10.1039/D3RA06647A>

- v. Hasan Parvej, Shahnaz Begum, Ramkrishna Dalui, **Swarnali Paul**, Barun Mondal, Subrata Sardar, Nayim Sepay, Gourhari Maiti and Umesh Chandra Halder. 2022. Coumarin derivatives inhibit the aggregation of β -lactoglobulin. RSC Adv.,12: 17020–17028, <https://doi.org/10.1039/D2RA01029A>
- vi. Sanhita Maity, Nayim Sepay, Sampa Pal, Subrata Sardar, Hasan Parvej, **Swarnali Paul**, Jishnu Chakraborty, Anirban Pradhan, and Umesh Chandra Halder. 2021. Modulation of amyloid fibrillation of bovine β -lactoglobulin by selective methionine oxidation, RSC Adv., 2021, 11, 11192-1120, [10.1039/d0ra09060c](https://doi.org/10.1039/d0ra09060c)
- vii. Sampa Pal, Sanhita Maity, Subrata Sardar, Shahnaz Begum, Ramkrishna Dalui, Hasan Parve, Kaushik Bera, Anirban Pradhan, Nayim Sepay, **Swarnali Paul** and Umesh Chandra Halder. 2020. Antioxidant ferulic acid prevents the aggregation of bovine β -lactoglobulin in vitro, J. Chem. Sci., 132: 103, <https://doi.org/10.1007/s12039-020-01796-z>

4. List of Presentations in National/ International Conferences/Workshops:

- Presentation of Poster entitled ‘Inhibition of amyloid fibrillation of human insulin by effective metal ions’ in an International Seminar on Recent Advances in Chemistry and Material Science [RACMS-2022] organized by the Indian Chemical Society in association with Bangladesh Chemical Society and Department of Chemistry, Jadavpur University held during 30th-31st July and 2nd-3rd August , 2022.
- Presented Poster entitled ‘Effect of metal ions on insulin aggregation in vitro’ in a National Seminar on Emerging Trends in Chemical Sciences [CAS II PROGRAM] organized by Department of Chemistry, Jadavpur University held on 7th January, 2020.
- Participated in National Seminar on ‘Chemical Sciences: Today and Tomorrow’, CSTT-2019 [CAS II PROGRAM] organized by the Department of Chemistry, Jadavpur University on 14th March, 2019.
- Participated in a 2-day workshop on ‘Introduction to Fractal Geometry and it’s application in Condensed Matter Physics’ organized by CMPRC, Jadavpur University on 13th -14th December, 2018.
- Participated of 2-days National seminar on ‘Twist and Turns of Physics research’, TTPR-2017 held on 21st - 22nd February, 2017 at the Department of Department of physics, Jadavpur University.

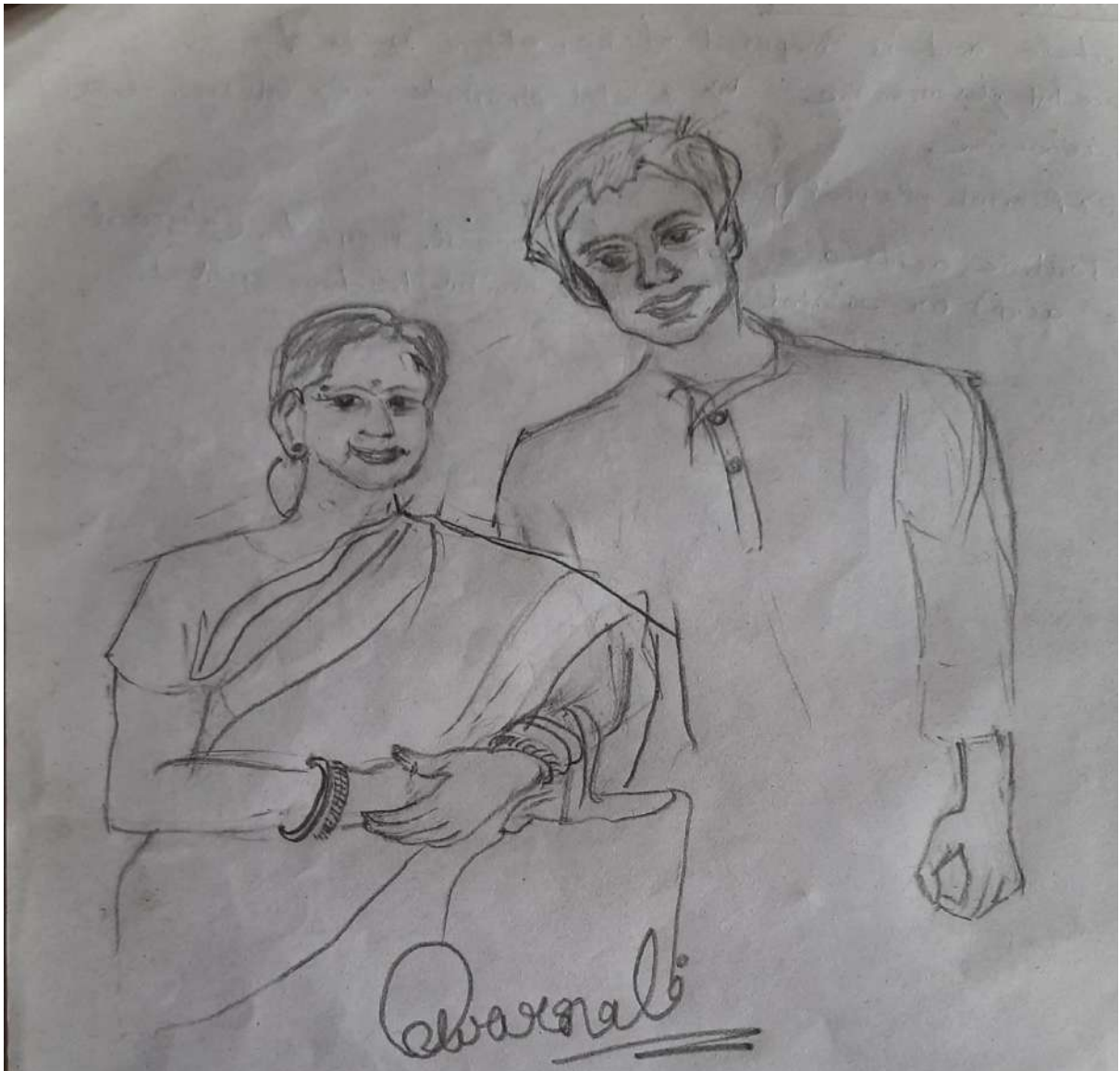
DECLARATION

*I, Swarnali Paul, Index no.168/18/Life Sc./26 do hereby declare that the work delineated in this thesis entitled “Interrupting the formation of harmful amyloid fibrils of human insulin with different co-solvents and small molecules” which is being submitted for the degree of Doctor of Philosophy (Science) has been carried out by me in the Organic Chemistry Laboratory, Department of Chemistry, Jadavpur University, under the supervision of **Professor (Dr.) Umesh Chandra Halder**, Professor, Department of Chemistry, Jadavpur University, Kolkata, India. Neither the thesis nor any part thereof has been presented anywhere earlier for any degree or award whatsoever.*

(SWARNALI PAUL)

Date:

Kolkata, India



DEDICATED TO

My Parents &

Younger Brother

"It is very easy to defeat someone, but it is very hard to win someone."

"We are all born with a divine fire in us. Our efforts should be to give wings to this fire and fill the world with the glow of its goodness."

"The only true wisdom is in knowing you know nothing."

"Wisdom is a weapon to ward off destruction; It is an inner fortress which enemies cannot destroy."

"Knowledge cannot be taken away from anyone except by obsolescence."

- Dr. A. P. J. Abdul Kalam

Acknowledgements

*The content embodied in this thesis submitted for the award of the Degree of Doctor of Philosophy in Science has taken its final shape. It is my great pleasure to acknowledge and show gratitude sincerely to those who helped me throughout my research work entitled “**Interrupting the formation of Harmful Amyloid Fibrils of Human Insulin with Different Co-Solvents and Small Molecules**”.*

*Firstly, from the core of my heart, I want to mention the names of my parents, **Dr. Santi Ranjan Paul** and **Smt. Anita Paul** and my little brother, **Shaswata Paul** for their efforts beyond limit to share and wipe out every obstacles of my path and their inseparable support to prepare me to approach each of my goals towards completion. The whole journey of doing Ph. D taught me a lot but I must mention the significant one is how consistently patience and self-trust to retain. According to my belief, this is the power given by my loving parents and the ‘**Almighty**, the supreme commander’.*

*With an unswerving respect, I wish to express my sincere veneration to my honorable Ph. D supervisor **Prof. (Dr.) Umesh Chandra Halder**, Professor, Organic Chemistry Section, Department of Chemistry, Jadavpur University for the significant scientific guidance, supervision and encouragement amidst difficulties faced during the execution of the work. I will try to follow the humbleness, time management, representation, skill acquisition, patience and sagacious leadership of Sir, Prof. U. C. Halder throughout my life. I am very much grateful to madam, **Mrs. Sraboni Halder** and younger sister like **Miss. Ishani Halder** for the priceless blessings and well wishes throughout my journey.*

*The research work for this thesis has been carried out in the Department of Chemistry, Organic Chemistry Section, Jadavpur University. In this regard, I would like to record my sincere thanks to **Prof. Bhaskar Gupta**, Vice-Chancellor and **Prof. Amitava Datta**, Dean – Faculty of Science of Jadavpur University. I am extremely grateful to **Prof. K. K. Rajak**, HOD (Chemistry), and the honorable faculty members of the Department of Chemistry, **Prof. Nitin Kumar Chattopadhyay**, **Prof. Chittaranjan Sinha**, **Prof. Soumen Ghosh**, **Dr. Arunabha Thakur**, **Dr. Samit Guha**, **Dr. Saubhik Haldar** for*

*providing me with various departmental and administrative facilities and encouraging me whenever I approached to them. I am highly obliged to the honorable faculty members of the Department of Physics, **Prof. Partha Pratim Ray, Professor Brajadulal Chattopadhyay, and Dr. Abiral Tamang** of Jadavpur University for their kind support and instrumental facilities.*

*The Ph. D course work has been done in the Department of Life Science and Biotechnology, Jadavpur University. I want to grab this scope to express humble gratitude to **Prof. Parimal Karmakar**, Head of the Department, Department of Life Science and Biotechnology, **Prof. Biswadip Das, Dr. Ratan Gachhui** and other faculty members of the Department of Life Science and Biotechnology for their constant help, support and administrative facilities. I also want to extend my humble thanks to all the **staff members** of Jadavpur University.*

*I am very much thankful to **Prof. Parthasarathi Dastidar**, Senior Professor, School of Chemical Sciences, Indian Association for the Cultivation of Science, Kolkata, for his constructive evaluation of my research work and expertise suggestions. With due respect and gratitude I want to mention **Prof. Pravash Chandra Chakraborti**, Professor, Department of Metallurgical & Material Engineering, Jadavpur University for providing me with necessary instrumental facilities.*

*I am highly obliged for getting the Swami Vivekananda Merit-cum-means scholarship from the **Govt. of West Bengal** during my research period for four years.*

*I would like to convey my deepest gratitude to my lab senior **Dr. Hasan Parvej** for guiding me in difficult situations, cordial advices and providing the necessary technical assistances. My sincere thanks also go to my seniors, colleagues and juniors, **Dr. Nayim Sepay, Dr. Barun Mondal, Shahnaz Begum, Ramkrishna Dalui, Falguni Mondal, Dr. Sanhita Maity, Dr. Sampa pal, Dr. Subrata Sardar, Dr. Dhananjoy Das, Rajibul Islam** for their valuable supports and invaluable motivations.*

Swarnali Paul

July 2024, Kolkata

PREFACE

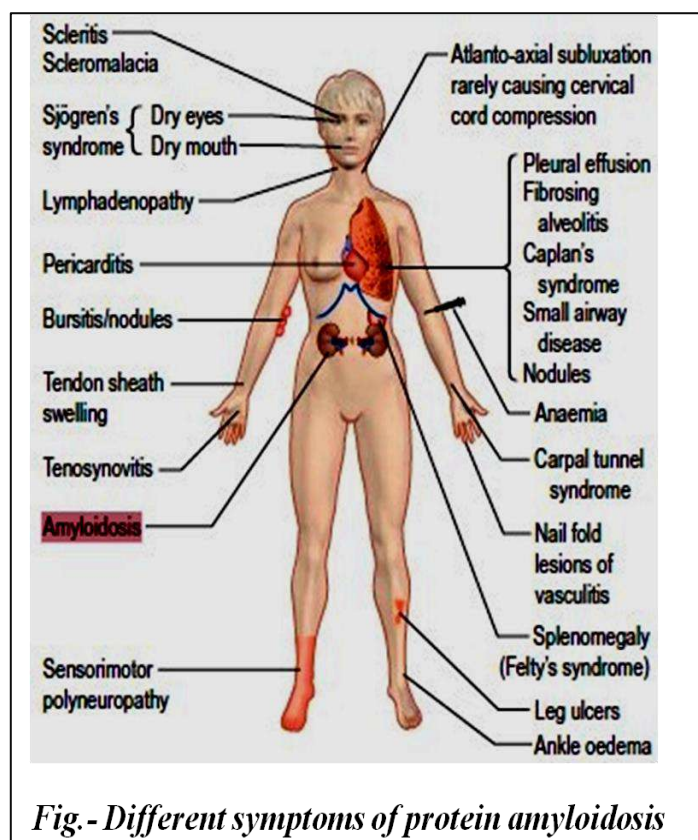
The foods we eat contain different biomolecules viz. carbohydrates, proteins, fat etc. Among them, carbohydrates after digestion, converted to monosaccharide like glucose, fructose, galactose. Glucose is the simplest form of carbohydrate and main fuel for our body activities. Blood glucose concentration is a vital parameter that is maintained majorly by two hormones secreted from pancreas namely insulin and glucagon. After digestion of food followed by absorption into bloodstream, the increased level of blood sugar signals the beta cells of pancreas to release insulin. Insulin helps to channelize the blood sugar into the body cells to oxidize them for energy production in the form of ATP. Insulin also signals the liver to store blood sugar for later use. However, if the pancreas does not produce



enough insulin or cells respond poorly to insulin and take in less sugar, then the fatal condition may lead to the development of type 2 diabetes. Eventually, high blood sugar levels can lead to disorders of the circulatory, nervous and immune systems.

Insulin therapy is common under such condition while initial fasting plasma glucose is greater than 250 mg/dl or the HbA1c is greater than 10%. Recombinant DNA technology advents execute the large-scale production of human insulin for therapeutic purpose. The first genetically engineered, synthetic human insulin, which was non-allergic and immunologically safe for human, was produced in 1978 using *E. coli* bacteria, and licensed as well as marketed by Eli Lilly in 1982 under the brand name Humulin. Though Humulin/other such market based therapeutic insulin are structurally identical to natural insulin, still their mode of action can be hampered if they would aggregate at the site of injection in diabetic patients taking insulin injections and thus cannot become absorbed in the body system. Such clump formation was reported in many people undergone insulin therapy through injection and common symptoms includes aesthetic discomfort, local site abscesses and may lead to chronic hyperglycemia and unpredictable hypoglycemia. This harmful event is known as **Insulin amyloidosis**. Such amyloidosis may take place with a number of other significant proteins like Apolipoprotein 1, Fibrinogen A alpha, Lysozyme, Atrial natriuretic factor, β 2-microglobulin etc and affect a number of organs like heart, kidneys, liver,

peripheral nervous system, skin, GI tract, osteo-articular tissue and circulatory system. Industrial processing of Insulin as well as its delivery confronts by the major problem of aggregation. Conventional pharmaceutical processing of insulin includes agitation, pH lowering, and different shearing forces generated by filtration, pumping, centrifugation and



administration. All these processes may account for conformational destabilization and partial unfolding of insulin followed by harmful amyloid generation. Amyloidosis collapses the functional properties of proteins and causes various neurodegenerative disorders like Alzheimer's disease, Parkinson's disease, Huntington's diseases, Spongiform encephalopathy etc. Diabetic patients taking regular insulin injections are commonly affected with the pathogenic deposition at the injection site followed by poor absorbance, reduced insulin functionality,

cytotoxicity and immunogenicity. Additionally, pharmaceutical and clinical formulations, storage and delivery of insulin require critical care against amyloid generation.

It is necessary to understand the mechanism of insulin aggregation and the ways that can potentially prevent amyloid formation. The insulin amyloid inhibitors should be specific enough to avoid interfering with the normal processes under physiological conditions. Naturally occurring compounds like micronutrients, vitamins, amino acids expected to show little/no side effects were chosen to proceed with the investigations of the present work. The stepwise approaches to attain the goal under the scope of the thesis were as follows. Firstly, the physical parameters (pH, temperature, duration of thermal exposure) were optimized to get the most aggregated/ amyloid form of insulin in vitro. The effects of micronutrients in the form of metal ions (Cu^{2+} and Fe^{3+}), water soluble B complex vitamins (Vitamin B₁, B₆ and B₁₂) and sulphur containing amino acids (cysteine and methionine) on insulin amyloidosis

were investigated with different in-vitro and in-silico approaches. In this regard, the influence of fluorinated co-solvent on insulin fibrillation was also examined.

Insulin composed of A and B polypeptide chains which are greatly stabilized by inter and intra-chain disulfide bonds. The fluorescence property of it is majorly rendered by the structural Tyrosine residues. The hexameric form of insulin found in its market available therapeutic formulations should be converted to monomeric form at acidic pH to proceed with the said objectives as the stability consideration of the monomeric form is vital in the functioning of insulin in vivo and also this form is susceptible to form amyloid structure.

The kinetics of insulin fibrillation is traced along with the effects of metal ions Fe^{3+} and Cu^{2+} in **Chapter1**. Fe^{3+} is more effective in inhibiting the heat induced amyloid generation than Cu^{2+} . Fe^{3+} maintains the alpha helical conformation of insulin by binding it with greater affinity. ΔG° for its binding is -7.02 kcal/mol where that for Cu^{2+} is -6.31 kcal/mol. Cu^{2+} has shortened the lag phase by promoting self association of insulin but decreases the propensity of its aggregation. Fe^{3+} treated insulin, under aggregated condition produces small spherule and ‘worm-like’ globular morphology of insulin as detected under FESEM imaging but Cu^{2+} causes ‘needle shaped’ fibrillar morphology. Being transition metal ions, both of them possess d-electrons and are assumed to form either octa or hexa-conjugated complex with water in aqueous media of interaction. They preferably access with protein side chains through surface H-bonds. Besides this, being very good heat and electrical conductors, these metal ions somehow have neutralized the thermal incubation effect on protein structure. The metal coordination sites are aspartate/asparagine, glutamate, histidine and cysteine residues of insulin as found in molecular docking simulations.

Chapter 2 explores the effect of vitamin B_1 , B_6 and B_{12} on insulin aggregation. Vitamin B_1 potentially retains the monomeric alpha helix rich conformation of insulin in aggregating conditions whereas vit. B_6 mediated inhibition is feeble. In contrast, vit. B_{12} aggravates the aggregation process. The thiazolium ring of vit. B_1 is assumed to favourably interact with insulin with H-bond and electrostatic interactions. The sulphur group present in vit. B_1 may form inter molecular disulphide bond within two or more vit. B_1 . This assembly in turn interacts with insulin side chains and serves as a shield to prevent more insulin molecules to come closer during aggregation. The resulting polar environment created in presence of Vitamin B_1 disfavours the hydrophobic association and burying event of non-polar residues of insulin. Vit. B_6 makes similar interactions but with lesser stability. Unlike the rest, Vit. B_{12}

induced the said aggregation of insulin. The bulky structure of vit.B₁₂ cannot fit itself to interact with insulin and induces the protein misfolding by hampering the stability and thus aggregation is favoured.

Chapter 3 addresses the influence of fluorinated co-solvents, 1,1,1,3,3,3-Hexafluoroisopropanol (HFIP) and 2, 2, 2-Trifluoroethanol (TFE) during the course of insulin aggregation. Maintenance of hydrophobicity of protein is critical in the inhibition of its amyloidogenic behaviour. Unlike HFIP, TFE greatly lengthened the Lag phase up to 150 minutes and thus assumed to delay the onset of fibrillation. Overall, HFIP at 10% v/v interaction ratio provided better protection to insulin monomeric form against the fibrillation. HFIP being a volatile solvent disrupts assembly of unfolded monomers to generate amyloid fibrils. Additionally, in aqueous solution the acidity of HFIP was enhanced which in turn maintained the monomer predominating form of insulin due to the protonation of its His residues. The possible formation of HFIP micro droplets at the amphoteric protein-alcohol interfaces in the aqueous medium can explain the results of the present study. However, above 10% v/v of fluorinated alcohol, the aggregation of insulin may take place. Then the HFIP mediated insulin fibrils gives needle shaped crystal-like morphologies whereas TFE mediated are of branched higher aggregates of insulin as revealed in Transmission Electron Microscopic imaging.

Chapter 4 gives a brief account of insulin aggregation in presence of sulphur containing amino acids. Cysteine and methionine when employed interact with insulin freely but cannot protect it against heat induced fibrillation. In the process of mature fibril formation, insulin first unfolds itself followed by refolded in an erroneous manner to generate the seed of nucleation. Here the data suggests, the unfolding of insulin is followed by a random coiling under the influence of Cys and Met individually. Increase in amount of beta-sheet and beta-turn rich species is prevalent in the aggregates. At higher interacting ratio with insulin, Cys produces larger particles than Met. However, at lower interacting ratio, the size of aggregating particle gets smaller under influence of Cys than Met.

ABBREVIATIONS

<i>Abbreviations used</i>	<i>Full form</i>	<i>Abbreviations used</i>	<i>Full form</i>
1. α	Alpha	2. A β	Amyloid-beta
3. ANS	8-Anilinonaphthalene-1-sulfonic acid	4. APS	Ammonium persulphate
5. Arg	Arginine	6. Asp	Aspartic acid
7. β	Beta	8. β -lg	β -lactoglobulin
9. $^{\circ}\text{C}$	degree Celsius	10. CD	Circular dichroism
11. CD4	Cluster of Differentiated cells	12. cm	centimeter
13. Cys	Cysteine	14. Da	dalton
15. DLS	Dynamic light scattering	16. DNA	Deoxyribonucleic Acid
17. <i>E.coli</i>	<i>Escherichia coli</i>	18. ex/em	excitation/emission
19. FTIR	Fourier Transform Infrared Spectroscopy	20. X g	relative centrifugal force
21. Gly	glycine	22. Glu	glutamic acid
23. h	hours	24. H bond	hydrogen bond
25. His	histidine	26. HFIP	1,1,1,3,3,3-Hexafluoroisopropanol
27. HPLC	High Performance Liquid Chromatography	28. Ile	isoleucine

29. IU	International unit	30. kV	kilo volt
31. Leu	leucine	32. Lys	lysine
33. M	Molar	34. mg	Milligram
35. mL	Milliliter	36. μL	Micro liter
37. mM	Milli molar	38. μM	Micro molar
39. MRE	Mean residual ellipticity	40. nm	nano meter
41. ns	nano second	42. PAGE	Polyacrylamide gel electrophoresis
43. Phe	phenyl-alanine	44. Pro	proline
45. RLS	Rayleigh light scattering	46. SDS	sodium dodecyl sulphate
47. Ser	serine	48. TFE	2, 2, 2-Trifluoroethanol
49. Thr	threonine	50. Tyr	tyrosine

TABLE OF CONTENTS

<i>HEADING OF CONTENT</i>	<i>TOPICS COVERED</i>	<i>PAGE NO.</i>
<i>Title</i>	Title page	i
<i>Certificate</i>	Certificate from the Supervisor	ii
<i>Particulars</i>	Particulars regarding Thesis submission	iii-iv
<i>Declaration</i>	Declaration	v
<i>Dedication</i>	Dedication page	vi
<i>Acknowledgements</i>	Acknowledgements	viii-ix
<i>Preface</i>	PREFACE	x-xiii
<i>Abbreviations</i>	Abbreviations used in the Thesis	xiv-xv
<i>Contents</i>	Table of Contents	xvi- xxii
<i>Figures</i>	List of Figures	xxiii-xxvii
<i>Introduction</i>	1. INTRODUCTION	1-44
	1.1. Protein-the indispensable biomolecule	1
	1.2. Structural organizations of proteins	1-3
	1.3. Protein folding	4

1.4. Forces orthodox to protein folding, stability and function	4-14
Primary forces	
1.4.1. The hydrophobic effect	4-5
1.4.2. Conventional Hydrogen bonding	5
1.4.3. Coulombic interactions	5-6
1.4.4. Van der Waals interaction	6
1.4.5. Disulfide linkage	7
1.4.6. Co-ordination with metal ions	7-9
Secondary forces	
1.4.7. C–H•••O H-Bonding	9-10
1.4.8. $n \rightarrow \pi^*$ Interactions	11
1.4.9. C δ Hydrogen Bonds	11
1.4.10. Cation– π Interaction	12
1.4.11. X–H••• π Interactions	12
1.4.12. π – π Interactions	13
1.4.13. Anion– π Interactions	13
1.4.14. Sulfur–Arene Interactions	13
1.4.15. Chalcogen Bonding	13-14
1.5. Protein misfolding: molecular and cellular implications	14-17
1.5.1. Oligomers	14
1.5.2. Protofibrils	14-15
1.5.3. Fibrils or Amyloid structures	15
1.5.4. Energy states of protein misfolding and aggregation	16-17

	1.5.5. Significance of determining energy landscapes and kinetics of folding	17
	1.6. In vivo consequences of protein misfolding	17-20
	1.7. Impact of protein aggregation in-vitro	20-22
	1.8. Human insulin - a therapeutic protein	22-25
	1.8.1. The need of insulin therapy and commercial production of human insulin	23-24
	1.8.2. The gradual development of insulin therapeutics	24-25
	1.9. Structural overview of human insulin	25-26
	1.10. Stability of native folds of insulin	27
	1.11. Insulin-derived amyloidosis	27-28
	1.12. References	29-44
<i>Objectives & Scopes</i>	2. OBJECTIVES & SCOPES	45-48
	2.1 Analysis of the research problem	45-47
	2.2. Summarized objectives	48
	2.3. Scopes of this study according to the objectives	48
<i>Materials and detailed methodologies</i>	3. MATERIALS AND METHODOLOGIES APPLIED THROUGHOUT THE STUDIES	49-63
	3.1 Reagents, Chemicals and Fine Equipments used	49-50
	Preparation of Monomeric insulin and Sample Solutions	
	3.2. Dialysis and preparation of insulin monomer	50-51
	3.3. Interaction of insulin with micronutrients	51
	3.4. Interaction of insulin with vitamins	51

	3.5. Interaction of insulin with fluorinated co-solvents	52
	3.6. Interaction of insulin with sulfur containing amino acids	52
	Preparation of Insulin Aggregates	
	3.7 Aggregation inhibition studies: thermal aggregation of insulin in presence and absence of modulators	52
	Electrophoresis Studies	
	3.8. Native Polyacrylamide Gel Electrophoresis (Native-PAGE) of Insulin Monomer and Aggregates	53
	3.9. Composition of solutions of native-PAGE	54-55
	Fluorimetric Studies	
	3.10. Intrinsic fluorescence emission study	55
	3.11. Thioflavin T (ThT) emission measurement	55-56
	3.12. Kinetic study for aggregation	56
	3.13.8-Anilinonaphthalene-1sulfonic acid(ANS)interaction study	56-57
	Conformational Studies	
	3.14. Far-UV Circular Dichroism (Far UV-CD) spectroscopy and Deconvolution studies	57
	3.15. Fourier-Transform Infrared (FT-IR) Spectroscopic studies	58
	Light Scattering Assays	
	3.16. Rayleigh Light Scattering (RLS) Study	58
	3.17. Dynamic light scattering (DLS) Assay	58-59

	Morphological Imaging	
	3.18. Surface morphology study with Field Emission Scanning Electron Microscope (FE-SEM)	59
	3.19. Transmission electron microscopic (TEM) study	59
	3.20. Atomic Force Microscopic imaging	60
	COMPUTATIONAL TECHNIQUES	
	3.21. Molecular docking	60
	3.22. References	61-63
<i>Chapter 1</i> <i>In vitro</i> <i>amyloid</i> <i>generation of</i> <i>insulin and</i> <i>study of the</i> <i>effects of</i> <i>metal ions</i>	4. CHAPTER 1	64-102
	4.1 Prologue of the study	65-66
	4.2 Amyloid inhibitors: Literature findings	
	4.2.1. Natural compounds	67-68
	4.2.2. Thermo stability contributors	68
	4.2.3. Dietary supplements	68
	4.2.4. Osmolytes and denaturants	69
	4.2.5. Molecular chaperones	69
	4.2.6. Several nanoparticles	69
	4.2.7. Conjugated polymers	70
	4.2.8. Monoclonal antibody	70
	4.3. Reason behind choosing metal ions to investigate insulin amyloid inhibition	
	4.3.1. Interaction of insulin with different metal ions	71-72
	4.4. Materials and Methodologies	73

	4.5. Results of research findings	
	4.5.1.Purification and monomeric conversion of Human Insulin	74
	4.5.2. Standardization of physical parameters (pH, temperature, heating duration) to get most irreversible aggregate formation i.e., amyloid fibril of human insulin	74-76
	4.5.3.Inhibition of in vitro fibrillation of human Insulin by Fe³⁺ and Cu²⁺ ions	76-89
	4.6 Discussions and Major Conclusions	89-92
	4.7 References	93-102
<i>Chapter 2 Employing water soluble B-complex vitamins to inhibit the process of insulin fibrillation</i>	5. CHAPTER 2	103-131
	5.1 Prologue of the study	104-105
	5.2. Interaction of vitamins with protein molecules	105-107
	5.3. Effects of vitamins in amyloid formation/related disorders: Literature findings	108-110
	5.4. Materials and Methodologies	111
	5.5. Results of research findings	112-122
	5.6 Discussions and major conclusions	123-125
	5.7 References	126-131
<i>Chapter 3 Investigation of the effect of fluorinated</i>	6. CHAPTER 3	132-157
	6.1 Prologue of the study	133-134
	6.2. Effect of Fluorinated alcohols on Protein structure and stability: a review of Literature	134-135

<i>co-solvents during in-vitro insulin fibrillation</i>	6.3. Materials and Methodologies	136
	6.4. Results of research findings	137-147
	6.5 Discussions and major conclusions	148-150
	6.6 References	151-157
<i>Chapter 4 Effect of sulfur containing amino acids on thermal fibrillation of insulin</i>	7. CHAPTER 4	158-176
	7.1 Prologue of the study	159-161
	7.2. Effect of free Cysteine and Methionine on protein stability : Literature evidences	162-163
	7.3. Materials and Methodologies	164
	7.4. Results of Research Findings	165-171
	7.5. Discussions and major conclusions	171
	7.6. References	173-176
<i>Summary</i>	Summarization of the thesis work	177-181
<i>Future Scopes</i>	Future Scopes of the work	182
<i>List of Publications</i>	List of Publications related to the Thesis	183
<i>Proceedings and Workshops</i>	Proceedings and Workshops	184
<i>Annexure</i>	Annexure of Result of PhD Course Work, Publications and Certificates of Proceedings and Workshops	

LIST OF FIGURES

<i>FIGURE NUMBER</i>	<i>FIGURE TITLE</i>	<i>PAGE NO.</i>
Figure 1.1	Protein sequence is coded by its particular gene (DNA)	1
Figure 1.2	General Structure of an amino acid and the Translation process	2
Figure 1.3	Secondary structures of protein- β -pleated sheet & α -helix	2
Figure 1.4	Development of protein structure (a) Primary structure, (b) secondary structure, (c) tertiary structure, and (d) quaternary structure.	3
Figure 1.5	Pathway of protein folding by chaperones and other factors	3
Figure 1.6	Illustration of the primary stabilizing forces in protein folding	5
Figure 1.7	Schematic illustration of coordination groups	7
Figure 1.8	Secondary interactions involving the main chain. (A) Structural model of an idealized β -sheet, showing conventional main-chain hydrogen bonds , C–H \cdots O hydrogen bonds , and C5 hydrogen bonds . (B) Structural model of an idealized α -helix, showing main-chain hydrogen bonds and n $\rightarrow\pi^*$ interactions. (C,D) Orbital overlap that underlies formation of n $\rightarrow\pi^*$ interactions (C) and C5 hydrogen bonds (D).	10
Figure 1.9	Stability of α -helix in the absence of hydrogen bonds	11
Figure 1.10	The possible secondary interactions in a protein involving side chains.	12
Figure 1.11	Schematic diagram showing different fates of unfolded/misfolded protein species due to the different stresses.	14
Figure 1.12	Amyloid fibrils showing the characteristic cross- β diffraction pattern under X-rays	15
Figure 1.13	The Energy landscape cartoons depicting native folding and aggregation of protein.	16
Figure 1.14	The Classical pathway of humoral immune response	21

Figure 1.15	Schematic representation of mode of action of human insulin	23
Figure 1.16	Schematic representation of human insulin production in <i>E.coli</i> by recombinant DNA technology	25
Figure 1.17	Schematic representation of sequence of human insulin in primary structure	25
Figure 1.18	a. The structures of insulin A- chain and b. B-chain of insulin. Both were determined from the three-dimensional X-ray analysis of the T 6 hexamer (2-Zn insulin) in perpendicular to the threefold symmetry axis.	26
Figure 1.19	Schematic diagram of pathway of insulin aggregation	27
Figure 2.1	The method of subcutaneous delivery of insulin	45
Figure 2.2	Clinical and paraclinical features of the patients under insulin therapy showing amyloid deposition	47
Figure 3.1	The dialysis of hexameric insulin against water [left] and the Millex –G Millipore syringe filter of pore size 0.22mm [right]	50
Figure 3.2	Schematic representation of insulin monomer formation from marketed hexamer	51
Figure 3.3	Schematic representation of general methodologies followed to study effect of metal ions, vitamins, amino acids and co-solvents on insulin aggregation	53
Figure 4.1	Three-dimensional structure of insulin monomer [left] and different forms of insulin association [right]	66
Figure 4.2	Schematic sketch of possible approaches of inhibition and destabilization of amyloidogenesis.	67
Figure 4.3	Schematic representation of the mode of action of nanogrenades	70
Figure 4.4	Native polyacrylamide gel electrophoresis of insulin	74
Figure 4.5	Results of different fluorimetric assays	75
Figure 4.6	Thioflavin T assay result of insulin aggregates in presence of metals	77
Figure 4.7	Kinetics of insulin aggregation in presence of metal ions	78
Figure 4.8	Conformational analysis of insulin aggregates in presence of metals	80

Figure 4.9	FTIR spectra of insulin aggregates under metal influences	82
Figure 4.10	Light scattering assay results in presence of metal ions	83
Figure 4.11	FE- SEM images of varied species of insulin aggregates in presence of metal ions	86
Figure 4.12	TEM images of insulin aggregates in presence of metal ions	87
Figure 4.13	Molecular Docking pose of hydrated metal ions treated insulin aggregates	88
Figure 4.14	The proposed mechanism of inhibition of partial unfolding and aggregation formation of human insulin by metal ions while co-incubated separately with insulin.	90
Figure 5.1	Prediction of VIRs by the TSL representation of sliding patterns	105
Figure 5.2	Comparative percentages of amino acids residues serving as non-VIRs, VIRs, VAIRs, VBIRs and PLPIRs	106
Figure 5.3	The representation of sliding patterns of TSL (17-residues length) for prediction of VBIRs.	107
Figure 5.4	Predictions of PLPIRs via the TSL representation of sliding patterns (17-residues length).	107
Figure 5.5	Schematic representation of the vitamins as potential therapeutics against Alzheimer's disease.	110
Figure 5.6	Relative Fluorescence emission Intensity (RFI) of tyrosyl residues of heat treated insulin in presence of B vitamins	112
Figure 5.7	ThT Assay results in presence of vitamins	114
Figure 5.8	Far-UV CD spectra of aggregated insulin in presence of B vitamins	115
Figure 5.9	FTIR spectra considering effects of vitamin B on insulin aggregation	118
Figure 5.10	Schematic depiction of the proportionality of particle size with light scattering	118
Figure 5.11	Rayleigh Light Scattering results showing effect of vitamin B on insulin aggregation	119

Figure 5.12	Particle size distribution patterns from DLS studies showing effect of vitamin B on aggregation of insulin	120
Figure 5.13	AFM images representing the aggregate morphologies of Insulin in presence of B vitamins	121
Figure 5.14	The chemical structures of a) Vit.B1, b) Vit. B6 (pyridoxal form) and c) Vit.B12	123
Figure 5.15	Schematic representation of the shielding effect imparted by thiamine against the aggregation event of insulin	124
Figure 6.1	Comparative effect of the Hydrogen bonding with TFE and Ethanol in solution, separately	135
Figure 6.2	Fluorescence emission spectra of Insulin aggregates in presence of co-solvents	137
Figure 6.3	ThT emission spectra of insulin and kinetics of aggregation in presence of co-solvents	138
Figure 6.4	ANS fluorescence emission spectra and Rayleigh scattering effects on insulin aggregation in presence of co-solvents	140
Figure 6.5	Conformational studies of insulin aggregation in presence of co-solvents	142
Figure 6.6	Representation in pie charts of CD Deconvolution data calculated by CDNN 2.1 software	143
Figure 6.7	The results of dynamic light scattering analysis in presence of co-solvents	144
Figure 6.8	TEM images of insulin aggregates having amyloid fibril network of insulin	145
Figure 6.9	TEM images showing insulin aggregates in presence of 10% and 20% HFIP	146
Figure 6.10	TEM images showing aggregated insulin in presence of 10% and 20% TFE	146
Figure 6.11	The physical and chemical properties of HFIP as a co-solvent	149
Figure 7.1	2D histograms of the frequencies of occurrence of the different amino acid-amino acid interactions, clustered according to the conformational space defined by the distance d and the angles P	159

	and θ .	
Figure 7.2	Stereo images of superimposition of cysteines on SARS 3CLpro (PDB code 1UJ1).	161
Figure 7.3	Different oxidation states of Cysteine	162
Figure 7.4	The S-aromatic motif of Methionine	163
Figure 7.5	Intrinsic fluorescence emission intensities of tyrosyl residues of insulin recorded in presence of Cys and Met	165
Figure 7.6	ThT assay results in presence of Cys and Met	167
Figure 7.7	The effects of Cys and Met on hydrophobicity and conformational changes of insulin during aggregation.	168
Figure 7.8	Dynamic Light scattering assay of different insulin aggregates formed under experimental conditions	170

INTRODUCTION

1.1. PROTEIN-THE INDISPENSABLE BIOMOLECULE

Every feature of any living organisms is defined in different genes located within its chromosome. A gene expresses (Fig.1.1) when the specified protein is produced through an mRNA intermediate from it. Proteins serve a number of fundamental functions in an organism. Their versatility of function nearly includes them in every cellular process.

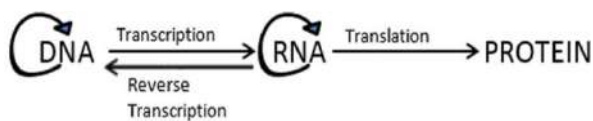


Table1.1: Biological significance of proteins

Functional area	Examples
Structural protein	Collagen
Enzymes	Pepsin
Hormones	Insulin
Transporters	Hemoglobin
Receptors	Ion channel
Storage protein	Casein
Immune response	γ -globulin
Motor protein	Actin, Myosin

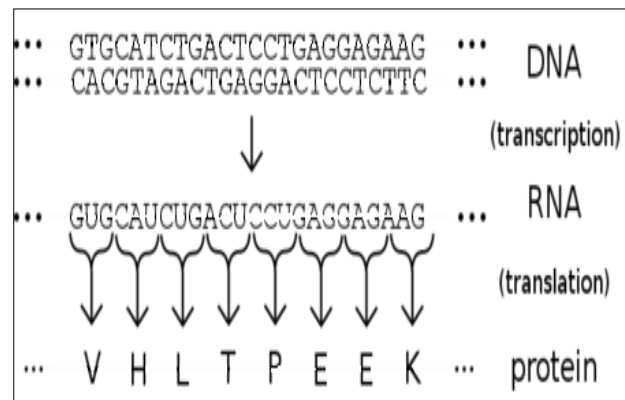


Fig.1.1 Protein sequence is coded by its particular gene (DNA)

As indicated in Table 1.1, proteins serve in various domains of life like the exoskeleton framework, enzymes, hormones, transporters, cellular receptors, different biological processes like DNA replication, cell division, cellular

metabolism, transcription of RNA, translation of proteins, and cellular apoptosis initiators.

1.2. STRUCTURAL ORGANIZATIONS OF PROTEINS

Proteins are synthesized in ribosome from its precursor mRNA as linear polypeptide chain (Fig.1.2, right panel) of amino acids by the process known as translation. Twenty types of biologically prevalent *L-amino acids* comprise the structure of proteins. These amino acids

having both carboxylic acid and amino group show amphoteric properties (Fig1.2, left panel).

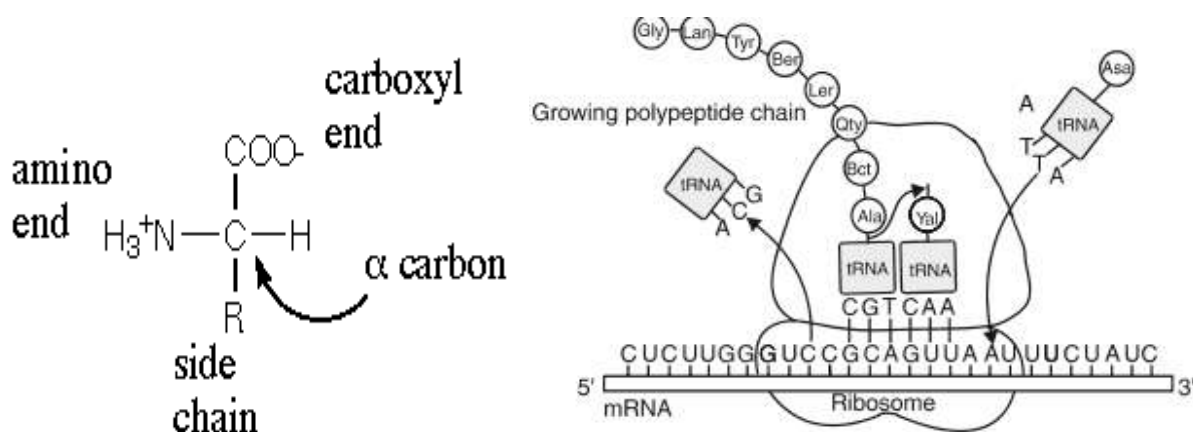


Fig.1.2 General Structure of an amino acid [left] and the Translation process [right]

Primary structure of protein formed primarily during the translation process is linear chain

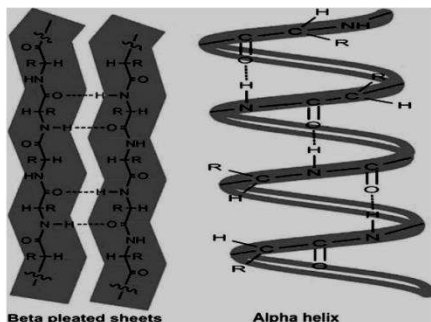
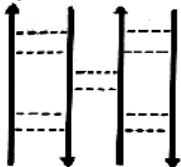


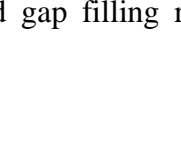
Fig 1.3. Secondary structures of protein- β -pleated sheet [left] & α -helix [right]

of amino acids joined with peptide linkages. The polypeptide chain should fold itself in a stepwise manner viz., primary \rightarrow secondary \rightarrow tertiary \rightarrow quaternary to perform a specified function. Primary structure then orients themselves through H-bonds to produce **secondary structure**. The most common of them are α -helix and β -pleated sheet (Fig.1.3). In **α -helix**, the carbonyl group ($\text{C}=\text{O}$) of one amino acid is hydrogen bonded to the amino H ($\text{N}-\text{H}$) of an amino acid that is four residues apart and thus forms a twisted ribbon like helical structure. There are 3.6 amino acids per turn. **β -pleated sheets** are lateral arrangements of β -strands connected by backbone hydrogen bonds. A β -strand consists of a polypeptide chain typically 3 to 10 amino acids long and is with right-handed twist due to of the L-amino acids. Two types of β -pleated sheets are parallel and

Antiparallel beta-sheet



Parallel beta-sheet



anti-parallel. If residue i in strand 1 forms a H-bond with residue j in strand 2, then the next bond can be formed in two different ways. Either residue $i+2$ in strand 1 binds to $j+2$ in strand 2 (referred to as a **parallel β -sheet**), or residue $i+2$ in strand 1 binds to $j-2$ in strand 2 (referred to as **anti-parallel β -sheet**). The increased stability of antiparallel β sheets compared to parallel one is due to more energetically favorable [1] H-bonding pattern in it. . Proline, the amino acid known as '**helix breaker**' is generally found in bends and gap filling regions between consecutive secondary structures. Similarly, the aromatic

amino acids like, tryptophan, tyrosine, and phenylalanine, having large ring structures inside chain, are favorably found in β pleated sheets. The groups on the amino acid side chains ($-R$) make stabilized bonds between side chain groups and the groups on the polymer backbone to

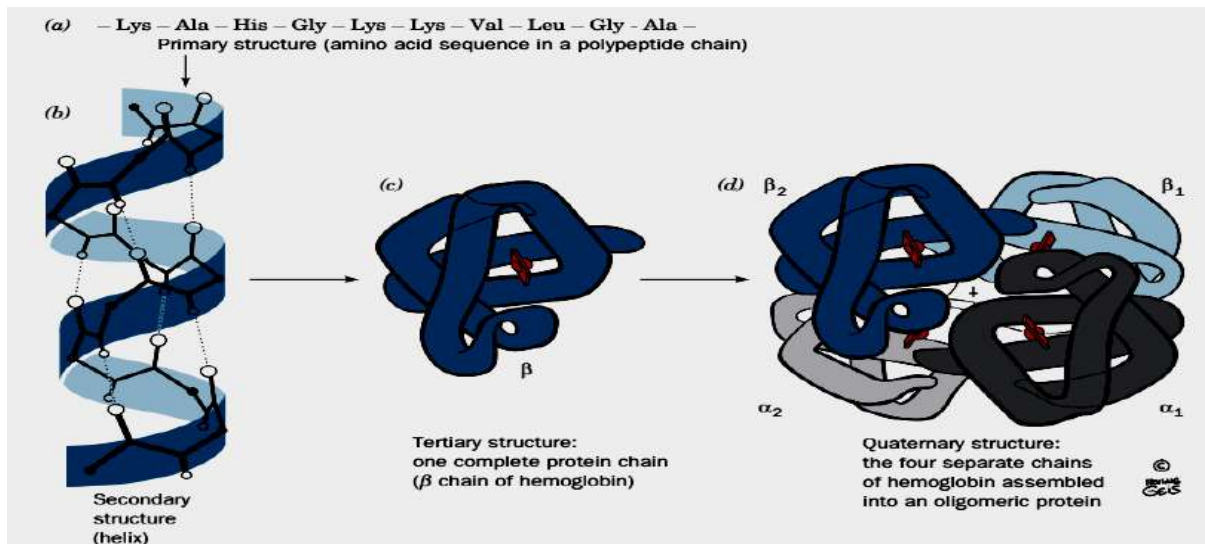


Fig.1.4 Development of protein structure (a) Primary structure, (b) secondary structure, (c) tertiary structure, and (d) quaternary structure. [Illustration, Irving Geis. adapted from *Biochemistry by Voet and Voet, 4th edition*]

get a more stable configuration of overall protein. This is defined as the **tertiary structure** of a single polypeptide chain (Fig. 1.4c) having three-dimensional arrangement [2]. The association of several same/different tertiary structures to have a specified function is known as the **quaternary structure of a protein**. If the subunits are identical, the protein is said to

be a **homomeric** but if the subunits are different, it is **heteromeric** [3]. E.g., Hemoglobin, the oxygen and carbon-dioxide transporter protein in the blood is made up of four polypeptides: two α and two β subunits (Fig.1.4d).

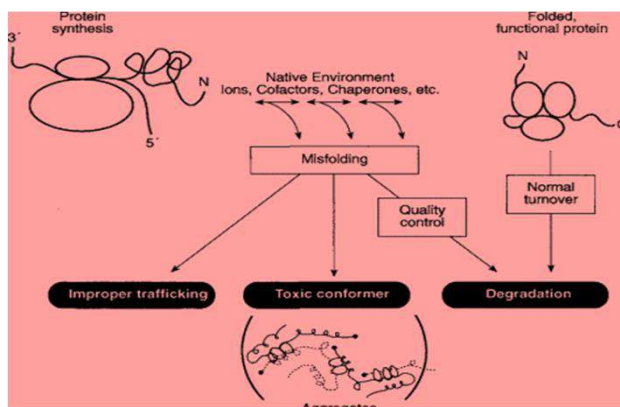


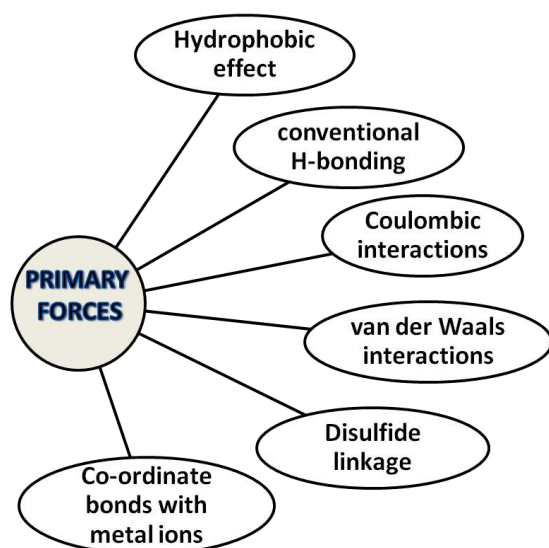
Fig 1.5. Pathway of protein folding by chaperones and other factors. Misfolding

leads to inappropriate trafficking or degradation or to aggregation. The aggregated product is often resistant to proteolysis and forms aggregates, such as amyloid plaques (adapted from Bhagavan N.V., 2002, Medical Biochemistry, Ed.4)

1.3. PROTEIN FOLDING

Nascent polypeptides are synthesized on ribosome located in the lumen of the endoplasmic reticulum (ER). Molecular chaperones (chaperonins) helps to direct and target the folding event of polypeptides to the fully folded structures. Chaperones are a family of proteins that bind hydrophobic patches of nascent polypeptide to prevent them from premature aggregation and become nonfunctional (Fig. 1.5). The folding event is necessary to expose the proper binding sites of the protein as per its role in biological system and thus it too maintains how it interacts with other proteins and molecules. Countless molecular processes and structural transitions are partly dependent on the proper folding of a protein. Thus, the stabilizing forces of a properly folded protein are of greater concern.

1.4. FORCES ORTHODOX TO PROTEIN FOLDING, STABILITY AND FUNCTION



Scheme 1.1: the major primary forces behind protein folding and stability

The primary forces behind protein folding are - the hydrophobic effect, conventional hydrogen bonding, Coulombic interaction, van der Waals interactions, disulphide linkage and co-ordinate bonds with metal ions (Fig. 1.6).

1.4.1. The hydrophobic effect is the major driving force for globular protein folding. The hydrophobic amino acid residues tend to bury in the core of the protein and there develops an

association between other hydrophobic residues buried similarly. The free energy of transfer of a non-polar compound from an organic solution into water, G_{tr} , is, $\Delta G_{tr} = \Delta H_{tr} - T\Delta S_{tr}$, where ΔH = enthalpy, T = absolute temperature and ΔS = Entropy. The size of globular proteins when is smaller, the hydrophobic residues then cannot be buried completely and the charged side chains are placed more closer than that of a larger protein [4]. Thus depending on the size of the protein the stability may change. Hydrophobic effect is dependent on temperature changes as entropy and enthalpy change

with it. It is observed that with lowering of temperature, the hydrophobic effect will be lowered and this event is termed as cold-denaturation of proteins [5].

1.4.2. Conventional Hydrogen bonding is crucial in stabilizing protein structure. Hydrogen atoms bonded to oxygen or nitrogen atoms can make H-bonds with any oxygen or nitrogen atom in vicinity. In case of protein, these bonds occur between side chains of amino acids like serine, asparagines, tyrosine, polar amino acids, backbone groups etc. The first experimental evidence was provided by Fersht et. al [6] in 1985 about the contribution of H-bonds in protein stability. 0.5–1.8 kcal/mol binding energies is provided by a single hydrogen bond [7]. The packing density within the interior of a protein is favorably increased by H-bonding

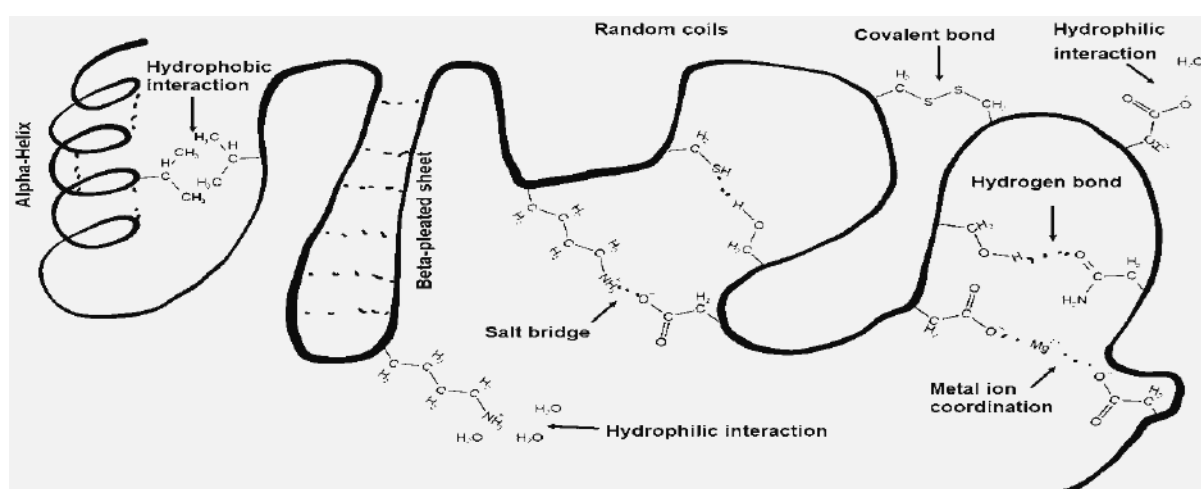


Fig.1.6 Illustration of the primary stabilizing forces in protein folding

[8]. A study revealed that, in a folded protein the average number of hydrogen bonds formed is 1.1 per residue, among which 65% are contributed by H-bonding within peptide groups, 23% by H-bonding between peptide groups and side chains, and just 12% for H-bonding within side chains [9]. Kelly et.al suggested that these are stronger in a nonpolar environment than a polar environment [10-11]. H-bonds are stronger in a lower dielectric constant environment [12-18].

1.4.3. Coulombic interactions accounts for the electrostatic interactions in protein structure. For protein in aqueous medium, the dielectric constant of water is ~80 at room temperature where the protein interior is being nonpolar possesses a dielectric constant generally 2–4, up to 40 [19-22]. This interaction can be affected majorly in the following three ways. Firstly, the charges of Asp, Glu, His, Lys, and Arg side chains of a protein can be modulated by pH [23] and may lead to denaturation of it [24]. Secondly, charge alteration can be done by

phosphorylation and dephosphorylation of Ser, Thr, and Tyr and it affect protein–protein interactions and also results in a cascade of signal transduction pathways in vivo [25]. Moreover, the posttranslational charge-altering events like acetylation of Lys can be a commonplace of the strength of protein–DNA association like in nucleosome. The pathogenic single amino acid change from glutamate (an ionizable amino acid) to valine (a non-polar amino acid) in the β -subunit results in production and polymerization followed by aggregation of sickle hemoglobin [26-27]. The long-range electrostatic interactions (placed 5–10 Å apart) within charged particles is very relevant in determination of rate constants for interactions of protein with small and large molecules [28-29]. Water solubility of protein is imparted by as well as aggregation is prevented by the electrostatic interactions of charged residues. Proteins involved in proton transport are largely dependent on the acidic amino acid residues [30-32]. Metal ion and ionic ligands mostly bind to the charged residues of proteins [33-35]. Under physiological ionic strengths (0.10 M), if two charges are 10 Å apart then the interaction energy is around 0.1 kcal/mole. This increases to 0.5 to 1.0 kcal/mole when the charges are separated by only 5 Å, which is similar to the energy of interaction in 0.01 M ionic strength at these short interchange distances. In 0.01 M, interaction energies of 0.1 kcal/mole are still present when the charges are separated by 20 Å. At ionic strength 1.5 M, charges separated by 5 Å or less in a protein structure have a measurable interaction, equivalent to 0.3 kcal/mole [36].

1.4.4. A Van der Waals interaction is a non-ionic weak force of about 0.5 to 1 kcal/mol. Electronegative atoms, like oxygen and nitrogen, tends to attract the electron cloud through the covalent bond toward itself and thus a charge dispersion; that is, a partial positive (δ^+) as well as a partial negative (δ^-) charge inside the same molecule. The attraction between opposite charges helps to align them in close proximity and strong electronegative atoms create permanent dipoles. In turn, their influences bring about induced dipole in neighboring molecules. The interaction between two permanent dipoles is known as **Keesom force** whereas between a permanent and an induced dipole is termed as **Debye force**. Another significant **London force** is within two induced dipoles located in two closely occurred neutral residues (e.g., aliphatic hydrocarbon) of amino acids. In particular, all the three forces named above contribute to the van der Waals interactions. As the van der waal force is inversely proportional in sixth power to the distance between interacting atoms thus it is termed as a short range interactions [37-38].

1.4.5. Disulfide linkage ($-S-S-$), occurs when the thiol ($-SH$) groups of two cysteine residues in a folded protein chain come closer and joined covalently. Intra-chain (within a single polypeptide chain) and inter-chain (within two or more polypeptide chains) disulfide linkages maintain and protects protein structure from unfolding and aggregation. The dihedral angle for disulfides is $\pm 90^\circ$, and deviation from this may lead to increase in redox potential by 10–100 mV [39]. Vicinal disulfides in chain or loops create strain in structure [40–41] even distortion of trans-planar conformation to cis conformation was reported [42]. Spontaneous formations of intra-molecular and inter-molecular disulfide bonds prevent the damage in the structure of secretory proteins caused by highly oxidizing environment of cells [43].

1.4.6. Co-ordination with metal ions. Protein structure bonded to a particular metal ion is formed by coordination and any residue/atom of protein capable of donating a pair of

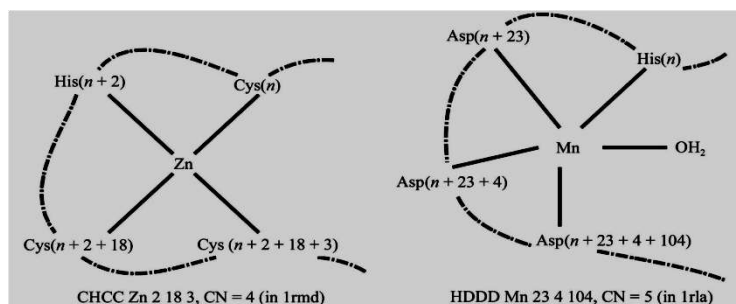


Fig.1.7 Schematic illustration of coordination groups. [adapted from Harding, M. M. (2004). *Acta Cryst. D60*, 849–859, 10.1107/S0907444904004081]

electrons to metal is called a ligand. Central metal ion with bound ligands forms a coordination sphere.

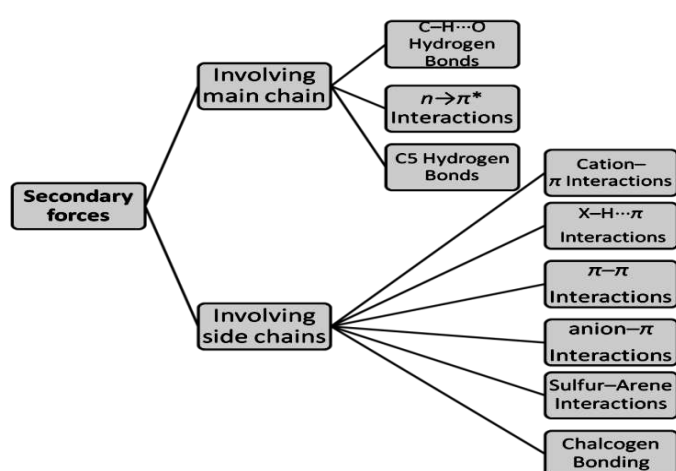
Coordination number is the number of donor atoms bound to the metal ion within the target distance + 0.75 Å. **Monodentate**

ligand refers to the ligands make coordination to the only site of a metal ion. Here only one pair of electrons is donated to the metal ion. **Bidentate ligands** are those that occupy two sites of a metal ion. **Polydentate ligands/ chelators** are formed when more than two sites are occupied of the same metal ion. Structural, regulatory and enzymatic properties as well as stability of proteins are majorly rendered by its co-ordinate metal-ion. The term “**Life metals**” is used to mention the significant contributions of sodium (Na), potassium (K), magnesium (Mg), calcium (Ca), manganese (Mn), iron (Fe), cobalt (Co), zinc (Zn), nickel (Ni), vanadium (V), molybdenum (Mb), and tungsten (W) in maintaining living state. The two types-nontransition metal ions having constant oxidation state (valency) and transition metal ions having variable oxidation state due to incompletely filled electron shells are involved. Irrespective of the large size of ions (0.95 and 1.33 Å, respectively), Na and K possess low ionization potentials where Mg and Ca have no preferences in bonds formation directions due to completely filled electron shells (2s² 2p⁶ and 3s² 3p⁶) and ionic radii of 0.65 and 0.99 Å,

respectively. Ca^{2+} , Mg^{2+} , Na^{+} and K^{+} , are preferably bind to “hard” (have more concentrated, less polarizable electron shells) oxygen ligands but not to nitrogen or sulfur ligands and thus forms purely electro-static interactions. In contrast, Zn^{2+} and transition metal ions select nitrogen, sulfur as well as oxygen ligands for coordination. In left panel of Fig. 1.7, the metal co-ordinations are CHCC Zn 2 18 3, since Zn is coordinated to the sulfur of cysteine (n) with sequence number n, N of histidine (n + 2), S of cysteine (n + 2 + 18) and S of cysteine (n + 2 + 18 + 3). The total coordination number (CN) is 4. The sequence differences (**seqdif**), in the three chelate loops are 2, 18 and 3. The relative sequence number of each donor amino acid in the coordination group is given by **relseq**. In this example there are cysteines at relseq = 0, 20 and 23, and histidine at relseq = 2. **nspan** is the sequence-number difference between the last and first amino-acid donors, which is the sum of all the seqdifs between them; nspan is 23 in this example. In the right panel of Fig. 1.7, the chelate loops i.e., the building blocks of coordination groups, such as CH 2, HC 18, CC 3 are shown. For full identification of a particular coordination group or a chelate loop, the protein name and the residue number and chain letter of the first amino acid is written e.g. the above group occurs in 1a1i at A137 (and another at A165). In comparing the Generally, the equilibrium association (binding) constant K_a is considered as $K_a = 1/K_d$ (M^{-1}), where K_d is equilibrium dissociation constant and is a ratio of dissociation (off) and association (on) rate constants $k_{\text{off}}/k_{\text{on}}$ ($\text{s}^{-1}/\text{M}^{-1} \text{s}^{-1}$ i.e., M) [44]. Mg^{2+} , Co^{2+} , Ni^{2+} due to of their rigid and stable first hydration shell, produces tetrahedral or octahedral geometry but Zn^{2+} possesses both of them. The calcium binding sites of proteins are found in coordination with oxygen atoms bestowed by carboxylates of Asp and Glu residues and carbonyls of polypeptide chain. This oxygen atom is placed in vertexes of a slightly distorted pentagonal bipyramide or octahedron [45- 47]. The Atomic radius of Mg^{2+} and oxygen are 0.65 Å and 0.99 Å respectively. This is why, in the octahedral geometry, only six oxygen atoms can be fitted near Mg^{2+} . Ca^{2+} having a greater atomic radius, forms bidentate ligand with carboxylates , while Zn^{2+} prefers soft ligands. Sulfur atoms of Cys and nitrogen atoms of His are considered soft ligands as they have less concentrated, more polarizable electron shell. Coordination with oxygen atoms of Asp and Glu are also observable for Zn^{2+} [47-48]. Generally, Zn^{2+} is coordinated tertahedrically in proteins with zinc fingers and zinc-containing enzymes whereas; the ligands used by transition metal ions are histidine, cysteine, and methionin residues of protein. Burying of residues into interior portion during protein folding involves 81% of the nonpolar side chains, 70% of the peptide groups, 63% of the polar side chains, and 54% of the charged side chains so that they can avoid the water contact [49].

Except the primary forces, additional contributors of protein folding involving main polypeptide chain (weak but plentiful) and side chain R groups (strong but scarce interactions) termed as **secondary forces** (Scheme 1.2, table 1.2) have been identified. They are C–H \cdots O hydrogen bonding, $n\rightarrow\pi^*$ interactions, C5 hydrogen bonding, cation– π , X–H $\cdots\pi$, π – π , anion– π , and sulfur–arene, chalcogen bonding interactions.

1.4.7. C–H \cdots O H-Bonding Commonly the C α –H protons donate for conventional H-bonds, there found some acidic protons serving same purpose, e.g., the C ϵ –H is donated by Histidine side chains [50]. This type of contacts occurring at a shorter distance that efficiently



Scheme 1.2: the major secondary forces behind protein folding and stability in Collagem triple helix [54] and transmembrane helices [55].

avoid repulsive van der Waals interactions and found mostly in interstand H-bonding (fig.1.8.A) in β -sheets [51-52]. The C–H \cdots O hydrogen bonds formed by a proline α -proton to carbonyl acceptors [53] may prevent proline from helix breaking. These bonds are also found

Table 1.2: The secondary forces behind protein folding

<i>Secondary force behind Protein folding</i>	<i>Type of interaction and Interacting residues</i>
C–H \cdots O Hydrogen bond	hydrogen bond between a carbon-based acid and an oxygen lone pair
$n\rightarrow\pi^*$ Interaction	stereo-electronic interaction between a lone pair and π anti-bonding orbital, especially that between two carbonyl groups
C5 Hydrogen bond	intra-residue hydrogen bond between backbone N–H and C=O groups in a β -strand
Cation– π interaction	interaction of a positive charge with the face of aromatic ring

X–H··· π Interaction	hydrogen bond donated to the face of an aromatic ring
π – π Interaction	interaction between two aromatic rings in either an edge-to-face or offset-stacked geometry
Anion– π interaction	interaction of a negative charge with the edge of an aromatic ring
Sulfur–arene interaction	short contact between sulfur atoms and aromatic rings
Chalcogen bonding	stereo-electronic interaction between a lone pair and σ anti-bonding orbital of a C–S or S–S bond

(*Table adapted from Newberry R.W. and Raines R.T. 2019. Secondary Forces in Protein Folding, ACS Chem Biol., 14(8): 1677–1686, [10.1021/acscchembio.9b00339](https://doi.org/10.1021/acscchembio.9b00339)).

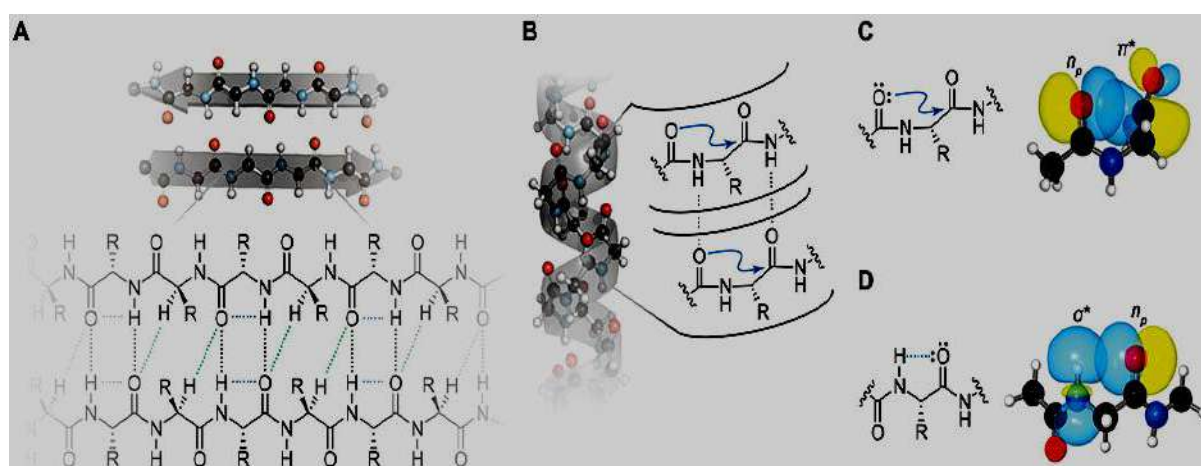


Fig. 1.8 Secondary interactions involving the main chain. (A) Structural model of an idealized β -sheet, showing conventional main-chain hydrogen bonds (black dashes), C–H···O hydrogen bonds (green dashes), and C5 hydrogen bonds (blue dashes). (B) Structural model of an idealized α -helix, showing main-chain hydrogen bonds (black dashes) and $n \rightarrow \pi^*$ interactions (blue arrows). (C,D) Orbital overlap that underlies formation of $n \rightarrow \pi^*$ interactions (C) and C5 hydrogen bonds (D). *Fig. adapted from Newberry R.W. et.al., 2019, ACS Chem Biol., 14(8): 1677-1686, [10.1021/acscchembio.9b00339](https://doi.org/10.1021/acscchembio.9b00339)

1.4.8. $n \rightarrow \pi^*$ Interactions Donation of lone pair (n) electron density from a carbonyl oxygen into the π^* orbital of another carbonyl group causes $n \rightarrow \pi^*$ interactions. Though they are weak, (Figures 8B and 8C) yet contribute a lot to proper protein folding [56-57]. There are a number of evidence that signify $n \rightarrow \pi^*$ Interactions in protein structure [58-60]. In collagen, the correspondence of pyrrolidine ring pucker with cis-trans conformation of prolyl peptide had explained by this interaction [61]. The energy of a typical $n \rightarrow \pi^*$ interaction is 0.3-0.7 kcal/mol as obtained from different experiment based [56] and reckoning [62] studies. It was found that the antecedent $n \rightarrow \pi^*$ Interactions potentially compete with H-bonds (Fig.1.9) in imparting protein stability [63]. One-third residues of a protein nearly show this type of interaction [57]. $n \rightarrow \pi^*$ Interactions are prevalent in stabilization of α -helices [57, 64], 3_{10} helix [57] and Poly Proline II helices [65-66] but less common in β -sheets [57].

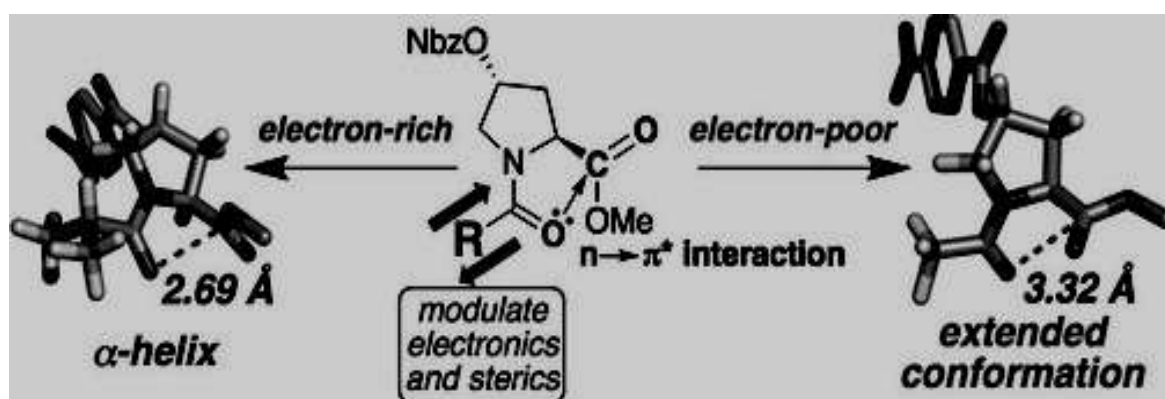


Fig.1.9 Stability of α -helix in the absence of hydrogen bonds: Modulation of the strength of $n \rightarrow \pi^*$ interactions with strong donors promoting α -helix and polyproline II helix conformations through peptide acyl N-cap, but weak donors resulting in more extended conformations. These results suggest the broader consideration of specific capping motifs for conformational control of peptides. *Fig. adapted from Wenzell NA. et al., *ChemBioChem.*, 20 : 963–967, <https://doi.org/10.1002/cbic.201800785>.

1.4.9. C5 Hydrogen Bonds refers to the intra residue hydrogen bonds between the β -strands amide proton and its carbonyl oxygen (Figures 1.8A and 1.8D) placed within 2.5 Å distance [67-68]. However, the energy contributions is very low (0.25 kcal/mol) compared to the canonical hydrogen bonds yet around 5% residues are engaged with this interaction in a stable folded protein making it significant. Even C5 hydrogen bonds contribute to the formation of harmful amyloid fibrils [68-69] during misfolding or aggregation event of biological proteins.

1.4.10. Cation- π Interaction occurs electrostatically within negatively charged residues of aromatic ring of amino acids and electric monopoles with corresponding quadrupole moments [70-71]. For each such interaction 0.5–1.0 kcal/mol energy is imparted to the stability of the protein [72]. The desolvation penalty of ion binding to protein cavities/pocket can be overcome by this energy [73]. The most important fact about this cation- π interaction is that this can be used to detect the smaller ligands [74] and post-translational modifications on histone proteins [75]. Cation- π interactions are formed with aromatic amino acid residues in the following relative frequency: tryptophan > tyrosine > phenylalanine whereas arginine interacts more than lysine [76]. These interactions are prevalent in protein-protein interfaces [77] and in protein secondary structures [78- 79].

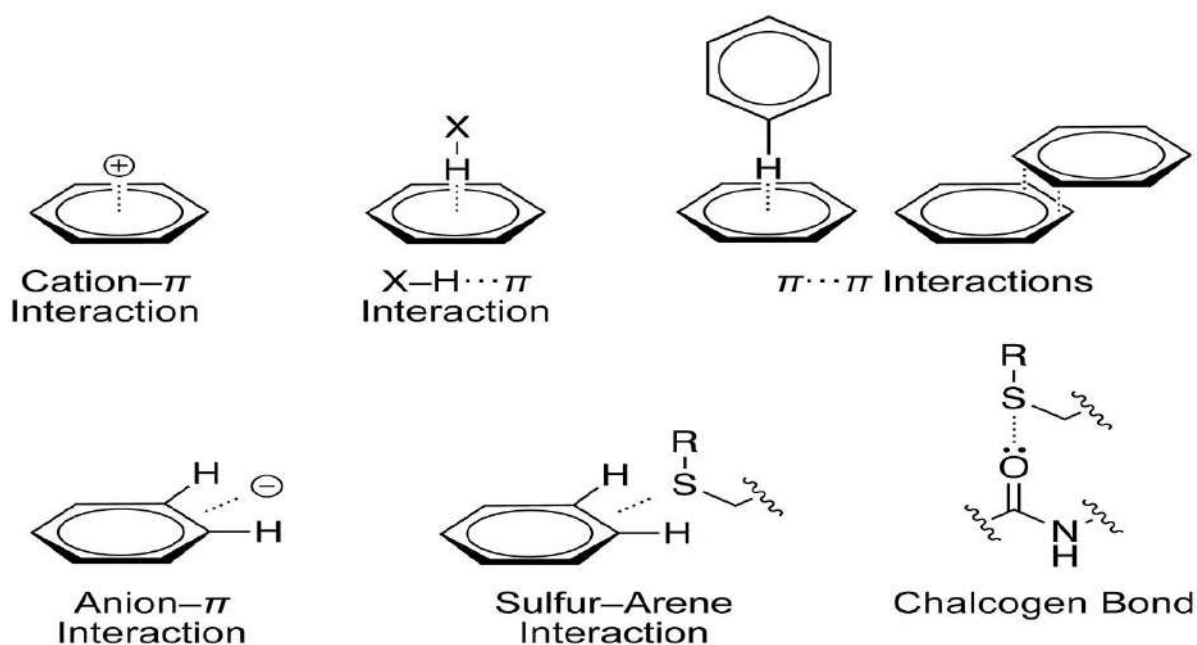


Fig.1.10 The possible secondary interactions in a protein involving side chains. * Fig. adapted from Newberry R.W. et.al., 2019, *ACS Chem Biol.*, 14(8): 1677-1686, [10.1021/acscchembio.9b00339](https://doi.org/10.1021/acscchembio.9b00339)

1.4.11. X-H $\cdots\pi$ Interactions. Besides engaging in cation- π interactions, aromatic rings of amino acids can form hydrogen bonds (Fig.1.10) donated from weaker acids [80]. This interaction is helpful in ligand binding especially for carbohydrates [81-83] e.g., tryptophan rich lectin binding site conformed via X-H $\cdots\pi$ interactions. Though weaker than Cation- π interaction, the individual strength of a C-H $\cdots\pi$ interaction confer thermo stability of designed mini-proteins [84].

1.4.12. π - π Interactions. The aromatic rings of proteins make attractive interactions within themselves at an inter-centroid distance of less than 7 Å through their preferable electron distributions [85]. It is known as the π - π Interactions of attraction and it engage nearly over half of the aromatic amino acid residues of a protein. There are two geometries of interactions of aromatic rings namely, T-shaped (or edge-to-face) and displaced-stacked (or offset-stacked) [86]. It was also shown to be prevalent in proteins of thermophilic organisms than do mesophilic organisms [87]. 0.5–1.5 kcal/mol energy is imparted by a single interaction [88–89]

1.4.13. Anion- π Interactions. It is a kind of electrostatic interactions in a protein within its aromatic rings and anions (Fig.1.10) e.g., carboxylate residues in an edge-to-edge fashion [90–91]. 0.5 kcal/mol energy is contributed by a single anion- π interaction [92]. Anion- π interactions occur more frequently with tryptophan may be due to its size and dipole moment than with phenyl alanine or tyrosine [93]. Anion- π interactions are co-operative with hydrogen bonds [94], π - π interactions [95] and cation- π interactions [95]. These types of interactions generally observed at protein-protein interfaces [94]. DNA having negatively charged phosphate groups and electron-deficient π -systems are more prone to form protein – DNA interactions through anion- π interactions [95]. Another example of stabilization by anion- π interaction is β -hairpin in the WW domain [96], which is an isolated three-stranded antiparallel beta-sheet domain.

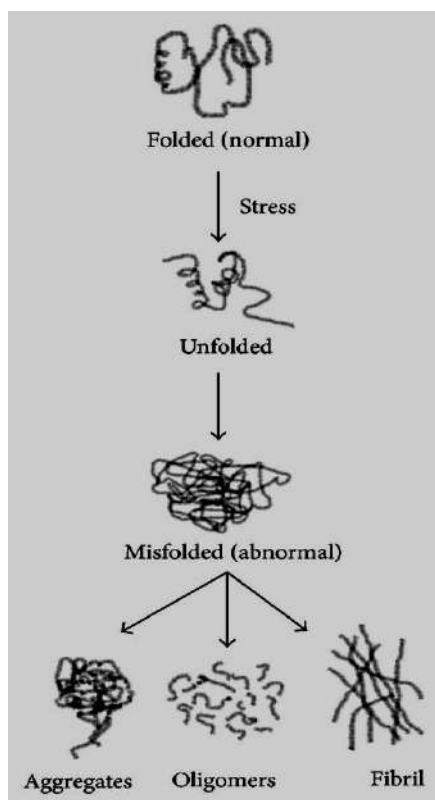
1.4.14. Sulfur-Arene Interactions. Frequent occurrence of cysteine, cystine, and methionine near the aromatic ring of protein structures [97] and protein-protein interfaces [97] had been documented many times in literature. This is due to the ability of aromatic rings in a protein structure to make contacts with lone pairs [98] through sulfur-arene interaction (Fig.10) and involve nearly 50% of sulfur residues with aromatic rings in a protein [99]. The energy of stabilization imparted by this type of interaction is 0.5 kcal/mol [100–101]. Though in this interaction, the hydrophobic effect is the dominating power [101] yet in protein this sulfur-arene interactions cannot be replaced by pure hydrophobic interactions [97].

1.4.15. Chalcogen Bonding is the stereoelectronic bond with sulfur atoms formed by transfer of electron cloud from a donor like carbonyl oxygen into any one of the σ^* orbital (Fig.1.10) of sulfur itself [102–103]. 0.64 kcal/mol energy is imparted to protein stability due to the said charge transfer [104]. Cystine disulfides interact strongly than thioesters of methionin [104].

The significant contributions of chalcogen bonding were observed mainly for heterocyclic ligands [105-106].

1.5. PROTEIN MISFOLDING: MOLECULAR AND CELLULAR IMPLICATIONS

Misfolding of protein is an intrinsic tendency of biological proteins unable to fold in a proper manner to get a functional form. It is attributed by several factors like (i) autosomal mutation



(ii) transcription or translation errors (iii) defective chaperone machinery (iv) error in post-translational modifications (v) mistakes in protein trafficking (vi) structural modification due to environmental factors or (vii) induction of the harmful events of protein misfolding and aggregation [107]. The self-aggregation of proteins while transition to large proportion of β -sheet motifs occurs is the most observed phenomenon generally contributed by exposure of otherwise buried residues of protein in the hydrophilic face [108]. The resulting large and heterogenous polymeric structure of protein is known as oligomers, protofibrils and fibrils (Fig. 1.11), among which oligomers are most toxic forms [109-111].

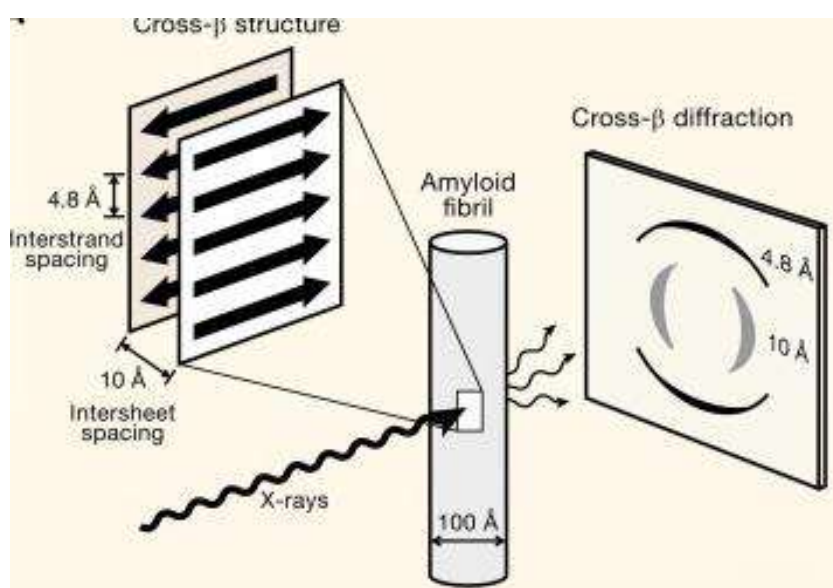
Fig. 1.11 Schematic diagram showing different fates of unfolded/misfolded protein species due to the different stresses. * Fig. adapted from Maiti P. et. al., 2014, *BioMed Research International*, 2014: 495091, <https://doi.org/10.1155/2014/495091>

1.5.1. Oligomers are generally soluble assemblies of 2-24 misfolded protein units [110-111]. Oligomers are involved in a numbers of harmful approaches viz., (i) even at minute concentrations, they are apoptosis or programmed cell death inducers in cell cultures both synthetically and naturally [112-114], (ii) long term potentiation in brain slice cultures is blocked by them [115] and (iii) in animals the synaptic plasticity and memory impairment is done by oligomers [116-117].

1.5.2. Protofibrils are arciform shaped structure of misfolded protein having 4–11 nm diameter, <200 nm long [109, 118] and they may elongate and grow more with time [119].

Protofibrils can form annular assemblies that form pores in cell membrane and thus disrupt osmotic balance of cell followed by cell death [120-121]. Besides this, the protofibrillar annular assemblies proved themselves harmful in various in –vitro systems also [121-122].

1.5.3. Fibrils or Amyloid structures are irreversibly formed, unbranched, non-functional harmful structures of misfolded/aggregated protein of around 10 nm diameter and several μm long [123]. In 1639, amyloid plaques were firstly observed [124] and in 1854, it got the name by Rudolph Virchow. The term amyloid coming from the Latin word ‘amylum’ and Greek word ‘amylon’ both of which means starch and this is due to the positive results of



iodine staining of cerebral plaques and thereby they were identified initially as starch. The identifying feature of amyloid fibrils is the perpendicular alignment of β -strands to the fibril axis forming extended regular ‘cross- β ’ (Fig. 1.12) form [125].

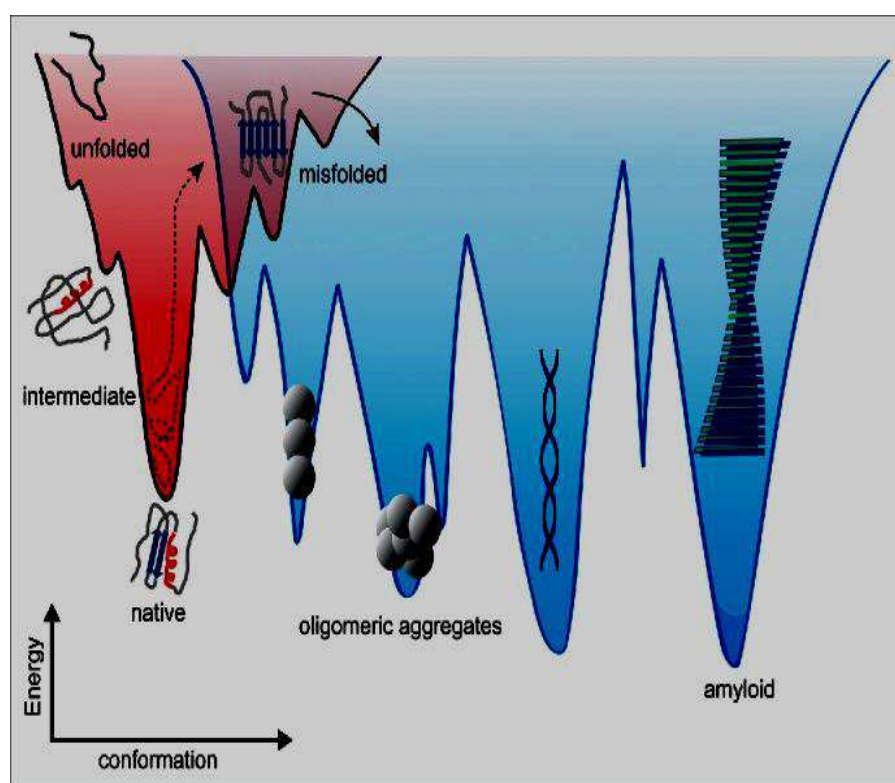
Fig. 1.12 Amyloid fibrils showing the characteristic cross- β diffraction pattern under X-rays. The extended protein chains running perpendicular to the fibril with diffuse reflection at 4.8 Å vertical spacing was shown. The sheets are placed ~ 10 Å apart. Reflection of the lesser-oriented fibrils blur into circular rings. *Fig. adapted from David Eisenberg D. et.al , 2012, <https://doi.org/10.1016/j.cell.2012.02.022>

The presence of amyloid fibrils in solution of protein can be sensed in vitro by different fluorescent dyes like Congo red and Thioflavin T. as shown in Fig.12, the peptide chains lay about 4.8 Å inter-stand spacing while the generated sheet are around 10 Å apart. Most importantly, the morphology of fibrils varies with types of protein, solvent/buffer system, concentration of protein and impurities, change in temperature and/or pH etc [126]. E.g., the hormonal protein insulin depending on pH, temperature and solvent conditions shows different level of organization and fibrillation [127- 129].

1.5.4. Energy states of Protein misfolding and aggregation

Levinthal's proposal about protein folding also known as **Levinthal's paradox**, 1968, [130] proposed that the rapid folding of a protein folds rapidly is due to the local interactions of its constituent amino acids. In this respect, the funnel-like energy landscape model that allows the protein to take most stable folded conformation is popular. In this model of energy landscape, unfolded states bearing high-energy and high-entropy are placed at the top of the funnel (Fig. 1.13). They subsequently fold themselves to acquire a low-energy, low-entropy native conformation [131] supported with stabilizing forces as discussed in paragraph 1.4.

Protein misfolding results due to improper interactions followed by folding in spaces of



actual folds and it results in development of energy - minimizing funnel where the involvement of multiple competing conformations [132] separated by substantial kinetic barriers are common.

Fig. 1.13 The Energy landscape

cartoons depicting native folding (left) and aggregation (right) of protein. The relative stabilities of different states (e.g. native, partially folded intermediate, unfolded, misfolded, soluble oligomer, or insoluble aggregate) and the separating energy barriers are shown.

**Adapted from Dee DR. et. al, 2016. Prion. 10 (3):207-220. doi: [10.1080/19336896.2016.1173297](https://doi.org/10.1080/19336896.2016.1173297)*

The aggregated structure of protein corresponds to rugged morphology (Fig. 1.13) in the landscape with deeper kinetic traps. Amyloid fibrillation is actually the structural transition of

protein from alpha helix to beta-sheet rich configuration [133] with resulting exposure of buried hydrophobic residues of protein.

1.5.5. Significance of determining energy landscapes and kinetics of folding

The energy landscape for a protein is a useful tool to determine the harmful transition from a natively folded protein into a disordered aggregate. Aggregation kinetics reveals the time scale and pattern of such transition event and thus very helpful in designing/ choosing inhibitors [134-137]. The ironic fact is that, if the aggregated form is found more thermodynamically stable than the native fold [138], the only way to prevent its spontaneous aggregation is the kinetic barriers. For example, ligands can be designed to stabilize native fold [139] of that particular protein and thus retaining its functional form while inhibiting the pathogenic aggregation. This is the basis of development of therapeutic strategies against the deadly diseases caused by protein aggregation. Simulation [140-142] and partial free-energy surfaces are calculated in Energy Landscapes. This also gives a view of activation energies along with thermodynamic stabilities for amyloid formation of protein [138, 143].

1.6. IN-VIVO CONSEQUENCES OF PROTEIN MISFOLDING

In a cellular system, the misfolded proteins at first are targeted to be degraded by chaperones or homeostasis oriented housekeeping mechanisms of the organism. If there is a deviation in the process of homeostasis, the pathogenic effects of generated fibrils can be of great concern [144]. The following table 1.3 shows some such fatal consequences of protein misfolding with their corresponding proteins of cause and target organs.

Table 1.3: Diseases associated with Protein misfolding

<i>Protein misfolding disorders</i>	<i>Protein involved</i>	<i>Affected organs</i>
Alzheimer's Disease	β-Amyloid	Hippocampus and cortex of brain
Amyloidoses	Insulin	Subcutaneous injection sites
Amyotrophic Lateral Sclerosis (ALS)	Superoxide dismutase (SOD1)	Motor cortex and Spinal motor neurons

α1-Antitrypsin deficiency	α1-Antitrypsin	Lungs, liver, skin
Atrial amyloidoses	Atrial natriuretic factor (ANF)	Heart
Cancer	P53	Any organ
Cataract	Crystallin	Mature fiber cells of eye lens
Cerebral amyloid angiopathy (Hereditary)	Cystatin C	Meninges of brain, central nervous system
Creutzfeldt Jakob Disease/ Scrapie	Prion protein PrP	Cerebellum , thalamus ,cortex, brain stem
Cystic fibrosis	Trans-membrane regulator protein	Lungs, pancreas, intestines
Diabetes (type II)	Islet amyloid polypeptide (IAPP)	Pancreatic islets
Familial amyloid polyneuropathy I	Transthyretin	Autonomic nervous system
Familial amyloid polyneuropathy III	Apolipoprotein A1	Peripheral nervous system, heart, liver, kidneys, skin
Finnish systemic amyloidoses (Hereditary)	Gelsolin	Eye cornea
Haemodialysis related amyloidoses	β2-Microglobulin	Joints of body
Huntington's Disease	Huntingtin	Basal ganglia, Striatum
Medullary carcinoma of thyroid	Calcitonin	Thyroid gland

Non-neuropathic systemic amyloidoses (Hereditary)	Lysozyme	Liver, kidneys
Parkinson's Disease	α-Synuclein	Basal ganglia, substantia nigra
Phenylketoneuria	Phenylalanine hydroxylase (PAH)	Brain tissue, Cerebrospinal fluid, Plasma
Primary systemic amyloidoses	Immunoglobulin light chain	Autonomic and peripheral nervous system, heart, liver, GI tract, kidneys
Renal amyloidoses (Hereditary)	Fibrinogen	Liver, kidneys
Senile systemic amyloidoses	Transthyretin	Heart
Sickle-cell anaemia	Haemoglobin	Heart, liver, kidneys, GI tract
Spongiform encephalopathies	Prion	Cerebellum , thalamus ,cortex, brain stem
Tay-Sach Disease	β-Hexosaminidase	Brain

Generally some proteins that possess repetitive amino acid motifs, such as poly-glutamine are prone to misfolding e.g., the cause of Huntington's disease [145]. **Cerebral proteopathies** is collectively used term indicative of the pathogenic conditions of accumulation of protease-resistant aggregated and misfolded proteins in different body sites due to the harmful transition of soluble proteins into insoluble plaques. These neurodegenerative disorders like Alzheimer's disease and Parkinson's disease are caused by endogenous errors of protein folding in vivo [146]. Sometimes, the misfolded configurations of protein are able to interact with other wild type copies of similar proteins to make them toxic unfolded aggregates. Proteins with such devastating contagious capabilities are known as **infective conformers**, e.g., **prion protein** [147], which repeats this process in a self-sustained manner and results in

amplification of toxic effects. In this way, a catastrophic effect, which disrupts the cell function or kills the cell, is generated.

1.7. IMPACT OF PROTEIN AGGREGATION IN-VITRO

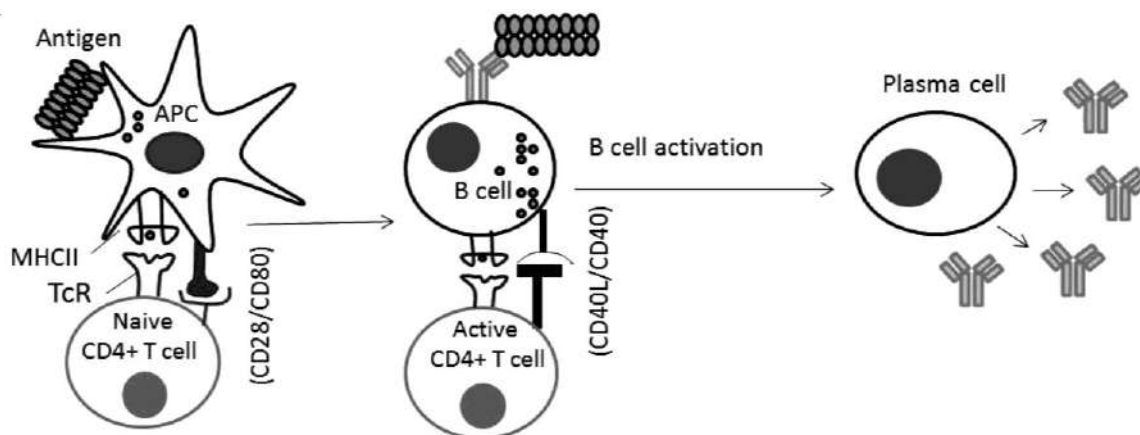
Protein aggregation arrives as a profound challenge in different fields like research, development, and commercialization of protein-based drugs and products. During the commercial processes of protein production, transport, and storage, various factors may lead to protein aggregation. Majorly this phenomenon affects the vast domain of Protein Pharmaceuticals based industry as follows:

Reduction in production yield: There are a large number of protein-based pharmaceuticals necessarily produced in industries on daily basis. Some of the examples of protein-based pharmaceuticals are Insulin, drugs against some cancer and autoimmune disorders, monoclonal antibodies, various drugs under clinical trials etc. The maintenance of quality standards is a necessity in this regard. Protein aggregation greatly hampers the functional ability and thus affecting the overall drug yield.

Product quality and efficacy compromisation : The alterations in protein configuration due to aggregation weaken/inactivate activity of proteins, leading to a reduction in therapeutic effectiveness. Most of the protein based drugs cannot be taken orally. They should be delivered via liquid injections viz., intravenous (IV), intramuscular (IM), or subcutaneous (SC). That is why the drugs are manufactured and stored in aqueous state [147]. Aggregation is reported also in aqueous phases of protein due to the solvent contributions, state of hydration and/or external effects.

Problems in dose generation: The general dosage of therapeutic proteins requires a certain amount of protein per unit mass of the patient body weight. IM and SC injections are preferred to deliver in the maximum volume of approximately 1 mL, while the target dose of protein to the patient can be over 200 mg. Therefore, the drug concentrations should be in the range of 10^2 mg/ml. such higher concentration is prone to aggregate formation [149].

Immunogenicity posed by aggregated therapeutic drug: Aggregated therapeutic protein naturally triggers immune system and may be a cause of heightened immunogenic properties.



If the aggregates form a larger size to be recognized as foreign antigen by body cells, then it induces a humoral immune response. In this response, the therapeutic agent is internalized,

Fig. 1.14 The Classical pathway of humoral immune response: the polymeric aggregates of the protein drug sensed as antigen, which is internalized by APC. APC process them to peptide fragments to be recognized by major histocompatibility complex II (MHCII). Subsequent interaction of CD4⁺ T-cells stimulates plasma B-cells to secrete antibody. *Fig. adapted from Ratanji KD. et. al., 2013, J. Immunotoxicol. 11(2):99-109, <https://doi.org/10.3109/1547691X.2013.821564>

processed, and presented by antigen-presenting cells (APC). CD4 T-cells are there to sense it (Fig. 1.14) and in turn activates plasma B-cells which secrete antibody to react with the antigen (here it is the therapeutic protein aggregates). Huge side effects can occur and adverse condition may leads to anaphylaxis (severe, instantaneous life-threatening allergic reaction) [150].

Harmful Impact on the Storage and Utilization of Protein Pharmaceuticals:

Environmental factors such as temperature and humidity may induce aggregation during storage of protein-based drugs. The high requirements for storage conditions increase the cost and complexity of pharmaceutical storage. The most terrifying factor is that, in most of the cases, the aggregates cannot be seen in naked eye as they are ‘**molecular**’ aggregates. It was also reported that pharmaceutical proteins may undergo crystallisation [151] or LLPS (liquid–liquid phase separation) [152].

Instability of Clinical Efficacy: The reasons behind untrustworthy efficiency of a protein-based drug are as follows: i. Aggregation followed by decreased solubility of the drug may

require low protein concentrations, and the maximum dose to be delivered via IM or SC should be compromised. IV delivery then is forced to be done.

ii. The solution viscosity of therapeutic protein may be altered that also affect IM or SC delivery. A compact aggregate like microcrystals or amorphous nanoparticles may lower the viscosity [153] while an aggregate with extended conformation can entangle within them and increases the viscosity [154].

Nowadays, the risk of protein aggregation in the drug design and production is a major concern. Standardization and unfolding the causes and mechanisms of protein misfolding/aggregation is necessary to develop safer and effective generations of protein-based therapeutics.

1.8. HUMAN INSULIN - A THERAPEUTIC PROTEIN

Technically, any protein-based drug is a “therapeutic protein,” but the term was first used to describe medicines that are genetically engineered versions [155] of naturally occurring human proteins. Protein therapeutics serve better than a small-molecular/chemical drugs in the following ways. Firstly, genetically engineered proteins often serve a highly complex set of functions that a chemical compound cannot do. Secondly, enzymatic/ therapeutic proteins produced through modified/controlled gene expression shows high specificity toward their target [156]. Third, normal biological processes are not hampered by them and thus show lesser side effects [157]. Fourth, the benefit of using genetically engineered proteins is – as they closely resemble the natural proteins, immunogenic induction of body can be eliminated [158]. Fifth, for a genetic disease where gene mutation/deletion is the cause of pathogenicity but gene therapy cannot be possible/ avoided, protein therapeutics is the option of treatment. Sixth, the clinical development of a protein therapeutic is more reliable and the following Food and Drug Administration (FDA) approval rate is faster in this case than that of small-molecule chemical drug [159]. Lastly, because of their uniqueness and high specificity in structure, they can be necessarily being patent-protected. Companies prefer the last two options for market based benefits from protein therapeutics.

Human insulin is a biological protein hormone produced by beta cells of islets of langerhans of pancreas. Its normal secretion in response to higher blood sugar level is to control the same. It performs the function by activating /deactivating a cascade of processes in the body. Some of which may include but not limited to activation of glycolysis (the first catabolic

pathway of glucose utilization in both aerobic and anaerobic organisms to get energy and product pyruvate) and glycogenesis (the process of formation of storage form of carbohydrate i.e., glycogen from glucose) [160]. While it causes simultaneous deactivation (fig.1.15) of glycogenolysis (the process of glycogen break down to release glucose) and gluconeogenesis (the process of synthesis of glucose from non-carbohydrate sources).

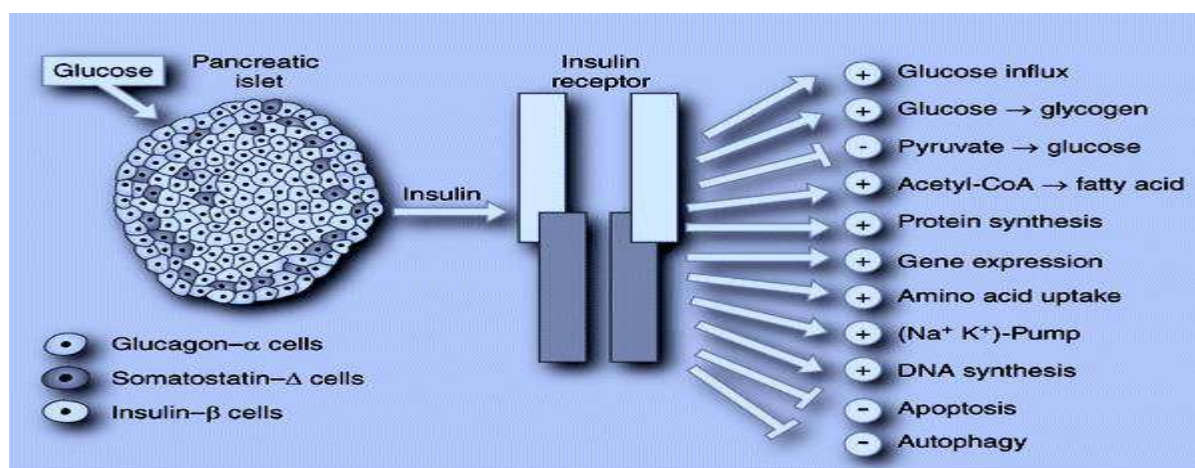


Fig. 1.15 Schematic representation of mode of action of human insulin. *Fig adapted from White, M.F. et. Al. 2012. In: Skyler, J. (eds) *Atlas of Diabetes*. Springer, Boston, MA. https://doi.org/10.1007/978-1-4614-1028-7_2

1.8.1. The need of insulin therapy and commercial production of human insulin

Medical treatment with insulin is required when there is inadequate/zero production or an increased insulin demand occurs in the body. The possible diseases requiring insulin treatment are as follows:

Type 1 Diabetes Mellitus (T1DM) or juvenile diabetes or insulin-dependent diabetes, is a chronic condition characterized by the body's inability to produce insulin due to the autoimmune destruction of the beta cells in the pancreas [161]. The disease may develop in adults too. As a result, the patients with type-1 diabetes are always in need of insulin therapy [162-163].

Type 2 Diabetes Mellitus (T2DM) is the commonest form of diabetes occurring generally after the age of 45 years. However, in children and teenagers the occurrence of this disease had reported. In type 2 diabetes, cells showing less/no response toward insulin i.e., they become resistant to the action of insulin. Although, the authentic cause is unknown still the

risk factors include hereditary occurrence, obesity, metabolic syndrome, high-calories in maximum diet or sluggish and lethargic habits in lifestyle. Body primarily makes more insulin to maintain glucose homeostasis, but over time, insulin production decreases and T2DM can be diagnosed. Treatment is done by changing diet; oral anti diabetic drugs and later stages of T2DM requires insulin therapy [164-165].

Maturity Onset Diabetes of Young (MODY): In this genetically inherited disease, a gene mutation disables the pancreatic beta cells to secrete insulin [166]. Here the young patients lack any antibodies against the islets of pancreas and have some siblings with this disease in common. Patients are recommended Insulin or sulfonylurea treatment.

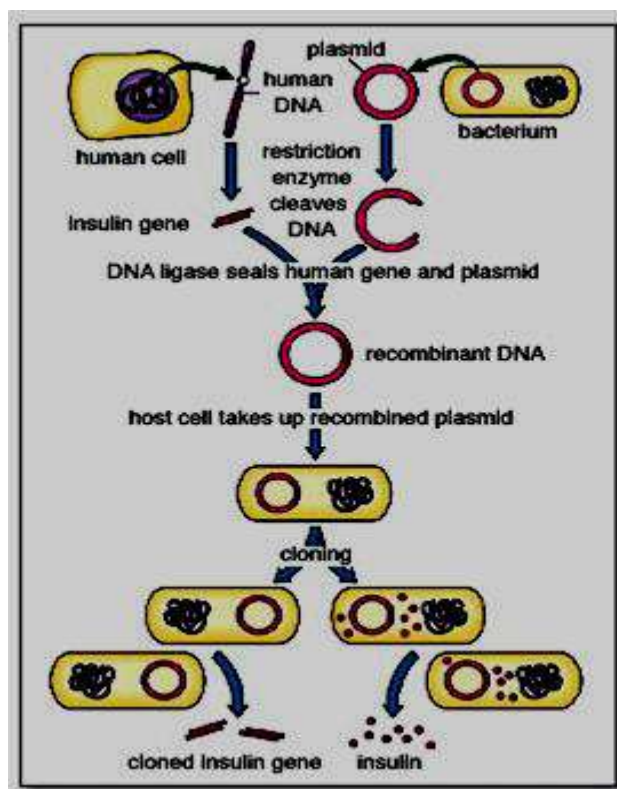
Gestational Diabetes Mellitus (GDM) is a condition seen in some pregnant women where the glucose cannot get into the cells, so the amount of glucose in the blood gets higher and higher. This is called Gestational Diabetes Mellitus (GDM). It is screened during 24 to 28 weeks of pregnancy, and initial treatment is done with diet and exercise. Such pregnant women are at higher risk of high blood pressure, preeclampsia (a sudden, dangerous rise in blood pressure), pregnancy loss during the last 4 weeks to 8 weeks, early/preterm labor and delivery leads to C-section Surgery to deliver the baby and the related infection risks. If diet and exercise fail to control the blood sugar level, insulin therapy is prescribed [167]

Cystic fibrosis is the related disease requiring insulin therapy as in this case, thick mucus is produced that causes scarring in the pancreas. This scarring can inhibit the pancreas to secrete sufficient insulin [168].

Hemochromatosis is a pathogenic condition that causes the body to store too much iron. If the disease is not treated, iron can build up in and damage the pancreas and other organs. Thus, insulin is required as one of the medications [169].

1.8.2.The gradual development of insulin therapeutics It was 1922 when, to treat patients having Diabetes Mellitus insulin was first purified from bovine and porcine pancreas [170]. The difficulties made during the extraction procedure of insulin are as follows: firstly, the fresh supply of animal pancreases for purification of insulin is challenging; secondly, the process of insulin purification from animal pancreas need expertise and very costly; and thirdly, a number of patients show immunogenic responses against the animal insulin.

To overcome the issues it is necessary to get human insulin only as the therapeutics and this was possible due to advent of recombinant DNA technology (RDT). In RDT, at first the gene responsible for insulin production in human is isolated and purified. Next, the gene is cloned and inserted into the chromosome of fast growing bacteria like *Escherichia coli*. The



successfully transformed bacteria having the recombinant insulin gene then allowed to grow in cultures (fig.1.16). In a very short time scale, huge amount of bacteria can grow and from which sufficient amount of recombinant insulin of human origin can be isolated and purified [171]. The advantages of this process over the rest are- large-scale commercial production can be attained in a short time, cost-effectiveness of the process, more reliability, insulin with lesser/no immunogenicity.

Fig.1.16 Schematic representation of human insulin production in E.coli by recombinant DNA technology

1.9. STRUCTURAL OVERVIEW OF HUMAN INSULIN

Insulin was discovered in 1922 [172] and after its discovery, the large-scale production of insulin was commenced in 1923 by the USA company Eli Lilly, Insulin was crystallized in 1926 [173] and the molecular weight was calculated in 1931 [174]. The consisting of A and B chains linked with disulfide bonds within insulin structure was revealed in 1949 [175] where the two chains were sequenced by Sanger in 1950 [176-177].

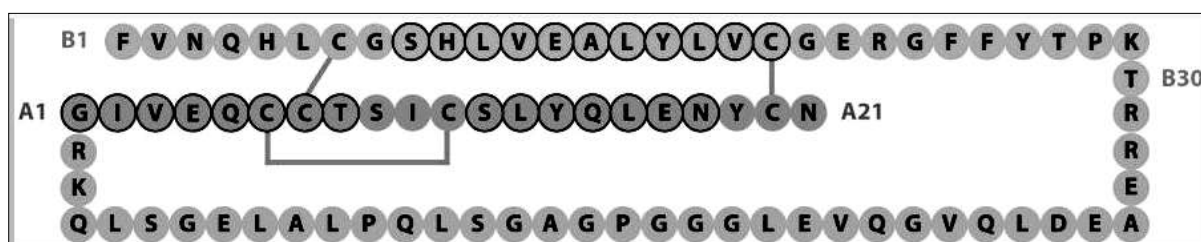
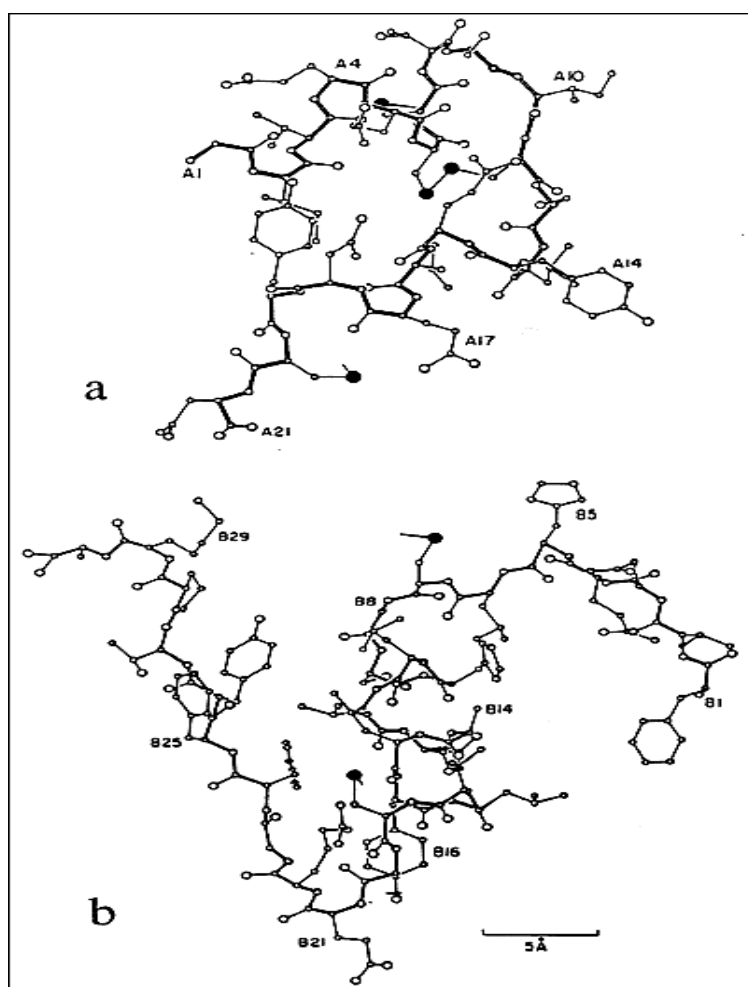


Fig.1.17 Schematic representation of sequence of human insulin in primary structure

Number of amino acid residues of human insulin is 51 while the molecular weight is 5808 Da. It has an A-chain (21 amino acids) and a B-chain (30 amino acids) linked by disulfide bonds (Fig.1.17).

The A chain possesses of two nearly antiparallel α -helical segments (A1-A8 and A12-A19). A non-canonical turn of residues A9-A12 connects the two helices (Fig.1.18a), to bring the N- and C-chain termini in close contact. The central α -helix (residues B9-B19) of B chain (Figure 1.18b) is flanked by disulfide bridges (cystines A7-B7 and A20-B19) and β -turns (B7-B10 and B20-B23). There is a β -strand within residues B24-B28. The noticeable α -turn- β super secondary structure occurred by close contact between the conserved aromatic side chains of Phe B24 and Tyr B26 with Leu B11, Val B12 and Leu B15 of the central α -helix of B chain.



Insulin at acidic pH and concentrations $\sim 10^{-6}$ M exists primarily as a monomer while it forms dimer at higher concentrations and a neutral pH. At high concentrations and in the presence of zinc ions, insulin generally forms hexameric structure [178].

Fig.1.18a. The structures of insulin A- chain b. B-chain of insulin. Both were determined from the three-dimensional X-ray analysis of the T_6 hexamer (2-Zn insulin) in perpendicular to the threefold symmetry axis.

*Fig adapted from Weiss M. et.

al, 201, <https://www.ncbi.nlm.nih.gov/books/NBK279029/>

1.10. STABILITY OF NATIVE FOLDS OF INSULIN

The sulfur atoms of cysteines A6-A11 and A20-B19 as well as the nonpolar side chains of Ile A2, Val A3, Leu A16, Tyr A19, Leu B6, Leu B11, and Leu B15 are buried in the properly folded insulin [179] in a conserved manner. Val A3, Ile A13, Val B12, Val B18, Phe B24, and Tyr B26 are exposed partly due to they are being located at edge of the above stated hydrophobic centre [180]. This is the basis of stability and surface interactions of insulin. There present three conserved amino acid Tyr A19 -Cys A20 -Asn A21 of special importance in the C-terminal of A-chain of insulin residues. Tyr A19 plays crucial role in packing of insulin in collaboration with Ile A2. While the hydroxyl group of it is being exposed towards the hydrophilic surfaces are ready to interact with solvents/ligands. It was revealed in mutagenic studies of insulin that, if Phe or Trp substitutes the Tyr A19, then the activity of insulin is badly hampered [180]. Though another tyrosine in the A-chain (Tyr A14) is not necessarily that much conserved.

1.11. INSULIN-DERIVED AMYLOIDOSIS

In 1982, the FDA (Food and Drug Administration) approved the insulin produced via recombinant DNA technology [181]. The recombinant human insulin pharmaceutical is in hexameric state which should be converted to monomer in order to become absorbed and remain in active state within body [182].

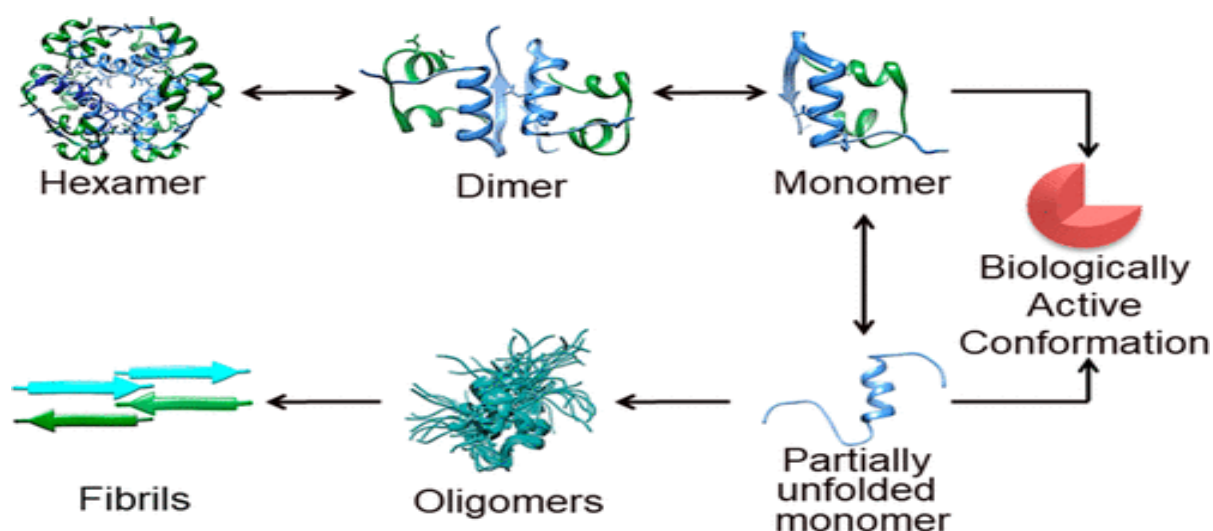


*Fig. 1.19 Schematic diagram of pathway of insulin aggregation *Fig adapted from Yang Y. et. al. 2010. J. Biol. Chem., 285 (14):10806– 10821, 10.1074/jbc.M109.067850*

Under different in vivo and in vitro conditions like repeated injection sites in case of diabetic patients or during formulation/storage / delivery of insulin, pH alteration, solvent condition, elevated temperature, and exposure to hydrophobic environment, insulin may undergo partial unfolding, seed generation followed by seed elongation i.e., irreversible fibrillation (Figure 1.19). This event is termed as **amyloidosis of insulin** [183].

The amino acid residues GlyB8, SerB9, GluB13, ValB12, TyrB16, GlyB23, PheB24, PheB25, TyrB26, and ThrB27 of insulin B chain are associated with this fibrillation process [184]. The seed nucleus for fibrillation is generated by the significant involvement of PheB1, ValB2, GluB13, GlnB4, AlaB14, LeuB17, ValB18, CysB19, and GlyB20 from the insulin B-chain and LeuA13, TyrA14, and GluA17 from the insulin A-chain. The amyloid structure is almost stabilized by Hydrogen bonding and hydrophobic interactions between the interacting amino acid residues. As per suggestions of Ivanova et al., the B-chain residues LVEALYLV form the core of insulin fibrils [185]. This is reason behind the findings of parallel β -sheets along the whole length of the fiber.

1.12. References

1. Kobayashi K., Granja J.R., Ghadiri M.R. 1995. β -Sheet Peptide Architecture: Measuring the Relative Stability of Parallel vs. Antiparallel β -Sheets, *Angew. Chem.*, 34(1): 95-98, <https://doi.org/10.1002/anie.199500951>
2. Bajaj M. and Blundell T. 1984. Evolution and the Tertiary Structure of Proteins, *Annu. Rev. Biophys.*, 13:453-492, <https://doi.org/10.1146/annurev.bb.13.060184.002321>
3. Pelley J.W. 2007. Protein Structure and Function, Elsevier's Integrated Biochemistry, Ch.3, 19-28, <https://doi.org/10.1016/B978-0-323-03410-4.50009-2>
4. Pace C.N., Fu H., Fryar K.L., Landua J., Trevino S.R., Shirley B.A., Hendricks M.M.N., Iimura S., Gajiwala K., Scholtz J.M. and Grimsley G.R. 2011. Contribution of Hydrophobic Interactions to Protein Stability, *J. Mol. Biol.*, 408(3): 514–528, [10.1016/j.jmb.2011.02.053](https://doi.org/10.1016/j.jmb.2011.02.053)
5. Sanfelicea D. and Temussi P.A. 2016. Cold denaturation as a tool to measure protein stability, *Biophys Chem.*, 208: 4–8, doi: [10.1016/j.bpc.2015.05.007](https://doi.org/10.1016/j.bpc.2015.05.007)
6. Fersht AR, Shi JP, Knill-Jones J, Lowe DM, Wilkinson AJ, Blow DM, Brick P, Carter P, Waye MM, Winter G. 1985. Hydrogen bonding and biological specificity analysed by protein engineering. *Nature*, 314:235–238, <https://doi.org/10.1038/314235a0>
7. Fersht AR. 1987, The hydrogen bond in molecular recognition. *Trends Biochem Sci.*, 12:301–304. [https://doi.org/10.1016/0968-0004\(87\)90146-0](https://doi.org/10.1016/0968-0004(87)90146-0)
8. Schell D, Tsai J, Scholtz JM, Pace CN. 2006. Hydrogen bonding increases packing density in the protein interior. *Proteins*. 63:278–282. [10.1002/prot.20826](https://doi.org/10.1002/prot.20826)
9. Stickle DF, Presta LG, Dill KA, Rose GD. 1992. Hydrogen bonding in globular proteins. *J Mol Biol.*, 226:1143–1159, [10.1016/0022-2836\(92\)91058-w](https://doi.org/10.1016/0022-2836(92)91058-w)
10. Gao J, Bosco DA, Powers ET, Kelly JW. 2009. Localized thermodynamic coupling between hydrogen bonding and microenvironment polarity substantially stabilizes proteins, *Nat Struct Mol Biol.*, 16:684–690, [10.1038/nsmb.1610](https://doi.org/10.1038/nsmb.1610)
11. Pace CN. 2009. Energetics of protein hydrogen bonds, *Nat Struct Mol Biol.*, 16:681–682, <https://doi.org/10.1038/nsmb0709-681>
12. Mitchell JBO, Price SL. 1991. On the relative strengths of amide..amide and amide..water hydrogen bonds. *Chem Phys Lett.*, 180:517–523. [https://doi.org/10.1016/0009-2614\(91\)85003-F](https://doi.org/10.1016/0009-2614(91)85003-F)

13. Baldwin RL. 2010. Desolvation penalty for burying hydrogen-bonded peptide groups in protein folding. *J Phys Chem B*, 114:16223–16227, [[Google Scholar](#)]
14. Worth CL and Blundell TL. 2009. Satisfaction of hydrogen-bonding potential influences the conservation of polar side chains. *Proteins*.75:413–429, [[Google Scholar](#)]
15. Tsemekhman K, Goldschmidt L, Eisenberg D, Baker D. 2007. Cooperative hydrogen bonding in amyloid formation. *Protein Sci.*,16:761–764, [[Google Scholar](#)]
16. Loladze VV, Ermolenko DN, Makhatadze GI. 2002. Thermodynamic consequences of burial of polar and non-polar amino acid residues in the protein interior. *J Mol Biol*.320:343–357, [[Google Scholar](#)]
17. Makhatadze GI, Privalov PL. 1995. Energetics of protein structure. *Adv Protein Chem.*, 47:307–425, [[Google Scholar](#)]
18. Brandts JF.,1964. The thermodynamics of protein denaturation. II. a model of reversible denaturation and interpretations regarding the stability of chymotrypsinogen. *J Am Chem Soc.*, 86:4302–4314, [[Google Scholar](#)].
19. Gilson MK, Honig BH. 1986. The Dielectric Constant of a Folded Protein. *Biopolymers*. 25:2097–2119, [[Google Scholar](#)].
20. Simonson T, Brooks CL. 1996. Charge Screening and the Dielectric Constant of Proteins: Insights from Molecular Dynamics. *J Am Chem. Soc.*,118:8452–8458, [[Google Scholar](#)]
21. Schutz CN, Warshel A. 2001, What Are the Dielectric “Constants” of Proteins and How to Validate Electrostatic Models? *Proteins: Struct, Funct Genet.*, 44:400–417, [[Google Scholar](#)]
22. Rossini E, Knapp EW.2017. Protonation Equilibria of Transition Metal Complexes: From Model Systems toward the Mn-Complex in Photosystem II. *Coord Chem Rev.*,345:16–30. [[Google Scholar](#)].
23. Linderström-Lang K. 1924, On the Ionisation of Proteins. *C R Trav Lab Carlsberg, Ser Chim.*,15:1–29, [[Google Scholar](#)]
24. Tanford C.1970, Protein Denaturation. C. Theoretical Models for the Mechanism of Denaturation. *Adv Protein Chem.*,24:1–95, [[Google Scholar](#)].
25. Hunter T. 2012. Why Nature Chose Phosphate to Modify Proteins. *Philos Trans R Soc, B*,367:2513–2516, [[Google Scholar](#)]
26. Pauling L, Itano HA, Singer SJ, Wells IC. 1949. Sickle-Cell Anemia, a Molecular Disease. *Science*. 110:543–548,[[Google Scholar](#)]

27. Ingram VM. 1956. A Specific Chemical Difference between the Globins of Normal Human and Sickle-Cell Anaemia Haemoglobin. *Nature*.178:792–794, [[Google Scholar](#)].
28. Schreiber G, Haran G, Zhou HX. 2009. Fundamental Aspects of Protein-Protein Association Kinetics. *Chem Rev.*,109:839–860, [[Google Scholar](#)]
29. Pang X, Zhou HX. 2017. Rate Constants and Mechanisms of Protein-Ligand Binding. *Annu Rev Biophys.*,46:105–130, [[Google Scholar](#)]
30. Iwata S, Ostermeier C, Ludwig B, Michel H. 1995. Structure at 2.8 Å Resolution of Cytochrome C Oxidase from *Paracoccus Denitrificans*. *Nature*. 376:660–669, [[Google Scholar](#)]
31. Hunte C, Screpanti E, Venturi M, Rimon A, Padan E, Michel H. 2005. Structure of a Na⁺/H⁺ Antiporter and Insights into Mechanism of Action and Regulation by pH. *Nature*. 435:1197–1202, [[Google Scholar](#)]
32. Feng L, Campbell EB, Hsiung Y, MacKinnon R. 2010. Structure of a Eukaryotic CLC Transporter Defines an Intermediate State in the Transport Cycle. *Science*.330:635–641, [[Google Scholar](#)]
33. Maniccia AW, Yang W, Johnson JA, Li S, Tjong H, Zhou HX, Shaket LA, Yang JJ. 2009. Inverse Tuning of Metal Binding Affinity and Protein Stability by Altering Charged Coordination Residues in Designed Calcium Binding Proteins. *PMC Biophys*.2:11,[[Google Scholar](#)]
34. Ennion S, Hagan S, Evans RJ., 2000. The Role of Positively Charged Amino Acids in ATP Recognition by Human P2X(1) Receptors. *J Biol Chem.*,275:29361–29367, [[Google Scholar](#)]
35. Jiang LH, Rassendren F, Surprenant A, North RA. 2000. Identification of Amino Acid Residues Contributing to the ATP-Binding Site of a Purinergic P2X Receptor. *J Biol Chem.*,275:34190–34196, [[Google Scholar](#)]
36. [Coleman E.](#), [Inusa B.](#) 2007. Sick cell anemia: targeting the role of fetal hemoglobin in therapy. *Clin Pediatr Phila.*,46 (5):386-91, doi: 10.1177/0009922806297751
37. Roy K., Kar S., Das R.N., 2015. Understanding the Basics of QSAR for Applications in Pharmaceutical Sciences and Risk Assessment. Background of QSAR and Historical Developments. Ch 1, 1-46, <https://doi.org/10.1016/B978-0-12-801505-6.00001-6>
38. Roth C.M., Neal B.L. and Lenhoff A.M. 1996. Van der Waals Interactions Involving Proteins. *Biophys J.*, 70(2): 977–987, [10.1016/S0006-3495\(96\)79641-8](https://doi.org/10.1016/S0006-3495(96)79641-8)

39. Katz BA, Kossiakoff A. 1986. The crystallographically determined structures of atypical strained disulfides engineered into subtilisin. *JBC*. 61:15480–15485, [[Google Scholar](#)]
40. Luken BM, Winn LY, Emsley J, Lane DA, Crawley JT. 2010. The importance of vicinal cysteines, C1669 and C1670, for von Willebrand factor A2 domain function. *Blood*. 115:4910–4913, [[Google Scholar](#)]
41. Mangan MS, Bird CH, Kaiserman D, Matthews AY. 2016. A Novel Serpin Regulatory Mechanism: SerpinB9 is reversibly inhibited by vicinal disulfide bond formation in the reactive center loop. *JBC*, 291:3626–3638, [[Google Scholar](#)]
42. Carugo O, Cemazar M, Zahariev S, Hudaky I. 2003. Vicinal disulfide turns. *Protein Eng.*, 16:637–639, [[Google Scholar](#)].
43. Feige MJ, Hendershot LM. 2011. Disulfide bonds in ER protein folding and homeostasis. *Curr Opin Cell Biol.*, 23:167–175, [[Google Scholar](#)]
44. Permyakov EA. 2021. Metal Binding Proteins. *Encyclopedia*. 1(1):261-292, <https://doi.org/10.3390/encyclopedia1010024>
45. Permyakov E.A. 2009. *Metalloproteomics*; Wiley: Hoboken, NJ, USA, [[Google Scholar](#)]
46. Permyakov E.A., Kretsinger R.H., 2010. *Calcium Binding Proteins*, Wiley: Hoboken, NJ, USA [[Google Scholar](#)]
47. Dudev T., Lim, C., 2003, Principles Governing Mg, Ca, and Zn Binding and Selectivity in Proteins. *Chem. Rev.*, 103:773–788. [[Google Scholar](#)]
48. Christianson D.W., 1991. Structural Biology of Zinc. *Protein Simul.* 42:281–355, [[Google Scholar](#)]
49. Lesser GJ, Rose GD. 1990. Hydrophobicity of amino acid subgroups in proteins. *Proteins*. 8:6–13, <https://doi.org/10.1002/prot.340080104>
50. Derewenda ZS, Derewenda U, Kobos PM. 1994. (His)C ϵ –H \cdots O=C< hydrogen bond in the active sites of serine hydrolases. *J. Mol. Biol.*, 241:83–93, <https://doi.org/10.1006/jmbi.1994.1475>
51. Derewenda ZS., Lee L., Derewenda U., 1995. The occurrence of C–H \cdots O hydrogen bonds in proteins. *J. Mol. Biol* 1995, 252: 248–262. <https://doi.org/10.1006/jmbi.1995.0492>

52. Scheiner S. 2006. Contributions of $\text{NH}\cdots\text{O}$ and $\text{CH}\cdots\text{O}$ hydrogen bonds to the stability of β -sheets in proteins. *J. Phys. Chem. B*, 110: 18670–18679, <https://doi.org/10.1021/jp063225q>
53. Chakrabarti P., Chakrabarti S., 1998. $\text{C-H}\cdots\text{O}$ Hydrogen bond involving proline residues in α -helices. *J. Mol. Biol.*, 284:867–873, <https://doi.org/10.1006/jmbi.1998.2199>
54. Bella J., Berman HM., 1996. Crystallographic evidence for $\text{C}^\alpha\text{-H}\cdots\text{O}=\text{C}$ hydrogen bonds in a collagen triple helix. *J. Mol. Biol.*, 264:734–742, <https://doi.org/10.1006/jmbi.1996.0673>
55. Mueller BK., Subramaniam S., Senes A., 2014. A frequent, GxxxG-mediated, transmembrane association motif is optimized for the formation of interhelical $\text{C}^\alpha\text{-H}$ hydrogen bonds. *Proc. Natl. Acad. Sci. U. S. A.*, 111:E888–E895, <https://doi.org/10.1073/pnas.1319944111>
56. Hinderaker MP., Raines RT., 2003. An electronic effect on protein structure. *Protein Sci.*, 12: 1188–1194, <https://doi.org/10.1110/ps.0241903>
57. Bartlett GJ., Choudhary A., Raines RT., Woolfson DN., 2010. $n\rightarrow\pi^*$ Interactions in proteins. *Nat. Chem. Biol.*, 6 : 615–620, <https://doi.org/10.1038/nchembio.406>
58. Singh SK., Das A., 2015. The $n\rightarrow\pi^*$ interaction: A rapidly emerging non-covalent interaction. *Phys. Chem. Chem. Phys.*, 17: 9596–9612, [10.1039/C4CP05536E](https://doi.org/10.1039/C4CP05536E)
59. Newberry RW., Raines RT., 2017. The $n\rightarrow\pi^*$ interaction. *Acc. Chem. Res.*, 50: 1838–1846, <https://doi.org/10.1021/acs.accounts.7b00121>
60. Sahariah B., Sarma BK. 2019. Relative orientation of the carbonyl groups determines the nature of orbital interactions in carbonyl–carbonyl short contacts. *Chem. Sci.*, 10:909–917, [10.1039/C8SC04221G](https://doi.org/10.1039/C8SC04221G)
61. Bretscher LE., Jenkins CL., Taylor KM., DeRider ML., Raines RT., 2001. Conformational stability of collagen relies on a stereoelectronic effect. *J. Am. Chem. Soc.*, 123:777–778, <https://doi.org/10.1021/ja005542v>
62. Newberry RW., VanVeller B., Guzei IA., Raines RT., 2013. $n\rightarrow\pi^*$ Interactions of amides and thioamides: Implications for protein stability. *J. Am. Chem. Soc.*, 135:7843–7846, <https://doi.org/10.1021/ja4033583>
63. Newberry RW., Orke SJ., Raines RT., 2016. $n\rightarrow\pi^*$ Interactions are competitive with hydrogen bonds. *Org. Lett.*, 18: 3614–3617, <https://doi.org/10.1021/acs.orglett.6b01655>.

64. Wenzell NA., Ganguly HK., Pandey AK., Bhatt MR., Yap GPA., Zondlo NJ., 2019. Electronic and steric control of $n \rightarrow \pi^*$ interactions: Stabilization of the α -helix conformation without a hydrogen bond. *ChemBioChem.*, 20 : 963–967, <https://doi.org/10.1002/cbic.201800785>
65. Horng JC., Raines RT., 2006. Stereoelectronic effects on polyproline conformation. *Protein Sci.*, 15:74–83, <https://doi.org/10.1110/ps.051779806>
66. Wilhelm P., Lewandowski B., Trapp N., Wennemers H A., 2014. crystal structure of an oligoproline PPII-helix, at last. *J. Am. Chem. Soc.*, 136: 15829–15832, <https://doi.org/10.1021/ja507405j>
67. Toniolo C., 1980. Intramolecularly hydrogen-bonded peptide conformations. *CRC Crit. Rev. Biochem.*, 9:1–44, <https://doi.org/10.3109/10409238009105471>
68. Newberry RW., Raines RT., 2016. A prevalent intraresidue hydrogen bond stabilizes proteins. *Nat. Chem. Biol.*, 12: 1084–1088, <https://doi.org/10.1038/nchembio.2206>
69. Gallagher-Jones M; Glynn C; Boyer DR; Martynowycz MW; Hernandez E; Miao J; Zee CT; Novikova IV; Goldschmidt L; McFarlane HT; Helguera GF; Evans JE; Sawaya MR; Cascio D; Eisenberg DS; Gonen T; Rodriguez JA Sub-ångström cryo-EM structure of a prion protofibril reveals a polar clasp. *Nat. Struct. Mol. Biol* 2018, 25:131–134.
70. Dougherty DA., 2013. The cation– π interaction. *Acc. Chem. Res.*, 46: 885–893, <https://doi.org/10.1021/ar300265y>.
71. Ma JC., Dougherty DA., 1997. The cation– π interaction. *Chem. Rev.*, 97: 1303–1324, <https://doi.org/10.1021/cr9603744>
72. Salonen LM; Ellermann M; Diederich F Aromatic rings in chemical and biological recognition: Energetics and structures. *Angew. Chem., Int. Ed* 2011, 50, 4808–4842
73. Kumpf RA., Dougherty DA., 1993. A mechanism for ion selectivity in potassium channels: Computational studies of cation– π interactions. *Science*. 261: 1708–1710
74. Dougherty DA., 1996. Cation– π interactions in chemistry and biology: A new view of benzene, Phe, Tyr, and Trp. *Science.*, 271: 163–168, [10.1126/science.271.5246.163](https://doi.org/10.1126/science.271.5246.163)
75. Taverna SD., Li H., Ruthenburg AJ., Allis CD., Patel DJ., 2007. How chromatin-binding modules interpret histone modifications: Lessons from professional pocket pickers. *Nat. Struct. Mol. Biol.* 14: 1025–1040, <https://doi.org/10.1038/nsmb1338>
76. Gallivan JP., Dougherty DA. 1999. Cation– π interactions in structural biology. *Proc. Natl. Acad. Sci. U. S. A.*, 98: 9459–9464, <https://doi.org/10.1073/pnas.96.17.9459>

77. Crowley PB., Golovin A., 2005. Cation- π interactions in protein-protein interfaces. *Proteins*, 59: 231–239, <https://doi.org/10.1002/prot.20417>
78. Tsou LK., Tatko CD., Waters ML., 2002. Simple cation- π interaction between a phenyl ring and a protonated amine stabilizes an α -helix in water. *J. Am. Chem. Soc.*, 124: 14917–14921, <https://doi.org/10.1021/ja026721a>
79. Waters ML., 2004. Aromatic interactions in peptides: Impact on structure and function. *Biopolymers*. 76: 435–445, <https://doi.org/10.1002/bip.20144>
80. Steiner T, Koellner G., 2001. Hydrogen bonds with π -acceptors in proteins: Frequencies and role in stabilizing local 3D structures. *J. Mol. Biol.*, 305: 535–557, <https://doi.org/10.1006/jmbi.2000.4301>
81. Chen W., Enck S., Price JL., Powers DL., Powers ET., Wong CH., Dyson HJ., Kelly JW. 2013. Structural and energetic basis of carbohydrate-aromatic packing interactions in proteins. *J. Am. Chem. Soc.*, 135: 9877–9884, <https://doi.org/10.1021/ja4040472>
82. Hudson KL., Bartlett GJ., Diehl RC., Agirre J., Gallagher T., Kiessling LL., Woolfson DN. 2015. Carbohydrate-aromatic interactions in proteins. *J. Am. Chem. Soc.*, 137: 15152–15160, <https://doi.org/10.1021/jacs.5b08424>
83. Kiessling LL., 2018. Chemistry-driven glycoscience. *Bioorg. Med. Chem.*, 26: 5229–5238, <https://doi.org/10.1016/j.bmc.2018.09.024>
84. Baker EG., Williams C., Hudson KL., Bartlett GJ., Heal JW., Porter Goff KL., Sessions RB., Crump MP., Woolfson DN. 2017. Engineering protein stability with atomic precision in a monomeric miniprotein. *Nat. Chem. Biol.*, 13: 764–770, <https://doi.org/10.1038/nchembio.2380>
85. Burley SK., Petsko GA., 1985. Aromatic-aromatic interaction: A mechanism of protein structure stabilization. *Science*. 229: 23–28, [10.1126/science.3892686](https://doi.org/10.1126/science.3892686)
86. Meyer EA., Castellano RK., Diederich F. 2003. Interactions with aromatic rings in chemical and biological recognition. *Angew. Chem., Int. Ed.*, 42: 1210–1250, <https://doi.org/10.1002/anie.200390319>
87. Kannan N., Wishveshwara S., 2000. Aromatic clusters: A determinant of thermal stability of thermophilic proteins. *Protein Eng.*, 13: 753–761, <https://doi.org/10.1093/protein/13.11.753>
88. Tatko CD., Waters ML., 2002. Selective aromatic interactions in β -hairpin peptides. *J. Am. Chem. Soc.*, 124: 9372–9373. <https://doi.org/10.1021/ja0262481>

89. Butterfield SM., Patel PR., Waters ML. 2002. Contribution of aromatic interactions to α -helix stability. *J. Am. Chem. Soc.*, 124: 9751–9755, <https://doi.org/10.1021/ja026668q>
90. Frontera A., Gamez P., Mascal M., Mooibroek TJ., Reedijk J. 2011. Putting anion– π interactions into perspective. *Angew. Chem., Int. Ed.*, 50: 9564–9583, <https://doi.org/10.1002/anie.201100208>
91. Jackson MR., Beahm R., Duvvuru S., Narasimhan C., Wu J., Wang H-N., Philip VM., Hinde RJ., Howell EE. 2007. A preference for edgewise interactions between aromatic rings and carboxylate anions: The biological relevance of anion–quadrupole interactions. *J. Phys. Chem. B.*, 111: 8242–8249, <https://doi.org/10.1021/jp0661995>
92. Shi Z., Olson CA., Bell AJ Jr., Kallenbach NR., 2002. Non-classical helix-stabilizing interactions: C–H \cdots O H-bonding between Phe and Glu side chains in α -helical peptides. *Biophys. Chem.*, 101: 267–279, [https://doi.org/10.1016/S0301-4622\(02\)00171-0](https://doi.org/10.1016/S0301-4622(02)00171-0)
93. Philip V., Harris J., Adams R., Nguyen D., Spiers J., Baudry J., Howell EE., Hinde RJ., 2011. A survey of aspartate–phenylalanine and glutamate–phenylalanine interactions in the protein data bank: Searching for anion– π pairs. *Biochemistry*, 50: 2939–2950, <https://doi.org/10.1021/bi200066k>
94. Chakravarty S., Ung AR., Moore B., Shore J., Alshamrani M A., 2018. Comprehensive analysis of anion–quadrupole interactions in protein structures. *Biochemistry*, 57: 1852–1867, <https://doi.org/10.1021/acs.biochem.7b01006>
95. Lucas X., Bauzá A., Frontera A., Quiñero D A., 2016. Thorough anion– π interaction study in biomolecules: On the importance of cooperativity effects. *Chem. Sci.*, 7: 1038–1050, [10.1039/C5SC01386K](https://doi.org/10.1039/C5SC01386K)
96. Smith MS., Lawrence EEK., Billings WM., Larsen KS., Bécarr NA., Price JL., 2017. An anion– π interaction strongly stabilizes the β -sheet protein WW. *ACS Chem. Biol.*, 12: 2535–2537, <https://doi.org/10.1021/acscchembio.7b00768>
97. Valley CC., Cembran A., Perlmutter JD., Lewis AK., Labello NP., Gao J., Sachs JN. 2012. The methionine–aromatic motif plays a unique role in stabilizing protein structure. *J. Biol. Chem.*, 287: 34979–34991, <https://doi.org/10.1074/jbc.M112.374504>
98. Egli M., Sarkhel S. 2007. Lone pair–aromatic interactions: To stabilize or not to stabilize. *Acc. Chem. Res.*, 40: 197–205, <https://doi.org/10.1021/ar068174u>

99. Reid KSC., Lindley PF., Thornton JM. 1985. Sulphur–aromatic interactions in proteins. *FEBS J.*, 190: 209–213, [https://doi.org/10.1016/0014-5793\(85\)81285-0](https://doi.org/10.1016/0014-5793(85)81285-0)
100. Viguera AR., Serrano L. 1995. Side-chain interactions between sulfur-containing amino acids and phenylalanine in α -helices. *Biochemistry*, 34: 8771–8779, <https://doi.org/10.1021/bi00027a028>
101. Tatko CD; Waters ML Investigation of the nature of the methionine– π interaction in β -hairpin peptide model systems. *Protein Sci.* 2004, 13: 2515–2522, <https://doi.org/10.1110/ps.04820104>
102. Iwaoka M., 2015. Chalcogen bonds in protein architecture In *Noncovalent Forces*, Scheiner S, Ed. Springer: Cham, Switzerland, 19 : 265–290, [Google Scholar]
103. Pascoe DJ., Ling KB., Cockroft SL., 2017. The origin of chalcogen-bonding interactions. *J. Am. Chem. Soc.*, 139 : 15160–15167, <https://doi.org/10.1021/jacs.7b08511>
104. Iwaoka M., Takemoto S., Okada M., Tomoda S. 2002. Weak nonbonded S...X (X = O, N, and S) interactions in proteins. Statistical and theoretical studies. *Bull. Chem. Soc. Japan.* 75: 1611–1625, <https://doi.org/10.1246/bcsj.75.1611>
105. Kříž K., Fanfrlík J., Lepšík M. 2018. Chalcogen bonding in protein–ligand complexes: PDB survey and quantum mechanical calculations. *ChemPhysChem.*, 19 : 2540–2548, <https://doi.org/10.1002/cphc.201800409>
106. Mitchell MO. 2017. Discovering protein–ligand chalcogen bonding in the protein data bank using endocyclic sulfur-containing heterocycles as ligand search subsets. *J. Mol. Model.* 23, 287, [Google Scholar]
107. Moreno-Gonzalez I., Soto C. 2011. Misfolded protein aggregates: mechanisms, structures and potential for disease transmission. *Semin Cell Dev Biol.* 22(5) : 482–487, [10.1016/j.semcdb.2011.04.002](https://doi.org/10.1016/j.semcdb.2011.04.002)
108. Nelson R., Sawaya MR., Balbirnie M., Madsen AO., Riekel C., Grothe R., Eisenberg D. 2005. Structure of the cross-beta spine of amyloid-like fibrils. *Nature.* 435:773–778, <https://doi.org/10.1038/nature03680>
109. Caughey B., Lansbury PT. 2003. Protofibrils, pores, fibrils, and neurodegeneration: separating the responsible protein aggregates from the innocent bystanders. *Annu Rev Neurosci.* 31:267–298, <https://doi.org/10.1146/annurev.neuro.26.010302.081142>

110. Glabe CG. 2006. Common mechanisms of amyloid oligomer pathogenesis in degenerative disease. *Neurobiol Aging.*, 27:570–575, <https://doi.org/10.1016/j.neurobiolaging.2005.04.017>
111. Walsh DM., Selkoe DJ. 2007. A beta oligomers - a decade of discovery. *J Neurochem.*, 101:1172–84, <https://doi.org/10.1111/j.1471-4159.2006.04426.x>
112. Demuro A., Mina E., Kaye R., Milton SC., Parker I., Glabe CG. 2005. Calcium dysregulation and membrane disruption as a ubiquitous neurotoxic mechanism of soluble amyloid oligomers. *J Biol Chem.* 280 (17) :17294–17300, <https://doi.org/10.1074/jbc.M500997200>
113. Bucciantini M., Calloni G., Chiti F., Formigli L., Nosi D., Dobson CM., Stefani M. 2004. Prefibrillar amyloid protein aggregates share common features of cytotoxicity. *J Biol Chem.*, 279 : 31374–31382, <https://doi.org/10.1074/jbc.M400348200>
114. Simoneau S., Rezaei H., Sales N., Kaiser-Schulz G., Lefebvre-Roque M., Vidal C., Fournier JG., 2007. In vitro and in vivo neurotoxicity of prion protein oligomers. *PLoS Pathog.*, 3: e125, <https://doi.org/10.1371/journal.ppat.0030125>
115. Wang HW., Pasternak JF., Kuo H., Ristic H., Lambert MP., Chromy B., Viola KL, 2002. Soluble oligomers of beta amyloid (1–42) inhibit long-term potentiation but not long-term depression in rat dentate gyrus. *Brain Res.*, 924:133–140, [https://doi.org/10.1016/S0006-8993\(01\)03058-X](https://doi.org/10.1016/S0006-8993(01)03058-X)
116. Cleary JP., Walsh DM., Hofmeister JJ., Shankar GM., Kuskowski MA., Selkoe DJ., Ashe KH. 2004. Natural oligomers of the amyloid-beta protein specifically disrupt cognitive function. *Nat Neurosci.*, 8(1) : 79–84, <https://doi.org/10.1038/nm1372>
117. Shankar GM., Li S., Mehta TH., Garcia-Munoz A., Shepardson NE., Smith I., Brett FM., 2008. Amyloid-beta protein dimers isolated directly from Alzheimer's brains impair synaptic plasticity and memory. *Nat Med.*, 14:837–842, <https://doi.org/10.1038/nm1782>
118. Walsh DM., Hartley DM., Kusumoto Y., Fezoui Y., Condron MM., Lomakin A., 1999. Amyloid beta-protein fibrillogenesis. Structure and biological activity of protofibrillar intermediates. *J Biol Chem.*, 274: 25945–25952, <https://doi.org/10.1074/jbc.274.36.25945>

119. Harper JD., Wong SS., Lieber CM., Lansbury PT. 1999. Jr Assembly of A beta amyloid protofibrils: an in vitro model for a possible early event in Alzheimer's disease. *Biochem.*,38 : 8972–80, <https://doi.org/10.1021/bi9904149>
120. Srinivasan R., Marchant RE., Zagorski MG. 2004. ABri peptide associated with familial British dementia forms annular and ring-like protofibrillar structures. *Amyloid*. 11:10–3, <https://doi.org/10.1080/13506120410001667872>
121. Lashuel HA., Hartley D., Petre BM., Walz T., Lansbury PT. 2002. Jr Neurodegenerative disease: amyloid pores from pathogenic mutations. *Nature*. 418 (6895) : 291, <https://doi.org/10.1038/418291a>
122. Hartley DM., Walsh DM., Ye CP., Diehl T., Vasquez S., Vassilev PM., 1999. Protofibrillar intermediates of amyloid beta-protein induce acute electrophysiological changes and progressive neurotoxicity in cortical neurons. *J Neurosci.*,19: 8876–8884, <https://doi.org/10.1523/JNEUROSCI.19-20-08876.1999>
123. Nelson R., Sawaya MR., Balbirnie M., Madsen AO., Riekel C., Grothe R., Eisenberg D. 2005. Structure of the cross-beta spine of amyloid-like fibrils. *Nature*, 435: 773–778, <https://doi.org/10.1038/nature03680>
124. Sipe J.D., Cohen A.S., 2000. Review: History of the Amyloid Fibril. *J Struct Biol.*, 130 : 88 –98, <https://doi.org/10.1006/jsbi.2000.4221>
125. Sunde M., Blake C. 1997. The Structure of Amyloid Fibrils by Electron Microscopy and X-Ray Diffraction, in: *Adv Prot Chem Elsevier*, pp. 123–159. [https://doi.org/10.1016/S0065-3233\(08\)60320-4](https://doi.org/10.1016/S0065-3233(08)60320-4)
126. Chaturvedi S.K., Siddiqi M.K., Alam P., Khan R.H., 2016. Protein misfolding and aggregation: Mechanism, factors and detection. *Process Biochem.*, 51: 1183–1192, <https://doi.org/10.1016/j.procbio.2016.05.015>
127. Darrington R.T., Anderson B.D., 1995. Evidence for a common intermediate in insulin deamidation and covalent dimer formation: effects of pH and aniline trapping in dilute acidic solutions. *J Pharm Sci.*, 84: 275–282, <https://doi.org/10.1002/jps.2600840303>
128. Sluzky V., Klibanov A.M., Langer R. 1992. Mechanism of insulin aggregation and stabilization in agitated aqueous solutions. *Biotechnol Bioeng.*, 40 : 895–903, <https://doi.org/10.1002/bit.260400805>
129. Sluzky V., Tamada J.A., Klibanov A.M., Langer, R., 1991. Kinetics of insulin aggregation in aqueous solutions upon agitation in the presence of hydrophobic

- surfaces. *Proc Natl Acad Sci USA*, 88: 9377–9381, <https://doi.org/10.1073/pnas.88.21.9377>
130. Zwanzig R, Szabo A, Bagchi B. 1992. Levinthal's paradox. *Proc Natl Acad Sci U S A*. 89(1) : 20-22, [10.1073/pnas.89.1.20](https://doi.org/10.1073/pnas.89.1.20)
 131. Ferreiro DU., Komives EA., Wolynes PG. 2014. Frustration in biomolecules. *Q Rev Biophys.*, 47: 285-363, <http://dx.doi.org/10.1017/S0033583514000092>
 132. Jahn TR., Radford SE. 2008. Folding vs. aggregation: Polypeptide conformations on competing pathways. *Arch Biochem Biophys.*, 469 : 100-17, <http://dx.doi.org/10.1016/j.abb.2007.05.015>
 133. Khammari, A., Arab, S.S., Ejtehadi, M.R. 2020. The hot sites of α -synuclein in amyloid fibril formation. *Sci Rep.*, 10:12175, <https://doi.org/10.1038/s41598-020-68887-2>
 134. Wetzel R. 2006. Kinetics and thermodynamics of amyloid fibril assembly. *Acc Chem Res.*, 39:671-679, <https://doi.org/10.1021/ar050069h>
 135. Ricchiuto P., Brukhno AV., Auer S. 2012. Protein aggregation: Kinetics versus thermodynamics. *J Phys Chem B*, 116:5384-5390, <https://doi.org/10.1021/jp302797c>
 136. Pellarin R., Schuetz P., Guarnera E., Caflisch A. 2010. Amyloid fibril polymorphism is under kinetic control. *J Am Chem Soc.*, 132:14960-14970, <https://doi.org/10.1021/ja106044u>
 137. Arosio P., Vendruscolo M., Dobson CM., Knowles TP. 2014. Chemical kinetics for drug discovery to combat protein aggregation diseases. *Trends Pharmacol Sci.*, 35:127-135, <https://doi.org/10.1016/j.tips.2013.12.00>
 138. Baldwin AJ., Knowles TP., Tartaglia GG., Fitzpatrick AW., Devlin GL., Shammass SL., Waudby CA., Mossuto MF., Meehan S., Gras SL., 2011. Metastability of native proteins and the phenomenon of amyloid formation. *J Am Chem Soc.*, 133:14160-14163, <https://doi.org/10.1021/ja2017703>
 139. Johnson SM., Wiseman RL., Sekijima Y., Green NS., Adamski-Werner S., Kelly JW. 2005. Native state kinetic stabilization as a strategy to ameliorate protein misfolding diseases: A focus on the transthyretin amyloidoses. *Acc Chem Res.*, 38:911-921, <https://doi.org/10.1021/ar020073i>

140. Zheng W., Schafer NP., Wolynes PG. 2013. Frustration in the energy landscapes of multidomain protein misfolding. *Proc Natl Acad Sci USA*. 110:1680-1685, <http://dx.doi.org/10.1073/pnas.1222130110>
141. Zheng W., Schafer NP., Wolynes PG. 2013. Free energy landscapes for initiation and branching of protein aggregation. *Proc Natl Acad Sci USA*, 110:20515-20520, <https://doi.org/10.1073/pnas.1320483111>
142. Baftizadeh F., Biarnes X., Pietrucci F., Affinito F., Laio A. 2012. Multidimensional view of amyloid fibril nucleation in atomistic detail. *J Am Chem Soc.*, 134:3886-3894, <https://doi.org/10.1021/ja210826a>
143. Buell AK., Dhulesia A., White DA., Knowles TP., Dobson CM., Welland ME. 2012. Detailed analysis of the energy barriers for amyloid fibril growth. *Angew Chem Int Ed.*, 51:5247-5251, <https://doi.org/10.1002/anie.201108040>
144. Bence N.F., Sampat R.M., Kopito R.R., 2001. Impairment of the ubiquitin-proteasome system by protein aggregation. *Science*, 292: 1552–1555, <https://doi.org/10.1126/science.292.5521.1552>
145. Reynaud E. 2010. Protein Misfolding and Degenerative Diseases. *Nat. Educ.*, 3(9):28, <https://www.researchgate.net/publication/284631720>
146. Bayer TA. 2015. Proteinopathies, a core concept for understanding and ultimately treating degenerative disorders? *Eur Neuropsychopharmacol.*, 25(5):713-724, [10.1016/j.euroneuro.2013.03.007](https://doi.org/10.1016/j.euroneuro.2013.03.007).
147. Jucker M., Walker L.C., 2013. Self-propagation of pathogenic protein aggregates in neurodegenerative diseases. *Nature*. 501:45–51, <https://doi.org/10.1038/nature12481>
148. Wang W. 2005. Protein aggregation and its inhibition in biopharmaceutics. *Int J Pharm.*, 289:1-30, <https://doi.org/10.1016/j.ijpharm.2004.11.014>
149. Roberts CJ. 2014. Protein aggregation and its impact on product quality. *Curr. Opin. Biotechnol.*, 30: 211-217, <http://dx.doi.org/10.1016/j.copbio.2014.08.001>
150. Ratanji KD., Derrick JP., Dearman RJ., Kimber I., 2013, Immunogenicity of therapeutic proteins: Influence of aggregation. *J. Immunotoxicol.* 11(2):99-109, <https://doi.org/10.3109/1547691X.2013.821564>
151. Smejkal B., Agrawal N.J., Helk B., Schulz H., Giffard M., Mechelke M., Ortner F., Heckmeier P., Trout B.L., Hekmat D. 2013. Fast and scalable purification of a therapeutic full-length antibody based on process crystallization. *Biotechnol Bioeng.*, 110: 2452-2461,

152. Mason B.D., Zhang-van Enk J., Zhang L., Remmele R.L., Zhang J. 2010. Liquid–liquid phase separation of a monoclonal antibody and nonmonotonic influence of Hofmeister anions. *Biophys J.*, 99: 3792-3800.
153. Johnston K.P., Maynard J.A., Truskett T.M., Borwankar A.U., Miller M.A., Wilson B.K., Dinin A.K., Khan T.A., Kaczorowski K.J. 2012. Concentrated dispersions of equilibrium protein nanoclusters that reversibly dissociate into active monomers. *ACS Nano.*, 6: 1357-1369.
154. Schmit J.D., He F., Mishra S., Ketchum R.R., Woods C.E., Kerwin B.A. 2014. Entanglement model of antibody viscosity. *J Phys Chem B.*, 118: 5044-5049.
155. Dimitrov DS. 2012. Therapeutic proteins. *Methods Mol Biol.*, 899:1-26, [10.1007/978-1-61779-921-1_1](https://doi.org/10.1007/978-1-61779-921-1_1)
156. Zhong X., Wright JF. 2013. Biological Insights into Therapeutic Protein Modifications throughout Trafficking and Their Biopharmaceutical Applications. *Int. J. Cell Biol.*, 2013:273086, <https://doi.org/10.1155/2013/273086>
157. Gupta V., Sengupta M., Prakash J., Tripathy BC. 2016. Production of Recombinant Pharmaceutical Proteins. Basic and Applied Aspects of Biotechnology. 23:77–101, [10.1007/978-981-10-0875-7_4](https://doi.org/10.1007/978-981-10-0875-7_4)
158. Dingman R, Balu-Iyer SV. 2019. Immunogenicity of Protein Pharmaceuticals. *J Pharm Sci.*, 108(5):1637-1654, [10.1016/j.xphs.2018.12.014](https://doi.org/10.1016/j.xphs.2018.12.014)
159. Leader B., Baca Q.J., Golan D.E. 2008. Protein therapeutics: a summary and pharmacological classification. *Nat. Rev. Drug Dis.*, 7(1):21–39, <https://doi.org/10.1038/nrd2399>
160. Petersen MC., Shulman GI. 2018. Mechanisms of Insulin Action and Insulin Resistance. *Physiol Rev.*, 98(4):2133-2223, [10.1152/physrev.00063.2017](https://doi.org/10.1152/physrev.00063.2017)
161. Krause M, De Vito G. 2023. Type 1 and Type 2 Diabetes Mellitus: Commonalities, Differences and the Importance of Exercise and Nutrition. *Nutrients.* 15(19):4279, [10.3390/nu15194279](https://doi.org/10.3390/nu15194279)
162. van Belle TL., Coppieters KT., von Herrath MG. 2011. Type 1 diabetes: etiology, immunology, and therapeutic strategies. *Physiol Rev.*, 91(1):79-118, [10.1152/physrev.00003.2010](https://doi.org/10.1152/physrev.00003.2010)
163. DiMeglio LA., Evans-Molina C., Oram RA. 2018. Type 1 diabetes. *Lancet.*, 391(10138):2449-2462, [10.1016/S0140-6736\(18\)31320-5](https://doi.org/10.1016/S0140-6736(18)31320-5).
164. Donner T., Muñoz M. 2012. Update on insulin therapy for type 2 diabetes. *J Clin Endocrinol Metab.*, 97(5):1405-13, [10.1210/jc.2011-2202](https://doi.org/10.1210/jc.2011-2202)

165. Howard-Thompson A., Khan M., Jones M., George CM. 2018. Type 2 Diabetes Mellitus: Outpatient Insulin Management. *Am Fam Physician.*,97(1):29-37, PMID: [29365240](#)
166. Anik A., Çatlı G., Abacı A., Böber E. 2015. Maturity-onset diabetes of the young (MODY): an update. *J Pediatr Endocrinol Metab.*, 28(3-4):251-63, [10.1515/jpem-2014-0384](#).
167. Patti AM., Giglio RV., Pafili K., Rizzo M., Papanas N. 2018. Pharmacotherapy for gestational diabetes. *Expert Opin Pharmacother.*, (13):1407-1414, [10.1080/14656566.2018.1509955](#)
168. Ode KL., Chan CL., Granados A., Moheet A., Moran A., Brennan AL., 2019. Cystic fibrosis related diabetes: Medical management. *J Cyst Fibros.*, 18(2):S10-S18, <https://doi.org/10.1016/j.jcf.2019.08.003>
169. McLaren GD., Gordeuk VR. 2009. Hereditary hemochromatosis: insights from the Hemochromatosis and Iron Overload Screening (HEIRS) Study. *Hematology Am Soc Hematol Educ Program.* 2009(1):195-206. [10.1182/asheducation-2009.1.195](#).
170. Rosenfeld L. 2002. Insulin: discovery and controversy. *Clin Chem.*, 48:2270–2288, <https://doi.org/10.1093/clinchem/48.12.2270>
171. Baeshen NA., Baeshen MN., Sheikh A., Bora RS., Ahmed MM., Ramadan HA., Saini KS., Redwan EM. 2014. Cell factories for insulin production. *Microb Cell Fact.*,13:141, [10.1186/s12934-014-0141-0](#).
172. Banting F. G., Best C. H., Collip J. B., Campbell W. R., Fletcher A. A., MacLeod J. J. R., Noble E. C. 1922. The effect produced on diabetes by extracts of pancreas. *Trans. Assoc. Am. Physicians* 37: 337–347, [[Google Scholar](#)]
173. Abel J. J. 1926. Crystalline insulin. *Proc. Natl. Acad. Sci. U.S.A.* 12: 132–136, [10.1073/pnas.12.2.132](#)
174. Sjögren B., Svedberg T. 1931. The molecular weight of insulin. *J. Am. Chem. Soc.* 53: 2657–2661, [10.1021/ja01358a029](#)
175. Sanger F. 1949. Fractionation of oxidized insulin. *Biochem. J.* 44: 126–128, [10.1042/bj0440126](#)
176. Sanger F., Tuppy H. 1951a . The amino-acid sequence in the phenylalanyl chain of insulin. 1. The identification of lower peptides from partial hydrolysates. *Biochem. J.* 49:463–481, [10.1042/bj0490481](#)

177. Sanger F., Tuppy H. (1951b). The amino-acid sequence in the phenylalanyl chain of insulin. 2. The investigation of peptides from enzymic hydrolysates. *Biochem. J.* 49: 481–490, [10.1042/bj0490481](https://doi.org/10.1042/bj0490481)
178. Smith GD., Pangborn WA., Blessing RH. 2003. The structure of T6 human insulin at 1.0Å resolution. *Acta Crystallogr D Biol Crystallogr.* 59(3):474–482, <https://doi.org/10.1107/S0907444902023685>
179. Bell G.I., Pictet R.L., Rutter W.J., Cordell B., Tischler E., Goodman, H.M. 1980. Sequence of the human insulin gene. *Nature*, 284:26-32. [10.1038/284026a0](https://doi.org/10.1038/284026a0)
180. Weiss M, Steiner DF, Philipson LH. Insulin Biosynthesis, Secretion, Structure, and Structure-Activity Relationships. 2014. In: Feingold KR, Anawalt B, Blackman MR, et al., <https://www.ncbi.nlm.nih.gov/books/NBK279029/>
181. Johnson IS. 1983. Human insulin from recombinant DNA technology. *Science*. 219(4585):632–637, [10.1126/science.6337396](https://doi.org/10.1126/science.6337396)
182. Crommelin DJ A., Sindelar RD, Meibohm B. 2008. *Pharmaceutical Biotechnology*; 3rd ed. New York: Informa Healthcare. <https://doi.org/10.3109/9780203508831>
183. Das A., Shah, M., Saraogi, I., 2022. Molecular aspects of insulin aggregation and various therapeutic interventions. *ACS bio & med Chem Au*, 2(3):205-221, <https://doi.org/10.1021/acsbiomedchemau.1c00054>
184. Jeffrey PD. 1982. The Interaction of Insulin with Its Receptor: Cross-Linking via Insulin Association as the Source of Receptor Clustering. *Diabetologia*, 23(5): 381– 385, *ISSN:0012-186X*.
185. Ivanova MI., Sievers SA., Sawaya MR., Wall JS., Eisenberg D. 2009. Molecular basis for insulin fibril assembly. *Proceedings of the National Academy of Sciences*, 106(45) :18990-18995.

OBJECTIVES & SCOPES

2.1 . ANALYSIS OF THE RESEARCH PROBLEM

Conformational changes of the native amyloidogenic therapeutic proteins leading to aggregation followed by deposition are detrimental to human system. When these natively folded proteins are converted into nonnative cross- β -sheet rich fibrous structures under different interacting or solvent conditions, their functional properties are lost forever. This process is called protein fibrillation or, more commonly, amyloid like aggregation. Neurodegenerative diseases and amyloidosis are closely related as the fibrils are the causative agents of many misfolding-based diseases such as Alzheimer's disease (ad), Parkinson's disease (pd), Huntington's diseases, Spongiform encephalopathy, Type 2 diabetes mellitus (type 2 DM) etc. Insulin, a therapeutic protein may undergo aggregation under stressful conditions and thus become misfolded and loses its functional ability by provoking the unwanted immune responses. Literature evidences indicates fatal consequences of the insulin amyloid formation in diabetic patients taking insulin .This is of great concern, as the number of people suffering from this disease is immense. In 2000, 171 million people were estimated to be suffering from diabetes and the number is expected to increase to 300 million in 2030. More than 20 neurodegenerative diseases have been found to owe their etiology to amyloid aggregation of proteins. Use of small molecules is considered an affordable method to counteract this aggregation process and stabilize insulin.

In vivo, human insulin is stored as a Zn-coordinated hexamer in β -cells of the pancreatic islets. In the active form of Insulin structure, there are two chains A and B chains. Both of

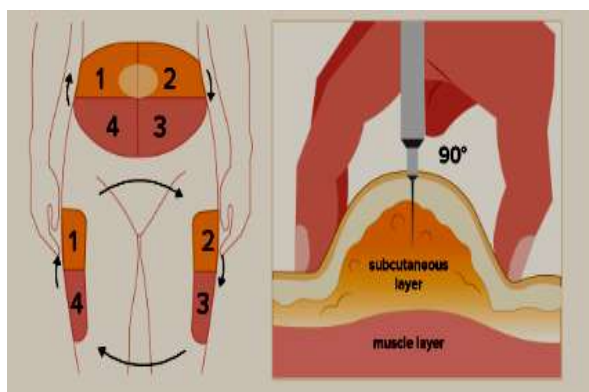


Fig.2.1 The method of subcutaneous delivery of insulin

which are covalently bonded through three disulfide linkages, among which two are inter-chain disulfide bonds, A7–B7 and A20–B19, covalently binding the two chains together, and the third one is an intra-chain disulfide bond within chain A, A6–A1.

At highly acidic pH, insulin assembles into oligomeric intermediates of non-native β -sheet rich structure and other secondary intermediates prior to fibril formation. Diabetic patients taking regular intravenous and subcutaneous insulin injections (Fig.19) are more prone to pathogenic insulin deposition due to high local concentration at the site of injection. Such patients are susceptible to have insulin fibril deposits in various body parts such as shoulders, arms (Fig. 20), thighs and abdominal walls at or around the site of injections. Insulin aggregates are present in the circulation of diabetic patients, treated with the, showing reduced biological activity, and increased immunogenicity. Besides, it is also a threat for pharmaceutical and clinical formulations. It is thus important to understand the mechanism of insulin aggregation and the ways that can potentially destabilize the preformed fibrils and/or prevent its formation. Amyloidogenesis is a major concern during insulin manufacture and storage too, as insulin in the amyloid form is not bio-available, and any degree of amyloid formation leads to reduced efficacy of insulin administration.

The amyloid inhibitors should be specific enough to avoid interfering with the normal processes under physiological conditions. One of the possible ways to achieve this criterion is to identify the inhibitors from natural products, which are consumed by us. The principle was taken in this work. The naturally occurring micronutrients, vitamins and sulfur containing amino acids were included in this research. Beside this solvent effect on inhibition of insulin fibrillation had also considered.

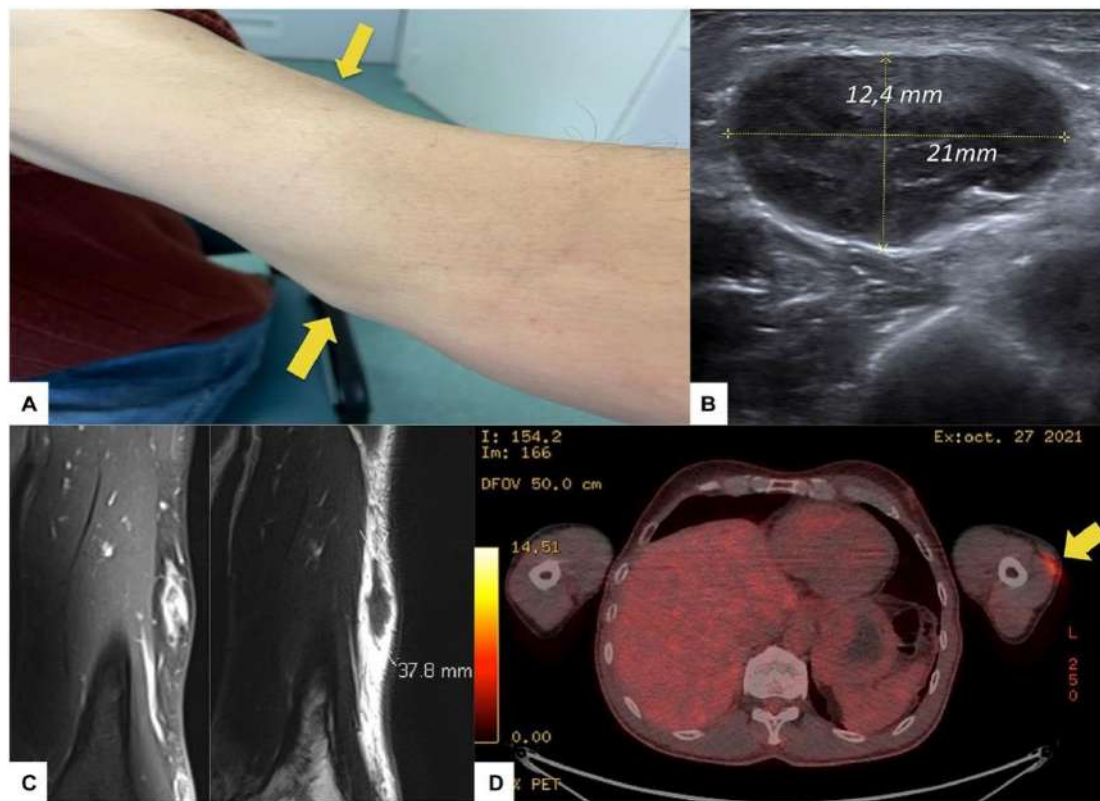


Fig. 2.2 *Clinical and paraclinical features of the patient under insulin therapy showing amyloid deposition (A) Two subcutaneous nodules on the left arm (arrows), (B) Ultrasound of the soft tissue of the left arm depicting one subcutaneous mass, (C) left upper limb MRI frontal slices of the (T1 with gadolinium injection on the left, and T2 on the right), and (D) 18-FDG-PET-CT scan of the left arm nodule considering a 18-FDG uptake (arrow) *Fig adapted from Dubernet A. et. al, 2023, Front. Med., <https://doi.org/10.3389/fmed.2023.1064832>*

2.2. SUMMARIZED OBJECTIVES

From the brief analysis of research problem, the major objectives can be summarized as follows. Protecting the native form of human Insulin by small biological molecules in vitro and thus inhibiting amyloid structure generation at the site of repeated injection is a necessary therapeutic strategy for diabetic type II patients.

- 1) During storage of human insulin, such kind of aggregation was also reported in literature. This problem should have to be addressed.
- 2) Various studies indicated the amyloid inhibitory property in a number of small molecules, antioxidants, synthetic peptides etc but biological molecules like micronutrients; vitamins etc can also be selected in this regard due to their negligible toxicities.
- 3) Standardization of the concentration of interacting residues is of significant importance as in high concentration of interacting molecules, the chances of toxicity will have to be considered. So it is required to be customized in such a way that they can be effective at very low interaction ratio with human insulin and thus can minimize the side effects and possible immunogenic development of body.
- 4) The study of co-solvent effects on human insulin can be very useful to compose solvents and physical standards for both short and long term storage of human insulin for clinical or laboratory purposes.

2.3. SCOPES OF THIS STUDY ACCORDING TO THE OBJECTIVES

- Optimization of physical parameters like pH, temperature, duration of thermal exposure to get the most aggregated form of protein i.e., insulin amyloid in vitro.
- Interrupting the process of in vitro fibrillation of human Insulin employing small interacting charged molecules like micronutrients.
- Employing water soluble B-complex vitamins to inhibit the process of fibrillation
- Investigation of the effect of fluorinated co-solvents during in-vitro insulin fibrillation
- Effect of sulfur containing amino acids on insulin fibrillation in-vitro

MATERIALS AND DETAILED METHODOLOGIES APPLIED THROUGHOUT THE STUDIES

3.1 Reagents, Chemicals and Fine Equipments used

Reagents and chemicals used for the studies narrated in the Thesis work were procured as follows

Table 3.1 The directory of chemicals and reagents and equipments

I T E M S	OBTAINED FROM
Human insulin (Huminsulin R)100 IU/ml (r-DNA origin)	Eli Lilly and Company India Pvt. Ltd.
HPLC grade 100% Pure Distilled Water, Acrylamide, N,N'-Methylenebisacrylamide,	Sigma-Aldrich
N,N,N,N tetramethylethylenediamine (TEMED), ammonium per sulphate(APS), bromophenol blue, Coomassie brilliant blue	Sigma-Aldrich
Methanol & Fluorescent probes, viz., 8-Anilinoanthralene-1-sulfonic acid (ANS), Thioflavin T (Th T)	Sigma Chemical Co. (St. Louis, USA)
Glycine, KOH, Acetone	Merck (Mumbai, India)
2, 2, 2-Trifluoroethanol (TFE)	Spectrochem Pvt. Ltd. (India).
1,1,1,3,3,3-Hexafluoroisopropanol (HFIP)	Sigma-Aldrich
Iron(III) chloride hexahydrate (FeCl ₃), Copper(II) chloride(CuCl ₂), HCl, NaOH	Sigma-Aldrich
Thiamine hydrochloride(Vitamin B ₁), Pyridoxine-HCl (Vitamin B ₆), Cyanocobalamin(Vitamin B ₁₂)	Sigma-Aldrich

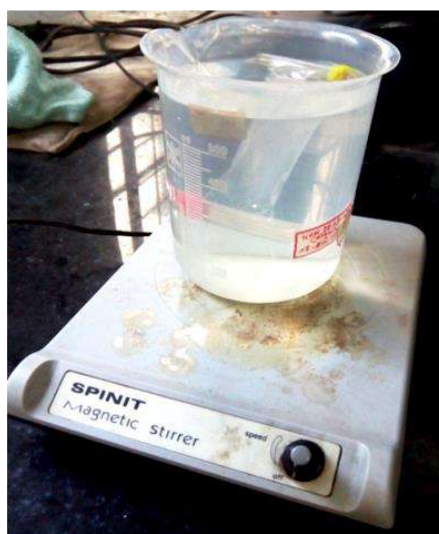
L-Cysteine ($C_3H_7NO_2S$)	Sigma-Aldrich
L-Methionine($C_5H_{11}NO_2S$)	Sigma-Aldrich
Copper grids (mesh size-300) for TEM	Sigma-Aldrich
Quartz cuvettes and Hellma absorption cuvettes	Sigma-Aldrich
Uranyl acetate	Sigma, Steinheim Germany
Glass plates for AFM	Merck (Mumbai, India)
Magnetic beads, Membrane dialysis tubing	Sigma-Aldrich

All the chemicals and reagents stated in the table 3.1 were of analytical grade and used without further purification. Human insulin was dialyzed and processed before use.

PREPARATION OF MONOMERIC INSULIN AND SAMPLE SOLUTIONS

3.2. Dialysis and preparation of insulin monomer

The insulin (Huminsulin R) 100 IU/ml purchased from pharmacies are in the hexameric state



[1] and there present 16mg glycerine/ml as tonicity modifier, 2.5 mg meta-cresol/ml as preservative and HCl/NaOH for pH adjustment purpose in it. In order to remove these compounds, dialysis was done against water (Fig. 3.1, left panel). The concentration of this dialyzed native insulin

of pH 5.0 was calculated using the molar extinction coefficient $5734 \text{ cm}^{-1}\text{M}^{-1}$ [2].

Fig. 3.1 The dialysis of hexameric insulin against water [left] and the Millex –G Millipore syringe filter of pore size 0.22mm [right]

The dialyzed protein was diluted with 80% glacial acetic acid to get a final concentration of 20% acetic acid in solution [3, 4]. The concentration of insulin was maintained at 1.5mg/ml (258.3 μ M). The resulting clear solution was filtered through 0.22 mm pore sized

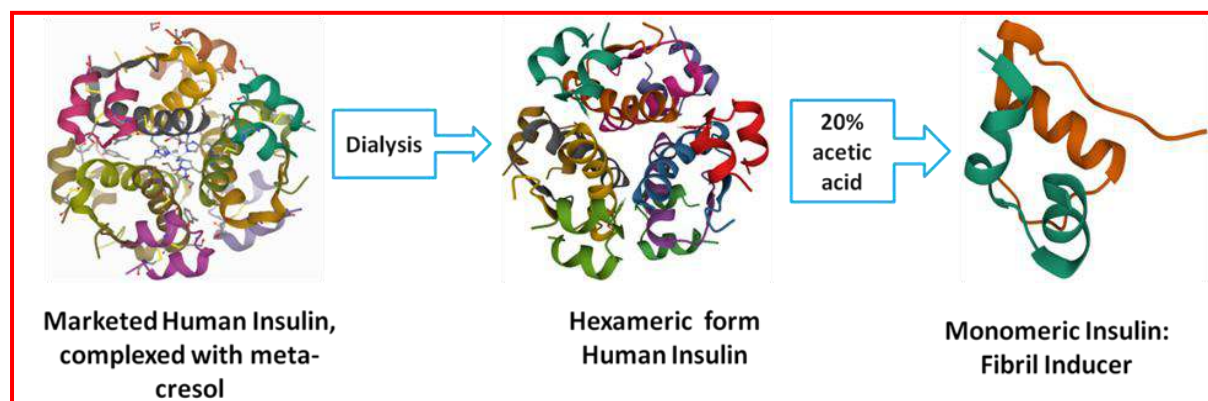


Fig. 3.2. Schematic representation of insulin monomer formation from marketed hexamer

Millipore filter membrane placed in a Millex-G filter (Fig. 3.1, right panel). In order to get homogeneous solution of monomeric insulin, the filtrate was maintained at 37°C overnight [3]. This solution was considered as stock insulin monomer having pH 1.6.

3.3. Interaction of insulin with micronutrients

Stock solution of chloride salts of important cationic micronutrients, viz., CuCl_2 , FeCl_3 were prepared in HPLC water while keeping concentration at 50mM freshly each time before use. From the stock, aliquots were taken and added with insulin keeping insulin concentration 1.16mg/ml (200 μ M) in final solution. While the interacting ratio of insulin and metal ion were 1:0.5, 1:1, 1:3, 1:5, 1:10, 1:15, 1:30 respectively in the said final solution prepared in separate sets for each of the metal ions.

3.4. Interaction of insulin with vitamins

Vitamin B₁, B₆ and B₁₂ stock solutions were prepared separately in HPLC water to get 10mM of concentration of each. At the time of interaction with insulin monomer, each of the vitamin solutions was added to obtain the ratio of Insulin: Vitamin as 1:0.5, 1:3, and 1:5 respectively. In each case, insulin concentration was kept 1.16mg/ml (200 μ M) in solution. Volume of the solutions had adjusted with HPLC water.

3.5. Interaction of insulin with fluorinated co-solvents Stock solutions for both HFIP (1, 1, 1, 3, 3, 3-Hexafluoro-2-propanol, $C_3H_2F_6O$) and TFE (2, 2, 2-Trifluoroethanol, $C_2H_3F_3O$) were prepared as 60% (v/v) with HPLC water. Each of the two co-solvents was added at 2%, 5%, 10%, 15% and 20% concentrations separately to make the final solution with fixed Insulin concentration of 1.16mg/ml (200 μ M).

3.6. Interaction of insulin with sulfur containing amino acids

The stock solutions of the two sulfur containing amino acids, L-Cysteine and L-Methionine each were prepared in HPLC water at a concentration of 20mM. From the freshly prepared stock, aliquots were taken and added with insulin keeping insulin concentration 1.16 mg/ml (200 μ M) in final solution. While the interacting ratio of insulin and each amino acid were 1:0.5, 1:3, 1:6, 1:12, 1:24 respectively. Separate sets were prepared for each of the two amino acids with their respective control set-up.

PREPARATION OF INSULIN AGGREGATES

3.7 Aggregation inhibition studies: thermal aggregation of insulin in presence and absence of modulators

Insulin fibrillates favorably from its monomer state when the pH is acidic [5-7]. Insulin monomer was diluted using 1(N) HCl to get final concentration of 1.16mg/ml (200 μ M). This is heat treated at 60-70°C for minimum 4 h [8-9] and was considered as heat treated (HT) insulin in all the forthcoming assays. In order to avoid premature aggregation, the optimum conditions were maintained throughout [10]. To study the effect of modulators on insulin aggregation, similar conditions of aggregation were followed for insulin with metal ions, vitamins and co-solvents separately. The solutions were prepared before aggregation as stated in paragraph 3.3, 3.4 and 3.5 respectively and were subjected to the aggregation conditions.

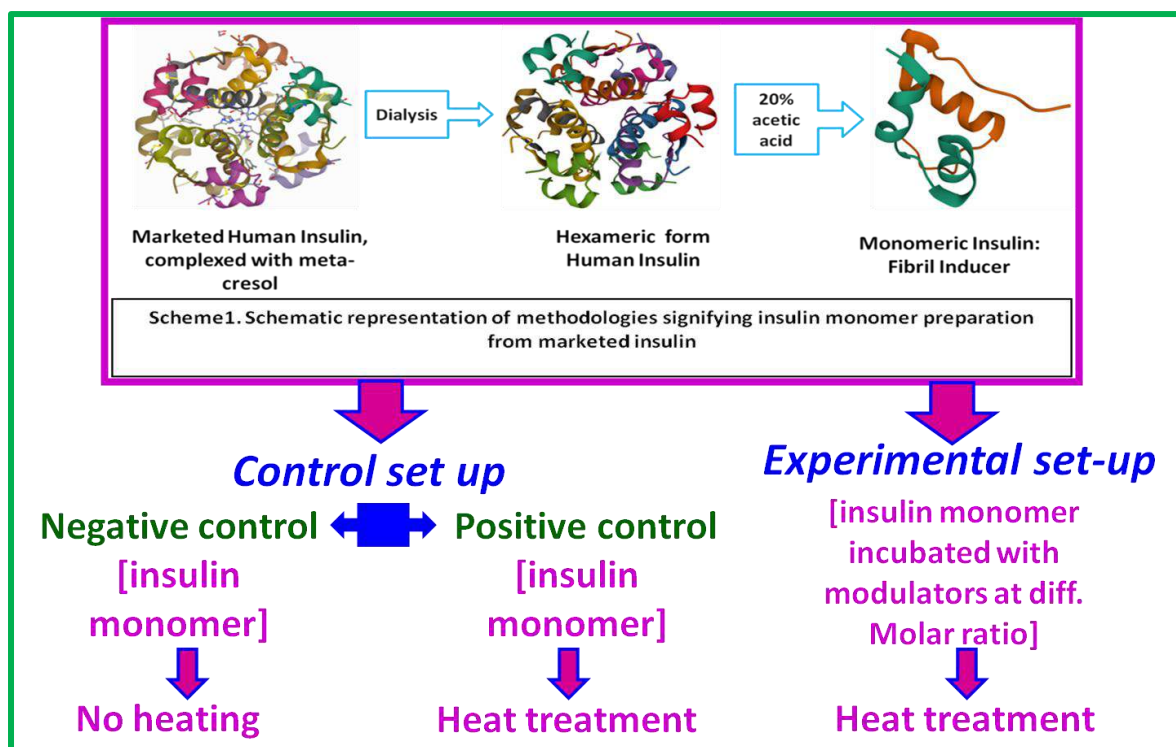


Fig. 3.3. Schematic representation of general methodologies followed to study effect of metal ions, vitamins, amino acids and co-solvents on insulin aggregation

ELECTROPHORESIS STUDIES

3.8. Native Polyacrylamide Gel Electrophoresis (Native-PAGE) of Insulin Monomer and Aggregates

Insulin possesses low molecular weight and inter-chain as well as intra-chain disulfide bonds in its structure and that's why the native-PAGE [11] was done for tracing insulin monomer under non-denaturing conditions. There was no use of SDS in preparation of gel, tray running buffer and sample loading buffer. 18% Polyacrylamide gel electrophoresis (Native-PAGE) was done to check the homogeneity of the purified monomeric insulin. It was performed according to the standard protocol [12]. The monomeric insulin and heat treated insulin each at a concentration of 1.16mg/ml (200 μ M) were loaded onto the wells after getting mixed with sample loading buffer. Electrophoresis was done applying an initial voltage of 50 volts to maximum voltage of 100 volts for 1.5 h. The gel was stained with Coomassie Brilliant Blue R-250 without any SDS and de-staining was done using the solution containing methanol and acetic acid.

3.9. Composition of solutions of native-PAGE

(A) Preparation of 18% resolving gel

Table 3.2 Composition of 7.5ml of 18% resolving gel

<u>Reagents</u>	<u>Volume</u>
30% acryl amide	4.5 ml
1.5(M) Tris-Cl, pH 8.8	2.34 ml
10% APS	75 µl
TEMED	5 µl
Water	0.58 ml

(B) Preparation of 5% stacking gel

Table 3.2 Composition of 2 ml of 5% stacking gel

<u>Reagents</u>	<u>Volume</u>
30% acryl amide	0.33 ml
1(M) Tris-Cl, pH6.8	0.25 ml
10% APS	20 µl
TEMED	2 µl
Water	1.4 ml

(C) Preparation of stock Running Buffer for native-PAGE

Table 3.3 Composition of 10X Running Buffer for native-PAGE (pH~ 8.3)

<u>Component</u>	<u>Amount</u>	<u>Concentration</u>
<u>Tris base</u> (mw: 121.14 g/mol)	30.3 g	0.2501 M
<u>Glycine</u> (mw: 75.07 g/mol)	144.4 g	1.924 M

Distill water was added to make up the volume of running buffer. This stock Running buffer was ten times diluted with cold distilled water to use as tray buffer in native-PAGE.

FLUORIMETRIC STUDIES

3.10. Intrinsic fluorescence emission study

The effect of metal ions, vitamins and fluorinated co-solvents on insulin aggregation was considered in separate set-ups. Each time under the same experimental condition as stated in paragraph 3.6, the heat-treated insulin in absence of any modulator i.e., (HT) was kept as positive control. The samples of all the set-ups were diluted with HPLC water to get 2 ml of total volume each having insulin concentration of 5.5 μ M. The fluorescence measurements had been done with a Horiba scientific Spectrofluorometer (Model: FLUOROMAX-4C, Serial no. 1734D-4018-FM). Excitation had done at 276 nm and emission recorded at 305 nm. 1 cm path-length rectangular quartz cuvette was used. Excitation and emission, both the slits were kept at 3 nm and each spectrum was an average of three scans having a scan rate of 100 nm s⁻¹.

3.11. Thioflavin T (ThT) emission measurement

Th T being a cationic dye and having benzothiazole ring that strongly binds with the amyloid fibrils rich in crossed β -sheet structure. This binding causes a notable rise of the emission intensity [13]. The stock solution of 3.136 mM (1mg/ml) concentration had prepared by dissolving ThT in HPLC water while the concentration was calculated by using a molar extinction coefficient of $\epsilon_{412} = 31600 \text{ M}^{-1}\text{cm}^{-1}$ [14]. All the samples sets had separately added with ThT to get 5.5 μ M and 31.36 μ M working concentration for the insulin and ThT

respectively and final volume of 2ml. Samples were excited at 440 nm in a Horiba Spectrofluorometer (Model: FLUOROMAX-4C, Serial no. 1734D-4018-FM) and emission were found in the range between 460 to 600 nm. The slits were kept at ex/em slit widths of 3 nm. Each spectrum was blank (spectra of ThT only) corrected. Each data averaged from triplicates.

3.12. Kinetic study for aggregation

The aggregation kinetics was studied by taking aliquots during heat treatment under experimental condition of insulin in absence and in presence of modulators [metal ions, vitamins and co-solvents, refer 3.6] at different time intervals ranging from 0-300 min. The aliquots were separately added with ThT as described in paragraph 3.10 and the emission spectra were recorded in the range of 460-600 nm after getting excited at 440nm.

F_p, the percent change in fluorescence intensity was calculated for each sample [15] using eqn. (1):

$$F_p = \{(F_t - F_0) / F_0\} \times 100 \dots \dots \dots \text{Eqn. 1}$$

Here, F_t is the fluorescence at a specific time point and F₀ is the fluorescence at the starting time of incubation.

Percent inhibition, F_x was also calculated [15] using eqn.(2):

$$F_x = 100 - (100F_s \div F_c) \dots \dots \dots \text{Eqn. 2}$$

Here, F_x is the percent inhibition; F_s is the percent increase in fluorescence intensity in the presence of the modulators and F_c is the percent increase in the fluorescence intensity of insulin monomer alone.

3.13. 8-Anilidonaphthalene-1-sulfonic acid (ANS) interaction study

Being an extrinsic fluorescent probe, ANS nonspecifically interact with any surface hydrophobic patches present in solution [16]. Aggregation directed exposure of hydrophobic clusters in proteins and change of its microenvironments can be traced by blue shift of emission wavelength with rise in intensity by ANS binding. The ANS stock solution of 1.2mM was prepared by dissolving ANS in methanol. Spectral corrections were done with only ANS as negative control for all experimental sets. ANS added with Insulin monomer

had served as positive control and heats incubated insulin samples with and without modulators and co-solvents (paragraph 3.6) separately were mixed with ANS. The concentrations of insulin and ANS in final solution were 5.5 μ M and 30 μ M respectively. The solutions were kept at room temperature in dark for 30 min. Excitation had been done at 350 nm while the ANS fluorescence intensities were recorded in the range of 390-600 nm with a Horiba Spectrofluorometer (FLUOROMAX-4C, Serial No.1734D-4018-FM and Fluoromax Software). Slit widths for excitation and emission were set at 3 nm. Each of the measurements was performed in triplicates.

CONFORMATIONAL STUDIES

3.14. Far-UV Circular Dichroism (Far UV-CD) spectroscopy and Deconvolution studies

CD measurements had been performed in a JASCO Spectropolarimeter (J-815, Jasco, Tokyo, Japan) and a thermostat cell holder equipped with a Peltier unit and MultiTech water circulator. Samples were diluted to 1 ml solution to get the final protein concentration of 6.5 μ M in each PerkinElmer quartz cuvette having 2mm path length. Subtraction of control i.e., solvent spectra were done for each sample. The range for far UV-CD was 190–260 nm and scanning speed maintained at 100nm/min. The purging of spectro-polarimeter was done with nitrogen gas before starting and continuously throughout the measuring process. All measurements had been performed in triplicates and averaged spectra were taken in each case. The mean residual ellipticity (MRE) values were obtained by following the Equation 1 [17] and the unit was deg.cm².dmol⁻¹

$$\text{MRE} = \theta_{\text{obs}} (\text{mdeg}) / 10 \times n \times C_p \times l \dots\dots\dots \text{Eqn. 3}$$

Here, θ_{obs} is the observed ellipticity (CD) in mill degree, n is the number of amino acid residues in protein monomer (for insulin, n is 51), l is the path length of the cell in centimeters (here l is 0.2 cm) and C_p is the molar fraction of proteins in solution.

Spectra analysis was done using Origin Lab 8.0 software while CDNN 2.1 software and BeStSel CD spectra analysis v1.3.230210 [was used to get a quantitative measurement of the beta-sheet rich amyloid transitions [18].

3.15. Fourier-Transform Infrared (FT-IR) Spectroscopic studies

For this assay, heat treated insulin samples both in presence and absence of metal ions/ vitamins /co-solvents had collected in micro filter device and prepared in 200 μL of D_2O . Centrifugation had done at 4000xg for 10 min to reduce the volume up to 50 μL . In this way, D_2O was exchanged 3–4 times. Thereafter, the samples were placed between two CaF_2 windows separated by a Teflon spacer (50 mm thick). A PerkinElmer Spectrum (Version 10.4.1) instrument (resolution 2 cm^{-1}) in N_2 environment had used in this assay. Solvent contribution was corrected by subtracting spectrum of D_2O at pD 7.5. The final spectra of each sample had acquired by average of 16 consecutive scans. From the gross range of spectra i.e., 4000-400 cm^{-1} , only selected region of amide-I (1800-1500 cm^{-1}) had normalized and under consideration in results.

LIGHT SCATTERING ASSAYS

3.16. Rayleigh Light Scattering (RLS) Study

RLS was a reliable tool to determine presence of higher ordered particles in solution [19]. Both the excitation and emission wavelength intensities were set at 307 nm and measured using a Horiba Scientific Spectrofluorometer (Model: FLUOROMAX-4C, Serial no. 1734D-4018-FM and Fluoromax Software). The assay had done at room temperature. The quartz cuvette of 1 cm path-length was used to measure the sample solutions for tracing effects of modulators on insulin amyloid fibrillation. In each solution, insulin concentration kept fixed at 5.5 μM .

3.17. Dynamic light scattering (DLS) Assay

The principle of DLS Assay lies in the fact that the fluctuations in the intensity of the scattered light by different sized particles in solution. Here the variable size of particle diameter in solution can be observed as different peaks having particular intensities [20-21]. The DLS instrument used for this analysis was a back-scatter apparatus (Malvern Nano ZS, Malvern, UK) performed at a constant scattering angle of 90° and temperature of $25 \pm 1^\circ\text{C}$. The instrument was equipped with 632.8 nm He/Ne laser. Rectangular Hellma cuvette of 10 mm path length was used to measure the samples. The changes in particle size distribution during the process of insulin aggregation in presence and absence of different modulators under study was observed. Concentration of insulin was maintained at 20 μM in

each solution. Auto correlation function was done by twelve consecutive acquisitions for each sample and was time dependant.

MORPHOLOGICAL IMAGING

3.18. Surface Morphology Study with Field Emission Scanning Electron Microscope (FE-SEM)

A scanning electron microscope (SEM) is a type of electron microscope that produces images of a sample by scanning it with a focused beam of electrons. The electrons interact with atoms in the sample, producing various signals that can be detected and that contain information about the sample's surface topography and composition. The morphology of the monomeric form of the insulin was compared with its aggregates formed in absence and presence of the modulators under experimental protocol using FE-SEM (Hitachi S-4800, JAPAN). The instrument had been operating with a voltage of 20 kV. The concentrations of proteins were maintained at 200 μ M. As the samples to observe were in aqueous media, the drop casting method of sample preparation was followed. One drop from each aliquot of sample was taken on a glass cover slip. The glass containing samples were allowed to dry by slow evaporation in open air and then under vacuum for further gold coating just prior the imaging.

3.19. Transmission electron microscopic (TEM) study

The aggregation-inhibitory effect of the three types of modulators, viz., metal ions, vitamins and co-solvents were further confirmed by TEM studies. The heat treated samples in presence and absence of modulators in minute volume was applied separately onto fine copper grid with 300 meshes and the sample number noted against its corresponding type. The grid was supported and coated with a thin, electron-transparent carbon film. Incubation at 25°C for 10 min of the sample loaded Grids were done. Excess solution was carefully wiped off and 1% uranyl acetate was applied to negatively stain the grids. Excess stain was removed by washing thoroughly with HPLC water. Complete air drying was required to visualize the sample under TEM. The instrument used for this study was Jeol-HRTEM-2011, Tokyo, Japan performing an accelerating voltage of 120 kV under different resolutions. 1,15,000x magnification in image view was achieved through it.

3.20. Atomic Force Microscopic imaging

Sample preparation for AFM included firstly the preparation of AFM grid slides. The glass was cleaned with detergent and water, then with acetone and water to remove oily and water soluble contaminants, respectively. Then it was dried under N₂ (g). Samples were drop casted each having protein concentrations of 200µM on a square AFM glass slide with plain surface. Samples included for AFM was heat-treated insulin in absence and presence of different modulators respectively. The drop-casted samples were homogenously spreaded over the slide and carefully air dried overnight. The instrument Bruker Multimode 8 Atomic Force Microscope had used in this study. In all the sets, the images of 512 by 512 pixels were captured at a scan size ranging between 0.6 and 9 µm. The images were captured at comfortable resolutions.

COMPUTATIONAL TECHNIQUES

3.21. Molecular docking

The conformation and orientation (pose) of modulators into the protein insulin during interaction was analyzed by molecular docking [22]. Auto Dock is a reliable software tool for this [23]. In the first step, the structure of insulin was retrieved from the RCSB Protein Data Bank (PDB ID: 3I40) and through analysis was done. Density Functional Theory (DFT) at the level of B3LYP/6-31G was utilized to optimize the structures with the minimized energy level to realize the most probable site of interaction for the protein. The software used was the grid-based docking program Auto Dock 4.2. And a default parameter and generic algorithm was used for the calculation. Atom Kollman charges was assigned to the protein whiles the ligand in the protein and water molecules were removed. Discovery Studio 4.1 Client was used to create the visual effects. Gibbs free internal energy change was calculated for separate interactions of modulator with insulin.

3.22. References

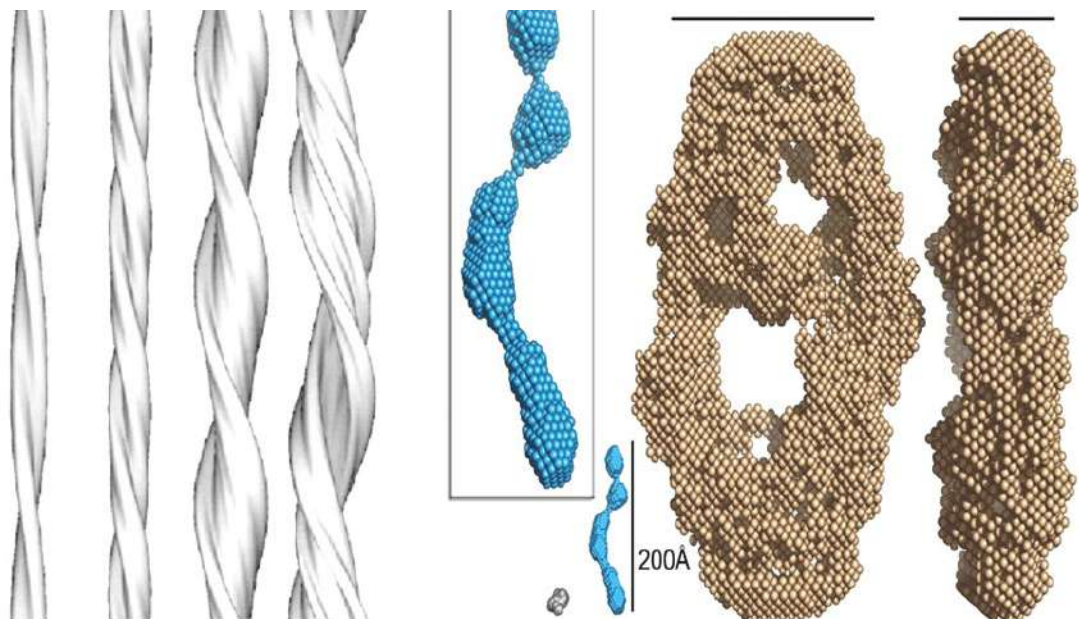
1. Bakaysa D.L., Radziuk J., Havel H.A., Brader M.L., Li S., Dodd S.W., Beals J.M., Pekar A.H., Brems, D.N. 1996. Physicochemical basis for the rapid time-action of LysB28ProB29-insulin: dissociation of a protein-ligand complex. *Protein Sci.*, 5: 2521–2531, <https://doi.org/10.1002/pro.5560051215>
2. Meesaragandla, B, Karanth S., Janke U. 2020. Biopolymer-coated gold nanoparticles inhibit human insulin amyloid fibrillation. *Sci Rep.*, 10:7862, <https://doi.org/10.1038/s41598-020-64010-7>
3. Ahmad A., Millett I.S., Doniach S., Uversky V.N., Fink A.L., 2003. Partially Folded Intermediates in Insulin Fibrillation. *Biochemistry* 42:11404–11416. <https://doi.org/10.1021/bi034868o>
4. Whittingham J.L., Scott D.J., Chance K., Wilson A., Finch J., Brange J., Guy Dodson G. 2002. Insulin at pH 2: Structural Analysis of the Conditions Promoting Insulin Fibre Formation. *J Mol Biol.*, 318:479–490. [https://doi.org/10.1016/S0022-2836\(02\)00021-9](https://doi.org/10.1016/S0022-2836(02)00021-9)
5. Nettleton E.J., Tito P., Sunde M., Bouchard M., Dobson C.M., Robinson C.V. 2000, Characterization of the oligomeric states of insulin in self-assembly and amyloid fibril formation by mass spectrometry, *Biophys. J.*, 79:1053–1065. [10.1016/S0006-3495\(00\)76359-4](https://doi.org/10.1016/S0006-3495(00)76359-4)
6. Smirnovas V., Winter R. 2008. Revealing different aggregation pathways of amyloidogenic proteins by ultrasound velocimetry, *Biophys. J.*, 94:3241–3246. [10.1529/biophysj.107.123133](https://doi.org/10.1529/biophysj.107.123133)
7. Vestergaard B., Groenning M., Roessle M., Kastrup J.S., van de Weert M., Flink J.M., Frokjaer S., Gajhede M., Svergun D.I., 200., A helical structural nucleus is the primary elongating unit of insulin amyloid fibrils, *PLoS Biol.*, 5:e134. <https://doi.org/10.1371/journal.pbio.0050134>
8. Krebs M.R.H., Bromley E.H.C., Donald, A.M., 2005. The binding of thioflavin-T to amyloid fibrils: localisation and implications. *J Struct Biol.*, 149:30–37. <https://doi.org/10.1016/j.jsb.2004.08.002>
9. Haas J., Vöhringer-Martinez E., Bögehold A., Matthes D., Hensen U., Pelah A., Abel B., Grubmüller H., 2009. Primary steps of pH-dependent insulin aggregation kinetics are governed by conformational flexibility. *Chembiochem.*, 10: 1816–1822. <https://doi.org/10.1002/cbic.200900266>

10. Brange J., Dodson G.G., Edwards D.J., Holden P.H., Whittingham J.L., 1997. A model of insulin fibrils derived from the x-ray crystal structure of a monomeric insulin (despentapeptide insulin). *Proteins*, 27:507–516. PMID: 9141131
11. Chi Q., Huang K. 2007. Polyacrylamide Gel Electrophoresis of Insulin. *Analytical Letters*, 40(1):95–102. <https://doi.org/10.1080/00032710600952432>
12. Arndt C., Koristka S., Feldmann A, Bachmann, M., 2019. Native Polyacrylamide Gels. In: Kurien, B., Scofield, R. (eds) *Electrophoretic Separation of Proteins. Methods in Molecular Biology*, vol 1855. Humana Press, New York, NY. https://doi.org/10.1007/978-1-4939-8793-1_8
13. Biancalana M., Koide S. 2010. Molecular mechanism of Thioflavin-T binding to amyloid fibrils. *Biochimica et Biophysica Acta (BBA)-Proteins and Proteomics*, 1804(7) : 1405-1412. [10.1016/j.bbapap.2010.04.001](https://doi.org/10.1016/j.bbapap.2010.04.001)
14. Sulatskaya A.I., Lavysh A.V., Maskevich A.A. 2017. Thioflavin T fluoresces as excimer in highly concentrated aqueous solutions and as monomer being incorporated in amyloid fibrils. *Sci Rep.*, 7 : 2146 (2017). <https://doi.org/10.1038/s41598-017-02237-7>
15. Maity S., Pal S., Sardar S., Sepay N., Parvej H., Begum S., Dalui R., Das N., Pradhan A., Halder U.C., 2018. Inhibition of amyloid fibril formation of beta-lactoglobulin by natural and synthetic curcuminoids, *New J. Chem.*, 42: 19260-19271, <https://doi.org/10.1039/C8NJ03194K>
16. L. Stryer. 1965. The interaction of a naphthalene dye with apomyoglobin and apohemoglobin. A fluorescent probe of non-polar binding sites. *J. Mol. Biol.* 13:482–495, [10.1016/s0022-2836\(65\)80111-5](https://doi.org/10.1016/s0022-2836(65)80111-5).
17. Patar M., Jalan A., Moyon N.S., 2024. A Spectroscopic and Molecular Docking Study on the Interaction of 2’Hydroxyflavanone with Bovine Serum Albumin, *Phys. Chem. Res.*, 12 (3) : 709-727, [10.22036/pcr.2024.416266.2415](https://doi.org/10.22036/pcr.2024.416266.2415)
18. Micsonai A., Wien F., Bulyaki E., Kun J., Moussong E., Lee Y-H., Goto Y, Refregiers M., Kardos J., 2018. BeStSel: a web server for accurate protein secondary structure prediction and fold recognition from the circular dichroism spectra, *Nucleic Acids Res.*, 46: W315–W322, [10.1093/nar/gky497](https://doi.org/10.1093/nar/gky497)

19. Brahma A., De D., Bhattacharyya D. 2009. Rayleigh scattering technique as a method to study protein–protein interaction using spectrofluorimeters, 2009, *Curr. Sci.*, 96 (7): 940-946, <https://www.researchgate.net/publication/228631298>
20. Yarmush DM., Morel G., Yarmush ML. 1987. A new technique for mapping epitope specificities of monoclonal antibodies using quasi-elastic light scattering spectroscopy. *J Biochem Biophys Methods.*, 14:279-289. [https://doi.org/10.1016/0165-022X\(87\)90054-6](https://doi.org/10.1016/0165-022X(87)90054-6)
21. Bohidar HB. 1989. Light scattering study of solution properties of bovine serum albumin, insulin, and polystyrene under moderate pressure. *Colloid Polymer Sci.*, 267:292–300. <https://doi.org/10.1007/BF01413622>
22. Muhammad E.F., Adnan R., Latif M.A.M. et al., 2016. Theoretical investigation on insulin dimer- β -cyclodextrin interactions using docking and molecular dynamics simulation. *J Incl Phenom Macrocycl Chem.*, 84:1–10, <https://doi.org/10.1007/s10847-015-0576-x>
23. Morris G.M., Goodsell D.S., Halliday R.S., Huey R., Hart W.E., Belew R.K., Olson A.J. 1998. Automated docking using a Lamarckian genetic algorithm and an empirical binding free energy function. *J. Comput. Chem.*, 19:1639–1662. doi: [10.1002/\(SICI\)1096-987X\(19981115\)19:14<1639::AID-JCC10>3.0.CO;2-B](https://doi.org/10.1002/(SICI)1096-987X(19981115)19:14<1639::AID-JCC10>3.0.CO;2-B).

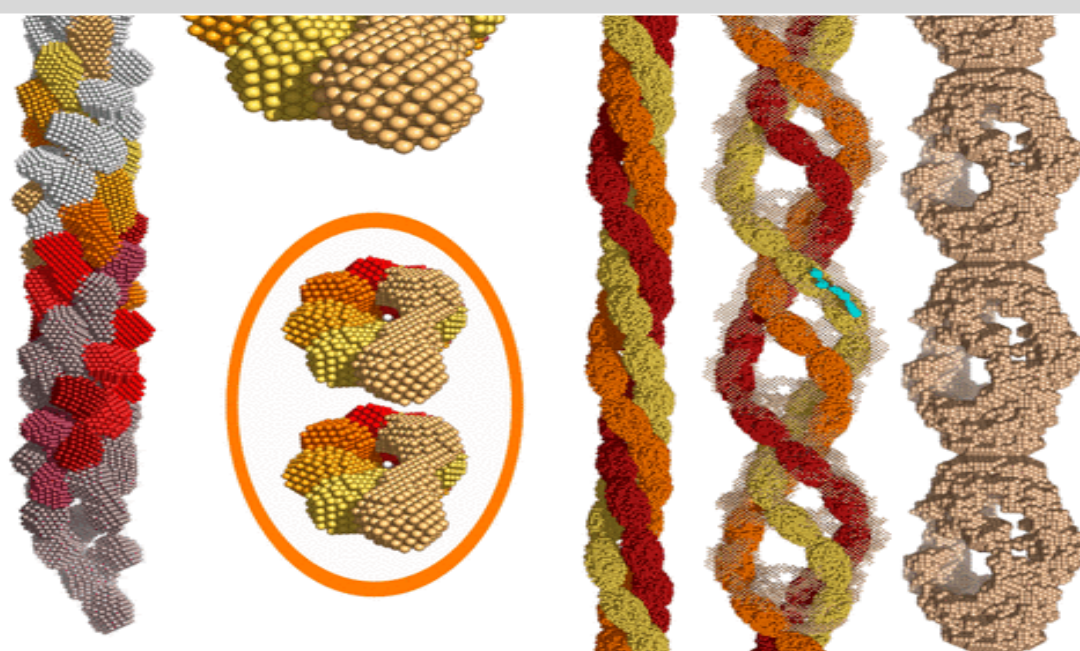
CHAPTER 1

In vitro amyloid generation of insulin and study of the effects of metal ions



Representative publication

New J. Chem., 2024, 48, 3120–3135 (DOI: 10.1039/d3nj04431a)



4.1 Prologue of the study

A protein has to maintain its properly folded conformation to become thermodynamically stable as well as functionally active [1]. Protein misfolding and aggregation (amyloidosis) leads to development of a number of different pathogenic conditions [2] collectively termed as ‘disorders due to amyloidosis’ depending on the nature and biological functions of that protein. Some well studied examples are Alzheimer’s disease, Huntington’s disease, Parkinson’s disease [3-4] etc. Therapeutic protein may undergo such amyloid generation under different in-vivo (when injected) or in-vitro (during storage) conditions. Such amyloid deposits are common at the insulin injection sites for patients undergoing insulin therapy [5]. Amyloids are insoluble cross- β -sheet rich irreversible fibril like forms that are generated via soluble toxic oligomeric intermediates [6]. Having mess of cytotoxic [7] fibrillar network in structure, they tend to deposit onto the cell membranes causing fatal membrane pores followed by cell lysis [8]. The proteins possessing marginal stability in secondary structures tends to form amyloid species under deviation from optimum conditions or in presence of stress inducers [9]. Thus it is also a great concern in vitro while proteins during commercial manufacture, processing, transportation, storage or delivery get fibrillated/ aggregated [10-11].

A number of proteins are reported to show amyloid fibrillation like Human insulin (amyloid deposition causing Alzheimer’s disease), amyloid precursor protein (Ab peptides causing Alzheimer’s disease), atrial natriuretic factor (amyloid ANF causing atrial amyloidosis), and prion protein (causing spongiform encephalopathies) etc. Among them human insulin showing similar type amyloid structure like the rest is a common model protein [12]. It is studied for the greater understanding of structural assemblies of amyloid and possible inhibition strategies of its formation. The pathogenic amyloidosis followed by deposition of insulin injected for therapeutic purpose was reported in various body parts like the shoulders [13], arms [14], thighs [15] and abdominal walls [16]. As amyloidogenesis and neurodegenerative diseases are closely related [17] thus the study can help to get rid of the fatal diseases [18].

While studying insulin amyloid inhibition, the knowledge of insulin amyloid formation mechanism is necessary. Prior to its biological hypoglycemic function, insulin is converted to monomeric form to become active. Therapeutic human insulin is formulated as hexamer.

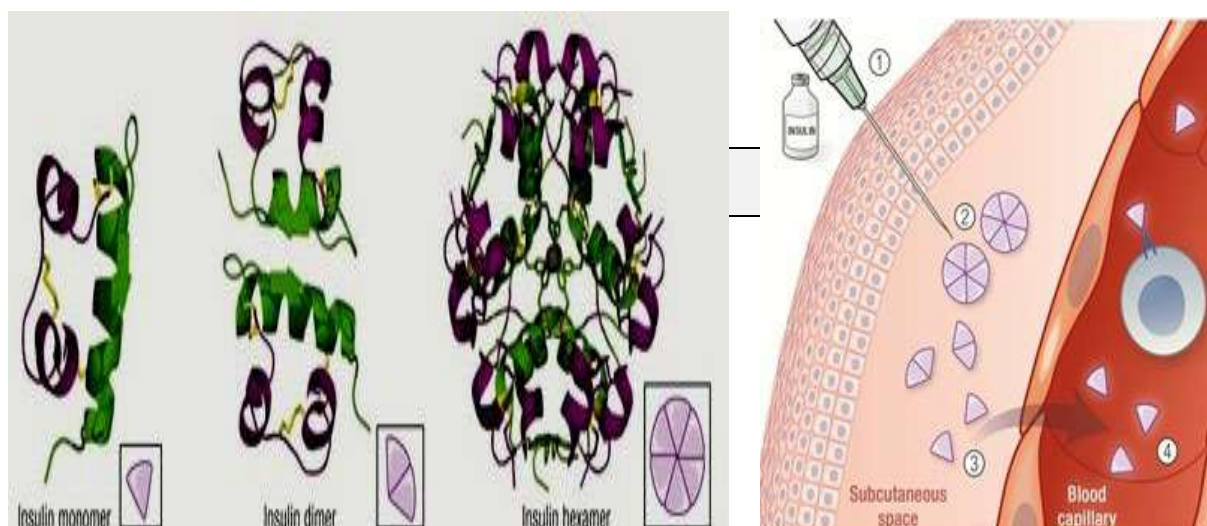


Fig.4.1. (left panel) Three-dimensional structure of insulin monomer (the A and B chains are in purple and green respectively; protein data bank [PDB] ID = 1LPH), insulin dimer (PDB ID = 1LPH), and insulin hexamer (three insulin dimers and 2 Zn^{2+}) (PDB ID = 2INS). (Right panel) (1) The hexameric form of regular huminsulin is formulated and (2) is subcutaneously injected (3) dissociation of insulin hexamers into dimers followed by monomer formation (4) absorption of monomers into the blood across the microvascular endothelium. *Fig adapted from https://www.rcsb.org/pdb/static.do?p=general_information/about_pdb/index.html and Pampanelli S., *Diabetes Care*. 1995.18(11):1452–1459.

But it will be converted to monomeric form (Fig 4.1. right panel). Hexamer to monomer conversion leads to shift and exposure of hydrophobic residues of the protein. This transition may promote amyloid generation [19]. Inhibition of amyloidogenesis is of significant importance in running the smooth application of insulin therapeutics. Before the research proceedings, the detail knowledge about interaction of protein with various molecules should have to be considered.

4.2 Amyloid inhibitors: Literature findings

The problem of amyloid generation was approached in two possible ways. Firstly, inhibition of the amyloid transition of via pre-interacting it with different molecules. Another approach was disintegrating already generated fibrils. The common goal was to either stabilize the native state of insulin by different additives or disorienting/destabilize the already misfolded proteins. The targets for inhibitors were also different as depicted in Fig. 4.2.

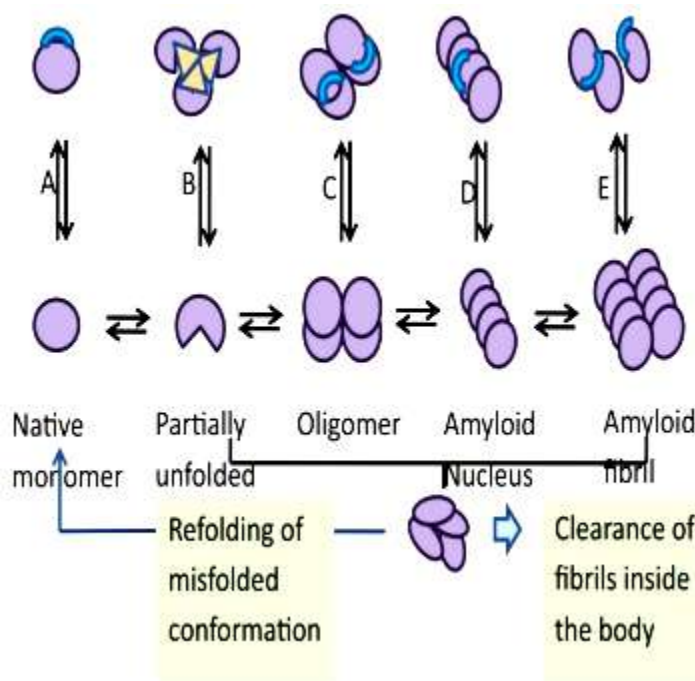


Fig.4.2. Schematic sketch of possible approaches of inhibition and destabilization of amyloidogenesis. (A) - (E) represent the proposed inhibitors either applied to stabilize protein or to destabilize its fibrils as follows: (A) stabilization of Native state (B) inducing protein refolding (C) preventing oligomerization (D) inhibiting fibril elongation (E) Disaggregation of amyloid fibrils.

**Fig adapted from Zaman M., 2019. Int. J. Biol. Macromol., 134: 1022-1037, <https://doi.org/10.1016/j.ijbiomac.2019.05.109>*

4.2.1. Natural compounds

Natural compounds employed for amyloidogenic inhibitions are flavonoids, phenolic compounds, quinones, pyridines, aldehydes, sugar alcohols, terpenes, etc. The **polyphenol compounds**, curcumin, resveratrol and **epigallocatechin-3-gallate (EGCG)** are popular for their metal chelating, anti-oxidant and anti-inflammatory properties. Their structural backbone are used in designing multifunctional anti-amyloid compounds [20-21]. Amyloid generation risk with aging is common and can be managed by diets supplemented with **oleuropein** and **oleocanthal** (present in olive oil), **resveratrol** (from fruit and red wine), **curcumin** (from turmeric), EGCG and **myricetin** (from green tea) [22-24]. The possible interactions between target protein and amyloid inhibitors are covalent bonds [25-26] and/or non-covalent interactions like π - π interactions, H-bond, or electrostatic interactions [27-28]. **Ferulic acid (FA)**, a phytochemical isolated from fruits and vegetables like tomatoes, sweet corn and rice bran, inhibits insulin fibrillation in vitro [29]. The said inhibitory activity of FA was shown to be contributed by the phenyl, hydroxyl, and carboxylic residues in it. Amino acids like **arginine** and its derivatives were proved to interact with proteins via hydrophobic, electrostatic and cation- π interactions [30] and suppresses heat stressed protein aggregation [31-32]. 4-7 Residues long arginine rich oligopeptides inhibited the fibrillation of amyloid β 42 [33]. **L-Cysteine (Cys)** interacted with lysozyme via thiophilic interactions between thiol

groups of side chain-Cys residues and in turn inhibited its fibrillation [34]. A β fibrillation was also shown to be inhibited by **D-amino acids** [35] and **Tannic acid** [36] and free A β binding to prevent its oligomerization was seen by curcumin, papain (from raw papaya), rosmarinic acid (herbs of the family Lamiaceae) and bromelain (from the fruit and stem of the pineapple plant) [37]. Inhibition of islet amyloid polypeptide (IAPP), Amyloid beta peptide (A β) and insulin amyloid were reported by **phensulfonphthaleine** while α -synuclein aggregation inhibition by **baicalein polyphenols** (present in the dry roots of *Scutellaria baicalensis Georgi*) [38]. **Gallic acid** (found in green tea) is a metal based amyloid inhibitor [39].

4.2.2. Thermo stability contributors

Some micro-organisms like *Pyrococcus aerophilum*, *Thermus thermophilus* were found to tolerate and grow at temperature above 100°C by accumulating some unusual organic solutes called stress molecules or thermo stability contributors [40-41]. **Trehalose** and **betaine** are such compounds found at high concentrations in the Thermophiles [40] and also shown to stabilize the native conformations of enzymatic proteins [41-42].

4.2.3. Dietary supplements

Morin is a dietary bioflavonoid compound of Moraceae family plants with antioxidant, anti-inflammatory, cardio protective, neuro-protective, anti-diabetic, and anti-microbial versatile properties. **Morin** was shown to interact and consequently inhibit the amyloid formation of human γ D-crystallin (HGD) through hydrogen bonding and van der Waals forces [43]. **Morin hydrate** (2', 3, 4', 5, 7-Pentahydroxyflavone) was found to inhibit the amyloid formation of the polypeptide hormone Islet Amyloid Polypeptide (IAPP, amylin) which is responsible for islet amyloid formation in type-2 diabetes [44]. IAPP was dangerous in islet cell transplants by causing graft failure. Peptides derived from **bromelain** found in fruit and stem of pineapple, was found effective in prevention of insulin amyloids [45]. **Vitamin C** was demonstrated to both inhibit the formation and disaggregate [46] the insulin amyloid fibrils while nullified the effect of amyloid induced cytotoxicities on human neuroblastoma cell line (SH- SY5Y). Slower rate of aggregation of hen egg-white (HEWL) as well as stabilization of its secondary structure was demonstrated by (–)-**epigallocatechin gallate (EGCG)**, a green tea constituent [47].

4.2.4. Osmolytes and denaturants

The native folds of globular proteins are naturally stabilized by small stabilizers and osmolytes and thus they can present themselves as inhibitors of amyloid formation. **Glucose, sucrose, trehalose** as well as **polyhydric alcohols** were shown to inhibit aggregation of HEWL [48-49], insulin [49-50], α -lactalbumin [51], bovine serum albumin [52] while **trimethylamine N-oxide (TMAO)** inhibited insulin fibrillation [53-54]. But some sugars were shown to aggravate β -amyloid fibrillation [55-56] though.

4.2.5. Molecular chaperones

Molecular chaperones, a class of molecules help in proper folding of protein in vivo was of a choice for amyloid inhibition. They were found to shield the effect of heat shock and other proteotoxic stresses [57-58] and secondary nucleation of the amyloid β aggregation in vitro [59]. The fibrillation of polyglutamine peptides responsible for Huntington disease development was inhibited by **DNAJB6** [60], a human molecular chaperone belonging to the Hsp40 heat shock protein family. α -Crystallin which is a small heat-shock protein in lens, possesses a peptide chaperone (functional site sequence DFVIFLDVKHFSPEDLTVK) known as **mini- α A-crystallin**. The fibril formation of A β peptides was arrested by application of Mini- α A-crystallin and rat pheochromocytoma (PC12) cells were protected [61].

4.2.6. Several nanoparticles

Stable gold (**AuNPs(Tyr)**, **AuNPs(Trp)**) and silver (**AgNPs(Tyr)**) nanoparticles were exhibited insulin amyloid inhibitory as well as amyloid disintegrating properties [62]. On the other hand, beta casein-coated iron oxide nanoparticles (**β Cas IONPs**) was found protective against oligomerization of Amyloid β and toxic effect like inflammation, apoptosis, and abundance of autophagy proteins in A β -injected mouse brain [63]. Additionally, insulin fibril formation inhibition was reported by stable **silver nanoparticles** [64] and gold nanoparticles **AuNPs functionalized with** linear- (i.e. **dextrin** and **chitosan**) and branched- (i.e. **dextran-40** and **dextran-10**) biopolymers [65]. Bovine Serum Albumin amyloid fibrillation was effectively inhibited by **Zinc Oxide Nanoparticles** [66].

4.2.7. Conjugated polymers

At physiological temperature, **conjugated polymer-based thermo responsive micelles** (CPMs) were surprisingly capable of capturing the harmful A β aggregates [67]. There present a reactive-oxygen-species (ROS)-generating core with thermo responsive surface in the structure of CPM. The ROS generated under white light irradiation were effective in disaggregating A β aggregates and thus reducing cytotoxicity. Another approach had shown amyloid inhibition, preformedfibril degradation and cytotoxicity prevention by poly (**p-phenylene vinylene**) derivative, **functionalized with p-nitrophenyl esters (PPV-NP)** [68]. A β plaques in brain slices were also eliminated by PPV-NP in ex vivo findings. The mechanism of interaction of PPV-NP with protein was found to be irreversible covalent interactions and non-covalent hydrophobic forces. **Fluorogenic “nanogrenades”** were prepared by supramolecular assemblies between conjugated polymers and fluorescent probes. They were very effective in irreversible destruction of amyloid β fibrils under white light as shown in fig 4.3 [69]

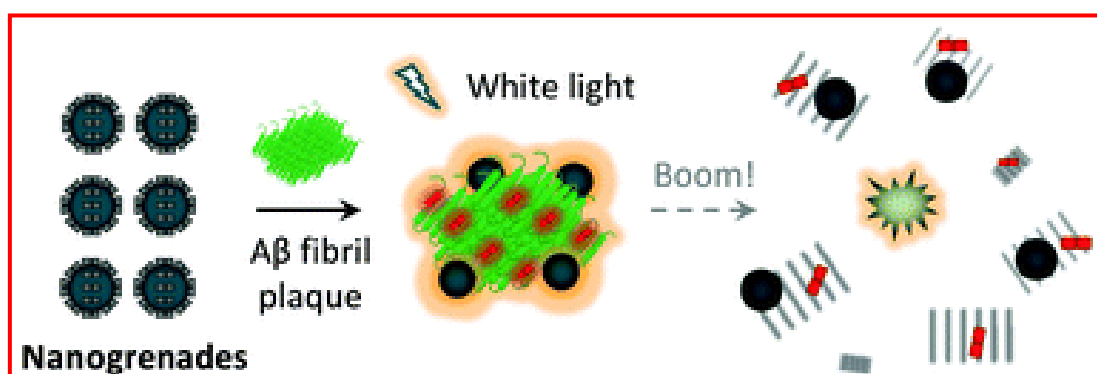


*Fig. 4.3. Schematic representation of the mode of action of nanogrenades. *Fig adapted from Dou W-T. et. al., 2016, J. Mater. Chem. B, 4: 4502-4506, <https://doi.org/10.1039/C6TB01351A>*

4.2.8. Monoclonal antibody

Food and Drug Administration (FDA) approved the only drug named, Aducanumab against Alzheimer’s disease (AD). Being a monoclonal antibody, **Aducanumab** sold under the brand name **Aduhelm** can selectively binds to oligomeric amyloid aggregates or mature fibrils and effectively reduced the number of beta-amyloid plaques. In this way, the neurological functions of patients were restored as well as the calcium permeability of neurons [70].

4.3. Selecting metal ions to investigate insulin amyloid inhibition

From the information of previous reports, amyloid inhibitors from natural sources and of synthetic origin were found maximum of which showed concentration dependent effects. In high or moderate concentrations side effect and effectors generated toxicities were of prime concern. Aducanumab applied to inhibit beta-amyloid plaques showed common side effects like headache, diarrhea, and other constitutional symptoms [71-73]. The most serious side effect of it as noted while applied against A β formation was Amyloid Related Imaging Abnormalities (ARIA-E) [74- 76]. Even death was reported in case of bapinezumab and solanezumab, another two anti A β drug treated patients [72-74]. Small molecules having binding efficacy and lesser side effects are considered in the present study regarding inhibition of insulin fibrillation. Metal ions can serve both the purposes as they are the important macro and micronutrients of our body.

4.3.1. Interaction of insulin with different metal ions

At minute concentrations, metal ions can interact well with insulin. During its storage in the secretory vesicles or granules, six monomers of insulin coordinates with two Zn²⁺ ions to form insulin hexamer [77]. Insulin secretion and activity is dependent on local Ca²⁺ and Mg²⁺ concentration [78]. Crystallization as well as aggregation of insulin is facilitated by Co²⁺ and Cd²⁺ [78]. The 10th positioned His residue of insulin B chain; HisB10 was found to interact with Co³⁺ ions or Zn²⁺ to impart thermodynamic stabilization to insulin [79] while GluB13 residue of insulin can easily bind with Zn²⁺, Cd²⁺, and Pb²⁺ separately [79]. Zn²⁺, Co²⁺ and Cd²⁺ conferred conformational changes in insulin structure as detected by red shift of tyrosine bands in absorption spectra of insulin [78] while Ca²⁺ and Mg²⁺ did not show any such effect. It was also prevalent that the specificity of the metal-binding center of insulin is not restricted for Zn²⁺ only; it was also shown to bind with Cu²⁺ with increasing affinity [80]. Beef and pork insulin were subjected to form larger aggregates with molecular weight ranging from 10⁵ to 2×10⁵ Da in artificial delivery systems under the influence of excess amounts of divalent metal ions, Zn²⁺, Cu²⁺, Fe²⁺ [81]. Zn²⁺ when coordinated at concentrations above 0.01 mM Zn–insulin with HisB10 of insulin, the hexameric form get stabilized [82]. At acidic pH the HisB12 gets protonated and releases zinc. This insists the prevalence of monomeric form of insulin [83] to become secreted. In this way, with decreasing pH, the hexameric insulin gradually forms dimer and then monomer to become functionally active.

In monomer state i.e., at acidic pH, the aggregation of insulin is favored at high temperature in vitro conditions [84-86]. The present study employed insulin at acidic pH (pH 1.6). The two transition metal ions, Fe^{3+} and Cu^{2+} relevant to macro and micronutrient respectively for our body were chosen for tracing the effect on insulin aggregation. These metal ions are included in our diet as they serve and regulate different metabolic functions by interacting with enzymes. Being block-d transition metal ions, they are very active in coordination with protein domains. E.g., iron in hemoglobin. They were found to serve as supplements of natural medicines too [87].

4.4. MATERIALS AND METHODOLOGIES

4.4.1.. The experiments were performed in HPLC water. All other reagents used were of analytical grade and listed as follows

Table 4.1. Chemicals and equipments required

I T E M S	OBTAINED FROM
Human insulin (Huminsulin R)100 IU/ml (r-DNA origin)	Eli Lilly and Company India Pvt. Ltd.
HPLC grade 100% Pure Distilled Water, Acrylamide, N,N'-Methylenebisacrylamide,	Sigma-Aldrich
N,N,N,N tetramethylethylenediamine (TEMED), ammonium per sulphate(APS), bromophenol blue, Coomassie brilliant blue	Sigma-Aldrich
Methanol & Fluorescent probes, viz., 8-Anilinoanthracene-1-sulfonic acid (ANS), Congo red (CR), Thioflavin T (Th T)	Sigma Chemical Co. (St. Louis, USA)
Glycine, KOH, Acetone	Merck (Mumbai, India)
Iron(III) chloride hexahydrate (FeCl ₃), Copper(II) chloride(CuCl ₂), HCl, NaOH	Sigma-Aldrich
Copper grids (mesh size-300) for TEM	Sigma-Aldrich
Quartz cuvettes and Hellma absorption cuvettes	Sigma-Aldrich
Glass plates for AFM	Merck (Mumbai, India)
Magnetic beads, Membrane dialysis tubing	Sigma-Aldrich

4.4.2. Methodologies

The stock solutions of metal ions were made as described in section 3.3. The aggregates were formed following the procedures described in the sections 3.7-3.17.

4.5. RESULTS OF RESEARCH FINDINGS

4.5.1. Purification and monomeric conversion of Human Insulin

After monomeric conversion of the protein, native polyacrylamide gel electrophoresis (native PAGE) experiment gave single band which confirmed the monomeric form of purified protein on 18% polyacrylamide gel bed shown in the following fig. 4.4

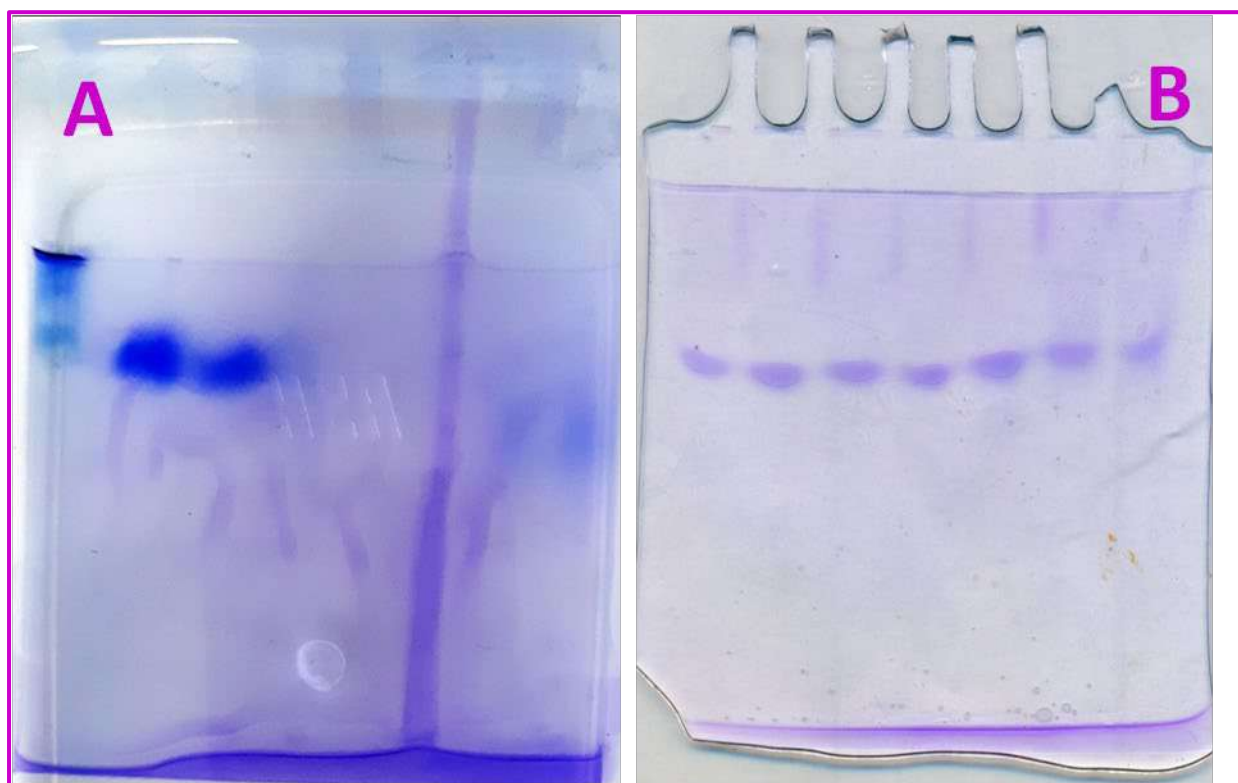


Fig.4.4. Native polyacrylamide gel electrophoresis (native PAGE) experiment showing single band which confirmed the monomeric form of purified protein on 18% polyacrylamide gel bed. The first lane of panel A shows the bands obtained for marker ladder while the rest bands of the lanes in both panels show monomeric insulin

4.5.2. Standardization of physical parameters (pH, temperature, heating duration) to get most irreversible aggregate formation i.e., amyloid fibril of human insulin

A wide range of pH was varied (from pH 1-11) while the insulin at different pH was allowed to aggregate under heating. The results of pH optimization for getting insulin amyloid are as follows:

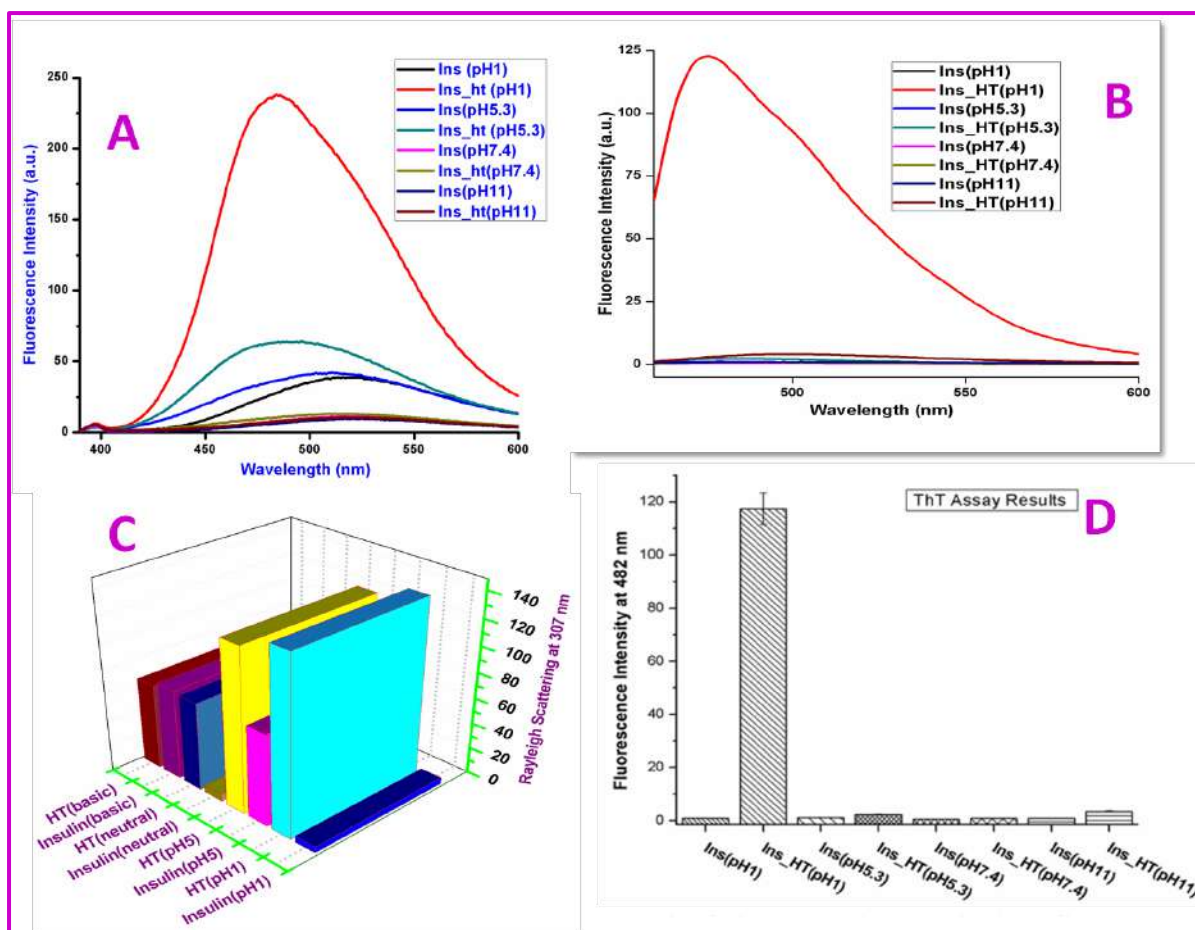


Fig. 4.5. Panel A. 8-anilino-1-naphthalene sulfonic Acid (ANS) Fluorescence emission assay showing increased fluorescence emission intensity accompanied by a blue shift from 512 nm (Ins only, black curve) to 475 nm, indicating the conformational change during aggregation. Panel B. Thioflavin T (Th T) assay results showing huge rise in emission intensity at 482 nm, which is a feature of amyloid structure in case insulin aggregated at pH1. Panel C. Rayleigh Scattering result showing highest scattering by fibril formed at pH 1.0. Panel D. ThT fluorescence emission intensity at 482 nm [characteristic wavelength of emission for protein insulin amyloids] also depicts highest intensity for fibril formed at pH 1 [2nd column in graph]

Results suggested that (Fig. 4.5, panel A), the blue shift obtained in aggregated structure through ANS assay indicated a decrease in wavelength thus increase in energy level i.e., the disorientation in monomeric structure of insulin. The most blue shift occurred in case of insulin heat treated at highly acidic pH shown in red curve. Panel B shows curves obtained from ThT assay where the amyloid generation can be understood by rise in emission intensity at 482 nm. This rise was prominent in case of insulin aggregated at highly acidic pH (red curve). Panel C showed the Rayleigh scattering pattern of insulin at different pHs and their

corresponding aggregates. Here it can be seen that with increasing pH, insulin itself scatter in higher intensities. While here also the greatest scattering was observed in case of insulin fibrillated at pH 1, and the difference in scattering intensity was largest between insulin and its corresponding aggregate at pH1. Rayleigh scattering is an indication of particle size in solution as higher scattering is observed in case of higher diameter particles or aggregates. Thus this study also agreed with the previous results. The ThT emission intensities of the insulin at different pHs and corresponding aggregated samples at 482nm were depicted in panel D bar diagram. Here also the highest scattering intensity [2nd column in the plot] in case of the fibril formed with monomeric protein at pH 1 was observed.

Similar experiments were done to optimize temperature of heating while incubating insulin at pH 1.6 at different temperatures ranging from 37- 80° C. Results showed that [data not shown] insulin aggregation take place within 3 hours at temperature range started from 60°C and reached plateau region after 4 hours. So, the monomeric insulin was found to be most aggregated while heating done at 60°C for at least 4 hours at the pH range of 1.4-1.8.

4.5.3. INHIBITION OF IN VITRO FIBRILLATION OF HUMAN INSULIN BY Fe^{3+} AND Cu^{2+} IONS

Th T fluorescence effectively measured the Insulin fibrillation propensity under the influence of metal ions, Fe^{3+} and Cu^{2+}

The principle of Thioflavin T (ThT) assay to detect amyloid fibril is, the dye upon binding to the amyloid fibrils give enhanced fluorescence intensity at 482 nm. The restricted rotation of the benzothiazole and benzaminic rings of ThT as shown in fig.4.6.A is responsible for the increase in intensity at a particular wavelength [88]. Fe^{3+} and Cu^{2+} ions effect on insulin fibrillation was monitored by ThT and the result was shown in fig. 4.6.B. HTI represented the heat treated insulin in absence of any metal ions and gave strong increase of ThT fluorescence emission around 482 nm (HTI in Fig 4.6.B). It indicated the formation of amyloid structure [89] of insulin under experimentally defined conditions i.e., at 60°C for 4h.

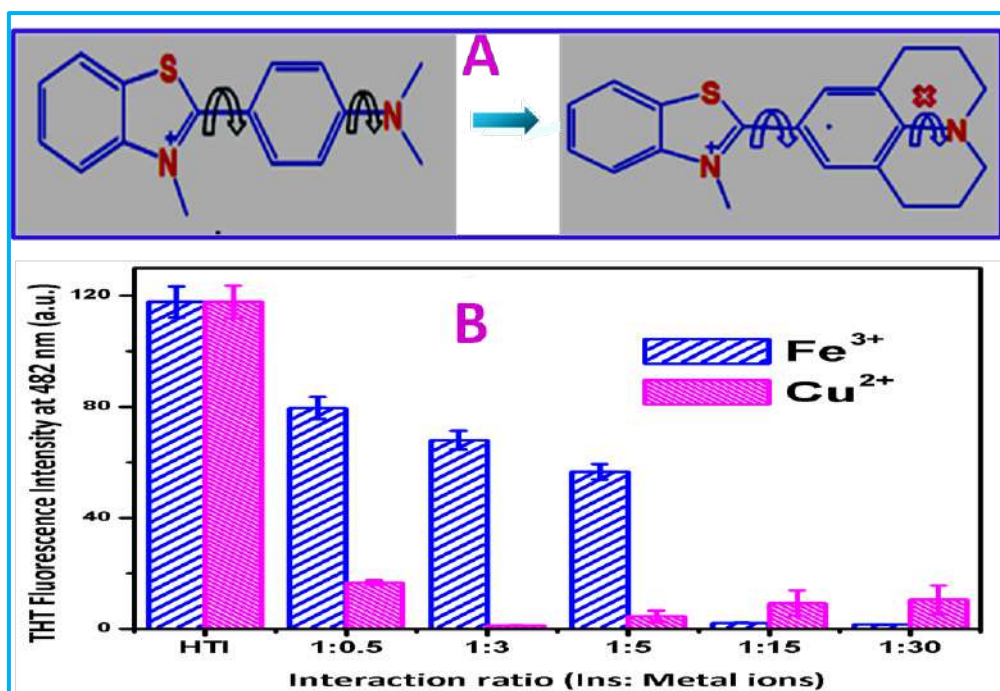


Fig. 4.6. A. Schematic representation of the immobilized rotation of central C—C bond of ThT upon binding to amyloid fibrils. B. End-point ThT emission intensity at 482nm of heat treated human insulin without metals (HTI) and in presence of Fe³⁺ (blue) and Cu²⁺ (magenta) separately at different millimolar ratios (from 1:0.5 up to 1:30) presented in Bar diagram. The range of standard deviations was ± 5.0 . Insulin conc. was fixed at 5.5 μ M for ThT assay. Excitation wavelength was 440 nm and each of the data presented were average of three scans. In positive control sample, the ThT assay was performed on only the monomeric protein, and the data were blank corrected using the data obtained from ThT solution alone (negative control).

The decrease in ThT fluorescence intensity with respect to HTI in presence of Fe³⁺ and Cu²⁺ ions individually were observed and were concentration dependant. Maximum decrease occurred at a molar ratio of insulin: Fe³⁺ as 1:30 and insulin: Cu as 1:3. Thus it can be stated that the amyloid fibril generation was minimized at higher conc. of Fe³⁺ but at lower conc. of Cu²⁺.

Aggregation kinetics in presence of metal ions

In order to get the aggregation kinetics, metal untreated insulin and metal treated insulin samples were heat incubated up to 300 min at 60⁰ C and aliquots were withdrawn at specific time intervals. The ThT assay was done with the aliquots separately. The results were presented following equation 1 and eqn.2 as discussed earlier in section 3.11. Fig 4.7.A

depicted the aggregation kinetics of insulin in absence and presence of metal ions.

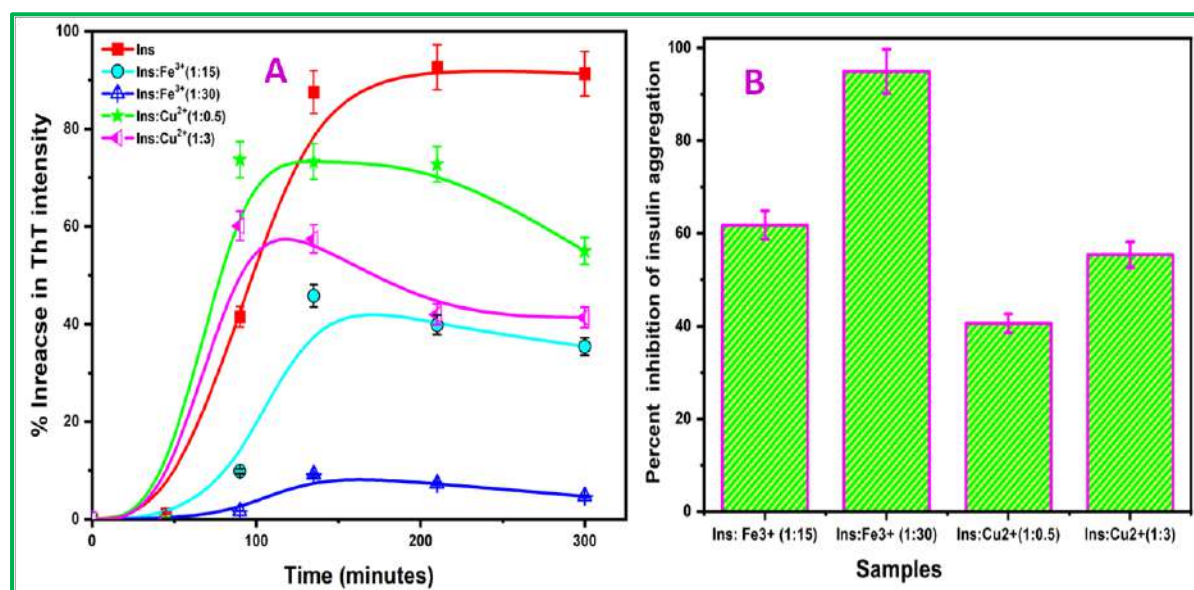


Fig. 4.7. *Insulin amyloid fibrillation kinetics as detected by ThT assay at pH 1.6. Panel A. shows percent increase in ThT fluorescence intensity calculated by following eqn.1, section 3.11 as a function of time. The aggregation kinetics of only insulin showed in red squares. Fe³⁺ treated insulin at ratio1:15 (cyan circle) and 1:30(upward blue triangle) were shown. Similar experiment results obtained with Cu²⁺ treated insulin at 1:0.5 (green star) and 1:3 ratio (left aligned magenta triangle) respectively were also shown. Error bars were given within the range of ± 2.0 . Panel B depicted the percentage inhibition of insulin aggregation individually by Fe³⁺ and Cu²⁺ ions as calculated from eqn.2, section 3.11. Standard errors were within the range of ± 5.0 . The insulin conc. was 5.5 μ M for all the samples examined.*

The aggregation of insulin in absence of any modulator showed the three phase kinetics, viz., a lag phase, a log phase followed by a stationary phase. The said kinetics is consistent with previous findings in literature. Unfolding of structure of insulin under heat influence followed by seed formation and initiation of oligomerization was said to be prevalent in the lag phase [90]. Elongation and growth of nascent fibrils occurred in the log phase [91]. The plateau region corresponds to attaining maximum fibril formation at that instance of experimental influences. **Fig.4.7.A** gave an idea of the mechanism of fibril inhibition by Fe³⁺ and Cu²⁺. Extension of lag phase of fibril initiation, shortening of the log phase was observed in Fe³⁺ treated samples. From **fig.4.7.B**, it was also evident that percent inhibition of insulin aggregation was maximized in presence of Fe³⁺. Both of the observations accounted for major inhibition posed by Fe³⁺ against insulin aggregation by decelerating the nucleation step of aggregation and simultaneous discouraging of the growth of the insulin fibril. However,

Cu^{2+} though cannot alter the onset of lag phase but effectively lower the amount of fibrillation compared to heat treated insulin samples under experimental condition. On the basis of aggregation inhibitory potentials, the two metal ions can be categorized as follows-
Ins: Fe^{3+} (1:30) > Ins: Fe^{3+} (1:15) > Ins: Cu^{2+} (1:3) > Ins: Cu^{2+} (1:0.5).

Alteration of hydrophobicity of insulin during aggregation in presence of metal ions

Hydrophobic changes in a protein structure are relevant to its aggregation. ANS, 8-Anilino-1-naphthalene-sulfonic acid is a fluorescent molecular probe effectively binds the solvent-exposed hydrophobic residues of the protein [92] upon aggregation. Enhanced fluorescence intensity with blue shift in wavelength of ANS emission is a greater indication of amyloid formation [93]. **Fig 4.8 A and B** showed the results obtained by ANS assay. Here the visible increase in fluorescence emission intensity along with a blue shift of wavelength maxima from 512 to 475 nm observed in case of heat treated insulin. This is due to the thermal unfolding of protein followed by exposure of hydrophobic amino acid residues which in turn facilitates ANS to bind more. If the said exposure can be prevented then protein aggregation may also be inhibited. As the curves depicted, the presence of ferric and cupric metal ions separately caused decrease in ANS emission intensity with red shift towards native like spectra. It was also shown of Fe^{3+} ions in increasing conc. while Cu^{2+} in decreasing conc. minimized the ANS emission. At millimolar ratio, 1: 30 for ins: Fe^{3+} and 1:0.5 for Ins: Cu^{2+} were observed maximum inhibition of exposure of hydrophobic residues of insulin under aggregation condition. Additionally, this suggested the interaction of metal ions with insulin in a way to prevent its unfolding followed by misfolding and thus stabilizing the monomeric form of human insulin in solution.

Monitoring secondary structural changes upon aggregation in experimental conditions

Circular Dichroism (CD) and Fourier transform infrared (FTIR) assays are considered to be standard methods for detecting secondary structural forms of protein. Far UV-CD results of insulin aggregation in presence of Fe^{3+} and Cu^{2+} was noted in **fig. 4.8.C and D** respectively.

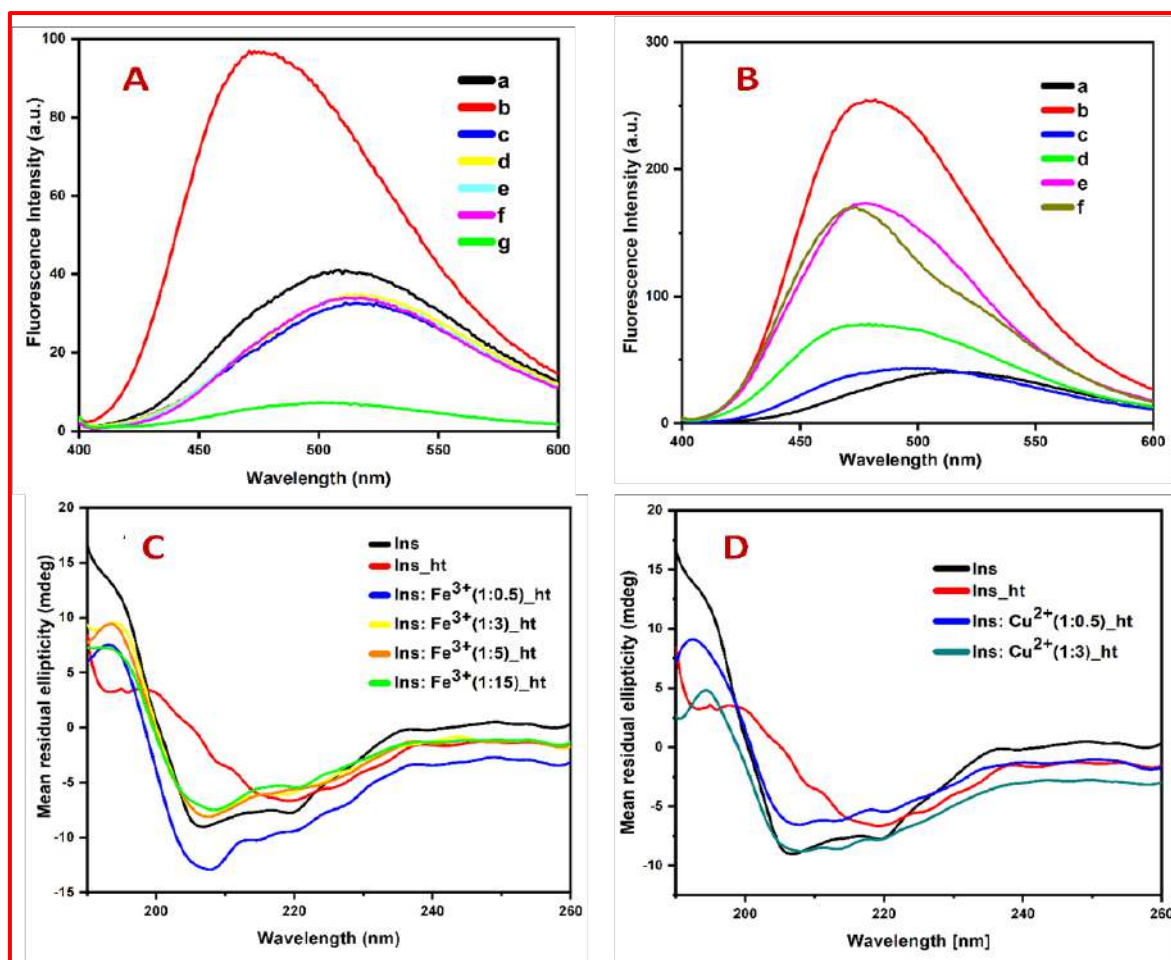


Fig.4.8. Monitoring conformational changes of insulin under experimental conditions. Fluorescence emission spectra as obtained by ANS assay (panels A and B) of monomeric insulin (curve a) and heat treated (60°C for 4h) insulin (curve b). (panel A) rest of the spectral curves were of thermally incubated insulin samples in presence of Fe^{3+} ions at different millimolar ratios viz., 1:0.5, 1:3, 1:5, 1:15 and 1:30 by curves c-g respectively. Panel B showed thermally incubated insulin in presence of Cu^{2+} ions at different millimolar ratios (1:0.5, 1:3, 1:5 and 1:15) by curves c-f respectively. Excitation wavelength was 350 nm while emissions range was 400–600 nm. Protein and ANS dye concentrations were 5.5 μM and 30 μM respectively. Path length of cuvette was 1 cm. Each scan was performed in triplicates and averaged. Blank values (only 30 μM ANS) were subtracted before presenting. Panels C and D showed Far-UV CD spectra of monomeric insulin (black, heat treated insulin (red), heat treated insulin in presence of Fe^{3+} ions (panel C) and in presence of Cu^{2+} ions (panel D) at different interaction ratio. The protein concentration for CD assay was maintained as 6.5 μM .

The spectra obtained for monomeric insulin (black curve, both panel C and D) had two prominent negative ellipticities at 208 and 222 nm. This is a characteristic feature of alpha-predominating conformation of protein like insulin. The minima alteration occurred in case of heat treated insulin to around 220 nm (red curve, in both Fig. 4.8 C and D), which is a significant indication of beta-sheet rich population in secondary structure causing due to amyloid formation.

Table. 4.1 Quantitative analysis of secondary structures of insulin under normal and aggregating conditions in absence and presence of metal ions (Fe^{3+} and Cu^{2+})^a

Samples	% of α -Helix	% of β -Sheet		% of β -Turn	% of Random coil
		Antiparallel	Parallel		
Monomeric Insulin (MI)	22.41	21.0	18.82	17.41	20.35
Heat treated (HT) Insulin	17.92	21.98	22.18	17.84	20.08
MI :Fe^{3+} (1:0.5)_HT	22.42	17.75	19.70	17.75	22.38
MI :Fe^{3+} (1:3)_HT	20.57	20.22	20.53	20.69	17.98
MI :Fe^{3+} (1:5)_HT	13.25	26.28	10.24	15.14	35.10
MI :Cu^{2+} (1:0.5)_HT	17.04	24.62	9.46	16.23	32.60
MI :Cu^{2+} (1:3)_HT	18.77	24.12	9.26	16.52	31.32

^a determined by CDNN 2.1 software

The decrease in percentage of alpha helix with concomitant increase of beta-sheet content after heat aggregation of insulin was quantified in Table 4.1. In case of iron treated samples the alpha helical conformation was greatly maintained near monomeric form. Negligible increase occurred in parallel beta-sheet percentages while the total percentages of beta-sheet remained same i.e., around 56 percent which closely resembled that of monomer form of insulin. Though in a higher percentage, iron induces random coiling in insulin during aggregation. Cu^{2+} on the other hand was not so effective in maintaining alpha helical form like Fe^{3+} . Though the total percentages of beta sheet population decreased slightly yet, percentages of antiparallel beta-sheet had increased. Cu^{2+} also increased the random coiling of insulin more than Fe^{3+} . Thus from results, it can be said that Fe^{3+} was more effective in insulin amyloid inhibition than Cu^{2+} even at lower interaction ratio.

FTIR was also done to confirm about the secondary structural changes of insulin under thermal incubation (60°C for 4h). Insulin aggregated both in absence and presence of Fe^{3+} and Cu^{2+} was analyzed by FTIR and illustrated in fig.4.9. Insulin monomer gave the amide-I transmittance minima around 1650 cm^{-1} (black curve in panel A and B, selected portion of IR

spectra [1800-1500 cm^{-1}] were shown in brown in both panels C and D of the same fig) due to the alpha-helical structure predominance. Where, the weaker amide-II band position at 1547 cm^{-1} was also confirmed the said predominance. After heat incubation, insulin showed an inverted maxima in the amide-I region at $\sim 1630 \text{ cm}^{-1}$ (red curve, panel C and D) indicating transformation of alpha-helix to cross-beta sheet which was due to insulin amyloid generation. A small shoulder around 1618 cm^{-1} was also confirmed the presence of stable beta-sheet in the fibrils. The small band at $\sim 1712 \text{ cm}^{-1}$ indicated the presence of deuterated carboxyl groups [94].

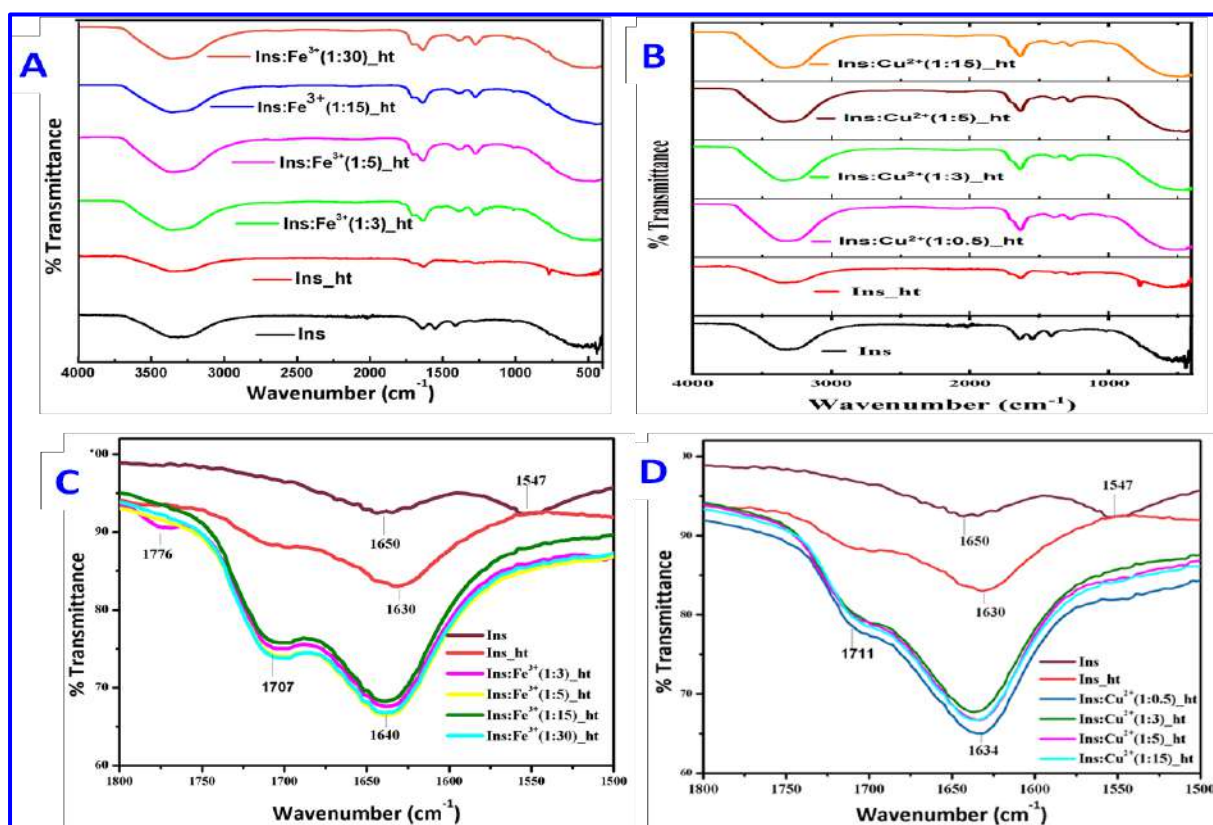


Fig. 4.9. Fourier transform infrared (FTIR) spectra of insulin under aggregation in presence and absence of Fe^{3+} ion [Panel A, C] and Cu^{2+} ions [Panel B, D] incubated at different milimolar ratio with insulin (Ins). Protein concentrations was maintained at 0.1722 mM throughout the assay. Selected region [1800-1500 cm^{-1}] was shown in panel C and D. Spectra of heat treated human insulin was shown in red curve while monomeric insulin was in brown curve. Aggregation of insulin in the presence of Fe^{3+} ion, i.e., ins: Fe^{3+} at milimolar ratio of 1:3, 1:5, 1:15, 1:30 was depicted in panel C while Cu^{2+} treated insulin, i.e., ins: Cu^{2+} (at milimolar ratio of 1:0.5, 1:3, 1:5, 1:15) was given in panel D. Each spectrum was obtained by average of 16 consecutive scans.

The pattern of spectra for the insulin aggregates formed in the presence of increasing concentrations of Fe^{3+} ions were found to have reduced transmittance and shifting of minima towards that of monomeric form (Panel C). The lowering of transmittance percentage in both the panels under metal influence was an indication of conjugation of insulin with metal ions [95]. Upon conjugation, Fe^{3+} ions prevented the thermal exposure of the hydrophobic clusters of insulin and thus inhibited the aggregation. Cu^{2+} ions affected the curve minima slightly shifted toward insulin monomer. Inhibition of fatal structural transitions (α -helix to β -sheet preminating structure) during thermal co-incubation of insulin with Cu^{2+} were also prominent at lower molar concentration of it.

Performing light scattering assays to monitor aggregation

Rayleigh scattering assay (RLS) and Dynamic Light Scattering assay (DLS) were performed to confirm about the particle size in solution under aggregating conditions with metal ions.

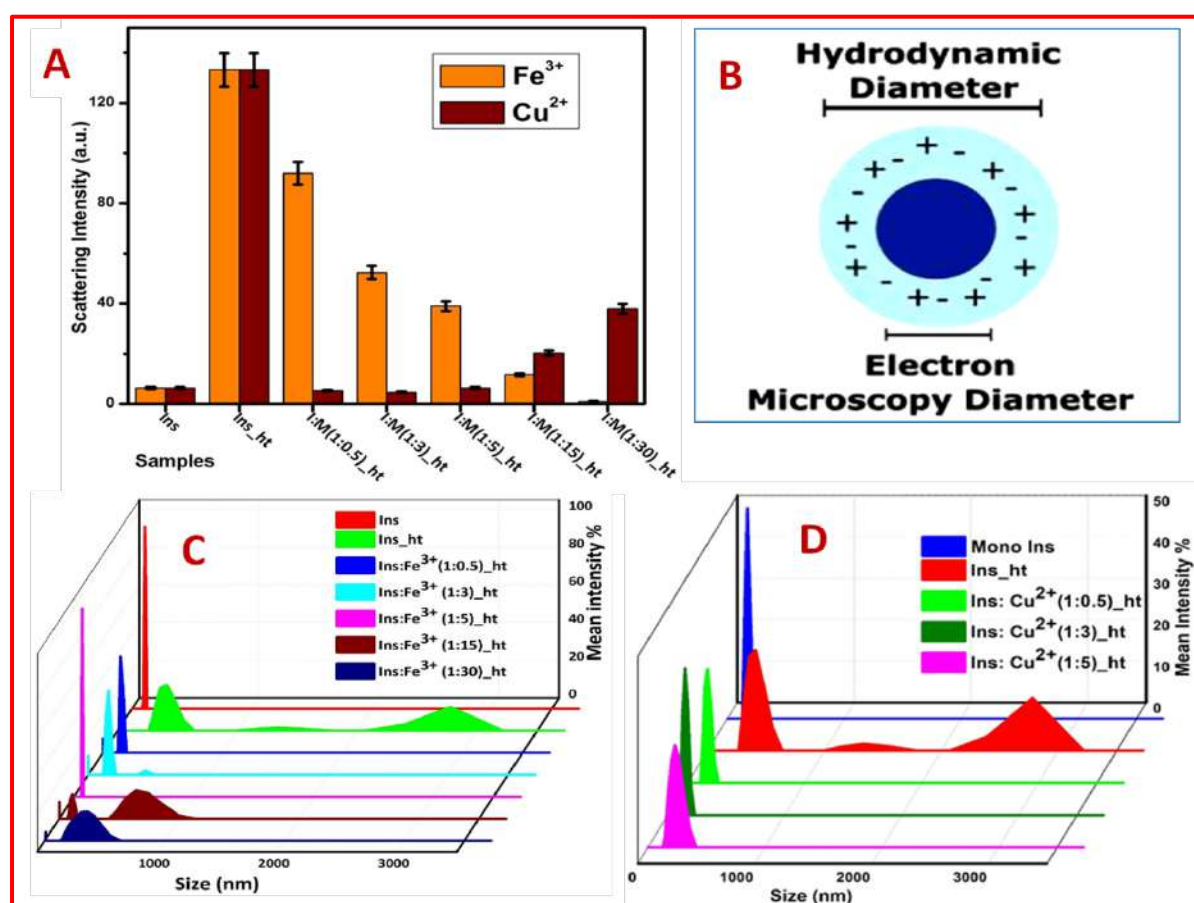


Fig. 4.10. A Bar diagram representing Rayleigh Light Scattering emission intensity of monomeric insulin (Ins), heat treated insulin (Ins_ht), heat-treated insulin co-incubated at different milimolar ratio, insulin: metal ion (I:M ratio) from 1:0.5 to 1:30 were shown both

in absence and presence of Fe^{3+} (in orange) and Cu^{2+} (in brown) separately. Excitation and emissions both wavelength was 307 nm. The data represented were blank corrected and averaged of three independent measurements. The error bars were within the range of ± 2.0 . Panel B. Schematic representation of Hydrodynamic radius (adapted from Maguire CM. et. al., 2018, Sci. Technol. Adv. Mater., 19(1), 732–745, <https://doi.org/10.1080/14686996.2018.1517587>). Panel C and D represented the DLS assay results of heat treated insulin in presence of Fe^{3+} and Cu^{2+} respectively. Particle size with respect to their distribution intensities were shown here. Increase in particle size of different range in aggregated form of insulin was compared with insulin in monomeric form and metal –incubated heat treated forms depicted by different colors. Insulin concentration was 20 μM in each sample.

Liquids with low concentrations of suspended particles may follow Rayleigh scattering event [96]. Here, both the excitation and emission wavelengths were 307nm, as it is known that neither loss nor any gain of energy is involved in this process. [97]. Significant rise of RLS scattering intensity was observed in heat treated insulin (2nd bar, Fig.4.10.A) compared to insulin monomer (1st bar, Fig.4.10.A) and is an indication of the presence of the aggregated structure. The degree of light scatterings by heat incubated insulin in presence of Fe^{3+} and Cu^{2+} ions were observed in orange and brown bars respectively in Fig.4.10.A. Both the metals lowered the scattering intensity of insulin under aggregating conditions and thus proved in maintenance of particle size like monomeric insulin by them during aggregating condition. At higher interacting conc., though Cu^{2+} showed slight increase in size of particles. Overall, the decrease in scattering intensity in presence of the two metal ions separately evidenced the presence of smaller aggregates of insulin instead of higher aggregates. Therefore, these two metal ions were considered to be possessing hindrance in thermal aggregation of insulin and this is in accordance with the findings of previous studies.

Another important approach to study the objectives is DLS also known as photon correlation spectroscopy (PCS). It employs a powerful light-scattering technique and reveals the particle size distributions of suspensions and solutions of colloids, biological solutions, macromolecules and polymers. The Brownian motion in solution caused by irradiating monochromatic light from a laser source, gives a Doppler shift. The hitting of light on a moving particle is sensed by alteration in wavelength (typically red light at 633 nm or near-infrared at 830 nm for bimolecular applications) of the incoming light. This change is corresponded to the size of the particles with their intensities in solution [98]. The

hydrodynamic diameter is greater than the particle diameter because of the presence of ligand and solvated water molecules as shown in Fig.4.10.B. Fig.4.10.C and D showed patterns of distribution of particle size of human insulin as well as insulin aggregates in the absence and presence of metal ions. Insulin aggregates expectedly showed significant increase in particle size than monomeric insulin (red, in fig.4.10.C and blue, in fig.4.10.D). The hydrodynamic radii of monomeric insulin were determined to be in the range of 95 to 110 nm but enhancement in its size up to 2.8 μm due to thermal incubation at 60 $^{\circ}\text{C}$ for 4h indicating the generation of amyloid fibrils. The realization of particle size in the lower range i.e., 95-127 nm in Fe^{3+} co-incubated insulin (Fig.4.10.C) proved the protection imposed by Fe^{3+} on insulin against thermal aggregation. Cupric ion also maintained the average size in between the ranges 127-198 nm (Fig.4.10.D) and also proved to be less effective in protecting the monomer form of insulin than Fe^{3+} . The best inhibition imposed by the two cations were in the interaction ratio as follows - Ins: Fe^{3+} (1: 5) and Ins: Cu^{2+} (1: 0.5).

Morphological revelation of different insulin aggregates

FE-SEM (Field Emission Scanning Electron Microscopy) and Transmission electron microscopy (TEM) are significant tools to confirm the previous studies and understanding of morphology of insulin fibrils generated under different experimental conditions. FE-SEM was used here to reveal the surface morphology of different aggregated species of human insulin. Fig.4.11.a and b discovered the surface morphologies of monomeric insulin while c and d showed the insulin aggregates. The aggregates were spherical having approximate diameter of around 489.6 nm (shown under 5 μM resolution in Fig. 4.11.d). In presence of Fe^{3+} ions (Fig.4.11.e and f) small spherules or very tiny worm-like aggregates were found. Under 5 μM resolution (Fig.4.11.f) the reduced size of the aggregates were determined to be approximately 125-280 nm. Fe^{3+} thus proved to be effective in reducing larger aggregate formation of insulin. Cu^{2+} under co-incubating conditions though formed small ragged fibrils (Fig.4.11.g) under 5 μm resolution. The fibrillar morphology was greatly transformed to ‘needle like shape’ from spherical clumps due to effect of Cu^{2+} ions as shown under 1 μm resolution (Fig.4.11.h).

For getting ultra structural views of insulin aggregates under different experimental conditions, TEM imaging was performed on samples. Insulin formed dense, thick, fibrillar network in absence of any metal ions under aggregation conditions. The said fibrils are identical with the amyloid structure of insulin [99] and shown in Fig. 4.12 A and B.

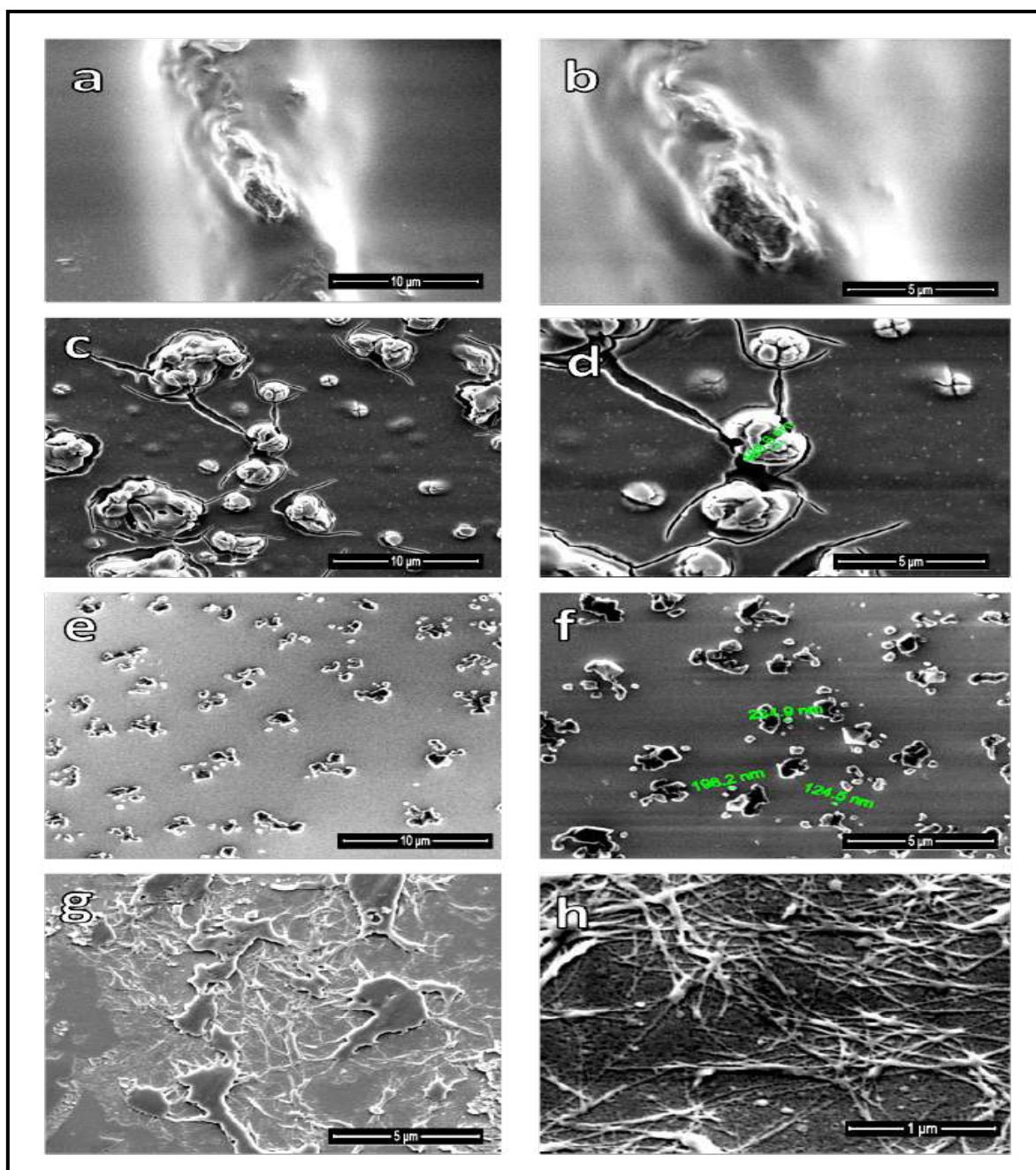


Fig. 4.11. FE-SEM images of varied species of insulin aggregates: images ‘a’ and ‘b’ were of surface morphology of monomeric insulin in absence of any metal ions. ‘c’ and ‘d’ represented the heat treated (60⁰ C, 4h) form of insulin. Figure ‘e’ and ‘f’ showed insulin aggregation in presence of Fe³⁺ ions while ‘g’ and ‘h’ exhibited the said aggregation in presence of Cu²⁺ ions. Vertically, all the four panels aligned left gave images of lower resolution while that of right the morphologies of heat aggregated insulin in the presence of, All images of left panel were produced under lower magnification where corresponding images of right panel were of higher magnifications.

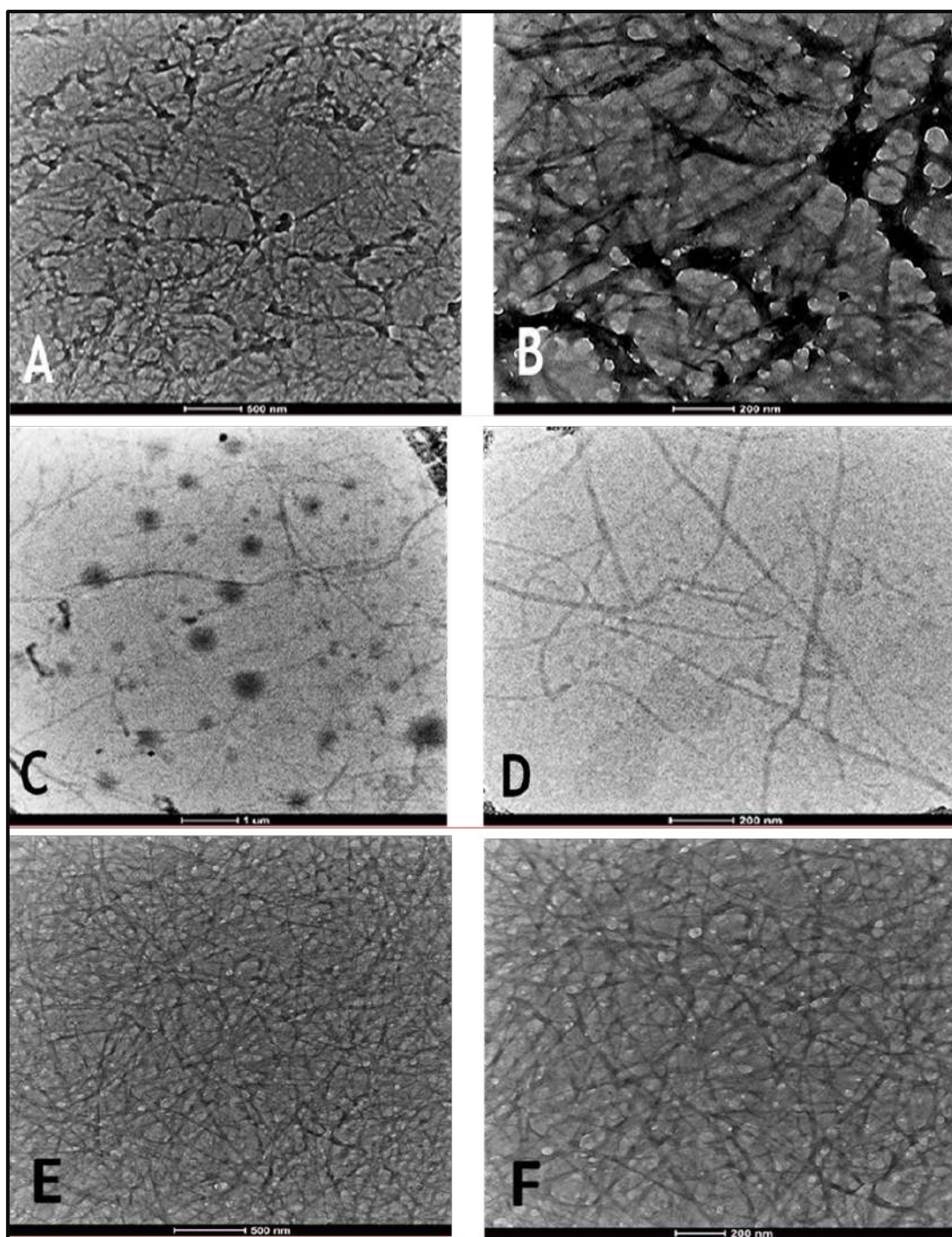


Fig. 4.12. The Transmission electron microscopic images of thermally incubated (at 60 °C for 4h) insulin aggregates in absence and presence of Fe^{3+} and Cu^{2+} ions: insulin aggregates (without metal ion) were shown in Panel A and B under 500 nm and 200 nm resolution respectively. Aggregated species in presence of Fe^{3+} were depicted in C and under 1 μm and 200 nm resolution respectively. Lastly, panel E and F represented the images of insulin aggregates formed in presence of Cu^{2+} under 500nm and 200nm resolution respectively.

Fe^{3+} insulin samples (Fig 4.12. C and D) revealed the inhibition posed by the metal on amyloid fibrillation as revealed by the appearance of very few fibrils. The fibrillar mesh like structure was almost getting vanished under the influence of iron. The fewer fibrils that were still formed showed thin and slender appearances. On the other hand, Fig. 4.12.E and F represented Cu^{2+} ion treated insulin aggregates. Here though the occurrence of generated fibrils was higher than that of Fe^{3+} treated one. The nature of the fibrils was less networked, shorter and thinner and ragged compared to insulin amyloids. Thus it can be said that, the metal ions Fe^{3+} and Cu^{2+} reduced the propensity of amyloid fibrillation where the former is more effective than the latter. Previous studies also supported the statement.

Molecular docking pose of metal ions on insulin

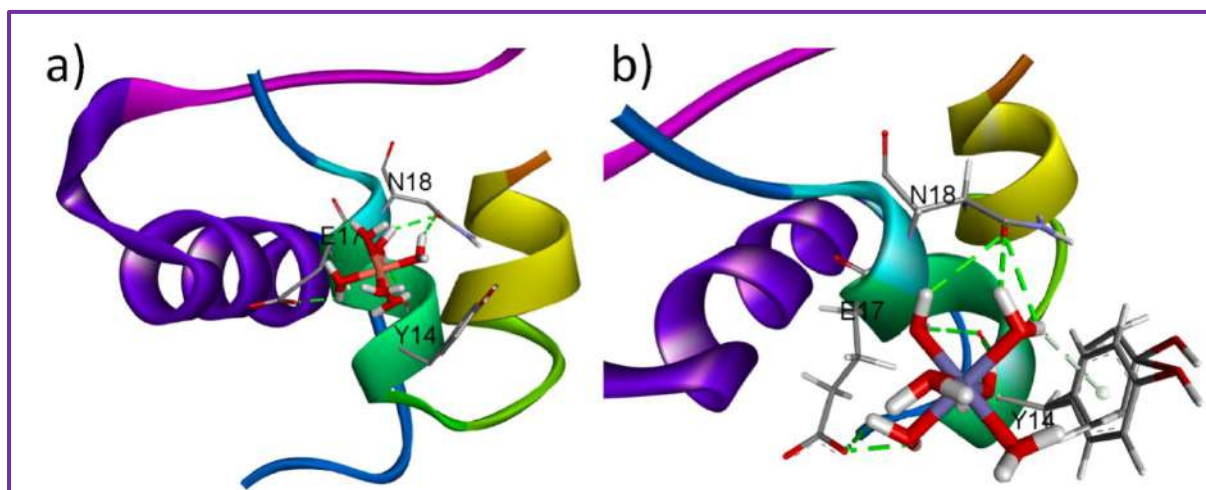


Fig. 4.13. Molecular Docking pose of hydrated (a) Cu^{2+} and (b) Fe^{3+} treated human insulin monomer

Binding of small molecules to proteins can be presumed by Molecular docking through software proceedings. Not only the most probable binding position but also the pose as well as the forces involved in the binding process can be determined. Here the metal ions used were intended to be hydrated in solution. For that reason, molecular docking was performed by presuming the hydrated of Cu^{2+} and Fe^{3+} with monomeric human insulin. The docking results shown in Fig. 4.13 gave individual poses posed by Cu^{2+} (a) and Fe^{3+} (b). the free energy changes due to insulin binding was calculated as -6.31 kcal/mol for Cu^{2+} and -7.02 kcal/mol for Fe^{3+} . These data clearly confirmed the more favorable and stable binding by Fe^{3+} than the other metal ion. Fe^{3+} upon binding may cause the increased positive charge density on the protein surface which leads to inhibition of aggregation by preventing self

assembly of insulin. Additionally, it was found that both the docking of hydrated Cu^{2+} and Fe^{3+} took place at similar position of the protein and they are Y14, E17, and N18 amino acid residues. The stabilizing force in this case was Hydrogen bonding between the water molecules attached to the metal ion and the amino acid residues of the protein. Besides this, polar interactions with Y14 may be the prime reason for the strong binding of Fe^{3+} ion to the protein.

4.6. DISCUSSIONS AND MAJOR CONCLUSIONS

Change of pH greatly alters the temperature driven human insulin fibrillation. Human insulin tends to remain monomeric at acidic pH but near the neutral pH, the hexameric form is prevalent. Temperature induction may aggregate insulin in storage conditions at low pH or through monomeric intermediate formation. In an approach to inhibit temperature induced aggregation, metal ions viz., Fe^{3+} and Cu^{2+} were employed and proved effective at low interacting concentrations. The supporting experiments were as follows:

Fluorescent probe, Th T along with the kinetics study of insulin amyloid fibrillation hinted that effectivity of Fe^{3+} was lies in the delay of nucleation or lag phase. Shortening of log phase by it also prevent fibril maturation and elongation event. Initiation of fibrillation cannot be affected by Cu^{2+} while it was effective only in preventing oligomerization during heating. Thus amount of mature fibril generated in the course of aggregation kinetics was lowered by it (Fig. 4.7.A). The order of the inhibitory potential on insulin aggregation was $\text{Ins: Fe}^{3+} (1:30) > \text{Ins: Fe}^{3+} (1:15) > \text{Ins: Cu}^{2+} (1:3) > \text{Ins: Cu}^{2+} (1:0.5)$.

Fe^{3+} and Cu^{2+} , the two abundant transition metal ions were proved effective in inhibition on insulin fibrillation, though Cu^{2+} inhibits the amyloid fibrillation in less molar concentration than Fe^{3+} . ANS spectral analysis showed the structural unfolding and subsequent misfolding of insulin during thermal incubation promoted it to expose the abundant buried hydrophobic amino acid residues. Fe^{3+} and Cu^{2+} both effectively inhibited this kind of exposure and thus maintained the hydrophobicity of the native fold (Fig.4.8.A and B). Far-UV circular dichroism (Far-UV CD) spectral data analysis gave another clue to the mechanism of inhibition by these two metal ions. Fe^{3+} maintained the percentages of alpha helices near that of monomeric form while Cu^{2+} inhibited the increased generation of cross beta sheet formation during aggregation (Table 4.1).

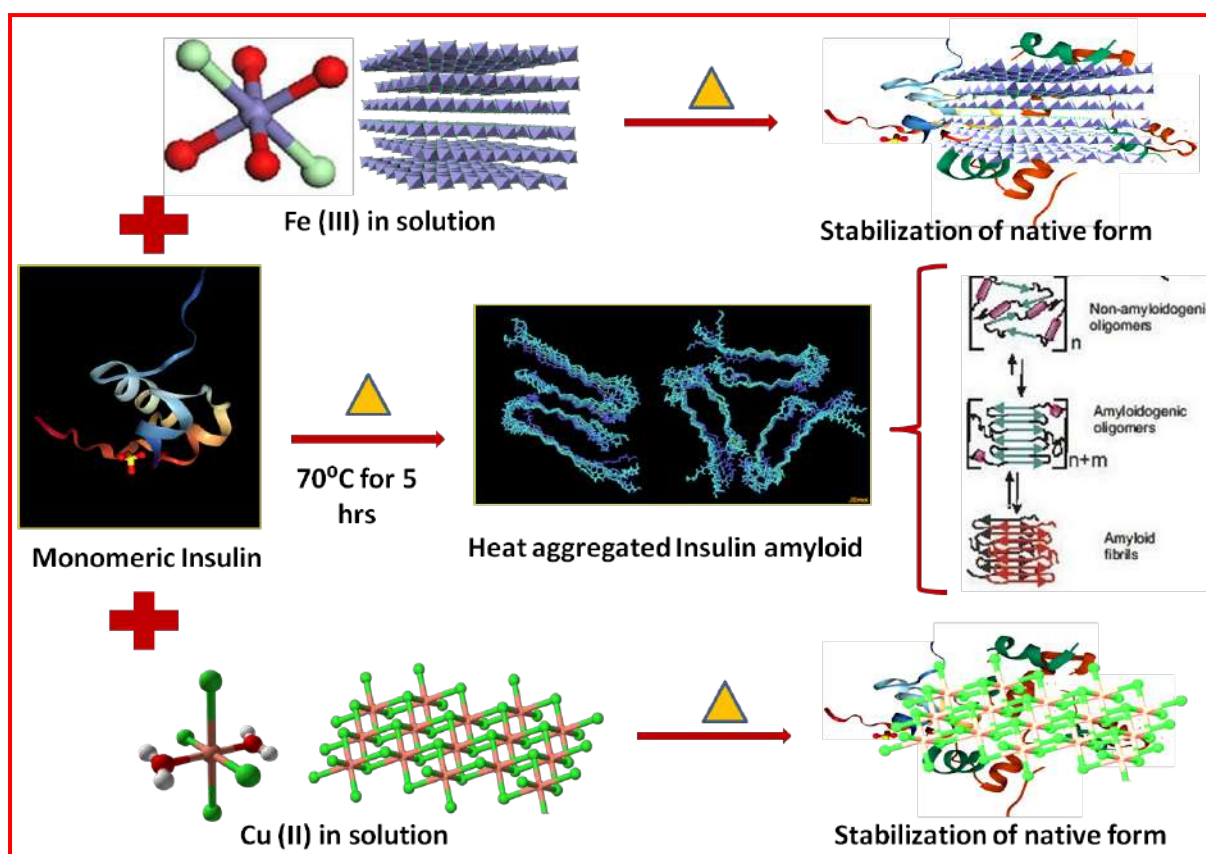


Fig.4.14. The proposed mechanism of inhibition of partial unfolding and aggregation formation of human insulin by Fe^{3+} and Cu^{2+} metal ions while co-incubated separately with insulin.

Dynamic light scattering study deciphered the diameter of monomeric insulin in the range 95-110 nm which greatly increased with varying intensity in thermally aggregated form. The aggregated diameter was shown to in a variable range of around 350-550 nm, 1.3-1.5 μm , and 2.4-2.7 μm (Fig.4.10.C and D). Fe^{3+} ions possessed a great reduction of the said diameters of insulin assembly which was ranging from 95-127 nm (majorly), 265-356nm (very few). Thus it can be said that Fe^{3+} ions help to retain the native like structure of insulin. Cu^{2+} also retained the native conformation of the insulin by maintaining the size of diameter in between 127-198nm (major), 300-550nm (very few). Morphological studies with FESEM technique were in accordance with the results obtained from the said experiments and added the information of the small spherule and worm-like structure formation in presence of Fe^{3+} and 'needle shaped' morphology of protein aggregates upon Cu^{2+} binding (Fig.4.11). However, although both Fe^{3+} and Cu^{2+} effectively reduced the diameter of aggregates separately by inhibiting or slowing down the process of fibrillation, Fe^{3+} reduced the affinity to form

cluster/aggregate of insulin as fewer aggregates were formed with lesser diameter. Transmission electron microscopic images also agreed with the FESEM data and shown the lesser fibril formation in case of iron and copper treated samples (Fig.4.12). Molecular docking result (Fig.4.13) also confirmed the favorable binding of Fe^{3+} with greater binding affinity than Cu^{2+} . ΔG° value for binding of Fe^{3+} with protein was found to be -7.02 kcal/mol where for that for Cu^{2+} was -6.31 kcal/mol.

The pHs for all of the experiments were acidic pH (pH 1.6). In that pH, the side chains of insulin are protonated and an overall positive charge is imparted to the said protein. However, the interaction of insulin with the positively charged metal ions may occur. The supporting information for the interactions is as follows: both of them are transition metal ions. The electronic configuration for Fe^{3+} is $3s^2 3p^6 3d^5$ and that of Cu^{2+} is $[\text{Ar}] 3d^9$. Both of them have d-electrons. The experiments were performed in aqueous media having water as solvent and both the metal ions favorably form either octa or hexa-coordinated complex with water in dissolved conditions (respective hydroxides are also formed with water). For that reason, they can easily interact with protein side chains while dissolved in solutions by means of water mediated hydrogen bonding. The similar occurrence was observed for iron in vivo cases where iron has made conjugation with protein like hemoglobin in order to perform oxygen transport and electron transferring reactions. Secondly, the two said metal ions are very good heat and electrical conductors and possibly because of their heat conducting nature they somehow neutralized the thermal incubation effect on protein structure. There are many evidences of co-ordination of insulin with Zn^{2+} [100], Mg^{2+} [101], Ca^{2+} [101]. Zn^{2+} stabilize the native structures of proteins with high binding affinity, better bioavailability, increased Lewis acidity, higher substitution rates for ligands, flexible geometry of coordination, and redox inactivity [100]. Similarly Fe^{3+} in a stable way makes co-ordination with proteins and the hydrophobic surface of porphyrins. It was evident that most transition metal ions (Fe, Co, Ni, Cu, Zn, and Hg) are generally present in the interface or in a non interfacial location and also the metal ions can contingently bind to protein surfaces [101]. A protein's native functional conformation may well be stabilized by metal coordination [102]. Generally, aspartate/asparagine, glutamate, histidine and cysteine residues of proteins coordinate with transition metal ions and strengthen the metal-protein interactions which further couples with the protein-protein interactions. Cu^{2+} is in an oxidized state and so a very good electron acceptor. Cu^{2+} at low pH may not fully bind with insulin monomeric form. Cu^{2+} compared to Cu^+ possess greater hydration energy and thus the binding of Cu^{2+} in water with protein is

avored. At highly acidic pH, Cu^{2+} ions in aqueous solution do not bind to proteins in an appreciative manner but it favors the self association of insulin at a faster rate than Fe^{3+} . The accelerated nucleation rate/self aggregation of insulin as well as quick nucleation (within 90 min) was the proof for it as compared to Fe^{3+} (lag phase is of around 150 min). Though, the aggregation propensity of insulin had greatly decreased in the presence of Cu^{2+} ions. Thus it can be stated that, Cu^{2+} favorably binds the self-aggregated structure of insulin with accessible surface interactions through Tyr, Glu and Asn side chains of insulin and thus preventing the extension of amyloid fibril of insulin and also inhibiting the formation of the higher sized aggregates. These two metal ions are essential micronutrients for human being at very low concentrations.

4.7. REFERENCES

1. Sorokina I., Mushegian A.R., Koonin E.V. 2022 Is Protein Folding a Thermodynamically Unfavorable, Active Energy-Dependent Process?. *Int. J. Mol. Sci.*, 23: 521, [10.3390/ijms23010521](https://doi.org/10.3390/ijms23010521).
2. Verma M., Vats A., Taneja V. 2015. Toxic species in amyloid disorders: Oligomers or mature fibrils. *Ann Indian Acad Neurol*, 18: 138-145, [10.4103/0972-2327.144284](https://doi.org/10.4103/0972-2327.144284)
3. Dikiy I., Eliezer D. 2012. Folding and misfolding of alpha-synuclein on membranes. *Biochim Biophys Acta.*, 1818: 1013–1018, <https://doi.org/10.1016/j.bbamem.2011.09.008>
4. Cao P., Abedini A., Raleigh D.P., 2013. Aggregation of islet amyloid polypeptide: from physical chemistry to cell biology. *Curr Opin Struct Biol.*, 23: 82–89, <https://doi.org/10.1016/j.sbi.2012.11.003>
5. Gupta Y., Singla G., Singla R. 2015. Insulin-derived amyloidosis, *Indian J. Endocrinol. Metab.*, 19 (1): 174–177, [10.4103/2230-8210.146879](https://doi.org/10.4103/2230-8210.146879)
6. Lopes D.H.J., Meister A., Gohlke A., Hauser A., Blume A., Winter R. 2007. Mechanism of Islet Amyloid Polypeptide Fibrillation at Lipid Interfaces Studied by Infrared Reflection Absorption Spectroscopy. *Biophys J.*, 93: 3132–3141, <https://doi.org/10.1529/biophysj.107.110635>
7. Yoshihara H., Saito J., Tanabe A., Amada T., Asakura T., Kitagawa K., Asada S., 2016, Characterization of novel insulin fibrils that show strong cytotoxicity under physiological pH, *Pharm. Biotechnol.*, 105(4), 1419–1426, <https://doi.org/10.1016/j.xphs.2016.01.025>
8. Oren Z., Shai Y. 1998. Mode of action of linear amphipathic alpha-helical antimicrobial peptides. *Biopolymers.* 47:451–463, [https://doi.org/10.1002/\(SICI\)1097-0282\(1998\)47:6<451::AID-BIP4>3.0.CO;2-F](https://doi.org/10.1002/(SICI)1097-0282(1998)47:6<451::AID-BIP4>3.0.CO;2-F)
9. Soto C., Pritzkow S. 2018. Protein misfolding, aggregation, and conformational strains in neurodegenerative diseases, *Nat Neurosci.*, 21(10):1332–1340, [10.1038/s41593-018-0235-9](https://doi.org/10.1038/s41593-018-0235-9)
10. Hjorth C.F., Norrman M., Wahlund P.O., Benie A.J., Petersen B.O., Jessen C.M., Pedersen T. Å., Vestergaard K., Steensgaard D.B., Pedersen J.S., Naver H., Hubálek F., Poulsen C., Otzen D., 2016. Structure, Aggregation, and Activity of a Covalent Insulin Dimer Formed During Storage of Neutral Formulation of Human Insulin, *J. Pharm. Sci.*, 105(4): 1376-1386, [10.1016/j.xphs.2016.01.003](https://doi.org/10.1016/j.xphs.2016.01.003).

11. Salahuddin P., Siddiqi M.K., Khan S., Abdelhameed A.S., Khan R.H. 2016. Mechanisms of protein misfolding: Novel therapeutic approaches to protein-misfolding diseases, *J. Mol. Struct.*, 1123: 311-326, [10.1016/j.molstruc.2016.06.046](https://doi.org/10.1016/j.molstruc.2016.06.046)
12. Rambaran R.N., Serpell L.C. 2008, Amyloid fibrils; Abnormal protein assembly, *Prion*, 2(3) : 112-117, <https://doi.org/10.4161/pri.2.3.7488>
13. Sahoo S., Reeves W., DeMay R.M. 2003, Amyloid tumor: A clinical and cytomorphologic study, *Diagn. Cytopathol.*, 28: 325–328, [10.1002/dc.10296](https://doi.org/10.1002/dc.10296)
14. Yumlu. S., Barany R., Eriksson M., Rocken C. 2009, Localized insulin-derived amyloidosis in patients with diabetes mellitus: A case report, *Human Pathol.* 40: 1655–1660. [10.1016/j.humpath.2009.02.019](https://doi.org/10.1016/j.humpath.2009.02.019)
15. Swift B., Hawkins P., Richards C., Gregory R. 2002, Examination of insulin injection sites: An unexpected finding of localized amyloidosis., *Diabet. Med.*, 19(10): 881–882, [10.1046/j.1464-5491.2002.07581.x](https://doi.org/10.1046/j.1464-5491.2002.07581.x)
16. Albert S.G., Obadijah J., Parseghian S.A., Hurley Y., Mooradian M. 2007, Severe insulin resistance associated with subcutaneous amyloid deposition, *Diabet. Res. Clin. Pract.*, 75: 374–376, [10.1016/j.diabres.2006.07.013](https://doi.org/10.1016/j.diabres.2006.07.013)
17. Wolfe K.J., Cyr D.M., 2011, Amyloid in neurodegenerative diseases: Friend or foe? *Semin. Cell Dev. Biol.*, 22, 476–481, <https://doi.org/10.1016/j.semcdb.2011.03.011>
18. Naiki H., Nagai, Y. 2009. Molecular pathogenesis of protein misfolding diseases: pathological molecular environments versus quality control systems against misfolded proteins. *J Biochem.*, 146: 751–756. <https://doi.org/10.1093/jb/mvp119>
19. Fagihi M.H.A. and Bhattacharjee S. 2022. *ACS Pharmacol. Transl.*, 5 (11) : 1050-1061. [10.1021/acsptsci.2c00174](https://doi.org/10.1021/acsptsci.2c00174)
20. Savelieff MG., DeToma AS., Derrick JS., Lim MH. 2014. The ongoing search for small molecules to study metal-associated amyloid-beta species in Alzheimer's disease. *Acc Chem Res.*, 47(8):2475–2482, <https://doi.org/10.1021/ar500152x>
21. Korshavn KJ., Jang M., Kwak YJ., Kochi A., Vertuani S., Bhunia A. 2015. Reactivity of metal-free and metal-associated amyloid-beta with glycosylated polyphenols and their esterified derivatives. *Sci Rep.*, 5:17842, <https://doi.org/10.1038/srep17842>
22. Yamada M., Ono K., Hamaguchi T., Noguchi-Shinohara M. 2015. Natural phenolic compounds as therapeutic and preventive agents for cerebral amyloidosis. *Adv Exp Med Biol.*, 863:79–94, https://doi.org/10.1007/978-3-319-18365-7_4
23. Mishra S., Palanivelu K. 2008. The effect of curcumin (turmeric) on Alzheimer's disease: an overview. *Ann Indian Acad Neurol.*, 11(1):13–19, [10.4103/0972-2327.40220](https://doi.org/10.4103/0972-2327.40220)

24. Rigacci S. 2015. Olive oil phenols as promising multi-targeting agents against Alzheimer's disease. *Adv Exp Med Biol*, 863:1–20, https://doi.org/10.1007/978-3-319-18365-7_1
25. Palhano FL., Lee J., Grimster NP., Kelly JW. 2013. Toward the molecular mechanism(s) by which EGCG treatment remodels mature Amyloid Fibrils. *J Am Chem Soc.*, 135(20):7503–7510, <https://doi.org/10.1021/ja3115696>
26. Ishii T., Mori T., Tanaka T., Mizuno D., Yamaji R., Kumazawa S. 2008. Covalent modification of proteins by green tea polyphenol (–)-epigallocatechin-3-gallate through autoxidation. *Free Radical Biol Med.*, 45(10):1384–1394, <https://doi.org/10.1016/j.freeradbiomed.2008.07.023>
27. Tu LH., Young LM., Wong AG., Ashcroft AE., Radford SE., Raleigh DP. 2015. Mutational analysis of the ability of resveratrol to inhibit amyloid formation by islet amyloid polypeptide: critical evaluation of the importance of aromatic-inhibitor and histidine-inhibitor interactions. *Biochemistry*. 54(3):666–676, <https://doi.org/10.1021/bi501016r>
28. Cheng B., Gong H., Xiao H., Petersen RB., Zheng L., Huang K. 2013. Inhibiting toxic aggregation of amyloidogenic proteins: a therapeutic strategy for protein misfolding diseases. *Biochim Biophys Acta.*, 1830 (10): 4860–4871. <https://doi.org/10.1016/j.bbagen.2013.06.029>
29. Jayamani J., Shanmugam G., Azhagiya Singam E.R. 2014., Inhibition of insulin amyloid fibril formation by ferulic acid, a natural compound found in many vegetables and fruits, *RSC Adv.*, 107(10)1074, 6232610.1039/C4RA11291A
30. Fukuda M., Kameoka D., Torizawa T. 2014. Thermodynamic and Fluorescence Analyses to Determine Mechanisms of IgG1 Stabilization and Destabilization by Arginine. *Pharm Res.*, 31: 992–1001, <https://doi.org/10.1007/s11095-013-1221-2>
31. Shiraki K., Kudou M., Fujiwara S., Imanaka T., Takagi M. 2002. Biophysical effect of amino acids on the prevention of protein aggregation. *J. Biochem.*, 132: 591-595, [10.1093/oxfordjournals.jbchem.a003261](https://doi.org/10.1093/oxfordjournals.jbchem.a003261)
32. Arakawa T., Ejima D., Tsumoto K., Obeyama N., Tanaka Y., Kita Y., Timasheff S.N. 2007. Suppression of protein interactions by arginine: A proposed mechanism of the arginine effects. *Biophys. Chem.*, 127: 1-8, [10.1016/j.bpc.2006.12.007](https://doi.org/10.1016/j.bpc.2006.12.007)
33. Kawasaki T., Kamijo S. 2012. Inhibition of aggregation of amyloid β 42 by arginine-containing small compounds. *Biosci Biotechnol Biochem.*, 76: 762–766, <https://doi.org/10.1271/bbb.110879>

34. Takai E., Uda K., Matsushita S., Shikiya Y., Yamada Y., Shiraki K., Zako T., Maeda M. 2014. Cysteine inhibits amyloid fibrillation of lysozyme and directs the formation of small worm-like aggregates through non-covalent interactions. *Biotechnol Prog.*, 30(2): 470-478, [10.1002/btpr.1866](https://doi.org/10.1002/btpr.1866).
35. Kumar J., Sim V. 2014. D-amino acid-based peptide inhibitors as early or preventative therapy in Alzheimer disease. *Prion*. 8: 119–124, <https://doi.org/10.4161/pri.28220>
36. Ono K., Hasegawa K., Naiki H., Yamada, M., 2004. Anti-amyloidogenic activity of tannic acid and its activity to destabilize Alzheimer's beta-amyloid fibrils in vitro. *Biochim Biophys Acta.*, 1690: 193–202, <https://doi.org/10.1016/j.bbadis.2004.06.008>
37. Yang Y., Wu Y., Zhang S., Song W. 2013. High glucose promotes A β production by inhibiting APP degradation. *PLoS One*. 8: e69824, <https://doi.org/10.1371/journal.pone.0069824>
38. Zhu M., Rajamani S., Kaylor J., Han S., Zhou F., Fink A.L. 2004. The flavonoid baicalein inhibits fibrillation of alpha-synuclein and disaggregates existing fibrils. *J Biol Chem*. 279 : 26846–26857, <https://doi.org/10.1074/jbc.M403129200>
39. Khan A.N., Hassan M.N., Khan R.H. 2019. Gallic acid: A naturally occurring bifunctional inhibitor of amyloid and metal induced aggregation with possible implication in metal-based therapy. *J Mol Liq*. 285: 27–37. <https://doi.org/10.1016/j.molliq.2019.04.059>
40. Nunes OC., Manaia CM., Da Costa MS., Santos H. 1995. Compatible Solutes in the Thermophilic Bacteria *Rhodothermus marinus* and "*Thermus thermophilus*". *Appl. Environ. Microbiol.*, 61: 2351-2355, <https://doi.org/10.1128/aem.61.6.2351-2355.1995H>.
41. Santos H., da Costa M.S. 2001. Organic solutes from thermophiles and hyperthermophiles. *Methods Enzymol.*, 334: 302-315, [https://doi.org/10.1016/S0076-6879\(01\)34478-6](https://doi.org/10.1016/S0076-6879(01)34478-6)
42. Borges N., Ramos A., Raven N. D. H., Sharp R. J., Santos H. 2002. Comparative study of the thermostabilizing properties of mannosylglycerate and other compatible solutes on model enzymes. *Extremophiles*, 6(3): 209-216, <https://doi.org/10.1007/s007920100236>
43. Rana S., Ghosh KS. 2021. Inhibition of fibrillation of human γ d-crystallin by a flavonoid morin. *J Biomol Struct Dyn.*, 39(12):4279-4289, [10.1080/07391102.2020.1775701](https://doi.org/10.1080/07391102.2020.1775701).
44. Noor H., Cao P., Raleigh DP. 2012. Morin hydrate inhibits amyloid formation by islet amyloid polypeptide and disaggregates amyloid fibers. *Protein Sci.*, 21(3):373-82, [10.1002/pro.2023](https://doi.org/10.1002/pro.2023).

45. Das S. and Bhattacharyya D. 2017. Destabilization of human insulin fibrils by peptides of fruit bromelain derived from *Ananas comosus* (pineapple). *J. Cell. Biochem.*, 118(12): 4881-4896, [10.1002/jcb.26173](https://doi.org/10.1002/jcb.26173)
46. Alam P., Beg AZ., Siddiqi MK., Chaturvedi SK., Rajpoot RK., Ajmal MR., Zaman M., Abdelhameed AS., Khan RH. 2017. Ascorbic acid inhibits human insulin aggregation and protects against amyloid induced cytotoxicity. *Arch Biochem Biophys.*, 621:54-62, [10.1016/j.ab.2017.04.005](https://doi.org/10.1016/j.ab.2017.04.005).
47. Gancar M., Kurin E., Bednarikova Z., Marek J., Mucaji P., Nagy M., Gazova Z. 2020. Amyloid aggregation of insulin: an interaction study of green tea constituents. *Int. J. Biol. Macromol.*, 242(2) : 124856, <https://doi.org/10.1016/j.ijbiomac.2023.124856>
48. Ueda T., Nagata M., Imoto T. 2001. Aggregation and Chemical Reaction in Hen Lysozyme Caused by Heating at PH 6 Are Depressed by Osmolytes, Sucrose and Trehalose. *J. Biochem.*, 130: 491–496, <https://doi.org/10.1093/oxfordjournals.jbchem.a003011>
49. White D.A., Buell A.K., Knowles T.P.J., Welland M.E., Dobson C.M. 2010. Protein Aggregation in Crowded Environments. *J. Am. Chem. Soc.*, 132: 5170–5175.
50. Arora A., Ha C., Park C.B. 2004. Inhibition of Insulin Amyloid Formation by Small Stress Molecules. *FEBS Lett.*, 564: 121–125, [https://doi.org/10.1016/S0014-5793\(04\)00326-6](https://doi.org/10.1016/S0014-5793(04)00326-6)
51. Ahmad AR., Mishra R. 2022. Polyol and Sugar Osmolytes Stabilize the Molten Globule State of α -Lactalbumin and Inhibit Amyloid Fibril Formation. *Biochim. Et Biophys. Acta (BBA)-Proteins Proteom.* 1870: 140853, <https://doi.org/10.1016/j.bbapap.2022.140853>
52. Sharma A., Pasha J.M., Deep S. 2010. Effect of the Sugar and Polyol Additives on the Aggregation Kinetics of BSA in the Presence of N-Cetyl-N,N,N-Trimethyl Ammonium Bromide. *J. Colloid Interface Sci.*, 350: 240–248, <https://doi.org/10.1016/j.jcis.2010.06.054>
53. Knowles T.P.J., Shu W., Devlin G.L., Meehan S., Auer S., Dobson C.M., Welland M.E. 2007. Kinetics and Thermodynamics of Amyloid Formation from Direct Measurements of Fluctuations in Fibril Mass. *Proc. Natl. Acad. Sci. USA.* 104: 10016–10021. <https://doi.org/10.1073/pnas.0610659104>
54. Nielsen L., Khurana R., Coats A., Frokjaer S., Brange J., Vyas S., Uversky V.N., Fink A.L. 2001. Effect of Environmental Factors on the Kinetics of Insulin Fibril Formation: Elucidation of the Molecular Mechanism. *Biochemistry*, 40: 6036–6046, <https://doi.org/10.1021/bi002555c>

55. Macchi F., Eisenkolb M., Kiefer H., Otzen D.E. 2012. The Effect of Osmolytes on Protein Fibrillation. *IJMS*. 13: 3801–3819. <https://doi.org/10.3390/ijms13033801>
56. Fung J., Darabie A.A., McLaurin J. 2005. Contribution of Simple Saccharides to the Stabilization of Amyloid Structure. *Biochem. Biophys. Res. Commun.* 328: 1067–1072, <https://doi.org/10.1016/j.bbrc.2005.01.068>
57. Morimoto RI. 2008. Proteotoxic stress and inducible chaperone networks in neurodegenerative disease and aging. *Genes & Dev.*, 22(11):1427-38. [10.1101/gad.1657108](https://doi.org/10.1101/gad.1657108)
58. Tyedmers J., Mogk A., Bukau B. 2010. Cellular strategies for controlling protein aggregation. *Nat. Rev. Mol. Cell Biol.*, 11(11):777-88. <https://doi.org/10.1038/nrm2993>
59. Abelein A., Johansson J. 2023. Amyloid inhibition by molecular chaperones *in vitro* can be translated to Alzheimer's pathology *in vivo*. *RSC Med Chem.*, 14(5):848-857, [10.1039/d3md00040k](https://doi.org/10.1039/d3md00040k).
60. Månsson C., Kakkar V., Monsellier E., Sourigues Y., Härmark J., Kampinga HH., Melki R., Emanuelsson C. 2014. DNAJB6 is a peptide-binding chaperone which can suppress amyloid fibrillation of polyglutamine peptides at substoichiometric molar ratios. *Cell Stress & Chaperones*, 19(2):227-39, <https://doi.org/10.1007/s12192-013-0448-5>
61. Santhoshkumar P., Sharma K.K. 2004. Inhibition of amyloid fibrillogenesis and toxicity by a peptide chaperone. *Mol Cell Biochem.*, 267: 147–155, <https://doi.org/10.1023/B:MCBI.0000049373.15558.b8>
62. Dubey K., Anand BG., Badhwar R., Bagler G., Navya PN., Daima HK., Kar K. 2015. Tyrosine- and tryptophan-coated gold nanoparticles inhibit amyloid aggregation of insulin. *Amino Acids*. 47(12):2551-60, [10.1007/s00726-015-2046-6](https://doi.org/10.1007/s00726-015-2046-6)
63. Andrikopoulos N., Song Z., Wan X., Douek AM., Javed I., Fu C., Xing Y., Xin F., Li Y., Kakinien A., Koppel K., Qiao R., Whittaker AK., Kaslin J., Davis TP., Song Y., Ding F., Ke PC. 2021. Inhibition of Amyloid Aggregation and Toxicity with Janus Iron Oxide Nanoparticles. *Chem Mater.*, 33(16):6484-6500, [10.1021/acs.chemmater.1c01947](https://doi.org/10.1021/acs.chemmater.1c01947)
64. Vus K., Tarabara U., Danylenko I., Pirko Y., Krupodorova T., Yemets A., Blume Y., Turchenko V., Klymchuk D., Smertenko P., Zhytniakivska O., Trusova V., Petrushenko S., Bogatyrenko S., Gorbenko G. 2021. Silver nanoparticles as inhibitors of insulin amyloid formation: A fluorescence study. *J. Mol. Liq.*, 342: 117508, <https://doi.org/10.1016/j.molliq.2021.117508>

65. Meesaragandla B., Karanth S., Janke U., Delcea M. 2020. Biopolymer-coated gold nanoparticles inhibit human insulin amyloid fibrillation. *Sci Rep.*, 10: 7862, <https://doi.org/10.1038/s41598-020-64010-7>
66. Sharma A., Ghosh K.S. 2023. Inhibition of Amyloid Fibrillation of Bovine Serum Albumin by Zinc Oxide Nanoparticles. *BioNanoSci.*, 13: 1243–1249. <https://doi.org/10.1007/s12668-023-01154-6>
67. Geng H., Yuan H., Qiu L., Gao D., Cheng Y., Xing C. 2020. Inhibition and disaggregation of amyloid β protein fibrils through conjugated polymer-core thermoresponsive micelles. *J Mater Chem B*, 8(44):10126-10135, [10.1039/d0tb01863e](https://doi.org/10.1039/d0tb01863e)
68. Sun H., Liu J., Li S., Zhou L., Wang J., Liu L., Lv F., Gu Q., Hu B., Ma Y., Wang S. 2019. Reactive Amphiphilic Conjugated Polymers for Inhibiting Amyloid β Assembly. *Angew Chem Int Ed Engl.*, 58(18): 5988-5993, [10.1002/anie.201901459](https://doi.org/10.1002/anie.201901459).
69. Dou W-T., Lv Y., Tan C., Chen G-R., He X-P. 2016. Irreversible destruction of amyloid fibril plaques by conjugated polymer based fluorogenic nanogrenades, *J. Mater. Chem. B*, 4: 4502-4506, <https://doi.org/10.1039/C6TB01351A>
70. Haddad HW., Malone GW., Comardelle NJ., et al. 2022. Aduhelm, a novel anti-amyloid monoclonal antibody, for the treatment of Alzheimer's Disease: A comprehensive review. *Health Psychol. Res.*, 10(2). [doi:10.52965/001c.37023](https://doi.org/10.52965/001c.37023)
71. Sevigny J., Chiao P., Bussière T. et al. 2016. The antibody aducanumab reduces A β plaques in Alzheimer's disease. *Nature*. 537(7618):50-56. [doi:10.1038/nature19323](https://doi.org/10.1038/nature19323)
72. Ferrero J., Williams L., Stella H., et al. 2016. First-in-human, double-blind, placebo-controlled, single-dose escalation study of aducanumab (BIIB037) in mild-to-moderate Alzheimer's disease. *Alzheimers Dement Transl Res Clin Interv.*, 2(3):169-176, [doi:10.1016/j.trci.2016.06.002](https://doi.org/10.1016/j.trci.2016.06.002)
73. Avgerinos KI., Ferrucci L., Kapogiannis D. 2021. Effects of monoclonal antibodies against amyloid- β on clinical and biomarker outcomes and adverse event risks: A systematic review and meta-analysis of phase III RCTs in Alzheimer's disease. *Ageing Res Rev.*, 68:101339. [doi:10.1016/j.arr.2021.101339](https://doi.org/10.1016/j.arr.2021.101339)
74. Mo JJ., Li JY., Yang Z., Liu Z., Feng JS. 2017. Efficacy and safety of anti-amyloid- β immunotherapy for Alzheimer's disease: a systematic review and network meta-analysis. *Ann Clin Transl Neurol.* 4(12):931-942. [doi:10.1002/acn3.469](https://doi.org/10.1002/acn3.469)
75. Tian Hui Kwan A, Arfaie S, Therriault J, Rosa-Neto P, Gauthier S. 2020, Lessons Learnt from the Second Generation of Anti-Amyloid Monoclonal Antibodies Clinical Trials. *Dement Geriatr Cogn Disord.* 2020;49(4):334-348. [doi:10.1159/000511506](https://doi.org/10.1159/000511506)

76. Avgerinos KI., Ferrucci L., Kapogiannis D. 2021. Effects of monoclonal antibodies against amyloid- β on clinical and biomarker outcomes and adverse event risks: A systematic review and meta-analysis of phase III RCTs in Alzheimer's disease. *Ageing Res Rev.* 68:101339. [doi:10.1016/j.arr.2021.101339](https://doi.org/10.1016/j.arr.2021.101339)
77. Li YV. 2014. Zinc and insulin in pancreatic beta-cells. *Endocrine.* 45(2):178-89, [10.1007/s12020-013-0032-x](https://doi.org/10.1007/s12020-013-0032-x)
78. Jiří H., Pavel A. and Vítěz K. 1979. Interaction of insulin with metal(II) ions, *FEBS Letters*, 100(2): 374– 376, [10.1016/0014-5793\(79\)80373-7](https://doi.org/10.1016/0014-5793(79)80373-7)
79. Coffman F. D., Dunn M. F. 1988. Insulin-Metal Ion Interactions: The Binding of Divalent Cations to Insulin Hexamers and Tetramers and the Assembly of Insulin Hexamers. *Biochemistry*, 27(16) : 6179– 6187, [10.1021/bi00416a053](https://doi.org/10.1021/bi00416a053)
80. Gavrilova J., Tõugu V., Palumaa P. 2014, Affinity of zinc and copper ions to insulin monomers, *Metallomics*, 6(7): 1296-300, [10.1039/c4mt00059e](https://doi.org/10.1039/c4mt00059e).
81. Loughheed W. D., Woulfe-Flanagan H., Clement J. R., Albisser A. M. 1980, Insulin Aggregation in Artificial Delivery Systems. *Diabetologia*, 19 (1): 1–9. [10.1007/BF00258302](https://doi.org/10.1007/BF00258302).
82. Yip C. M., Brader M. L., DeFelippis M. R., Ward M. D. 1998. Atomic Force Microscopy of Crystalline Insulins: The Influence of Sequence Variation on Crystallization and Interfacial Structure. *Biophys. J.*, 74 (5): 2199–2209. [10.1016/S0006-3495\(98\)77929-9](https://doi.org/10.1016/S0006-3495(98)77929-9).
83. Dathe M., Gast K., Zirwer D., Welfle H., Mehlis B. 1990. Insulin Aggregation in Solution. *Int. J. Pept. Protein Res.*, 36 (4): 344–349. [10.1111/j.1399-3011.1990.tb01292.x](https://doi.org/10.1111/j.1399-3011.1990.tb01292.x).
84. Sharp J.S., Forrest J.A., Jones R.A.L. 2002. Surface denaturation and amyloid fibril formation of insulin at model lipid–water interfaces. *Biochemistry*. 41: 15810–15819, <https://doi.org/10.1021/bi020525z>
85. Ahmad A., Millett I.S., Doniach S., Uversky V.N., Fink A.L. 2003. Partially folded intermediates in insulin fibrillation. *Biochemistry*. 42: 11404–11416. [10.1021/bi034868o](https://doi.org/10.1021/bi034868o)
86. Hua Q.X. and Weiss M.A. 2004. Mechanism of insulin fibrillation: The structure of insulin under amyloidogenic conditions resembles a protein-folding intermediate. *J. Biol. Chem.*, 279: 21449–21460. <https://doi.org/10.1074/jbc.M314141200>
87. Md. Mannan A., Nasiruddin , MdHossain S., Nipa N.N., Khatun A., Md Amin R., Sarkar M.K., MdZahan K-E. 2019. Macro and micro nutrients in Holy basil (Tulsi): A possible supplement for natural medicine, *Int. J. Chem. Stud.*, 3(4) : 43-47, <https://www.researchgate.net/publication/338682578>

88. Naiki H, Higuchi K., Hosokawa M., Takeda T. 1989. Fluorometric determination of amyloid fibrils in vitro using the fluorescent dye, thioflavine T. *Anal. Biochem.*, 177: 244–249, [10.1016/0003-2697\(89\)90046-8](https://doi.org/10.1016/0003-2697(89)90046-8)
89. Ziaunys M., Sakalauskas A., Smirnovas V. 2020. Identifying Insulin Fibril Conformational Differences by Thioflavin-T Binding Characteristics. *Biomacromolecules*. 21(12):4989-4997, [10.1021/acs.biomac.0c01178](https://doi.org/10.1021/acs.biomac.0c01178)
90. Waugh D. F., Wilhemson D. F., Commerford S. L., Sackler, M. L. 1953, Studies of the nucleation and growth reactions of selected types of insulin fibrils. *J. Am. Chem. Soc.*, 75: 2592–2600, <https://doi.org/10.1021/ja01107a013>
91. Manno M., Craparo E.F., Podestà A., Bulone D., Carrotta R., Martorana V., Tiana G., San Biagio P.L. 2007. Kinetics of Different Processes in Human Insulin Amyloid Formation, *J. Mol. Biol.*, 366: 258–274, [10.1016/j.jmb.2006.11.008](https://doi.org/10.1016/j.jmb.2006.11.008)
92. Nowacka O., Shcharbin D., Klajnert-Maculewicz B., Bryszewska M. 2014. Stabilizing effect of small concentrations of PAMAM dendrimers at the insulin aggregation. *Colloids Surf B Biointerfaces*, 116: 757-760. <https://doi.org/10.1016/j.colsurfb.2014.01.056>.
93. Zand Z., Khaki PA., Salihi A., Sharifi M., Qadir Nanakali NM., Alasady AA., Aziz FM., Shahpasand K., Hasan A., Falahati M. 2019. Cerium oxide NPs mitigate the amyloid formation of α -synuclein and associated cytotoxicity. *Int J Nanomedicine*. 14: 6989-7000, [10.2147/IJN.S220380](https://doi.org/10.2147/IJN.S220380).
94. Surmacz-Chwedoruk W., Babenko V., Dzwolak W. 2014, Master and Slave Relationship Between Two Types of Self-Propagating Insulin Amyloid Fibrils, *J Phys Chem B*, 118:13582–13589, [10.1021/jp510980b](https://doi.org/10.1021/jp510980b)
95. Yang H., Yang S., Kong J., Dong A., Yu S. 2015. Obtaining information about protein secondary structures in aqueous solution using Fourier transform IR spectroscopy. *Nat Protoc.*, 10(3): 382-396, [10.1038/nprot.2015.024](https://doi.org/10.1038/nprot.2015.024).
96. D.M. Lawler ,Spectrophotometry, Turbidimetry and Nephelometry, Encyclopedia of Analytical Science (Second Edition), 2005.
97. D. L. Andrews Rayleigh Scattering and Raman Effect, Theory, 2017 Encyclopedia of Spectroscopy and Spectrometry (Third Edition).
98. Nielsen L., Khurana R., Coats A., Frokjaer S., Brange J., Vyas S., Uversky VN., Fink AL. 2001. Effect of environmental factors on the kinetics of insulin fibril formation: elucidation of the molecular mechanism. *Biochemistry*. 40 (20): 6036-46, [10.1021/bi002555c](https://doi.org/10.1021/bi002555c).

99. Mahendra VP., Prasad KY., Ganesan P., Kumar R. 2021. Mechanism of rutin mediated inhibition of insulin amyloid formation and protection of Neuro-2a cells from fibril-induced apoptosis. *Mol. Biol. Rep.*, 47. [10.1007/s11033-020-05393-8](https://doi.org/10.1007/s11033-020-05393-8).
100. Frankær C. G., SønderbyP., Bang M.B., MateiuR.V., Groenning M., BukrinskiJ., Harris P. 2017. Insulin fibrillation: The influence and coordination of Zn^{2+} . *J Struct Bio.*, 199(1):27-38. [10.1016/j.jsb.2017.05.006](https://doi.org/10.1016/j.jsb.2017.05.006).
101. Duboué-Dijon E., Delcroix P., Martinez-Seara H., Hladílková J., Coufal P., Křížek T., JungwirthP., Binding of Divalent Cations to Insulin: Capillary Electrophoresis and Molecular Simulations. 2018. *J. Phys. Chem. B.*, 122(21):5640–5648, <https://doi.org/10.1021/acs.jpcb.7b12097>
102. Bertini I, Decaria L, Rosato A. 2010. The annotation of full zinc proteomes. *J. Biol. Inorg. Chem.* 15:1071–78

CHAPTER 2

Employing water soluble B-complex vitamins to inhibit the process of insulin fibrillation



5.1 Prologue of the study

Interaction study of different biological proteins with selected ligands is very helpful to figure out various accelerating and inhibitory effects of the ligands on the protein function as well as maintenance of native structure of it. It is quite common that sometimes the protein structure get disassembled spontaneously or by some internal/external forces and render the protein mal/non-functional. In that case, also such interacting molecules can act as shielding agent from the adverse event of misfolding/fibrillation of it. Huminsulin (recombinant DNA origin) is a therapeutic protein widely used against the disease Diabetes mellitus [1] and there are many case reports of insulin aggregation at different body sites [2] after its administration. Aggregation may occur during in vitro production and purification of insulin in commercial scale or during delivery of it [3]. The elaborative study on such aggregation event reveals the highly fibrillated beta-sheet rich irreversible non-functional form of Insulin known as Amyloid [4]. The Amyloid/fibrillated structures were found in other significant proteins also and are the reason behind a number of dreadful disorders like Creutzfeldt-Jakob disease, Alzheimer's disease, Parkinson's disease, and lifestyle-related Type II diabetes [5]. Number of case reports regarding fatal insulin deposition is alarmingly high [6]. Amyloid formation at injection site may extend upto strong pathogenic attack to erythrocytes and nearby tissues followed by fibril toxicity and deposition causing lump formation [7]. Amyloid fibril elongation occurs in a positive co-operative manner and thus freshly incorporated insulin even cannot be absorbed into blood of affected patient [8]. Mature amyloid fibrils can serve as the source of harmful oligomers [9]. Therapeutic strategy development should precede the understanding of protein-effectors interactions in vitro [10].

Vitamins and minerals are essentially required by the body to carry out a range of normal functions. However, these micronutrients are not produced in our bodies and must be derived from the food we eat. Vitamins are organic substances that are generally classified as either fat-soluble or water-soluble. Fat-soluble vitamins (vitamin A, vitamin D, vitamin E, and vitamin K) dissolve in fat and tend to accumulate in the body if ingested in large amounts. Water-soluble vitamins (vitamin C and the B-complex vitamins, such as vitamin B6, vitamin B12, and folate) are absorbed in solubilized form. The majority of B complex vitamins help enzymes to function by serving as cofactor/precursors of co-factors [11]. More than 140 enzymes among which most are involved in amino acid metabolism are PLP-dependent (vitamin B6-derived pyridoxal 5'-phosphate) [12]. There are many evidences in literature of

interaction of vitamins with proteins like prediction of vitamin B interacting residues (VBIRs) showed that Gly, His, Asn, Ser, Thr, Trp and Tyr were more abundant in VBIRs [13]. Water soluble B-complex vitamins can be a great choice for interacting with protein and tracing their effects on protein fibrillation.

5.2. Interaction of vitamins with protein molecules

To employ vitamins as amyloid inhibitors, it is of primary concern to understand the interactions and interacting residues of vitamins with various proteins. The versatile roles of Vitamins in vivo and also the necessary involvements in the various enzymatic reactions as cofactors are well known. A web-based application, Two Sample Logo (TSL) and a SVM (Support Vector Machines) based prediction method, VitaPred can calculate and visualize the differences between two sets of aligned samples of amino acids and predict the vitamin-interacting residues in protein sequences respectively [14- 17]. These techniques revealed slight different preferences of vitamins than ATP, GTP, NAD, FAD and mannose binding to proteins. The ATP, GTP, NAD, FAD and mannose interacted via {G,R,K,S,H}, {G,K,T,S,D,N}, {T,G,Y}, {G,Y,W} and {Y,D,W,N,E} residues of protein respectively

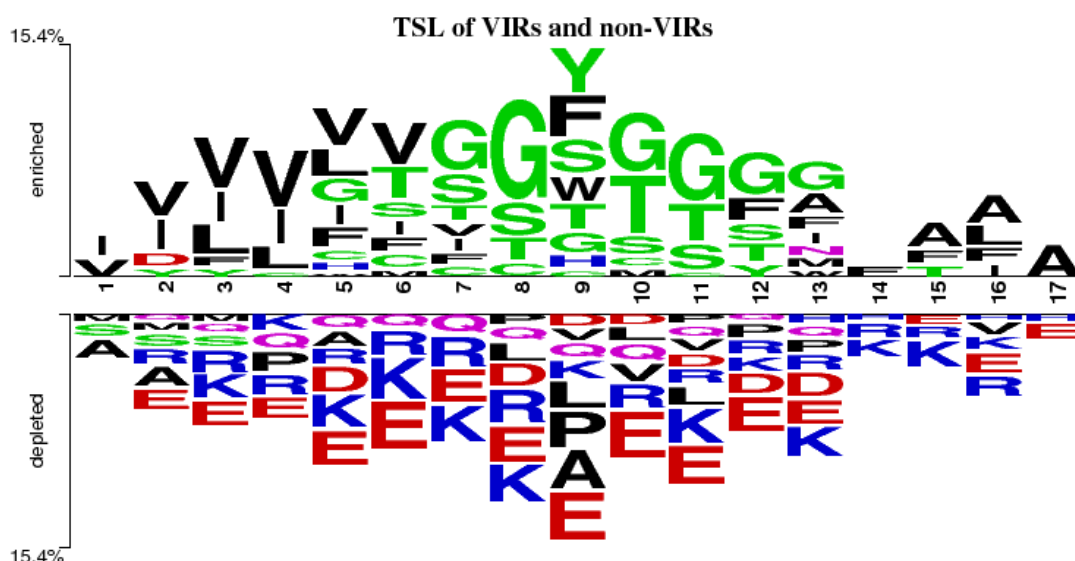


Fig.5.1. Prediction of VIRs by the TSL representation of sliding patterns (17-residues length). The central residue (9th position) is showing VIRs (positive) and non-VIRs (negative). *Fig. adapted from 13. Panwar B. et.al., 2013, BMC Bioinformatics, 14:44, [10.1186/1471-2105-14-44](https://doi.org/10.1186/1471-2105-14-44)

But the binding preferences for vitamins are different in some aspects (Fig. 5.1). The predictions categorized vitamin interactions to protein in four different levels; they are (i) vitamin interacting residues (VIRs), (ii) vitamin-A interacting residues (VAIRs), (iii) vitamin-B interacting residues (VBIRs) and (iv) pyridoxal-5-phosphate (vitamin B6) interacting residues (PLPIRs). Actually VIRs consists of the three rest categories, VAIRs, VBIRs and PLPIRs howbeit prediction tools are available for all the four categories. Literature reports showed that, Vitamin A make interactions with proteins preferably via {Phe, Ile, Trp, Tyr, Leu, Val} residues, while Vitamin B (Fig.5.3) and PLP (Fig.5.4) preferred {Ser, Tyr, Gly, Thr, His, Trp, Asn, Glu} and {Ser, Thr, Gly, His, Tyr, Asn} residues respectively. The non-preferred residues were also predicted as {Glu, Pro, Asp, Asn, Ser, Arg, Gln}, {Leu, Glu, Ala, Pro, Val, Ile, Lys} and {Leu, Glu, Ala, Pro, Val, Ile, Ala} for Vitamin A, B and PLP respectively [13]. It can thus be said that, the mode and occurrence of interaction of vitamins with protein may differ even within the sub-classes of vitamins.

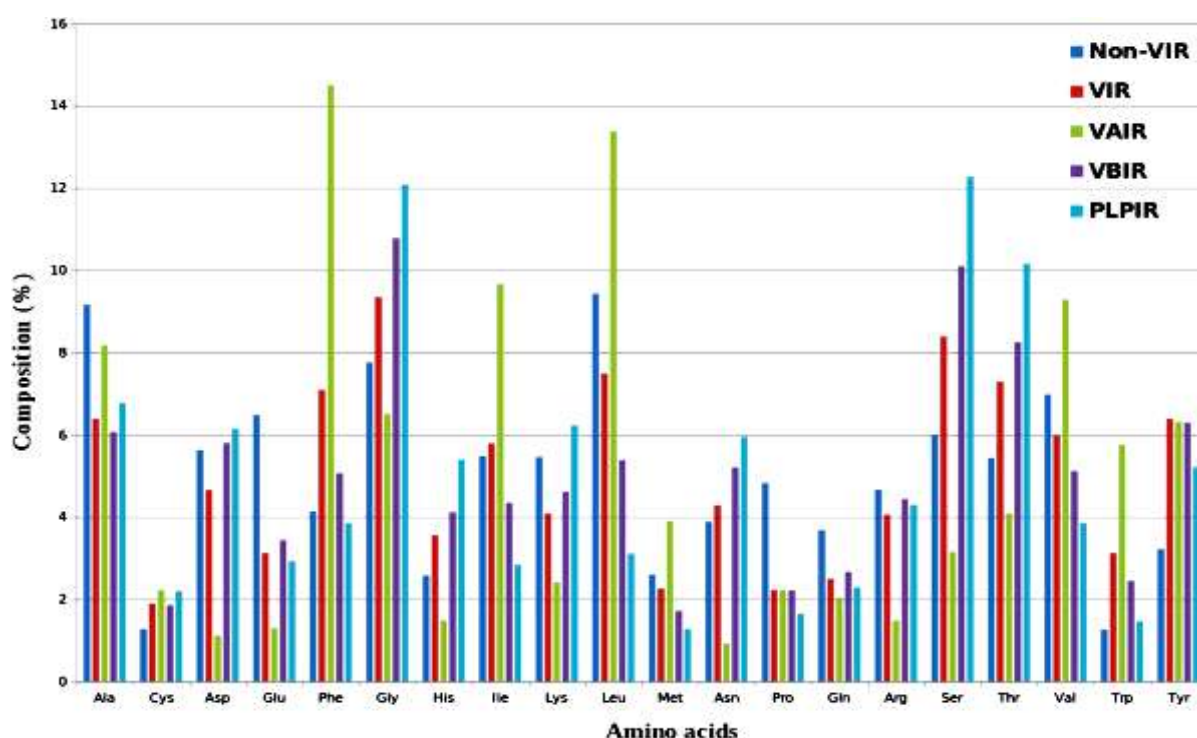


Fig.5.2. Comparative percentages of amino acids residues serving as non-VIRs, VIRs, VAIRs, VBIRs and PLPIRs. *Fig. adapted from Panwar B. et.al., 2013, BMC Bioinformatics, 14:44, [10.1186/1471-2105-14-44](https://doi.org/10.1186/1471-2105-14-44)

The water soluble B-complex groups of vitamins were chosen in the current study. Their interaction patterns are as follows:

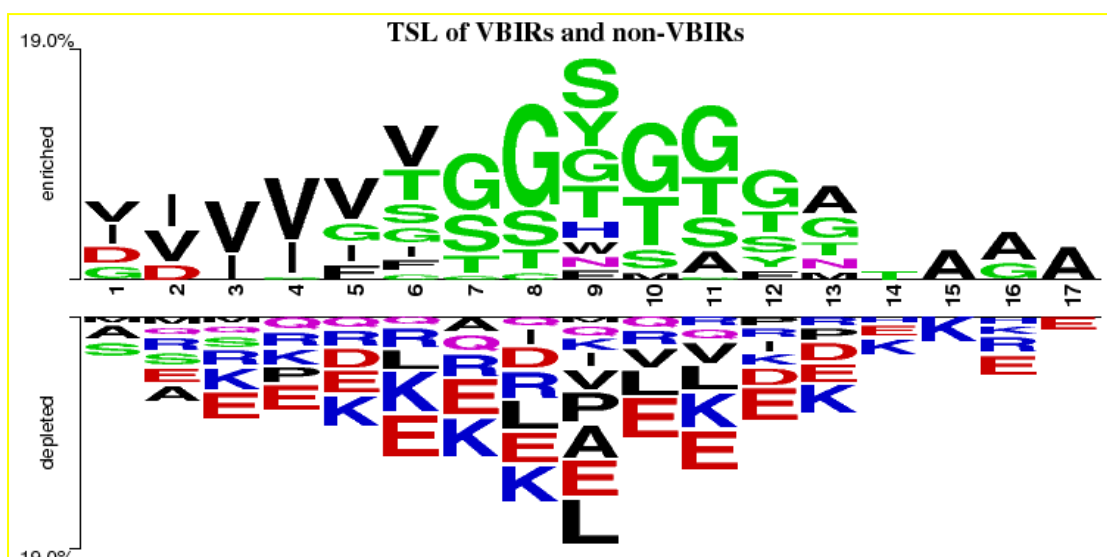


Fig.5.3. The representation of sliding patterns of TSL (17-residues length) for prediction of VBIRs. The central residue at position 9 is showing VBIRs (positive) and non-VBIRs (negative). *Fig. adapted from 13. Panwar B. et.al., 2013, BMC Bioinformatics, 14:44, [10.1186/1471-2105-14-44](https://doi.org/10.1186/1471-2105-14-44)

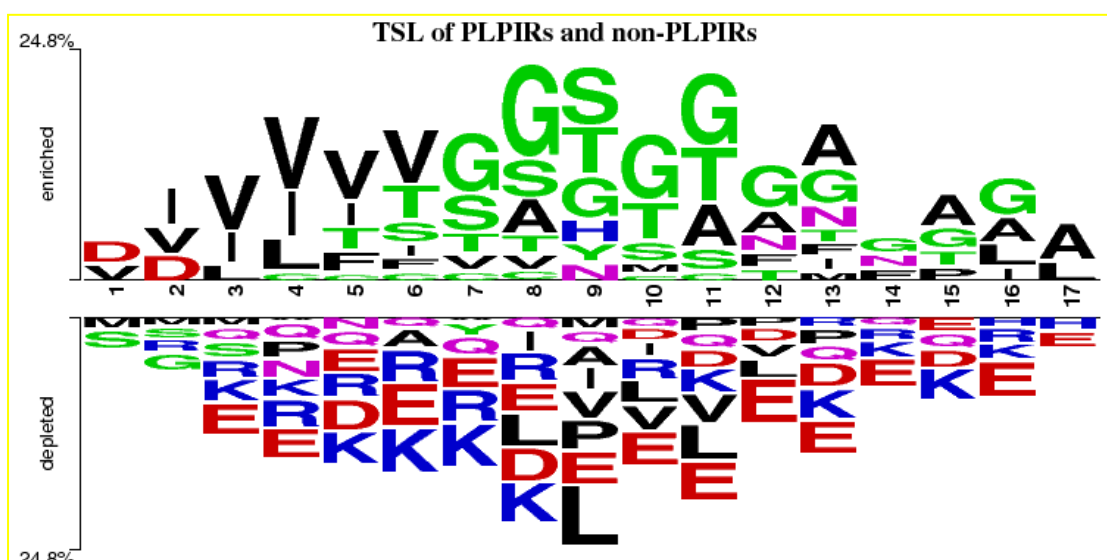


Fig.5.4. Predictions of PLPIRs via the TSL representation of sliding patterns (17-residues length). The centrally positioned 9th residue represents PLPIRs (positive) and non-PLPIRs (negative). *Fig. adapted from 13. Panwar B. et.al., 2013, BMC Bioinformatics, 14:44, [10.1186/1471-2105-14-44](https://doi.org/10.1186/1471-2105-14-44)

5.3. Effects of vitamins in amyloid formation/related disorders: Literature findings

There are many evidences of anti-amyloidogenic activities of fat-soluble vitamins. Literature reports showed that vitamin K3 inhibit the fibrillation of hen egg white lysozyme (HEWL) and A β -42 (amyloid beta 1- 42) peptide [18]. Deposition of amyloid beta followed by inflammation is a common cause behind age-related macular degeneration (AMD) and blindness, that can be overcome by the amyloid clearing effect of Vit.D [19]. Vit.D when combined with memantine, an effective drug, synergistically prevents the A β -peptide and glutamate toxicity in cortical neuronal cultures [20]. Vitamin A also showed in vitro anti amyloidogenic activity against amyloid β -peptide [21]. Another study revealed that, retinoic acid (Vit. A) and α -tocopherol (Vit.E) individually disrupt the process of A β aggregation both in vitro and in vivo model of a *C. elegans* (a nematode) [22]. Some study on water-soluble vitamins also proved beneficial. The inhibitory effect conferred by vitamin B12 against fibrillation of A β -42 and amyloid induced cytotoxicity had been shown in human neuronal cell line [23]. Ascorbic acid (Vit.C) had found to inhibit the A β 42 aggregation [24]. Vitamin B6 derivatives viz., pyridoxamine (PM), pyridoxine (PN), pyridoxal (PL), and pyridoxal-5'-phosphate (PLP) were shown to inhibit the metal complexes of β -amyloid (A β) peptides responsible for fatal cases of Alzheimer's disease [25].

Because of such inherent capability, in this work some of the B complex group vitamins (Vit. B1, B6 and B12) had chosen to interact with insulin ex vivo followed by investigation on their any amyloid inhibitory activities separately. The important point for choosing these vitamins was, being soluble in water they are not stored in the body and generally shows no toxicity in case of excess intake. Any water-soluble vitamins unused by the body are primarily lost through urine. All the three vitamins are inevitable in maintenance of our nervous system [26].

Vit.B1 i.e., thiamine or anti-beriberi factor is very significant in monosaccharide/glucose catabolism [27]. The Thiamine level of body is significant in activation of thiamine-dependent enzymes. It was reported that, in patients having amyloid generated disorders like Alzheimer's disease, the thiamine level is greatly reduced in the brains and peripheral tissues. The cognitive functions had found to improve by oral thiamine trials [28]. Another study [29] had also found that, Thiamine deficiency (TD) was found to involve with development of fatal cases of protein amyloid generations. TD was found to play important role in processing of amyloid precursor protein (APP) in cellular and animal models. Study was done on

population of SH-SY5Y neuroblastoma cells that over-expresses APP. In that case maturation of β -site APP cleaving enzyme 1 (BACE1) was promoted by TD. TD there also advanced the β -secretase activity and in turn results in elevated production of β -amyloid ($A\beta$). $A\beta$ accumulation exacerbated oxidative stress in cells. Here also thiamine supplementation is very important in reversing the adverse phenomenon of TD-induced alterations. So, it can be undisputedly stated that, vitamin B1 is required in glucose metabolism, neuro-transmission, and inhibition of amyloid formation. Therefore in the present study, thiamine was chosen along with other two B-complexes.

Besides being a part of protein metabolism, Vit.B6 also helps in the formation of RBCs, fatty acids, neurotransmitters [30] etc. Reports found that, B vitamins (Folate, B6, B12) deprived diet if applied on TgCRND8 mouse model of AD that over express APP, hyper homocysteinemia, $A\beta$ accumulation, and impaired spatial memory were caused [31]. Pyridoxal 5'-phosphate (PLP) served as a cofactor for a number of metabolic enzymes. Vitamin B6 shows anti-inflammatory effects and therapeutic potential for different inflammatory diseases. High-dose vitamin B6 supplementation (100 mg/day) is required to suppress the levels of plasma IL-6 and TNF- α in patient with rheumatoid arthritis [32]. Vitamin B6 was shown to discourage the occurrence of colon cancer in both human and animal model [33]. Though there is no direct evidence of amyloid inhibition, still recently it was observed that, the shrinkage of the whole brain as well as atrophy in specific regions of brain were diminished in Alzheimer's patients with vitamin-B supplementation (folic acid, vitamin B6, and vitamin B12) [34]. The risk of developing Parkinson's disease was assessed to high in case of low vitamin B6 intake [35].

Vit.B12 required during hematopoiesis, cell division, myelin formation and re-myelination of neurons and managing the oxidative stress on cells [26]. The fibrillization of tau protein and the formation of the neurofibrillary tangle were prevented by Vitamin B12 (Figure 5.4). This is why the severity and progress of AD was greatly hampered by VitB12 [36]. Besides this, proteotoxic stress generated due to protein aggregation disorders like AD, can be neutralized by Vitamin B₁₂ supplementation [37]. The anti-oxidative property of vitamin B12 render itself effective against oxidation of lipids, proteins and nucleic acids within body cells and thus an important contributing factor inhibiting the development of age-related diseases where oxidative stress is the causing factor like AD, Parkinson disease and type 2 diabetes [38-39].

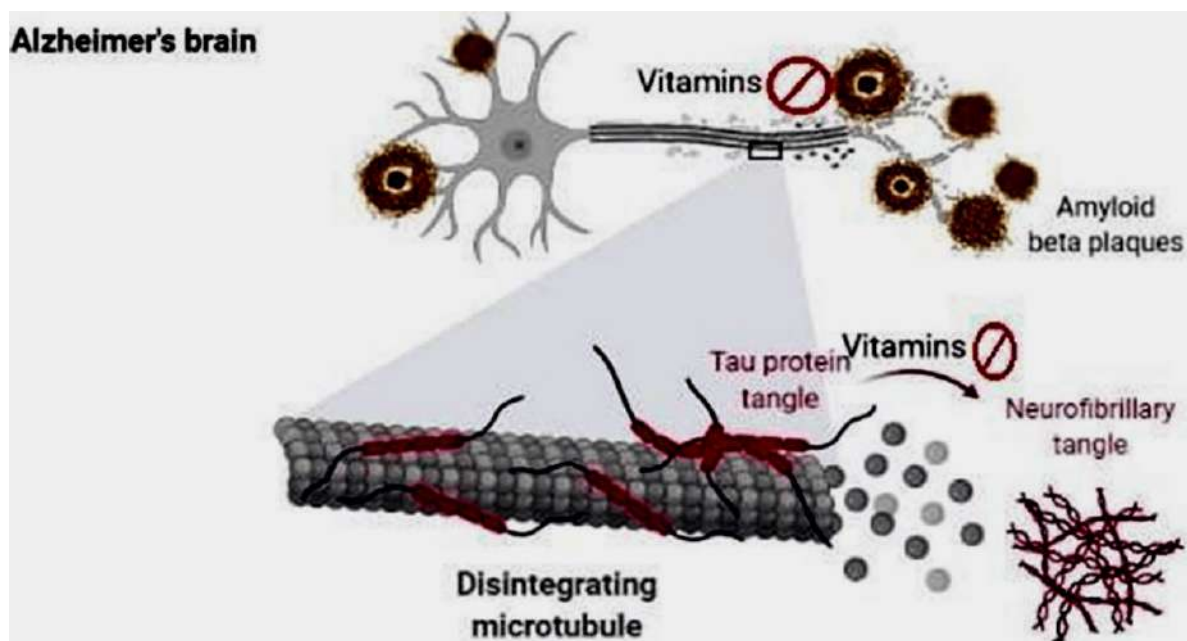


*Figure 5.5. Schematic representation of the vitamins as potential therapeutics against Alzheimer's disease. $A\beta$ plaque formation is prevented by vitamins. Tau protein oligomerization and aggregation followed by formation of neurofibrillary tangles were also supposed to be prevented by Vitamins. *Fig. adapted from Rai SN. et.al., 2021. Biomedicines. 9(10):1284. <https://doi.org/10.3390/biomedicines9101284>*

5.4. MATERIALS AND METHODOLOGIES

5.4.1. Different fluorescent probes namely, ANS, Thioflavin T (ThT) were used as received without further purification. The experiments were performed in HPLC water. All other reagents used were of analytical grade.

Table 5.1. Chemicals and equipments required

ITEMS	OBTAINED FROM
Human insulin (Huminsulin R)100 IU/ml (r-DNA origin)	Eli Lilly and Company India Pvt. Ltd.
HPLC grade 100% Pure Distilled Water, Acrylamide, N,N'-Methylenebisacrylamide,	Sigma-Aldrich
N,N,N,N tetramethylethylenediamine (TEMED), ammonium per sulphate (APS), bromophenol blue, Coomassie brilliant blue	Sigma-Aldrich
Methanol & Fluorescent probes, viz., 8-Anilinoanthracene-1-sulfonic acid (ANS), Congo red (CR), Thioflavin T (Th T)	Sigma Chemical Co. (St. Louis, USA)
Glycine, KOH, Acetone	Merck (Mumbai, India)
Thiamine hydrochloride (Vitamin B ₁), Pyridoxine-HCl (Vitamin B ₆), Cyanocobalamin (Vitamin B ₁₂)	Sigma-Aldrich
Quartz cuvettes and Hellma absorption cuvettes	Sigma-Aldrich
Glass plates for AFM	Merck (Mumbai, India)
Magnetic beads, Membrane dialysis tubing	Sigma-Aldrich

5.4.2. Methodologies employed

In order to investigate the effects of vitamin on insulin aggregation, the stock solution of vitamins were made as described in section 3.4. The insulin aggregates were formed in absence and in presence of vitamins and experimented as described in the sections 3.7-3.17.

5.5. RESULTS OF RESEARCH FINDINGS

Intrinsic fluorescence as a Measure of structural deformation of Insulin

Among the three aromatic amino acid residues responsible for intrinsic fluorescence of protein, tryptophan is absent [40] in case of insulin. Therefore, the contribution of Tyr chromophore is major in this study. Here the change of Tyr fluorescence was observed at fixed wavelengths (excitation 276 nm, emission 305 nm) under non-aggregating and aggregating conditions [at 60° C, 4h] in absence and presence of the three B-complex vitamins.

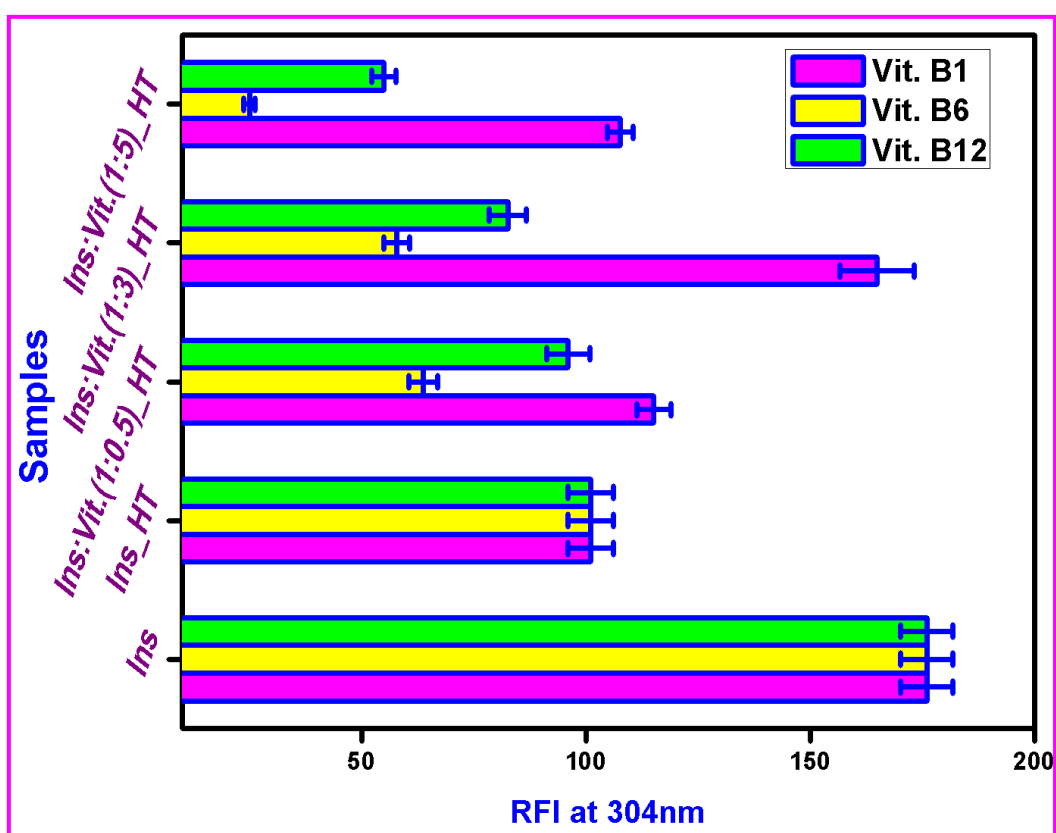


Fig.5.6. Relative Fluorescence emission Intensity (RFI) of tyrosyl residues of monomeric (Ins), heat treated ins (Ins_HT) and insulin in the presence of Vit.B1, B6 and B12 separately followed by heat application at different mill molar ratios(1:0.5, 1:3, 1:5).The excited and emitted wavelengths were 274 nm and 304 nm respectively. The protein concentration had been kept 5.5 μ M in solution and cuvette path length was 1 cm. Each reading was blank corrected and was an average of three different scans. Standard deviations were within the range of ± 4.13 .

At ambient temperature, upon excitation at 274 nm, Insulin gave emission maxima at 304 nm, which is majorly due to the Tyrosyl residues (Tyr-A14, Tyr-A19, Tyr-B16, and Tyr-B26) present in both A and B chains of it. The relative fluorescence intensity (RFI) decreased for insulin under aggregating conditions. This fluorescence-quenching event of Tyr may be due to the burying event of Tyr into more hydrophobic region during aggregation and thus become less accessible to act as a fluorophore [41]. Diminished RFI also indicated structural deformation without the involvement of any chemical changes during the process of aggregation [42]. In the vitamin B1 treated samples (showed in pink, Fig.5.5), the reverse phenomenon was observed i.e., intrinsic fluorescence remain unchanged or slightly raised and such observation may account for the fact of unchanged accessibility of Tyrosyl residues in aggregation favored conditions in presence of Vit. B1. This hints to the inhibitory effect exerted by Vit. B1 on insulin aggregation as well as helped to retain the initial folds of insulin before fibrillation. In similar experiments with Vitamin B6 (yellow bars, Fig.5.5) and Vitamin B 12 (green bars, Fig.5.5), gradual decrease in RFI was observed with higher conc. of vitamins. Thus, it can be said that both of them helped the burying event of Tyr more and so favored insulin aggregation under heating.

Thoflavin T Fluorescence emission spectra marked the comparative effects of three water soluble Vit. B complexes on human insulin aggregation

ThT indicates the presence of amyloid fibrils in solution by giving a strong peak at 482 nm [43] as shown in red curves, while this peak is missing in the emission curves of only insulin samples showed in black curves in each of the above three panels. Such strong emission accounts for the fact that the rotation of the C—C bond of Th T connecting between the benzothiazole and aniline rings get blocked (Fig. 4.6.A) upon binding of the amyloid fibrils [44].

Here ThT assay was performed to detect in-vitro formation of amyloid fibrils of human insulin in presence of three water soluble vitamin B complexes. It was already reported that ThT itself did not interfere with the event of insulin fibrillation at 60°C [45]. Results showed that, Vit.B1 effectively nullified (panel A, Fig.5.6) the amyloid generation under aggregation favoring condition as the peak intensity at 482 nm gradually decreased with increasing concentration of it and reached to a monomer like state at 1:5 milimolar ratio of Ins: Vit. B1. But the rate of amyloid generation was inconsistent with the concentration of Vit.B6 (Fig.5.6, panel B). On the other hand, Vit. B12 strongly aggravated the amyloid formation

phenomenon with increasing molar ratio (Fig. 5.6.C) revealed by the sharp rise in emission intensity than heat treated insulin itself at 482nm. ThT binding requires minimum involvement of four successive β -strands [46, 47] in amyloid structure and thus it can be said that among the three vitamins under observation, Vit. B1 prevented the mesh like network formation of consecutive β -strands in amyloid fibrils.

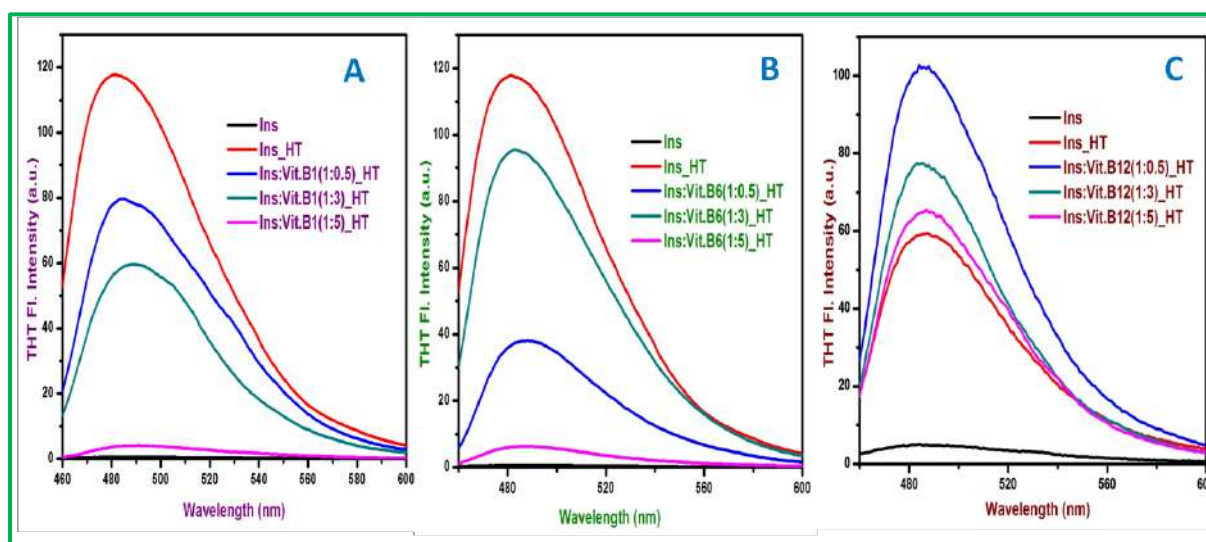


Fig.5.7. Thioflavin T (Th T) fluorescence emission spectral curves as monitored in three sets of experiment. Each set up is blank corrected by subtracting the emission values of only Th T (negative control) while the positive control set up i.e., ThT emission spectra of monomeric insulin only was shown in black curve in each of the above three panels. The excitation wavelength is 440 nm where the emission spectras were recorded in the range 460-600 nm. ThT effectively indicated the presence of amyloid fibrils after heat treatment of insulin at 60°C for 5hrs as shown in red curves. The above three panels showed the individual effects of co-incubation of insulin with Vit. B1 (panel A), Vit. B6 (panel B) and Vit. B12 (panel C) during heat treatment. Protein concentrations were kept 5.5 μ M and the data presented here were average of three consecutive scans.

Circular Dichroism (CD) spectra and Deconvolution studies helped to quantify the protein secondary structural measurements under experimental conditions

Far UV-CD spectral curve minimas are characteristic to realize the secondary structure of protein. The black curve in each of the panels in Fig.3 represents the CD spectra of monomeric human insulin where two inverted peak were found, viz., at 207 nm and 222 nm. This corresponds to the alpha helical dominating structure of the protein insulin [48].

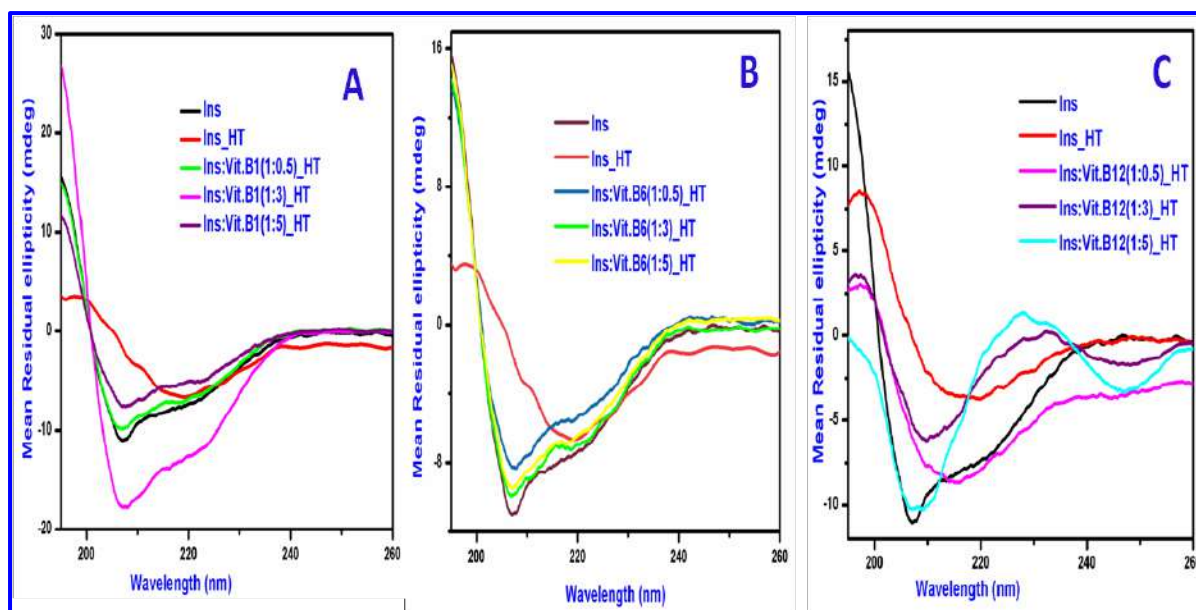


Fig. 5.8. Circular Dichroism spectra in the Far UV-CD range of monomeric form of human insulin (in black), heat treated form of the same (in red), in presence of Vit. B1 (panel A), Vit. B6 (panel B) and Vit. B12 (panel C) at molar ratios Ins: Vit. solution of 1:0.5, 1:3 and 1:5. The protein concentration was $6.5\mu\text{M}$ and path length was 2 mm in each measurement.

After heat treatment, the obtained curve (in red, all panels, Fig.5.7) showed a negative band at 218 nm and a positive one at 196 nm. This clearly revealed the presence of beta-sheet rich conformation [49] generated during amyloid transition. Vit. B1 co-incubated insulin samples at three different conc (Fig.5.7.A) showed the monomer like pattern that is earlier alpha helix rich structural conformation having negative peaks at both 207nm and 222 nm were conserved. In Vit.B6 treated samples (Fig. 5.7. B), though the monomer like conformation peaks were obtained, still they gradually lost their peak minima i.e., the negative intensity of mean residual ellipticity. The decrease in the said intensity can be understood as the partial but not full inhibition of insulin amyloid generation by Vit. B6. In Vit.B12 treated protein (Fig 5.7.C), the prominent transition toward beta-rich orientation from alpha helical primary conformation was accountable for the fact that Vit.B12 itself exasperated the aggregation process of insulin.

The CD deconvolution study helped to get a quantitative idea about the secondary structure of insulin undergoing harmful amyloid transition as indicated in the table 5.1.

Table 5.1: A quantitative measurement of secondary structural transition using CD
Deconvolution method under experimental conditions

<i>Samples</i>	<i>% of α-helix</i>	<i>% of β-sheet</i>		<i>% of β-turn</i>	<i>% of random coil</i>
		<i>Antiparallel</i>	<i>Parallel</i>		
<i>Monomeric Insulin (MI)</i>	<i>33.8</i>	<i>8.1</i>	<i>1.1</i>	<i>8.8</i>	<i>48.2</i>
<i>Heat treated (HT) Insulin</i>	<i>22.4</i>	<i>24.3</i>	<i>7.5</i>	<i>12.4</i>	<i>33.4</i>
<i>MI :Vit.B1 (1:0.5)_HT</i>	<i>30.7</i>	<i>13.3</i>	<i>3.0</i>	<i>10.3</i>	<i>42.7</i>
<i>MI :Vit.B1 (1:3)_HT</i>	<i>31.3</i>	<i>4.0</i>	<i>2.9</i>	<i>9.9</i>	<i>51.9</i>
<i>MI :Vit.B1 (1:5)_HT</i>	<i>32.1</i>	<i>8.2</i>	<i>1.2</i>	<i>9.1</i>	<i>49.4</i>
<i>MI :Vit.B6 (1:0.5)_HT</i>	<i>23.9</i>	<i>19.4</i>	<i>2.5</i>	<i>11.1</i>	<i>43.1</i>
<i>MI :Vit.B6 (1:3)_HT</i>	<i>28.6</i>	<i>11.1</i>	<i>1.7</i>	<i>10.6</i>	<i>48.0</i>
<i>MI :Vit.B6 (1:5)_HT</i>	<i>30.4</i>	<i>13.0</i>	<i>1.6</i>	<i>10.0</i>	<i>45.0</i>
<i>MI :Vit.B12 (1:0.5)_HT</i>	<i>17.0</i>	<i>8.2</i>	<i>3.7</i>	<i>20.0</i>	<i>51.1</i>
<i>MI :Vit.B12 (1:3)_HT</i>	<i>17.3</i>	<i>17.8</i>	<i>7.0</i>	<i>7.5</i>	<i>50.4</i>
<i>MI :Vit.B12 (1:5)_HT</i>	<i>13.3</i>	<i>20.0</i>	<i>5.7</i>	<i>10.2</i>	<i>50.8</i>

* Calculated by BeStSel CD spectra analysis v1.3.230210

Here we can found that, the percentage of alpha helix was higher in monomer sample where the antiparallel beta-sheet was dominated in insulin undergone aggregation process. Vitamin B1 when incubated with the protein in higher ratio (1:5) prior aggregation then not only the percentages of alpha helix but also the overall secondary structural composition majorly was changed to the initial monomeric form. Vitamin B6 incubated samples could not effectively maintain the dominating helical form and slight increase in the percentage of parallel beta-sheet was recorded. Vitamin B12 treated samples completely reversed the scenario. With Vitamin B12, major loss of helical structure, which indicated greater disorientation of stable folds, were found. Increase in both the percentages of beta-sheet and beta-turns in insulin secondary structure in the said case referred to the stimulatory effect of vitamin B12.

The Analytical aspects of Fourier transform infrared spectroscopy (FTIR) on insulin aggregation under influence of vitamins

The wave numbers of amide I band was to monitor the structural conducts of insulin before and after aggregation and a deliberate pursuit for knowing the effect of vitamin's under observation on it. The spectrum recorded before heating of insulin monomer (Fig.5.8, black curve), had two minima at 1550 and 1650 cm^{-1} . This clearly confirmed the presence of alpha helical structure [50-52] in higher percentages. After heat treatment, the minima were transitioned to 1628 cm^{-1} and a small shoulder at 1697 cm^{-1} was appeared. The former peak was due to the extended beta-sheet structures [53] that was in consistent with the CD results and formed during heat aggregation. The shoulder in higher wavelength corresponds to beta-turns and some off-diagonal involvement of beta-sheets [52]. In case of vitamin co-incubated heating samples, peak minima transfer along with more deepening of curves had found (Fig.5.8, blue, green and magenta curves). The more the negative intensity of transmission indicated both the more the energy was absorbed and rise in polarity. Polarity decrease is an indication of insoluble aggregates in solution [54] thus here the reverse phenomenon of polarity increase may emphasize the percent decrease of insoluble mature fibrils with the involvement of vitamins. The FT-IR peak at 1631 cm^{-1} and 1694 cm^{-1} may account for the presence of some 3_{10} -Helix [52] which may be found during the misfolding followed by refolding of the protein to native state. [55]

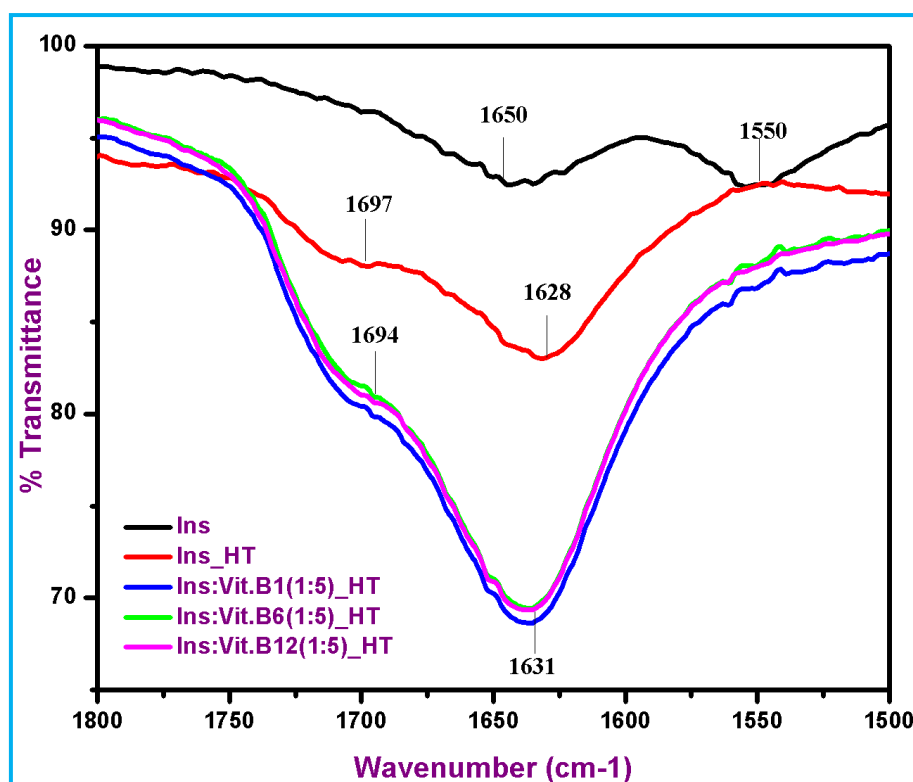


Fig.5.9. FTIR spectra considering percentage of transmittance with corresponding wave-numbers of monomeric insulin (black), only heat treated protein (red) and heat treated insulin in presence of Vit.B1 (blue), Vit.B6 (green) and Vit. B12 (magenta). Data shown in the curve was selected for amide I region [1800-1500 cm⁻¹] only. In each sample, protein concentrations were kept at 0.172 mm. Every spectrum was an average of 16 scans.

Rayleigh scattering assay as a measure of larger particles in solution

Liquids with low concentrations of suspended particles may follow Rayleigh scattering event [56]. Here, both the excitation and emission wavelengths were 307nm, as it is known that neither loss nor any gain of energy is involved in this process [57].

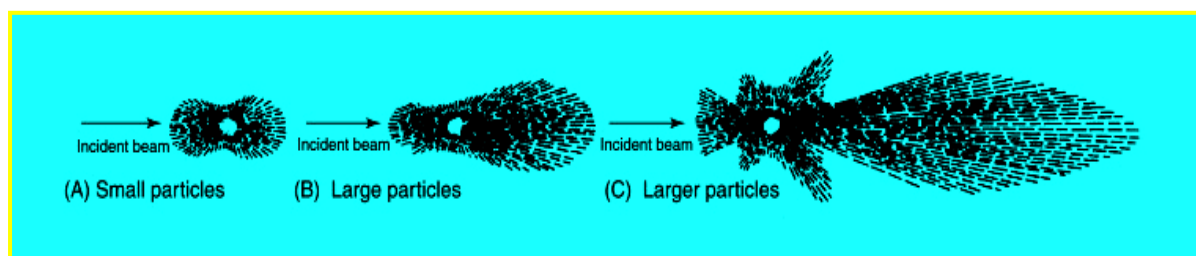


Fig.5.10. Schematic depiction of the proportionality of particle size with light scattering.
*Fig. adapted from Vanous RD. et. al., 1982.

From the bar diagram of Fig.5.10, it was evident that aggregation of insulin is responsible for the elevation of scattering intensity. Here it can be said due to the rise in particle size followed by aggregation [58]. The more the size of the particle the more is the scattering as shown in Fig.5.9.

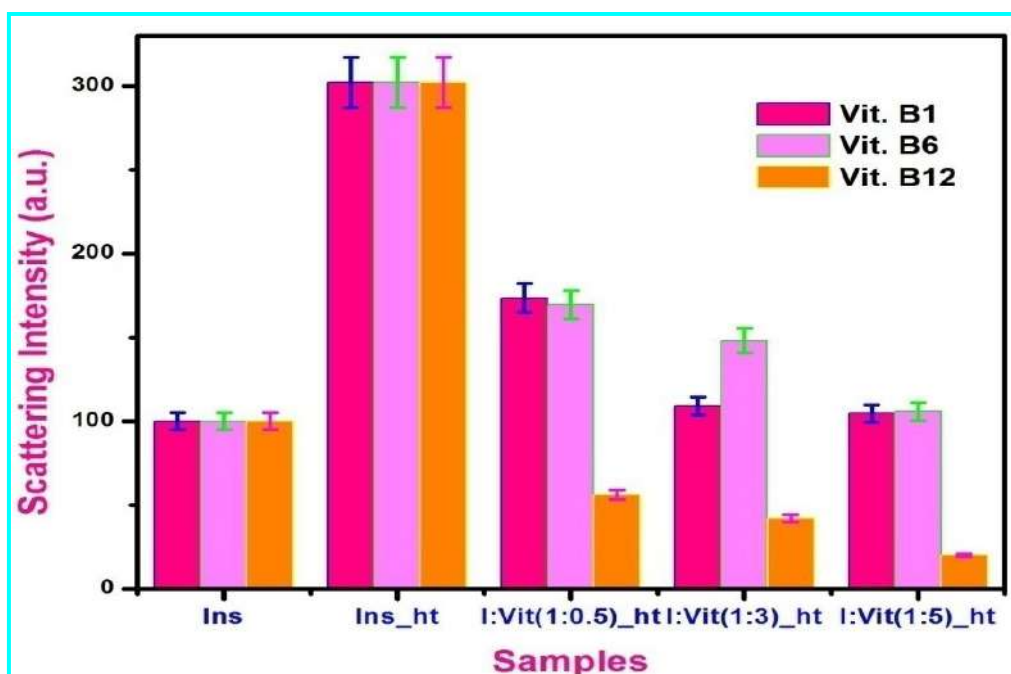


Fig.5.11. Results showing increase in intensity of Rayleigh Light Scattering of heat treated (60°C for 4h) insulin (Ins_ht) than the monomeric insulin (Ins). The effect of Vit. B1 (red bars), Vit.B6 (pink bars) and Vit.B12 (yellow bars) under experimental conditions on insulin aggregation at different ratio (Ins:Vit.) viz.1:0.5 to 1:5 were shown. Both the excitation and emissions were at 307 nm wavelength. Each data was average of three independent measurements. Error bars were given within the range of ± 5.0 .

From the Fig.5.10, it was clear that presence of Vit.B1 greatly reduced the scattering event of insulin and thus inhibited the formation of larger aggregates. The scattering shown by the samples treated with Vit.B1 with the ratio up to 1:5 was much like the scattering intensity obtained for monomeric insulin (in red, fig.5.10). Vit. B6 (pink bars, fig.5.10) also reduced the scattering up to a limit but presence of some higher order structure was accounted due to the appearance of moderate level scattering. Vit.B12 (yellow bars, fig.5.10) though greatly diminished the particle scattering with increasing concentration of the vitamin even the scattering was lower than that of monomeric form. This abnormal decrease may be realized as the misfolding/ disruption of monomeric configuration of insulin.

5.5.6. Measures of Hydrodynamic radius by Dynamic Light Scattering Assay of insulin and aggregates under experimental conditions

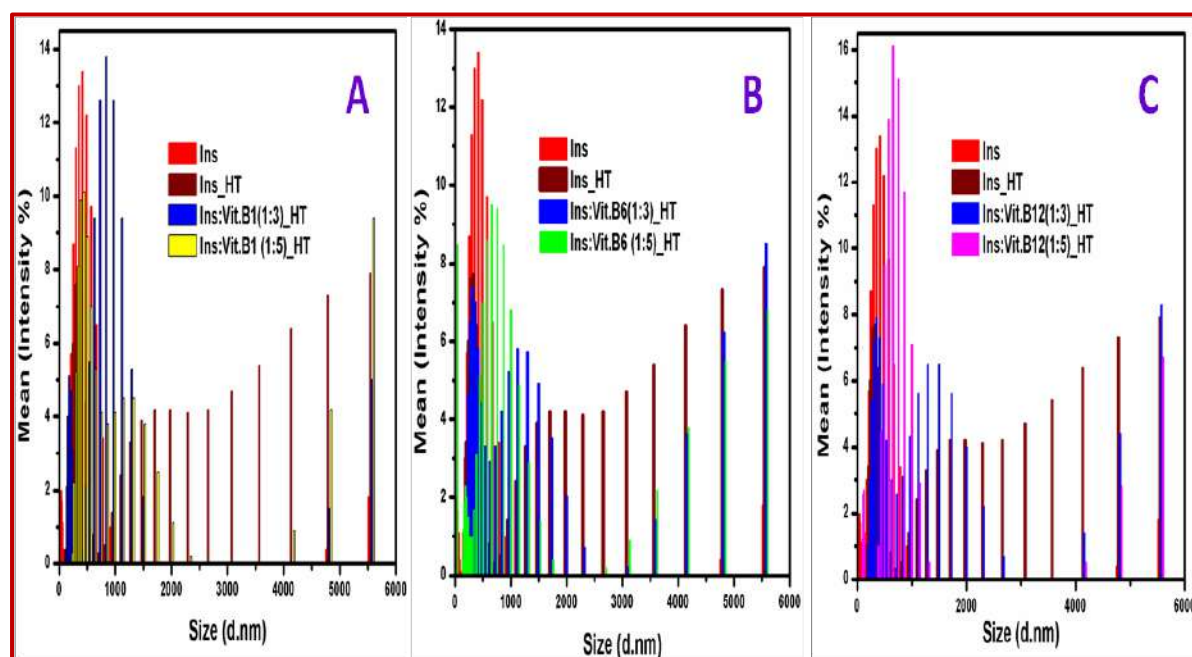


Fig.5.12. Particle size distribution patterns from DLS studies. Monomeric Insulin (red, each panel), heat treated (brown, each panel), heat treated in presence of Vit. B1 (panel A), Vit. B6 (panel B), Vit. B12 (panel C) at different interacting ratio. Protein concentration was maintained 20 μ M in each solution.

The physicochemical quantity of Particle size distribution by DLS can easily correlates the fluctuations in scattered light intensity proportionally to the sixth power of the corresponding diameter [59]. The hydrodynamic diameter is greater than the particle diameter because of the presence of ligand and solvated water molecules as shown in Fig.4.10.B.

From fig. 5.11, the particle size for monomeric insulin was condensed in the range of 95 to 110 nm (red, each panel), which was expected [60], but different size of particle distributed in varying intensities were yielded upon heat aggregation (brown, each panel). The 190-458 nm particles may be assigned as dimeric/tetrameric structural transition of insulin during the process and 2.6-5.5 μ m sized particles may be of higher ordered aggregated fibrils of insulin. Vit. B1 though effectively maintained the particle size near the range of monomeric insulin as shown in panel A. Vit.B1 treated samples after aggregation showed particle size within the range of 105-255nm (Ins:Vit.B1=1:3). Very few particles were found having larger size. Vit.B6 maintained the size of aggregated particles within the range of 220-825nm (panel B,

Fig.6), while co-incubating with insulin and Vit. B12 yielded 531nm-955nm size particles (panel C, Fig.6), during the said process. Some aggregates in the range of 3.1-5.5 μm size were also formed in Vit.B6 and Vit.B12 treated samples separately. Thus it can be said that, the phenomenon of inhibition of insulin aggregation was comparable in the order Vit.B1>Vit.B6> Vit.B12.

Atomic Force Microscopic (AFM) view of Insulin aggregation under the influence of Vit.B1,Vit. B6 and Vit. B12

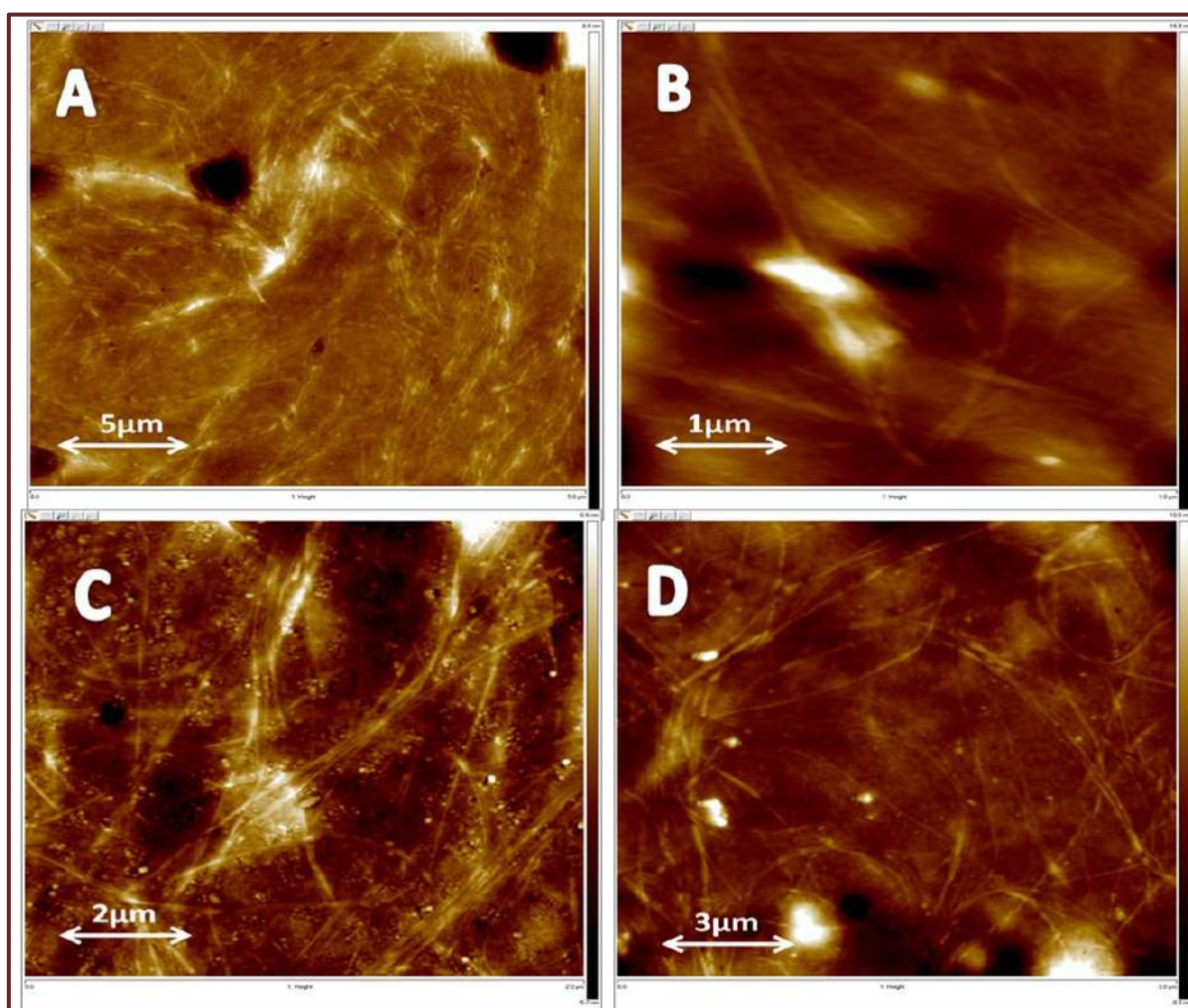


Fig.5.13. AFM images representing the aggregate morphologies of Insulin only at 5 μm resolution [A] and in the presence of Vit.B1 [B], Vit.B6 [C], Vit.B12[D] at 1 μm , 2 μm and 3 μm respectively

The huge mesh of needle like sharp aggregates in Fig.5.12.a was confirmed as amyloid fibrils [61] of insulin obtained under experimental condition. Vitamin B1 treated samples after heating however showed very few fibrils even in five times zoomed image than the former, as

the image resolution was 1 μm instead of 5 μm . thus Vit.B1 can be considered as an effective inhibitor of human insulin amyloid formation under experimental conditions. Fibrils were found in both the cases of Vit.B6 and Vit. B12 treated samples but the amount of fibrils was less in Vi.B6 treated samples compared to Vit.B12. The AFM study results were consistent with the previous experimental follow-ups.

5.6. DISCUSSIONS AND MAJOR CONCLUSIONS

The results showed that vitamin B1 was effective in inhibiting the amyloid fibrillation of insulin whereas vit.B6 partly did and vit.B12 aggravates the said process. In the chemical structure of vit.B1, there present an aminopyrimidine and a thiazolium ring linked by a methylene bridge (Fig 5.13.a). The thiazole is substituted with methyl and hydroxyethyl side chains. Thiamine had found to bind directly with different proteins like malate dehydrogenase, glutamate dehydrogenase and pyridoxal kinase with its thiazolium ring [62]. Because of the presence of cationic charge and hydroxyl group, there is a chance of interaction of vit.B1 with polar R groups of insulin side chain by H-bond and electrostatic interactions. The sulphur group present in vit.B1 may form inter molecular disulphide bond within two or more vit.B1 and thus can form a shield to prevent more numbers of insulin molecules to come closer during aggregation as shown in Fig.5.14.

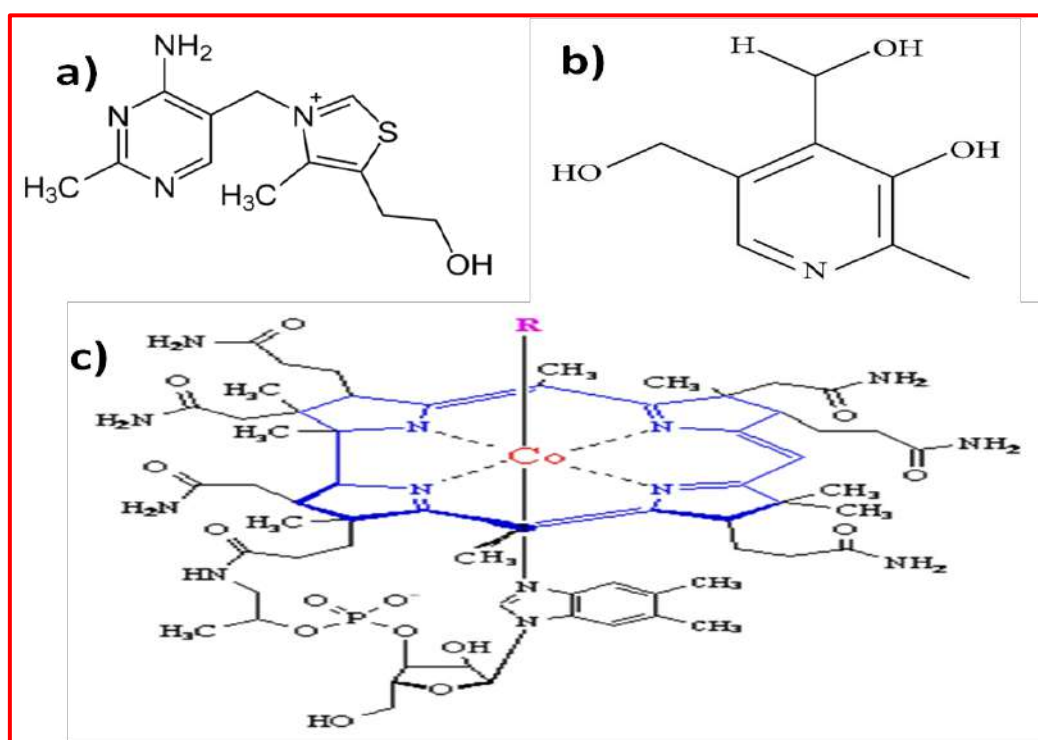


Fig.5.14. The chemical structures of a) Vit.B1, b) Vit. B6 (pyridoxal form) and c) Vit.B12

As found in experimental results, Vit.B1 had shown best inhibitory activity against aggregation at an interacting ratio of 1:5 (Insulin: Vit.B1). That means at a conc. five times more than insulin it will properly shield the protein to prevent aggregation. It had also known that thiamin is much stable at the acidic pH of experimental conditions [63].

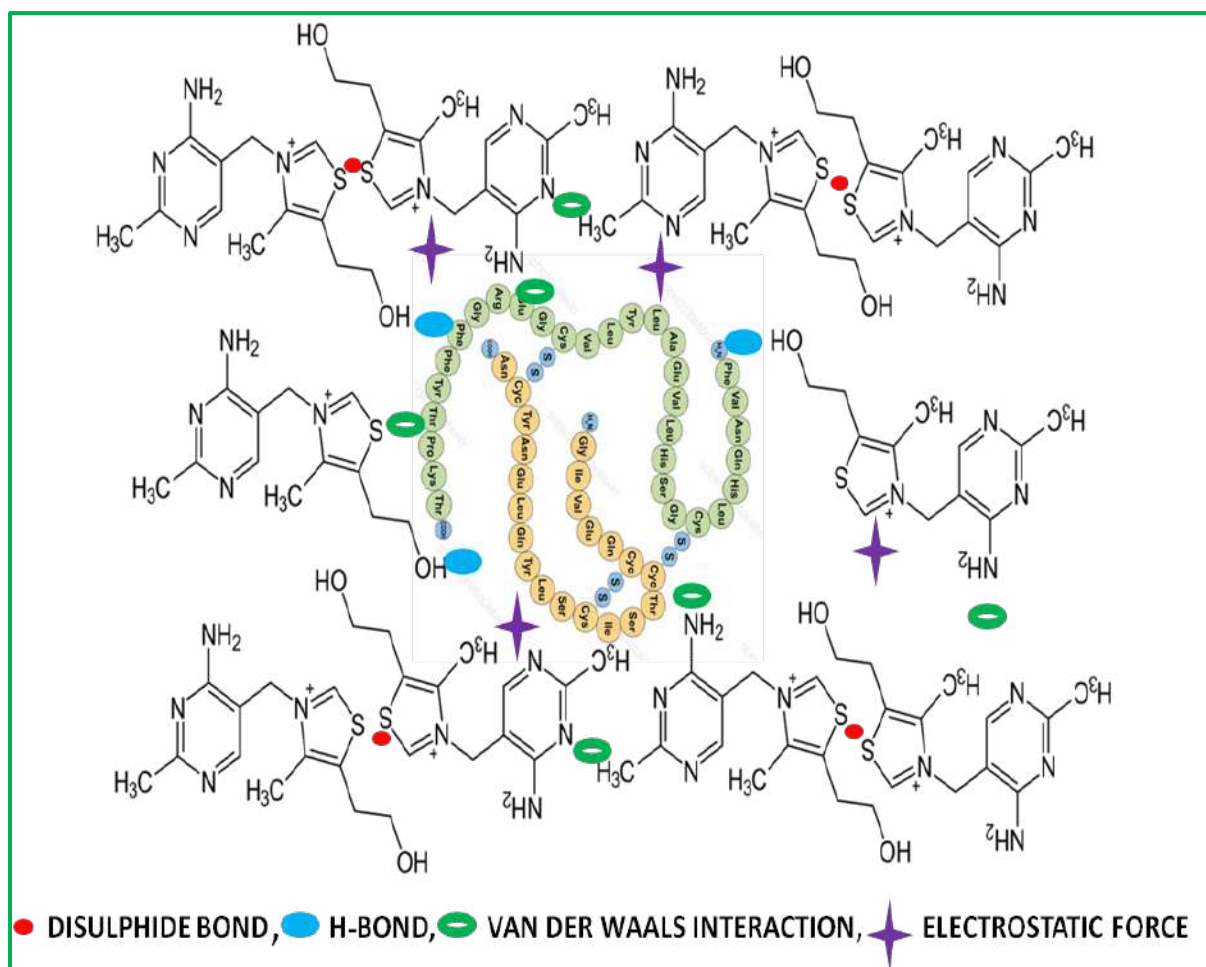


Fig.5.15. Schematic representation of the shielding effect imparted by thiamine against the aggregation event of insulin: many thiamine residues encircle single insulin molecule with the help of different stabilizing forces in order to prevent the aggregation of insulin

The stabilization of Insulin–Vit.B1 interaction may be imparted by formation of H-bond between insulin and vit.B1, disulfide bond within adjacent vitamin molecules, electrostatic interactions, van der waal forces etc. In this polar environment, the formation of hydrophobic association and burying event of non-polar residues of insulin followed by misfolding and self-aggregation had potentially disfavored. Vit.B6 in pyridoxal form, the aldehyde derivative of 3-hydroxy-2-methylpyridine (Fig 5.13.b) also was suitable to maintain the polar environment because of presence of three exposed hydroxyl groups and thereby involve insulin to interact with it through the polar side chains. However, the absence of any sulfur/other interacting residues may not sufficient to stabilize the interaction between insulin and vitamin B6. Thus during the course of heat treatment some insulin can be freed to form self-aggregates. The metallo enzyme structure of Cobalamin i.e., VitB12 represents a corrin ring with Cobalt positioned right in the center of the structure by four coordinated bonds of

nitrogen from four pyrrole groups. These four subunit groups have separated evenly across each other on the same plane (Fig 5.13.c). The fifth ligand connected to Cobalt is a nitrogen of the 5, 6-dimethylbenzimidazole. This benzimidazole is also connected to a five carbon sugar, which eventually attaches itself to a phosphate group, and then straps back to the rest of the structure. Vit.B12 though had found to aggravate the said aggregation of insulin. This was due to the probable poor accommodation of such bulky structure of Vit.B12 within the folds of insulin. The inner stability of Vit.B12 and decrease in sphere of solvation due to unavailability of exposed polar residues made Vit.B12 poor ligand for insulin. This also favors the separate accumulation of insulin in solution. Thus, the hydrophobic burying event during heat treatment leads to aggregate formation of the said protein.

While drawing conclusions from the comparative study on effects of the three vitamins on insulin aggregation, it can be conferred that, vitamin B1 was effectively maintained the alpha helical fold of insulin by protecting it in solution from forming higher aggregates. It was so as the potency of interaction with insulin was more profound for vitamin B1 than the rest two vitamins. The morphology of aggregates was also very slender comparatively than other forms. The quantity of aggregates though was less in vitamin B6 treated samples, yet the nature of fibrils found were same for both the Vit.B6 and B12 treated samples. In both the cases, long fibrils with blunt stems were observed which was mostly unlike the insulin amyloid fibrils. The fibrillar morphology of insulin amyloid was needle like and messy. Thus from the results it was evident that the inhibitory effect of vitamin B1 on insulin fibrillation was considerable at an interacting ratio of 1:5 for insulin: vitamin.

5.7. REFERENCES

1. Demain AL, Vaishnav P. 2009. Production of recombinant proteins by microbes and higher organisms. *Biotechnol. Adv.*, 27 (3) : 297-306, <https://doi.org/10.1016/j.biotechadv.2009.01.008>
2. Shikama Y., Kitazawa J-I., Yagihashi N., Uehara O., Murata Y., Yajima N., Wada R., Yagihashi S. 2010. Localized Amyloidosis at the Site of Repeated Insulin Injection in a Diabetic Patient. *Int. Med.*, 49: 397–401. [10.2169/internalmedicine.49.2633](https://doi.org/10.2169/internalmedicine.49.2633)
3. Das A, Shah M. and Saraogi I. 2022. Molecular Aspects of Insulin Aggregation and Various Therapeutic Interventions. *ACS Bio Med Chem Au.*, 2(3) : 205–221, [10.1021/acsbiochemau.1c00054](https://doi.org/10.1021/acsbiochemau.1c00054)
4. Endo JO., Röcken C., Lamb S., Harris RM., Bowen AR. 2010. Nodular Amyloidosis in a Diabetic Patient with Frequent Hypoglycemia: Sequelae of Repeatedly Injecting Insulin without Site Rotation, 2010, *J. Am. Acad. Dermatol.*, 63 (6): e113 [10.1016/j.jaad.2010.03.001](https://doi.org/10.1016/j.jaad.2010.03.001).
5. Rambaran RN., Serpell LC. 2008. Amyloid fibrils: abnormal protein assembly. *Prion*, 2(3) : 112–117, [10.4161/pri.2.3.7488](https://doi.org/10.4161/pri.2.3.7488)
6. Nilsson MR. 2016. Insulin amyloid at injection sites of patients with diabetes. *Amyloid*, 23 (3) : 139–147, [10.1080/13506129.2016.1179183](https://doi.org/10.1080/13506129.2016.1179183)
7. D'Souza A., Theis JD., Vrana JA., Dogan A. 2014. Pharmaceutical amyloidosis associated with subcutaneous insulin and enfuvirtide administration. *Amyloid*, 21(2) : 71–75, [10.3109/13506129.2013.876984](https://doi.org/10.3109/13506129.2013.876984)
8. Gupta Y., Singla G., Singla R. 2015. Insulin-derived amyloidosis. *Indian J. Endocrinol. Metab.*, 19 (1) : 174-177, [10.4103/2230-8210.146879](https://doi.org/10.4103/2230-8210.146879)
9. Bigi A., Cascella R., Chiti F., Cecchi C. 2022. Amyloid fibrils act as a reservoir of soluble oligomers, the main culprits in protein deposition diseases. *BioEssays*, 44: 2200086, [10.1002/bies.202200086](https://doi.org/10.1002/bies.202200086)
10. Cremades N., Dobson CM. 2018. The contribution of biophysical and structural studies of protein self-assembly to the design of therapeutic strategies for amyloid diseases. *Neurobiol. Dis.*, 109: 178–190, [10.1016/j.nbd.2017.07.009](https://doi.org/10.1016/j.nbd.2017.07.009)
11. Bender DA: Nutritional biochemistry of the vitamins. Cambridge, U.K.: Cambridge University Press; 2003. ISBN 978-0-521-80388-5.

12. Percudani R., Peracchi A. 2003. A genomic overview of pyridoxal-phosphate dependent enzymes. *EMBO Rep.*, 4 (9): 850–854, [10.1038/sj.embor.embor914](https://doi.org/10.1038/sj.embor.embor914).
13. Panwar B., Gupta S. and Raghava GPS. 2013. Prediction of vitamin interacting residues in a vitamin binding protein using evolutionary Information, 2013, *BMC Bioinformatics*, 14:44, [10.1186/1471-2105-14-44](https://doi.org/10.1186/1471-2105-14-44)
14. Rangwala H, Kauffman C, Karypis G. 2009. svmPRAT: SVM-based protein residue annotation toolkit. *BMC Bioinformatics*.10: 439. [10.1186/1471-2105-10-439](https://doi.org/10.1186/1471-2105-10-439).
15. Li N., Sun Z., Jiang F. 2008. Prediction of protein-protein binding site by using core interface residue and support vector machine. *BMC Bioinformatics.*, 9:553. [10.1186/1471-2105-9-553](https://doi.org/10.1186/1471-2105-9-553)
16. Shamim MT., Anwaruddin M., Nagarajaram HA. 2007. Support Vector Machine-based classification of protein folds using the structural properties of amino acid residues and amino acid residue pairs. *Bioinformatics*. 23(24):3320–3327, [10.1093/bioinformatics/btm527](https://doi.org/10.1093/bioinformatics/btm527).
17. Huang J., Li T., Chen K., Wu J. 2006. An approach of encoding for prediction of splice sites using SVM. *Biochimie.*, 88(7): 923–929, [10.1016/j.biochi.2006.03.006](https://doi.org/10.1016/j.biochi.2006.03.006).
18. Alam P., Chaturvedi SK., Siddiqi MK., Rajpoot RK., Ajmal MR., Zaman M and Khan RH. 2016. Vitamin k3 inhibits protein aggregation: Implication in the treatment of amyloid diseases. *Sci Rep.*, 6: 26759, [10.1038/srep26759](https://doi.org/10.1038/srep26759)
19. Lee V., Rekhi E., Kam JH., Jeffery G. 2012. Vitamin D rejuvenates aging eyes by reducing inflammation, clearing amyloid beta and improving visual function. *Neurobiol. Aging.*, 33 (10) : 2382-2389, <https://doi.org/10.1016/j.neurobiolaging.2011.12.002>
20. Annweiler C., Brugg B., Peyrin J-M., Bartha R., Beauchet O. 2014. Combination of memantine and vitamin D prevents axon degeneration induced by amyloid-beta and glutamate. *Neurobiol. Aging.*, 35 (2) : 331-335, <https://doi.org/10.1016/j.neurobiolaging.2013.07.029>
21. Ono K., Yoshiike Y., Takashima A., Hasegawa K., Naiki H., Yamada M. 2004. Vitamin A exhibits potent antiamyloidogenic and fibril-destabilizing effects in vitro. *Exp. Neurol.*, 189 (2): 380-392, <https://doi.org/10.1016/j.expneurol.2004.05.035>
22. Joshi P., Chia S., Yang X., Perni M, Habchi J., Vendruscolo M. 2021. Vitamin A and vitamin E metabolites comodulate amyloid- β aggregation. *bioRxiv*, I, <https://doi.org/10.1101/2021.10.30.466561>

23. Alam P., Siddiqi MK., Chaturvedi SK., Zaman M., Khan RH. 2017. Vitamin B12 offers neuronal cell protection by inhibiting A β -42 amyloid fibrillation, 2017, *Int J Biol Macromol.*, 99: 477-482, [10.1016/j.ijbiomac.2017.03.001](https://doi.org/10.1016/j.ijbiomac.2017.03.001)
24. Sampaio I., Quatroni FD., Lins PMP., Nascimento AS., Zucolotto V. 2022. Modulation of beta-amyloid aggregation using ascorbic acid. *Biochim.*, 200: 36-43, <https://doi.org/10.1016/j.biochi.2022.05.006>
25. Hashim A., Wang L., Juneja K., Ye Y., Zhao Y., Ming L-J. 2011. Vitamin B6s inhibit oxidative stress caused by Alzheimer's disease-related Cu (II)- β -amyloid complexes-cooperative action of phospho-moiety. *Bioorg Med Chem Lett.*, 21(21): 6430-6432, [10.1016/j.bmcl.2011.08.123](https://doi.org/10.1016/j.bmcl.2011.08.123).
26. C-Ospina CA. and N-Mesa MO. 2020. B Vitamins in the nervous system: Current knowledge of the biochemical modes of action and synergies of thiamine, pyridoxine, and cobalamin. *CNS Neurosci Ther.*, 26(1) : 5–13, [10.1111/cns.13207](https://doi.org/10.1111/cns.13207)
27. Lonsdale D. 2006. A Review of the Biochemistry, Metabolism and Clinical Benefits of Thiamin(e) and Its Derivatives. *Evid Based Complement Alternat Med.*, 3(1): 49–59. [10.1093/ecam/nek009](https://doi.org/10.1093/ecam/nek009)
28. Lu'o'ng K vinh quốc, Nguyễn LTH. 2011. Role of Thiamine in Alzheimer's Disease. *Am. J. Alzheimer's Dis.*, 26(8): 588-598, [10.1177/1533317511432736](https://doi.org/10.1177/1533317511432736)
29. Zhang Q., Yang G., Li W., Fan Z., Sun A., Luo J., Ke Z-J. 2011. Thiamine deficiency increases β -secretase activity and accumulation of β -amyloid peptides. *Neurobiol. Aging.*, 32(1) : 42-53, <https://doi.org/10.1016/j.neurobiolaging.2009.01.005>.
30. Parra M., Stahl S. and Hellmann H. 2018. Vitamin B6 and Its Role in Cell Metabolism and Physiology. *Cells*, 7(7): 84, [10.3390/cells7070084](https://doi.org/10.3390/cells7070084)
31. Fuso A., Nicolai V., Cavallaro R.A. Ricceri L., D'Anselmi F., Coluccia P., Calamandrei G., Scarpa S. 2008. B-vitamin deprivation induces hyperhomocysteinemia and brain S-adenosylhomocysteine, depletes brain S-adenosylmethionine, and enhances PS1 and BACE expression and amyloid-beta deposition in mice., *Mol. Cell. Neurosci.*, 37: 731–746. <https://doi.org/10.1016/j.mcn.2007.12.018>
32. Huang S. C., Wei J. C., Wu D. J., Huang Y. C. 2010. Vitamin B6 supplementation improves pro-inflammatory responses in patients with rheumatoid arthritis. *Eur. J. Clin. Nutr.*, 64(9) : 1007-1013, <https://doi.org/10.1038/ejcn.2010.107>.
33. Galluzzi L., Vacchelli E., Michels J., Garcia P., Kepp O., Senovilla L., Vitale I., Kroemer G., 2013. Effects of vitamin B6 metabolism on oncogenesis, tumor progression and therapeutic responses. *Oncogene* .32 : 4995–5004, <https://doi.org/10.1038/onc.2012.623>

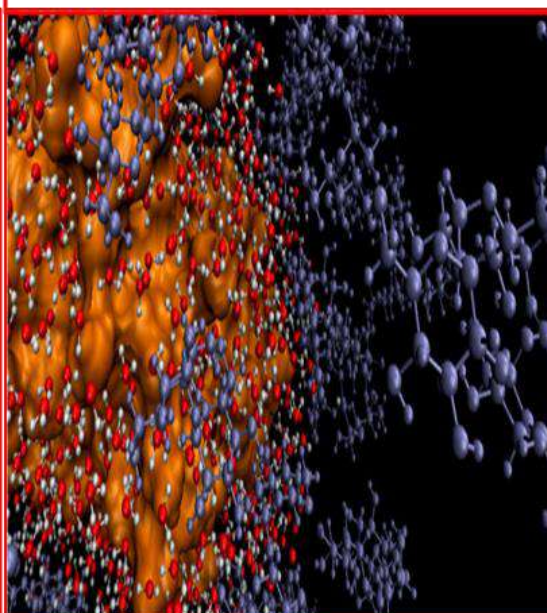
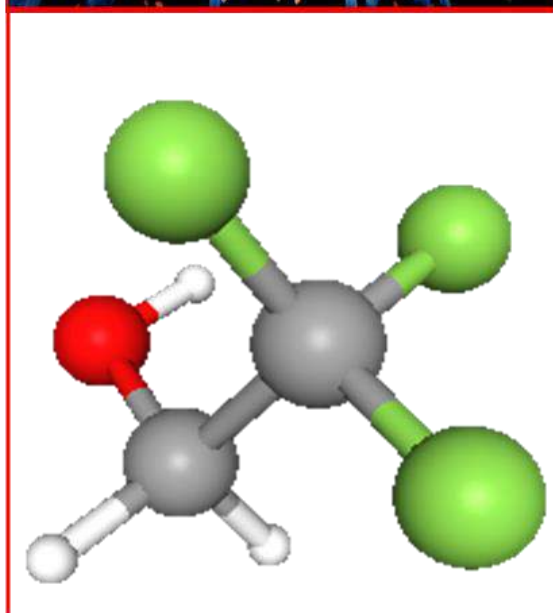
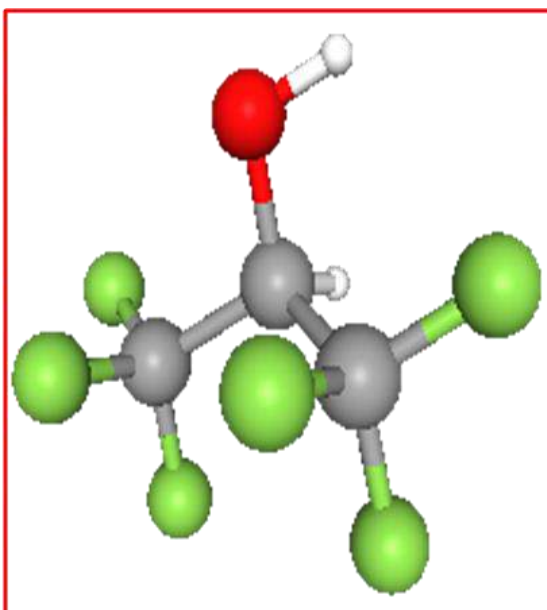
34. Douaud G., Refsum H., de Jager C. A., Jacoby R., Nichols T.E., Smith S. M., Smith A. D. 2013. Preventing Alzheimer's disease-related gray matter atrophy by B-vitamin treatment. *Proc. Natl. Acad. Sci.*, 110(23): 9523-9528. <https://doi.org/10.1073/pnas.1301816110>
35. Murakami K., Miyake Y., Sasaki S., Tanaka K., Fukushima W., Kiyohara C., Tsuboi Y., Yamada T., Oeda T., Miki T. and Kawamura N. 2010. Dietary intake of folate, vitamin B6, vitamin B12 and riboflavin and risk of Parkinson's disease: a case-control study in Japan. *Br J Nutr.*, 104(5): 757-764. [10.1017/S0007114510001005](https://doi.org/10.1017/S0007114510001005)
36. Rafiee S., Asadollahi K., Riazi G., Ahmadian S., Saboury A.A. 2017. Vitamin B12 inhibits tau fibrillization via binding to cysteine residues of tau. *ACS Chem. Neurosci.*, 8: 2676–2682, <https://doi.org/10.1021/acschemneuro.7b00230>
37. Lam AB., Kervin K., Tanis JE. 2021. Vitamin B₁₂ impacts amyloid beta-induced proteotoxicity by regulating the methionine/S-adenosylmethionine cycle. *Cell Rep.*, 36(13): 109753, [10.1016/j.celrep.2021.109753](https://doi.org/10.1016/j.celrep.2021.109753)
38. McCaddon A., Regland B., Hudson P., Davies G. 2002. Functional vitamin b(12) deficiency and Alzheimer disease. *Neurology*. 58:1395–1399. [10.1212/WNL.58.9.1395](https://doi.org/10.1212/WNL.58.9.1395).
39. McCaddon A. 2013. Vitamin b12 in neurology and ageing; clinical and genetic aspects. *Biochimie.*, 95:1066–1076, [10.1016/j.biochi.2012.11.017](https://doi.org/10.1016/j.biochi.2012.11.017).
40. Brange J., Langkjaer L., Insulin structure and stability. Book, Stability and Characterization of Protein and Peptide Drugs: Case Histories, Editors: Y. J. Wang, R. Pearlman, Springer; New York: 1993, 315–350. [\[Google Scholar\]](#)
41. Bekard IB. and Dunstan DE. 2009. Tyrosine Autofluorescence as a Measure of Bovine Insulin Fibrillation. *Biophys. J.*, 97: 2521–2531, [10.1016/j.bpj.2009.07.064](https://doi.org/10.1016/j.bpj.2009.07.064)
42. Waugh DF. 1946. A fibrous modification of insulin. I. The heat precipitate of insulin. *J. Am. Chem. Soc.* 68: 247–250, <https://doi.org/10.1021/ja01206a030>
43. Naiki H., Higuchi K., Hosokawa H., Takeda T. 1989. Fluorometric determination of amyloid fibrils in vitro using the fluorescent dye, thioflavine T. *Anal. Biochem.* 177: 244–249, [10.1016/0003-2697\(89\)90046-8](https://doi.org/10.1016/0003-2697(89)90046-8)
44. Srivastava A., Singh PK., Kumbhakar M., Mukherjee T., Chattopadhyay S., Pal H., Nath S. 2010. Identifying the bond responsible for the fluorescence modulation in an amyloid fibril sensor. *Chemistry*. 16: 9257–9263, [10.1002/chem.200902968](https://doi.org/10.1002/chem.200902968)
45. Nielsen L., Khurana R., Coats A., Frokjaer S, Brange J., Vyas S., Uversky VN., Fink AL. 2001. Effect of environmental factors on the kinetics of insulin fibril formation:

- elucidation of the molecular mechanism. 2001, *Biochemistry*, 40: 6036–6046, [10.1021/bi002555c](https://doi.org/10.1021/bi002555c)
46. Wu C., Biancalana M., Koide S., Shea J-E. 2009. Binding modes of thioflavin-T to the single-layer β -sheet of the peptide self-assembly mimics. *J. Mol. Biol.*, 394: 627–633. [10.1016/j.jmb.2009.09.056](https://doi.org/10.1016/j.jmb.2009.09.056)
 47. Biancalana M., Makabe K., Koide A., Koide S. 2009. Molecular mechanism of thioflavin-T binding to the surface of β -rich peptide self-assemblies. *J. Mol. Biol.*, 385: 1052–1063. [10.1016/j.jmb.2008.11.006](https://doi.org/10.1016/j.jmb.2008.11.006)
 48. Ivancic V.K., Krasinski CA., Zheng Q., Meservier RJ., Spratt DE., and Lazo ND. 2018. Enzyme kinetics from circular dichroism of insulin reveals mechanistic insights into the regulation of insulin-degrading enzyme, *Biosci. Rep.*, 38 : BSR20181416, <https://doi.org/10.1042/BSR20181416>
 49. Sreerama N., Woody RW. 2004. Computation and Analysis of Protein Circular Dichroism Spectra. *Methods Enzymol*, 383: 318-351
 50. Jackson M, Mantsch HH. 1995. The use and misuse of FTIR spectroscopy in the determination of protein structure. *Crit. Rev. Biochem. Mol. Biol.*, 30: 95–120, <https://doi.org/10.3109/10409239509085140>
 51. Cai S., Singh B.R. 2004. A distinct utility of the amide III infrared band for secondary structure estimation of aqueous protein solutions using partial least squares methods. *Biochemistry*, 43: 2541–2549, <https://doi.org/10.1021/bi030149y>
 52. Goormaghtigh E., Ruyschaert J-M., Raussens V. 2006. Evaluation of the Information Content in Infrared Spectra for Protein Secondary Structure Determination. *Biophys. J.*, 90 (8) : 2946-2957, <https://doi.org/10.1529/biophysj.105.072017>
 53. van Velzen EJJ., van Duynhoven JPM., Pudney P., Weegels PL., van der Maas JH. 2003. Factors Associated with Dough Stickiness as Sensed by Attenuated Total Reflectance Infrared Spectroscopy. *Cereal Chem.*, 80 (4) : 378-382, [10.1094/cchem.2003.80.4.378](https://doi.org/10.1094/cchem.2003.80.4.378)
 54. Ye S., Hsiung C-H., Tang Y., Zhang X. 2022. Visualizing the multi-step process of protein aggregation in live cells. *Acc Chem Res.*, 55(3) : 381–390, [10.1021/acs.accounts.1c00648](https://doi.org/10.1021/acs.accounts.1c00648)
 55. Armen R., Alonso DOV., Daggett V. 2003. The role of α -, 3_{10} -, and π -helix in helix→coil transitions. *Protein Sci.*, 12(6) : 1145–1157, [10.1110/ps.0240103](https://doi.org/10.1110/ps.0240103)
 56. Lawler DM. 2005. Spectrophotometry, Turbidimetry and Nephelometry, *Encyclopedia of Analytical Science (Second Edition)*, 2005

57. Andrews DL. 2017. Rayleigh Scattering and Raman Effect, Theory, Encyclopedia of Spectroscopy and Spectrometry (Third Edition)
58. Wade DM. and Drake JD. 2019. A Brief Review of Modern Uses of Scattering Techniques. *Georgia J. Sci.*, 77 (2) : 7, <https://digitalcommons.gaacademy.org/gjs/vol77/iss2/7>
59. Frisken B. 2001. Revisiting the method of cumulants for the analysis of dynamic light-scattering data. *Applied Optics*, 40(24) : 4087–4091, <https://doi.org/10.1364/AO.40.004087>
60. Paul S., Begum S., Parvej H., Dalui R., Sardar S., Mondal F., Sepay N and Halder U.C. 2024. In vitro retardation and modulation of human insulin amyloid fibrillation by Fe³⁺ and Cu²⁺ ions. *New J. Chem.*, 48: 3120–3135, <https://doi.org/10.1039/D3NJ04431A>
61. Siposova K., Kubovcikova M., Bednarikova Z., Koneracka M., Zavisova V., Antosova A., Kopcansky P., Daxnerova Z. and Gazova Z. 2012. Depolymerization of insulin amyloid fibrils by albumin-modified magnetic fluid. *Nanotechnology*, 23: 055101, [10.1088/0957-4484/23/5/055101](https://doi.org/10.1088/0957-4484/23/5/055101)
62. Bunik VI. and Aleshin VA. 2017. Analysis of the Protein Binding Sites for Thiamin and Its Derivatives to Elucidate the Molecular Mechanisms of the Noncoenzyme Action of Thiamin (Vitamin B1), *Stud. Nat. Prod. Chem.*, 53: 375-419, <http://dx.doi.org/10.1016/B978-0-444-63930-1.00011-9>
63. Voelker AL., Taylor LS. and Mauer LJ. 2021. Effect of pH and concentration on the chemical stability and reaction kinetics of thiamine mononitrate and thiamine chloride hydrochloride in solution. *BMC Chemistry*, 15: 47, <https://doi.org/10.1186/s13065-021-00773-y>

CHAPTER 3

Investigation of the effect of fluorinated co-solvents during in-vitro insulin fibrillation



6.1 Prologue of the study

Co-solvent can be defined as a solvent that in conjunction with another solvent can better dissolve a solute. In aqueous solution, the folding/unfolding equilibrium of marginally stabilized proteins can be moderated by co-solvents. If in presence of co-solvents, the said equilibrium shifts toward the unfolded state then the co-solvent can be specified as denaturants [1]. Urea for example, mainly serves as denaturants for maximum protein. On the other hand, if folded native form is favored in presence of it, then it is termed as protein stabilizing osmolytes. Some common and effective protein stabilizers are glucose [2], sucrose [2-3], trehalose [3] etc. Trehalose was shown to impart thermodynamic stability against chemical denaturation induced by guanidinium chloride (Gdn.HCl) to β -lactoglobulin at pH 6 and 2 [4]. Monohydric and polyhydric alcohols served well in protein stabilization. The different modes of action of Polyols to confer protein stability are: (i) increasing retention of structural conformation of protein to inhibit thermal [5] or chemical denaturation [6] (ii) protecting the structure of protein during freezing [7] and drying [8-9] to prevent loss of structure/activity. Temperature-induced denaturation of beta-lactoglobulin was shown to overcome by polyols and sugars [10]. The exposure of buried residues in a protein structure is mainly inhibited by the stabilizers as revealed by Hydrogen exchange studies. They do so by preventing partial or total unfolding of protein under stress [11-14]. Reports also said that, protein volume and compressibility also get decreased by polyols [15-16]. However, primarily alcohols were thought to denature protein still there are great evidences as their protective roles on protein stability [17]. In a study, polyhydric glycol and glycerol were shown to protect the assembly of the α - and β -domains of the model polypeptide BBA5 [17].

Fluorinated alcohols (fluoroalcohols) are considered as excellent solvents of peptides, proteins, and other compounds due to of their favourable physicochemical properties [18]. Trifluoroethanol (2,2,2-trifluoroethanol; TFE), hexafluoroisopropanol (1,1,1,3,3,3-hexafluoro-2-propanol; HFIP), and perfluoro-*tert*-butanol (1,1,1,3,3,3-hexafluoro-2-(trifluoromethyl)-2-propanol; PFTB) are commonly used as solvents, cosolvents, and additives in synthetic chemistry division [19]. Fluorinated alcohols like HFIP ($C_3H_2F_6O$) and TFE ($C_2H_3F_3O$) are most notable performer.

Fluorinated alcohols were known inducers of alpha helices, though they are also effective in disruption of native oligomeric forms of protein. These two are relevant criteria in affecting insulin fibrillation. The current investigation on insulin fibrillation in vitro in presence of

HFIP and TFE was preceded by the detailed inquiry on the effects of the two said alcohols on protein as follows in the next passage.

6.2. Effect of Fluorinated alcohols on Protein structure and stability: a review of Literature

HFIP was shown to induce alpha-helices in beta-lactoglobulin [20]. Fluorinated alcohols tend to form clusters and thus impact largely on protein or peptide structures in solution [21]. Thus they can favourably disorient the aggregated structures of Alzheimer's amyloid- β ($A\beta$) peptides [22]. Reports showed that TFE as well as some small alcohols can dissociate the tetrameric potassium channel KcsA present in a lipid bilayer [23]. Fluoroalcohols can interact well with proteins and there is a lot of evidence in literature of these interactions. There found many membrane proteins whose functions were altered by fluoroalcohols at low-to-mid mM concentrations. Some of such important membrane proteins are P2X receptors [24], nicotinic acetylcholine receptors [25], the mechanosensitive channel of small conductance (MscS) [26], KcsA channels [27], and Kv1.3 potassium channels [28]. HFIP on the other hand was found to decrease the rate of human islet amyloid polypeptide fibrillation at lipid bilayer interfaces [29].

A study to measure the effects of 2, 2, 2-trifluoroethanol (TFE) at low concentrations as helix-stabilizing co-solvents, gained light about the mechanisms of TFE in this regard. The study employed the dimeric α -helical coiled coil derived from the leucine zipper region of bZIP transcriptional activator GCN4 to follow its thermodynamics and kinetics of folding both in absence and presence of 5% (v/v) TFE. Results indicated that, the expenditure of energy associated with solvation of the polypeptide backbone had increased to a greater extent due to of the increase in structure of the binary alcohol/water solvent by TFE. This in turn destabilizes the unfolded species that indirectly hastens the kinetics of folding of the coiled coil. This study emphasized that, the leading cause of the transition state for folding of this small dimeric protein was the polypeptide backbone desolvation by TFE in higher degrees [30].

Another study proved the effect of 1, 1, 1, 3, 3, 3-hexafluoroisopropanol (HFIP) under acidic and neutral pH conditions in the formation of fibrils of human islet amyloid polypeptide associated with type II diabetes. The formation of amorphous aggregates was greatly suppressed by addition of HFIP with an optimum effect at 25% (v/v) [31]. Low

concentrations of HFIP strengthen both hydrophobic interactions and electrostatic interactions [31].

Although it was believed that individual hydrogen bonds were weakened under the influence of certain alcohols. But latter studies disclosed that the number of backbone hydrogen bonds formed in alcohol/water solutions compared to that in pure water had built up under impact of fluorinated co-solvents like TFE. In a comparative study (Fig.6.1) between normal and fluorinated alcohols on the patterns of hydrogen bonding pattern revealed that, the ability of the hydroxyl hydrogen of TFE is more than EtOH, but the TFE oxygen ability is much lowered than ethanol [32]. The lower capacity of electron donation by the two lone pairs of the oxygen was due to the higher hydrophobicity of TFE compared to EtOH.

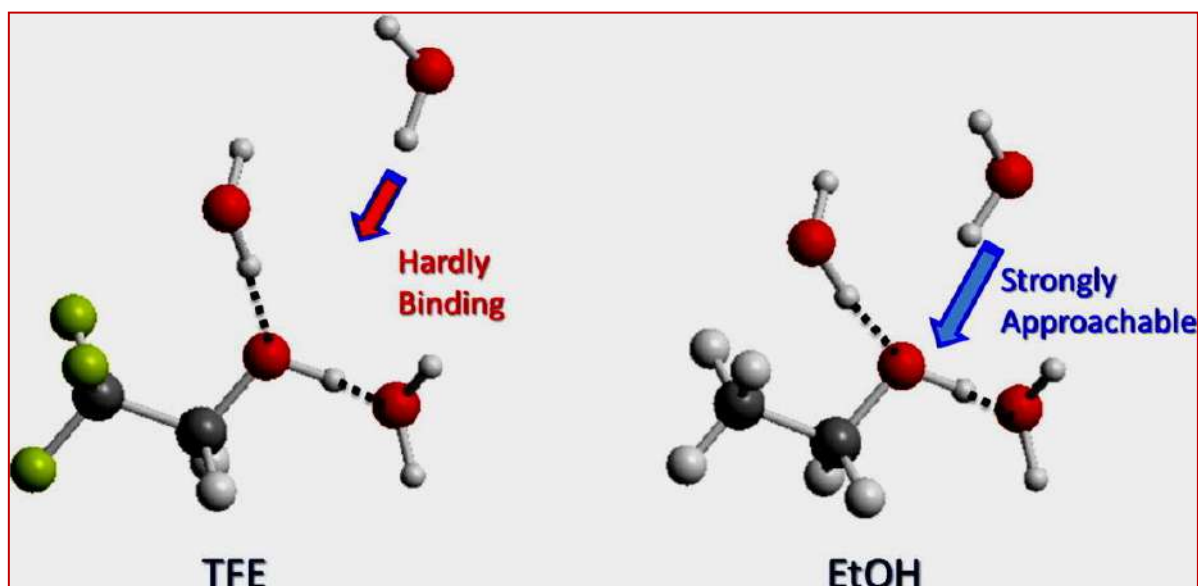


*Fig. 6.1. Comparative effect of the Hydrogen bonding with TFE and Ethanol in solution, separately. *Fig. adapted from Matsugami M. et. al., 2016, J. Mol. Liq., 217: 3-11, [10.1016/J.MOLLIQ.2015.06.050](https://doi.org/10.1016/J.MOLLIQ.2015.06.050)*

It was also revealed while comparing TFE with Methanol, that the stability conferred by the two was different. Methanol enhances the stability of backbone hydrogen bonds of which the carbonyl groups came from polar residues. However, TFE tends to stabilize the same involving non-polar residues [17]. Hydrophobicity is closely related to the amyloidogenicity of a protein. Insulin amyloid structure is dominated by the cross- β structure with an unavoidable mess of hydrogen bond network of fibrils [33]. For that reason the co-solvent effect should be considered in terms of hydrogen bonding propensities with native protein. In this study, HFIP and TFE were used separately to trace the effects on insulin aggregation.

6.3. MATERIALS AND METHODOLOGIES

6.3.1. Different fluorescent probes namely, ANS, Thioflavin T (ThT) were used as received without further purification. The experiments were performed in HPLC water. All other reagents used were of analytical grade.

Table 6.1. Chemicals and equipments required

ITEMS	OBTAINED FROM
Human insulin (Huminsulin R)100 IU/ml (r-DNA origin)	Eli Lilly and Company India Pvt. Ltd.
HPLC grade 100% Pure Distilled Water, Acrylamide, N,N'-Methylenebisacrylamide,	Sigma-Aldrich
Methanol & Fluorescent probes, viz., 8-Anilinonaphthalene-1-sulfonic acid (ANS), Congo red (CR), Thioflavin T (Th T)	Sigma Chemical Co. (St. Louis, USA)
Glycine, KOH, Acetone	Merck (Mumbai, India)
2, 2, 2-Trifluoroethanol (TFE)	Spectrochem Pvt. Ltd. (India).
1,1,1,3,3,3-Hexafluoroisopropanol (HFIP)	Sigma-Aldrich
Copper grids (mesh size-300) for TEM	Sigma-Aldrich
Quartz cuvettes and Hellma absorption cuvettes	Sigma-Aldrich
Magnetic beads, Membrane dialysis tubing	Sigma-Aldrich

6.3.2. Methodologies employed

In order to investigate the effects of co-solvents individually on insulin aggregation, the stock percentages of fluorinated co-solvents were made as described in section 3.5. The aggregates formed in absence and in presence of co-solvents were experimented through different spectroscopic, fluorimetric, light scattering approaches as detailed in the sections 3.7-3.17.

6.4. RESULTS OF RESEARCH FINDINGS

Intrinsic Fluorescence measurements

To determine the effects of fluorinated co-solvent on thermally induced insulin fibrillation, the intrinsic tyrosine emission spectra of insulin was compared with that of fibrillated form. The result was presented in Fig.6.2 where a decrease in Tyr fluorescence intensity during insulin fibrillation was prevalent at emission intensity of 304nm. Tyrosine, being one of the best intrinsic fluorophores, can speculate about the microenvironments [34] of the aromatic moieties of insulin in TFE and HFIP solutions. Here the fluorescence quenching in heat treated insulin [35] was very much relevant due to the placement of accessible tyrosine residues into hydrophobic grooves generated during its fibrillation. Both HFIP and TFE treated samples did not show any significant difference in the fluorescence wavelength maxima (~ 304 nm) as well as the maximum fluorescence emission intensity (I_{\max}) (Fig. 6.2.A and B respectively). However, the addition of HFIP and TFE at different percentages to the insulin did not increase the emission intensity like that of insulin monomer at 306 nm except at 5 and 10 percent for HFIP (depicted in pink and cyan, Fig.6.2 A) and 10 percent for TFE (depicted in pink, Fig.6.2 B).

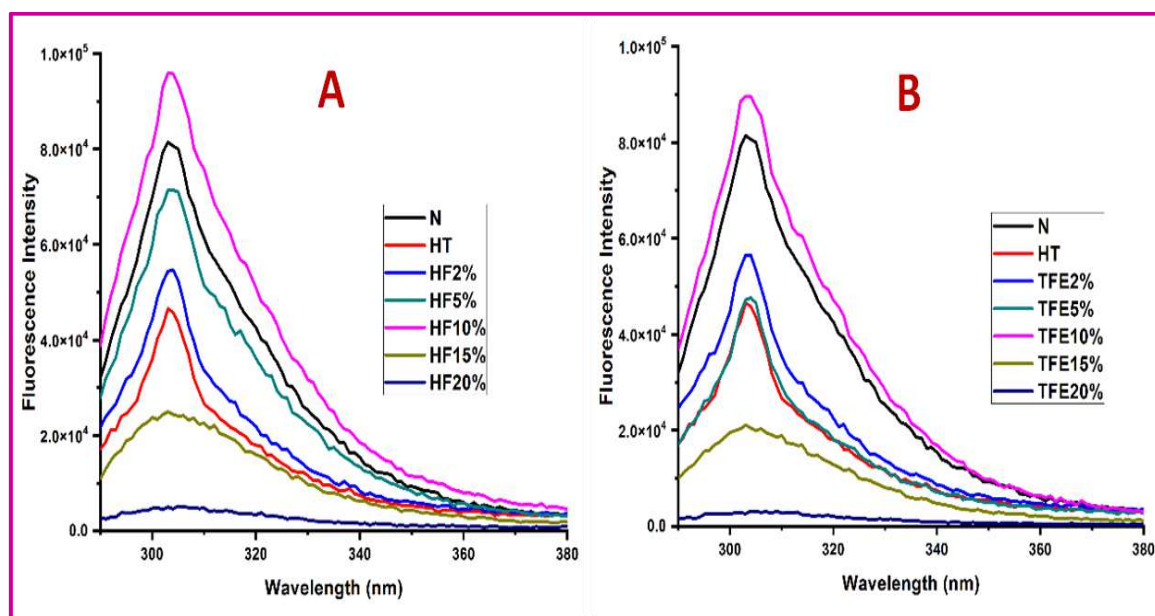


Fig. 6.2. Fluorescence emission spectra of Insulin monomer (black), heat aggregated form of Insulin (red), in presence of 2-20% HFIP (panel A) and TFE (panel B) respectively.

The said scenario may account for the maintenance of monomeric form of insulin effectively by fluorinated alcohols at lower concentrations. The inhibition of burying event of tyrosine

due to thermal effect at lower pH can thus said to be optimized when 5-10% fluorinated alcohol were used as co-solvents.

Effect of co-solvents on fibrillation propensity of insulin measured by Thioflavin T (ThT) fluorescence and Kinetic studies

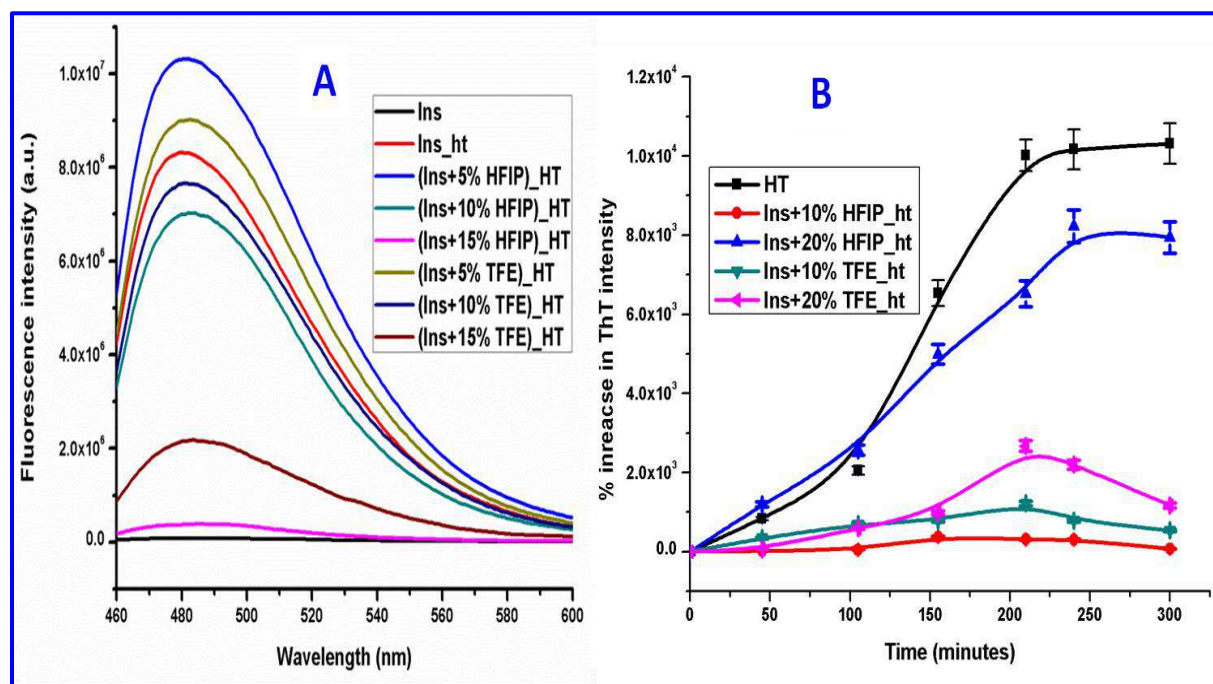


Fig. 6.3.A. ThT emission spectra of insulin monomer (black), insulin amyloid (red) and heat treated insulin with diff. conc. (5-15%) of co-solvents-HFIP and TFE. Panel B shows kinetics of Insulin amyloid fibrillation in absence and presence of co-solvents. The percent increase in ThT fluorescence intensity was calculated by eqn.1, section 3.11. The aggregation kinetics of insulin was showed in black squares. Insulin aggregated in presence of HFIP as well as TFE was shown accordingly in different colored symbols at interacting percentages of 10% and 20% respectively. Error bars were given consequently.

Thioflavin T assay is an indicative tool of amyloid fibrillation [36-37]. Increase in ThT fluorescence emission intensity of heat treated insulin at 482 nm as shown in red curve in Fig. 6.3.A is expected due to amyloid generation during thermal incubation [38-40] when excited at 440 nm. The decrease in ThT emission intensity was observed in presence of HFIP and TFE separately at an interaction ratio of 10% or more.

To clarify the effect of co-solvents, investigation was done on the kinetics of insulin aggregation via ThT assay. Fig.6.3.B showed that insulin followed sigmoidal pattern kinetics

for fibril growth and it was one of the characteristic features of insulin fibrillation [41]. The sigmoidal pattern also known as nucleation-elongation kinetics for heat treated insulin was depicted in black squares in Fig.6.3.B. This growth curve of untreated human insulin showed a considerable Lag phase of around ~ 100 min. The Lag phase is characterized by seed/nuclei formations which give rise due to intermolecular interactions of non-native monomeric insulin species followed by inevitable oligomerization [42]. However, the sharp elongation of fibrils got a peak value at ~ 200 min. Once the fibrillation propensity reached peak value, further elongation of fibrillation was inhibited. Rather the amount of mature fibril generated maintained a constant value though heat incubation had been continued [43]. Both the HFIP and TFE had best reduced the fibrillation growth kinetics of insulin at 10% v/v. Although HFIP gave steeper curves with lower intensities at both low and high interacting concentrations with insulin. This data indicated the slow rate of gradual fibrillation of insulin in presence of HFIP accompanied by slight acceleration of Lag phase and fix duration of Log phase. TFE on the other hand greatly reduced amount of mature fibril generation of insulin. But the irony was, it somehow shortened the elongation phase. The most noticeable thing was, TFE greatly lengthened the Lag phase up to 150 minutes for fibril growth as depicted in green and blue shapes in Fig 6.3.B.

Monitoring the hydrophobicity changes of insulin in absence and presence of the fluorinated alcohols by 8-Anilino-1-Naphthalene sulfonic Acid (ANS) assay

1-Anilino-8-naphthalene-sulfonic Acid (ANS) is a solvato-chromic dye that may differentiate between partially folded and molten globule states of a protein [44]. In this study, the ANS assay was proved very relevant in showing the solvent-dependent shift in its emission spectra. The dramatic increase in ANS fluorescence intensity along with visible blue shift (from 512 nm to around 475 nm) in thermally incubated insulin from monomeric no-heat incubated insulin was portrayed in red curves and black curves, respectively in Fig .6.4.A and B. In general, for most fluorophores, a blue shift and increased fluorescence intensity are seen with decreasing polarity of the medium. In this case- the first excited electronic state of the fluorophore is more polar than the ground state. If there are more polar groups around to form stronger interactions with the fluorophore, these interactions will be even stronger for the excited state, since it is more polar. Hence, in more polar environment, the difference in energy between the excited state and the ground state will be smaller, and the fluorescence red-shifted, and, vice versa, in less polar environment the energy difference will be larger,

and the fluorescence will be blue-shifted [45]. Accordingly, the most suitable explanation for the result is that insulin was becoming partially or fully unfolded so the ANS fluorophore got access to less polar environment.

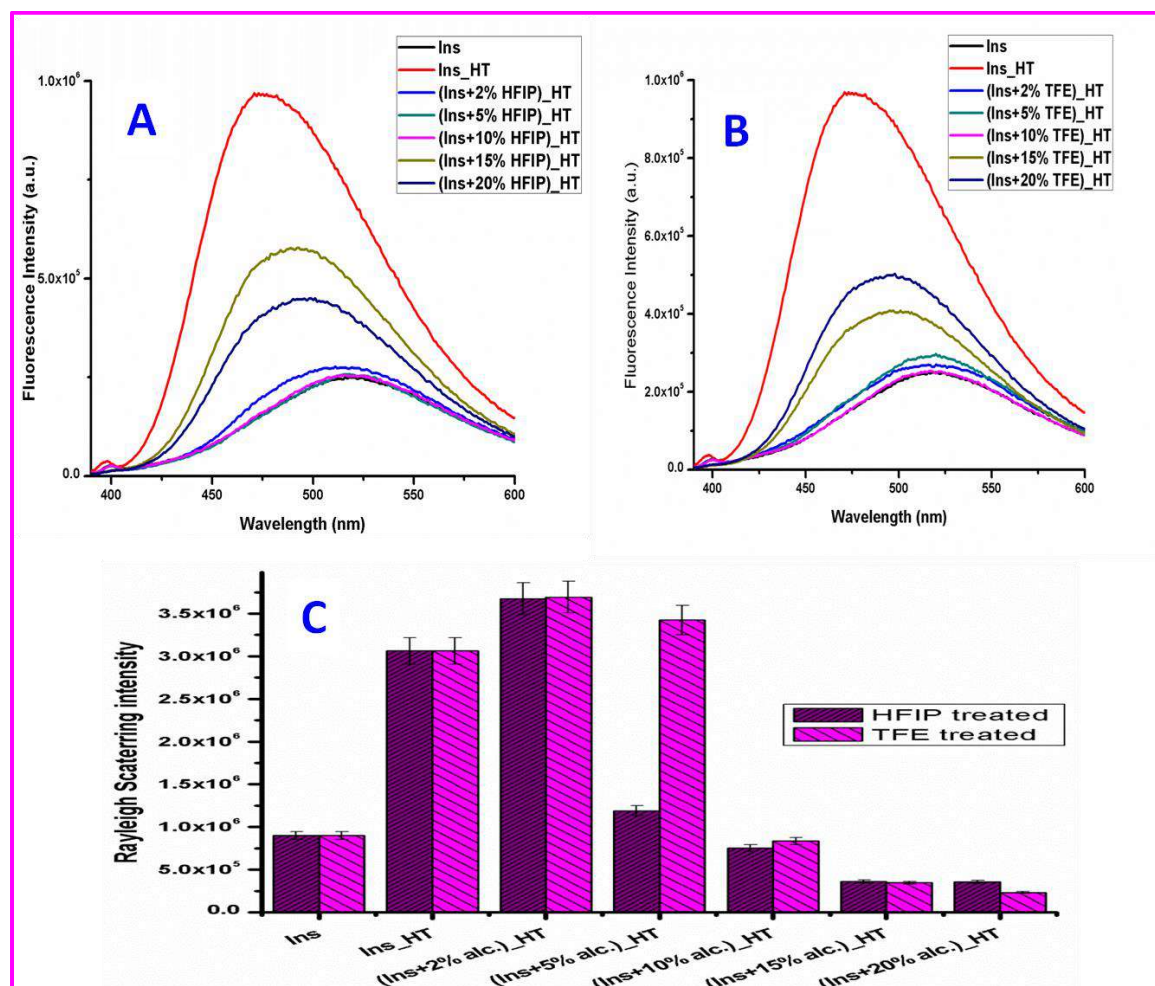


Fig.6.4. ANS fluorescence emission spectra of monomeric (black curve, panel A and B) and heat aggregated insulin (red curve, Panel A and B). The aggregation of insulin followed by ANS assay was shown in the presence of 2-20% HFIP (Panel A), same in the presence of 2-20% TFE (Panel B). Excitation was done at 350 nm and emission range 400–600nm. Panel C showed the Bar diagram of the Rayleigh Light Scattering emission intensity to compare monomeric insulin with heat treated samples both without and with fluorinated alcohol, HFIP (dark violet) and TFE (magenta) in the conc. range (2-20%). Error bars were given accordingly.

From the ANS result, it was evident that, both the alcohols HFIP and TFE at lower concentrations, 5-10% v/v, maintained the insulin monomer like spectra having λ_{max} of around 510nm with very low fluorescence intensity. So it can be stated that, the two

fluoroalcohols did not permit the access of ANS by preventing unfolding of protein and thus indirectly prevented the misfolding and aggregation of insulin.

Rayleigh Light Scattering (RLS) Measurements

Rayleigh scattering assay showed in Fig 6.4.C. clearly indicated the occurrence of around 3.5 fold multiplied scattering by heat treated insulin (second couple of bars) compared to not-heated monomer form (first couple of bars). The said increase can be explained in terms of presence of larger particle size in solution after heat treatment. Consequently, the alcohol incubated samples showed lower scattering but the degree of scattering was varied differently for the two. TFE in very lower interacting percentages increased the scattering [46] which was though decreased with increasing percentages of TFE. But above 15% v/v concentration, HFIP and TFE both diminished the scattering than even the native monomeric form of insulin. It though indicated the disruption of stable monomeric form of insulin itself. But at moderate interacting ratio i.e., at 10% v/v, both the HFIP and TFE gave the monomer like scattering. It also can be said that, decreasing the light scattering followed sharp fall pattern with HFIP.

Interpreting Fourier Transform Infra Red (FTIR) spectral Peaks

Native spectra of insulin monomer (black curve, both panels A and B, Fig 6.5) grown at pH 1.6 exhibited maxima in the amide I' region with the main minimum of 1640 cm^{-1} and a weaker one at 1550 cm^{-1} , this indicates alpha helix predominating form of monomer [47]. While Insulin at Ph 1.6 fibrillated at 60°C for 4hrs at exhibited inverted maxima in the amide I' region at $\sim 1627\text{ cm}^{-1}$ which largely revealed the formation of predominantly cross beta-sheet structures [48]. A small band outside of the amide I' region at $\sim 1712\text{ cm}^{-1}$ was present and can be attributed to deuterated carboxyl groups. There found reduced transmittance as well as minima shift towards native spectra, optimized when HFIP and TFE concentration reached 10% (depicted by green and brown curves in panel A and B respectively, Fig 6.5). HFIP and TFE individually though partly reduced the said transition towards beta-sheet rich spectra yet the results also showed presence of cross-beta structures in these two fluorinated alcohol treated samples separately. The amide I bands found in the regions of $1638\text{--}1634\text{ cm}^{-1}$ attributed to N-H bending [49]. It was too observed that the use of HFIP and TFE as co-solvents of insulin leads to a fall in the transmittance as shown by the sharp minima which corresponds to higher absorption. The intensity of an absorption band depends on the polarity

of the bond, the bond with higher polarity will show more intense absorption band. The intensity also depends on the number of bonds responsible for the absorption; the absorption band with more bonds involved has higher intensity. This indicates the interaction of HFIP and TFE with insulin separately under experimental conditions.

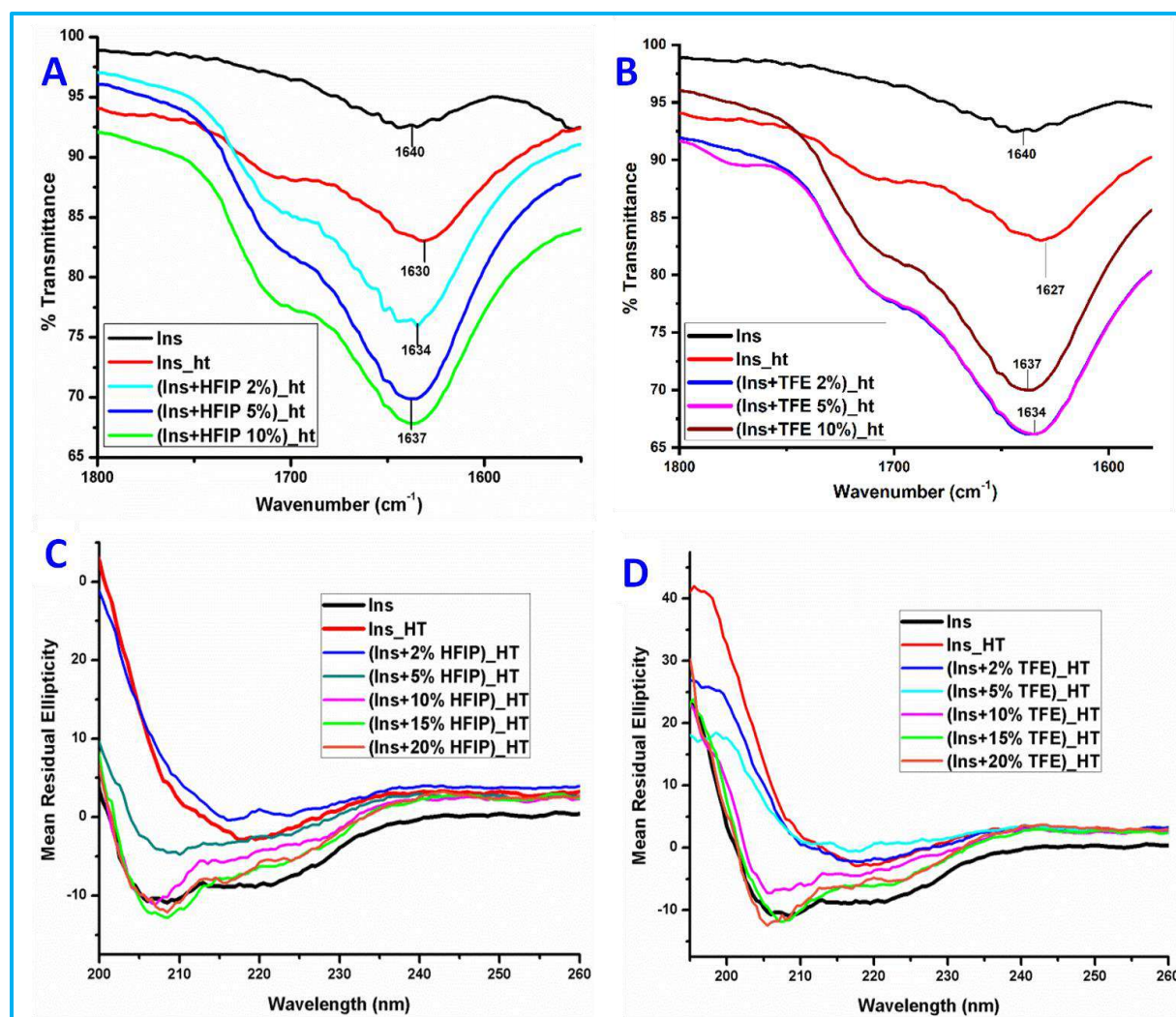


Fig.6.5. A and B showing selected region of FTIR spectra (1550 cm⁻¹ to 1800 cm⁻¹) of native Insulin (black curves, both A and B panels) and insulin under different experimental conditions. Heat treated insulin in absence (red curves, both A and B panels) and in presence of 2-10% HFIP (Panel A) and TFE (Panel B) were depicted. Each spectrum was an average of 32 scans. Panel C and D is showing Far-UV CD spectra of monomeric insulin (black curves, both panels C and D) and heat incubated insulin (red curves, both panels C and D) in the presence of HFIP (panel C) and TFE (panel D) at 2-20% interacting concentrations with insulin. The insulin concentration was kept 6.5μM in each of the cuvette.

Far UV-Circular Dichroism (CD) spectra and deconvolution analyses

CD spectroscopy was used to examine the secondary structure of non-aggregated insulin at pH 1.6 (black curve, in both Fig. 6.5.C and D) along with aggregated (red curve, in both Fig. 6.5.C and D) one. Peak minima occurred in case of insulin monomer at 208 nm (major) and 222nm (minor) were due to alpha helix rich secondary structure of insulin whereas mean residual ellipticity at around 216 nm which was found in case of heat aggregated insulin was due to of β -sheet predominating structure [50]. Increasing concentrations of HFIP and TFE treated insulin separately were also thermally incubated and scanned for Far UV-CD and depicted in Fig.6.5 C and D respectively. In cases of alcohol treated samples, the gradual disappearing of ellipticity at 216nm and reappearance of ellipticity at around 207 nm were found and optimized at low conc. (at 10%) of alcohol treatment.

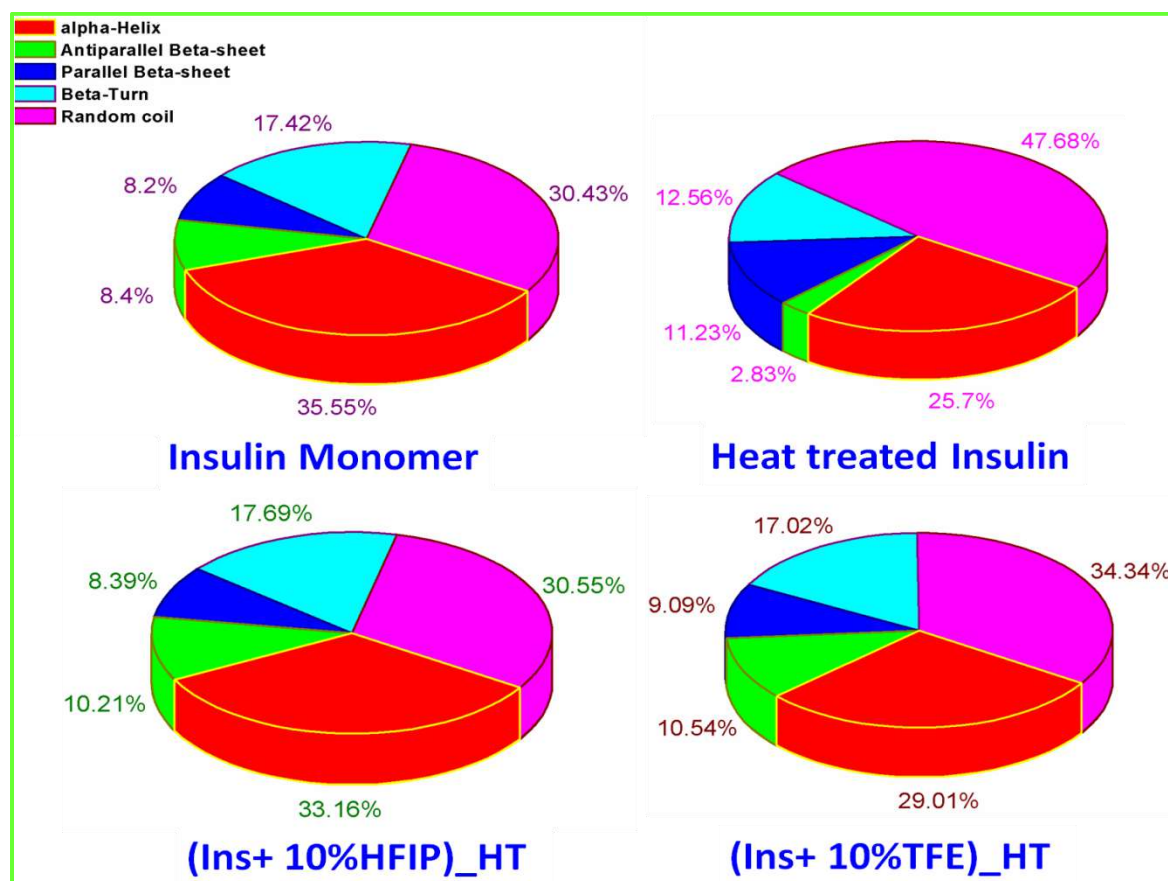


Fig.6.6 Representation in pie charts of CD Deconvolution data calculated by CDNN 2.1 software. Samples notified in the diagram are insulin (upper left), heat treated insulin in absence (upper right) and in presence of 10% HFIP (lower left) and TFE (lower right).

The Far UV-CD signals were deconvoluted using CDNN 2.1 software and represented as pie charts in Fig.6.6. Pie Chart clearly depicted that HFIP when used as co-solvent (Fig. 6.6, lower left panel) before heat treatment, greatly retained the alpha helical secondary conformation of insulin monomer and thus protected insulin against fibrillation. Though some rise in antiparallel beta-sheet percentage was prevalent and this may indicate formation of mature fibrils in smaller extents in spite of the protection of HFIP. Similar experiment with TFE (Fig. 6.6, lower right panel) revealed decrease in alpha helical percentages while increase in both parallel and antiparallel beta-sheet percentages. This proved the occurrence of insulin fibrils in solution. Though the percentage of random coiling was greatly reduced with TFE and thus indicated the poor protection provided by TFE against fibrillation of insulin.

Dynamic Light Scattering (DLS) of insulin fibrillation as monitored under co-solvent influence

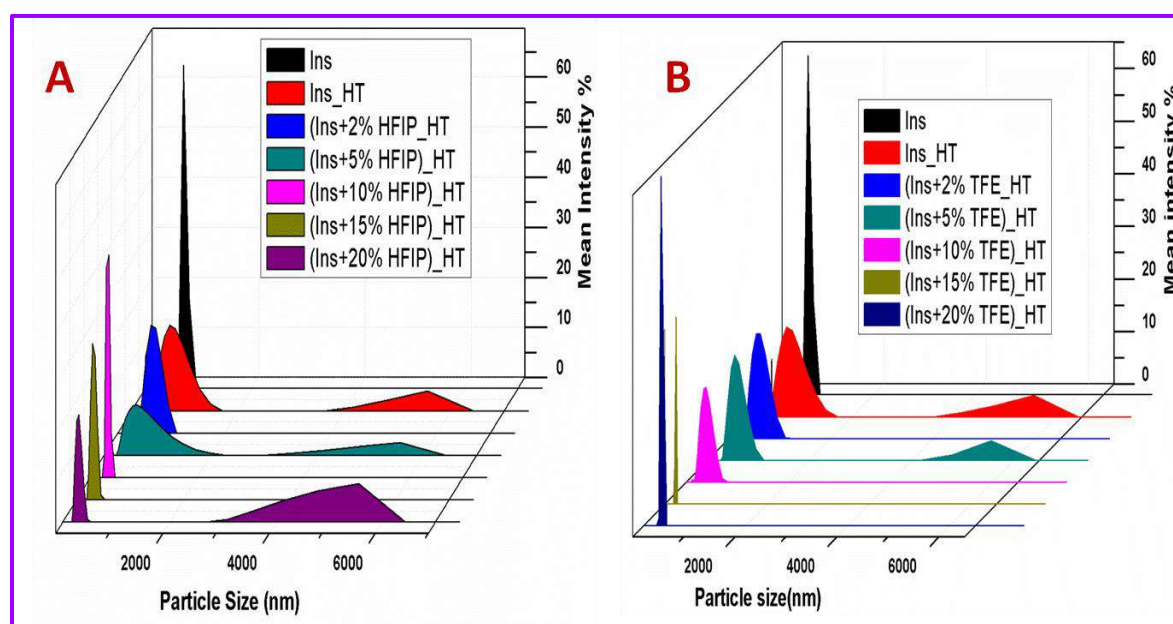


Fig.6.7. The results of dynamic light scattering analysis as a function of particle size. Changes in the particle size of insulin monomer (in black color, both panels) during heat incubation in at 60 °C for 4 hrs without (in red color, both panels) and with co-solvents, HFIP (panel A) and TFE (panel B) at different percentages v/v interactions depicted by different colors. Each of the spectra was an average of 12 scans.

Based on the DLS assay results (Fig.6.7), it was found that the particle size of monomeric human insulin ranged between 100-150nm whereas, in insulin aggregates there was

significant increase in particle size, ranging from 350-550nm, 1.3-1.5 μm , 2.4-2.7 μm [51]. The different sizes of particles mixed in a population were an indication of presence of mature amyloid fibrils as well as soluble oligomeric intermediates of unfolded insulin. HFIP remarkably restored the hydrodynamic radius of insulin within the range of 342 nm under aggregating condition. TFE though showed the presence of some higher aggregates of having maximum radius up to 530 nm. Another notable thing was that HFIP at higher interacting percentages (>15%) could not exert any protective effect on aggregation (Fig.6.7.A) whereas TFE at higher percentages yielded very small sized particles in solution having range of 20-40 nm. This can be explained as the shattering of inter-chain and intra-chain disulfide bond stabilized A and B chains of insulin monomeric form at higher percentages of TFE.

Transmission electron microscopic study (TEM) of Insulin Amyloid generation in presence of HFIP and TFE

TEM imaging of heat aggregated insulin (Figure 6.8 A and B) showed the long unbranched rod-like nature of insulin aggregates that were identical to amyloid fibrils as reported previous literatures [52-53]. The fibrils generated in presence of 10% HFIP (Figure 6.9 A and B) were found to be very few and slender whereas the same in presence of 20% HFIP (Figure 6.9 C and D) revealed with needle-like morphologies. This finding is consistent with previous results in that the lower percentage of HFIP is more effective in protecting the monomer form of insulin under heat treatment.

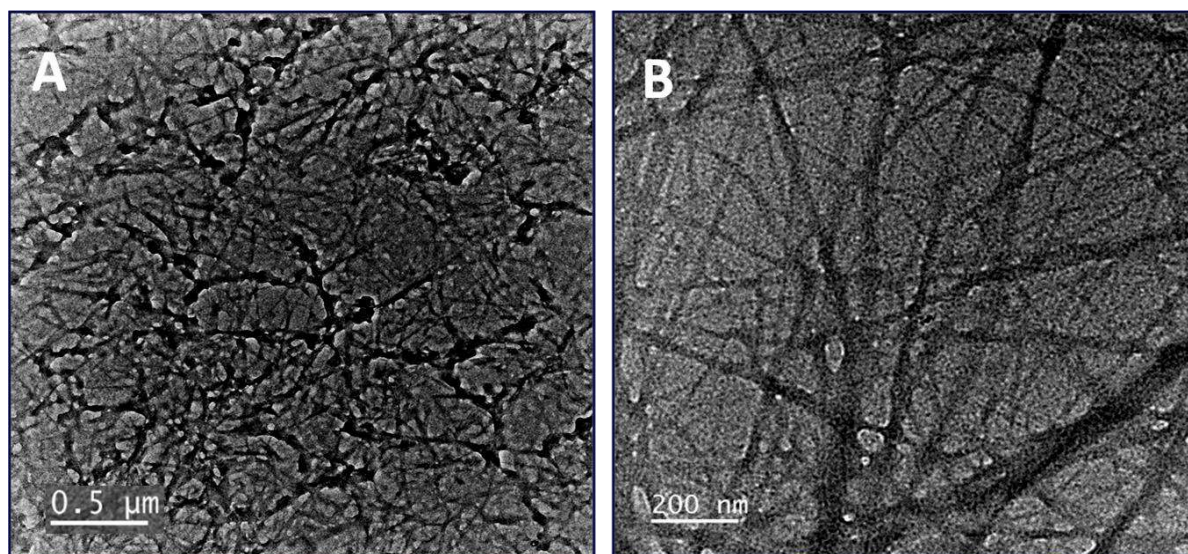


Fig.6.8. TEM images of insulin aggregates having amyloid fibril network viewed under 500 nm (panel A) and 200 nm resolution (panel B) respectively.

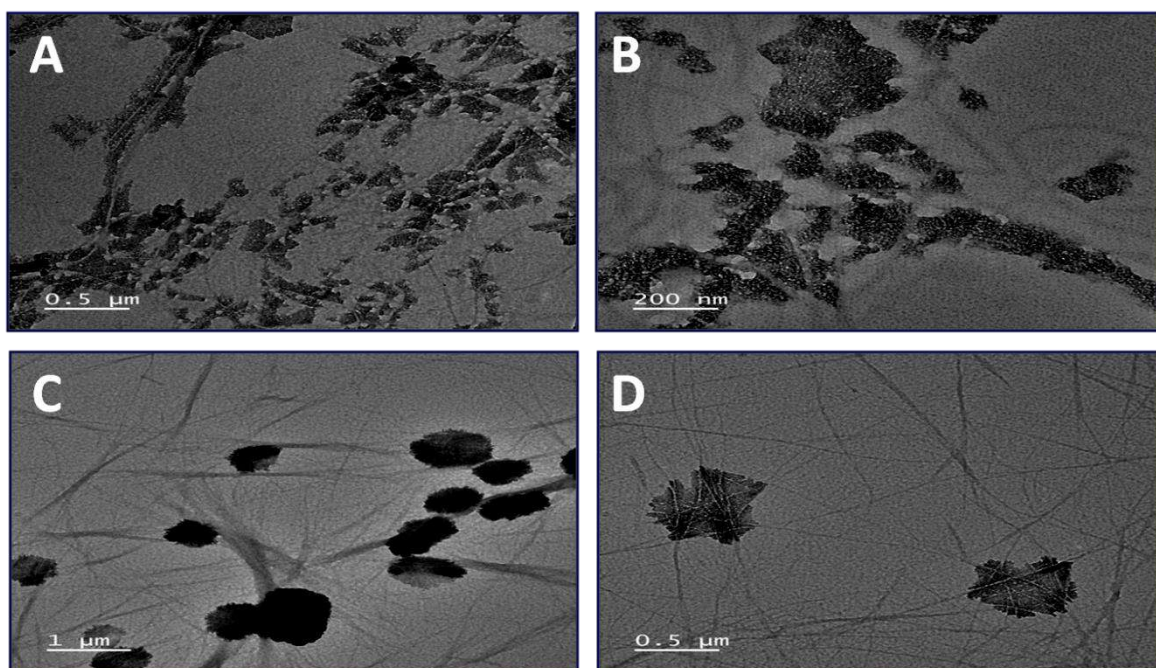


Fig.6.9. TEM images showing insulin aggregates in presence of 10% HFIP under 500nm (panel A) and 200nm resolution (panel B) respectively. Whereas, heat treated insulin in presence of 20% HFIP were shown under 1μm (panel C) and 500nm resolution (panel D) respectively.

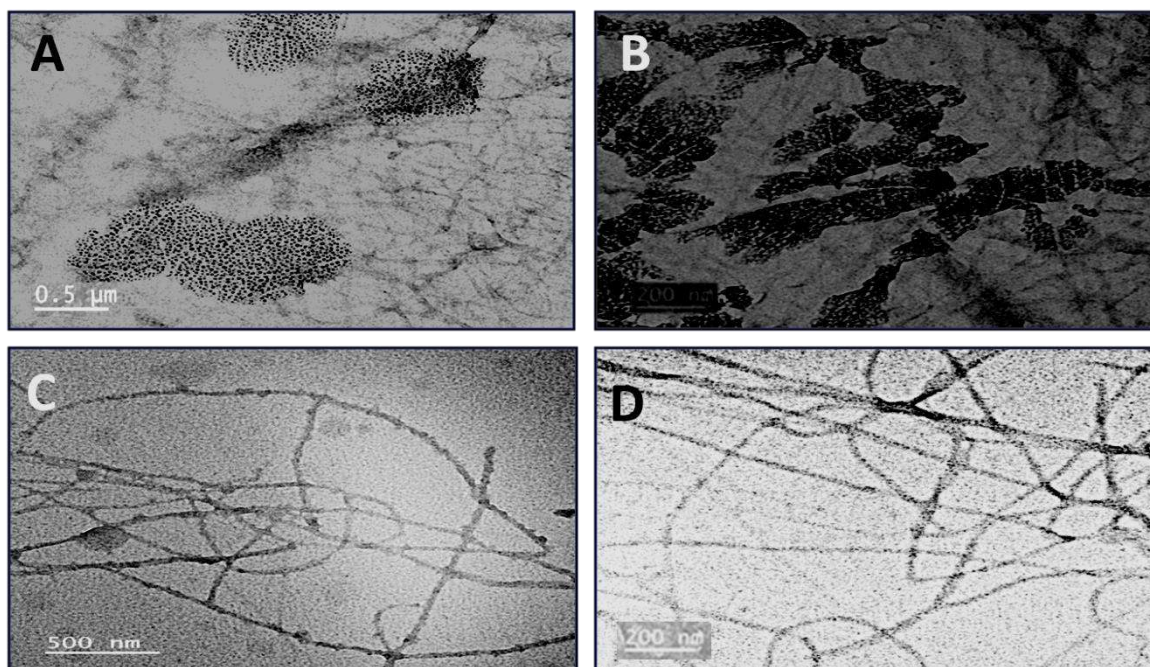


Fig.6.10. TEM images showing aggregated insulin in presence of 10% TFE under 500nm (panel A) and 200nm resolution (panel B) respectively, and in presence of 20% TFE under 500nm (panel C) and 200nm resolution (panel D) respectively.

TFE presented difference in fibrillar aggregates under similar experimental conditions as shown in Fig.6.10. Here also the lower percentage of TFE showed better protection against fibrillation of insulin. 10% TFE treated insulin formed fine mesh like fibrillar network as shown under 500 nm and 200 nm resolutions in Fig.6.10 A and B. On the other hand, 20% TFE treated samples (Figure 6.10 C and D) formed long, branched, scattered fibrils of insulin which possessed subsequent difference from insulin amyloid structure (Figure 6.8 A and B). The TEM results of TFE treated samples were also in agreement with the previous experimental interpretations.

6.5 DISCUSSIONS AND MAJOR CONCLUSIONS

It was also revealed while comparing TFE with Methanol, that the stability conferred by the two was different. Methanol enhances the stability of backbone hydrogen bonds of which the carbonyl groups came from polar residues. However, TFE tends to stabilize the same involving non-polar residues [17]. Hydrophobicity is closely related to the amyloidogenicity of a protein. Insulin amyloid structure is dominated by the cross- β structure with an unavoidable mess of hydrogen bond network of fibrils [33]. For that reason the co-solvent effect should be considered in terms of hydrogen bonding propensities with native protein. In this study, HFIP and TFE were used separately to trace the effects on insulin aggregation. The amounts of mature amyloid fibrils was greatly reduced. This study found that HFIP is better protector of insulin monomeric form at pH1.6 than TFE. It also showed that 10 % v/v interaction ratio is optimal for both HFIP and TFE to favor aggregation-limiting conditions.

The possible explanation of the observations can be, HFIP being a volatile solvent, may disrupts assembly of unfolded monomers to generate amyloid fibrils under heating conditions and thus the alpha-helical predominating structure of insulin persisted [55]. It was also reported earlier in literature that at higher percentages of HFIP, protein tends to undergo a molten globule state [56] which is an intermediate stage of amyloid generation. Thus this present study results are logical and consistent with previous findings of literature. Another report from literature showed that, low conc. of HFIP induced amyloid beta aggregation whereas in the same study it was also reported that at 10 % v/v of HFIP interaction ratio, exhibited no aggregation [57].

The acidity of HFIP is enhanced in aqueous solution [58]. Insulin in acidic pH tends to remain in monomeric form due to the protonation of HisB10 [59]. In solution, the HFIP's nucleophilicity is reduced as shown in Fig.6.11 but hydrogen bond donating ability of HFIP is markedly increased [60]. This also indicates favorable interaction of HFIP with insulin side chains via H-bond.

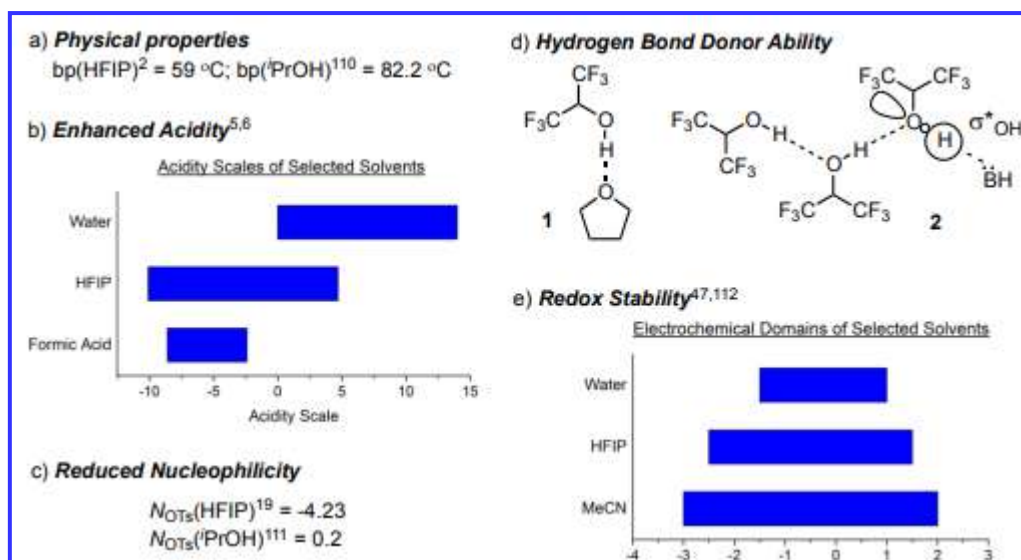


Fig. 6.11. The physical and chemical properties of HFIP as a co-solvent. In the fig., *bp* = boiling point. *N_{OTs}* is the solvent nucleophilicity parameter (the higher the value, the greater the nucleophilic strength of the solvent). *Fig. adapted from Colomer I. et. al., 2017.

Super saturation had been considered to be a trivial factor that retards the initiation of fibrillation. A study on protein super saturation and influence of HFIP and TFE [61] showed that water/alcohol mixtures of TFE and HFIP separately decreased the solubility of insulin and when supersaturated, the denatured insulin being metastable remained soluble. The study used through strong agitation through ultrasonication and yielded of crystal-like amyloid fibrils. This study also explained why lower-moderate concentrations of even highly amyloidogenic protein remained stable until got supersaturated in alcohol-water mixtures. Additionally, the ultrasonication mediated disruption indicated the stability of insulin in fluorinated alcohol-water mixture involved protein-alcohol interfaces [62-63]. The possibility of generation of HFIP microdroplets at the amphoteric protein-alcohol interfaces in the aqueous medium can explain the finding of the present study. Previous reports on biophysical analyses of aqueous HFIP solutions gave an idea of a micro droplet structure of HFIP [64]. Investigation and determination of protein stability under influence of HFIP as well as TFE found that the two co-solvents were very much suitable in stabilizing the secondary structure of peptides and also in inducing the alpha helical state of protein [65-68]. The interaction mainly involves hydrophobic surfaces of protein and the cluster of HFIP molecules in a way that resembles the interior of a hydrophobic lipid membrane or the interior of a folded protein [65, 69].

So it can be concluded that, the partial stability optimization of insulin in HFIP-water or TFE-water system was done at 10% v/v concentration of alcohol. The possible interaction site is hydrophobic surfaces of protein in aqueous solution with fluorinated alcohols. Above this concentration range, insulin amyloid may form in alcohol-water mixture. The HFIP induced fibrils are needle shaped crystal-like morphologies but TFE can give rise to branched higher aggregates of insulin.

6.6. REFERENCES

1. Canchi DR., García AE. 2013. Cosolvent effects on protein stability. *Annu Rev Phys Chem.*, 64: 273-293, [10.1146/annurev-physchem-040412-110156](https://doi.org/10.1146/annurev-physchem-040412-110156).
2. Oshima H., Kinoshita M. 2013. Effects of sugars on the thermal stability of a protein. *J Chem Phys.*, 138(24): 245101, [10.1063/1.4811287](https://doi.org/10.1063/1.4811287)
3. Jonsson O., Lundell A., Rosell J., You S., Ahlgren K., Swenson J. 2024. Comparison of Sucrose and Trehalose for Protein Stabilization Using Differential Scanning Calorimetry. *J Phys Chem B.*, 128(20):4922-4930, [10.1021/acs.jpcc.4c00022](https://doi.org/10.1021/acs.jpcc.4c00022).
4. D'Alfonso L., Collini M. and Baldini G. 2003. Trehalose influence on beta-lactoglobulin stability and hydration by time resolved fluorescence. *Eur. J. Biochem.*, 270(11): 2497-2504, <https://doi.org/10.1046/j.1432-1033.2003.03621.x>
5. Back JF., Oakenfull D., Smith MB. 1979. Increased thermal stability of proteins in the presence of sugars and polyols. *Biochemistry.* 18(23): 5191-5196, [10.1021/bi00590a025](https://doi.org/10.1021/bi00590a025)
6. Sola-Penna M., Ferreira-Pereira A., Lemos A.d.P. and Meyer-Ferwandes J.R. 1997. Carbohydrate Protection of Enzyme Structure and Function against Guanidinium Chloride Treatment Depends on the Nature of Carbohydrate and Enzyme. *Eur. J. Biochem.*, 248: 24-29, <https://doi.org/10.1111/j.1432-1033.1997.00024.x>
7. Carpenter JF., Crowe JH. 1988. The mechanism of cryoprotection of proteins by solutes. *Cryobiology.* 25(3):244-255. [10.1016/0011-2240\(88\)90032-6](https://doi.org/10.1016/0011-2240(88)90032-6).
8. Colaço C., Sen S., Thangavelu M., Pinder S., Roser B. 1992. Extraordinary Stability of Enzymes Dried in Trehalose: Simplified Molecular Biology. *Nat Biotechnol.*, 10: 1007–1011, <https://doi.org/10.1038/nbt0992-1007>
9. Sun WQ., Davidson P. 1998. Protein inactivation in amorphous sucrose and trehalose matrices: effects of phase separation and crystallization. *Biochim Biophys Acta.*, 1425(1): 235-244, [10.1016/s0304-4165\(98\)00076-2](https://doi.org/10.1016/s0304-4165(98)00076-2).
10. Barbiroli A., Marengo M., Fessas D., Ragg E., Renzetti S., Bonomi F., Iametti S. 2017. Stabilization of beta-lactoglobulin by polyols and sugars against temperature-induced denaturation involves diverse and specific structural regions of the protein. *Food Chem.*, 234:155-162, [10.1016/j.foodchem.2017.04.132](https://doi.org/10.1016/j.foodchem.2017.04.132)
11. Wang A., Robertson AD., Bolen DW. 1995. Effects of a naturally occurring compatible osmolyte on the internal dynamics of ribonuclease A. *Biochemistry.* 1995; 34:15096–15104, <https://doi.org/10.1021/bi00046a016>

12. Gregory RB. 1988. *Biopolymers*. The influence of glycerol on hydrogen isotope exchange in lysozyme. 27: 1699–1709, <https://doi.org/10.1002/bip.360271102>
13. Calhoun DB., Englander SW. 1985. Internal protein motions, concentrated glycerol, and hydrogen exchange studied in myoglobin. *Biochemistry.*, 24(8):2095-100, <https://doi.org/10.1021/bi00329a043>.
14. Knox DG., Rosenberg A. 1980. Fluctuations of protein structure as expressed in the distribution of hydrogen exchange rate constants. *Biopolymers*. 19:1049–1068. [10.1002/bip.1980.360190509](https://doi.org/10.1002/bip.1980.360190509)
15. Priev A., Almagor A., Yedgar S., Gavish B. 1996. Glycerol decreases the volume and compressibility of protein interior. *Biochemistry.* 35(7): 2061-2066. <https://doi.org/10.1021/bi951842r>
16. Cioni P., Strambini GB. 1994. Pressure effects on protein flexibility monomeric proteins. *J. Mol. Biol.*, 242(3): 291-301. <https://doi.org/10.1006/jmbi.1994.1579>
17. Shao Q., Fan Y., Yang L., Gao YQ. 2012. From protein denaturant to protectant: comparative molecular dynamics study of alcohol/protein interactions. *J Chem Phys*. 136(11):115101. [10.1063/1.3692801](https://doi.org/10.1063/1.3692801)
18. Shuklov I.A., Dubrovina N.V., Börner A. 2007. Fluorinated alcohols as solvents, cosolvents and additives in homogeneous catalysis. *Synthesis*. 19:2925–2943, [10.1055/s-2007-983902](https://doi.org/10.1055/s-2007-983902).
19. Bégué J.-P., Bonnet-Delpon D., Crousse B. 2004. Fluorinated alcohols: a new medium for selective and clean reaction. *Synlett.*, 2004(01):18–29, [10.1055/s-2003-44973](https://doi.org/10.1055/s-2003-44973).
20. Hirota N., Mizuno K., Goto Y. 1997. Cooperative α -helix formation of β -lactoglobulin and melittin induced by hexafluoroisopropanol. *Protein Sci.*, 6:416–421, <https://doi.org/10.1002/pro.5560060218>
21. Hong D.-P., Hoshino M., Goto Y. 1999. Clustering of fluorine-substituted alcohols as a factor responsible for their marked effects on proteins and peptides. *J. Am. Chem. Soc.*, 121:8427–8433, <https://doi.org/10.1021/ja990833t>
22. Barrow C.J., Yasuda A., Zagorski M.G. 1992. Solution conformations and aggregational properties of synthetic amyloid β -peptides of Alzheimer's disease. Analysis of circular dichroism spectra. *J. Mol. Biol.*, 225:1075–1093, [https://doi.org/10.1016/0022-2836\(92\)90106-T](https://doi.org/10.1016/0022-2836(92)90106-T)

23. van den Brink-van der Laan E., Chupin V., de Kruijff B. 2004. Small alcohols destabilize the KcsA tetramer via their effect on the membrane lateral pressure. *Biochemistry*. 43: 5937–5942. <https://doi.org/10.1021/bi0496079>
24. Weight F.F., Li C., Peoples R.W. 1999. Alcohol action on membrane ion channels gated by extracellular ATP (P2X receptors) *Neurochem. Int.*, 35:143–152, [https://doi.org/10.1016/S0197-0186\(99\)00056-X](https://doi.org/10.1016/S0197-0186(99)00056-X)
25. Godden E.L., Harris R.A., Dunwiddie T.V. 2001. Correlation between molecular volume and effects of n-alcohols on human neuronal nicotinic acetylcholine receptors expressed in *Xenopus* oocytes. *J. Pharmacol. Exp. Ther.* 296:716–722. PMID: 11181898
26. Akitake B., Spelbrink R.E., Sukharev S. 2007. 2,2,2-Trifluoroethanol changes the transition kinetics and subunit interactions in the small bacterial mechanosensitive channel MscS. *Biophys. J.*, 92: 2771–2784. <https://doi.org/10.1529/biophysj.106.098715>
27. Imai S., Osawa M., Shimada I. 2012. Functional equilibrium of the KcsA structure revealed by NMR. *J. Biol. Chem.*, 287: 39634–39641. <https://doi.org/10.1074/jbc.M112.401265>
28. Lioudyno M.I., Broccio M., Hall J.E. 2012. Effect of synthetic $\alpha\beta$ peptide oligomers and fluorinated solvents on Kv1.3 channel properties and membrane conductance. *PLoS One*, 7:e35090, <https://doi.org/10.1371/journal.pone.0035090>
29. Wang L., Li Y., Li F. 2014. The effects of organic solvents on the membrane-induced fibrillation of human islet amyloid polypeptide and on the inhibition of the fibrillation. *Biochim. Biophys. Acta*, 1838: 3162–3170. <https://doi.org/10.1016/j.bbamem.2014.09.002>
30. Kentsis A, Sosnick TR. 1998. Trifluoroethanol promotes helix formation by destabilizing backbone exposure: desolvation rather than native hydrogen bonding defines the kinetic pathway of dimeric coiled coil folding. *Biochemistry*., 37(41): 14613-14622, [10.1021/bi981641y](https://doi.org/10.1021/bi981641y).
31. Yanagi K., Ashizaki M., Yagi H., Sakurai K., Lee YH., Goto Y. 2011. Hexafluoroisopropanol induces amyloid fibrils of islet amyloid polypeptide by enhancing both hydrophobic and electrostatic interactions. *J Biol Chem.*, 286(27): 23959-23966, [10.1074/jbc.M111.226688](https://doi.org/10.1074/jbc.M111.226688).
32. Matsugami M., Yamamoto R., Kumai T., Tanaka M., Umecky T., Takamuku, T. 2016. Hydrogen bonding in ethanol–water and trifluoroethanol–water mixtures

- studied by NMR and molecular dynamics simulation. *J. Mol. Liq.*, 217: 3-11, [10.1016/J.MOLLIQ.2015.06.050](https://doi.org/10.1016/J.MOLLIQ.2015.06.050)
33. Nelson R., Eisenberg D. 2006. Structural models of amyloid-like fibrils. *Advances in protein chemistry*. 73: 235-82, [https://doi.org/10.1016/S0065-3233\(06\)73008-X](https://doi.org/10.1016/S0065-3233(06)73008-X)
 34. Reddy SMM., Shanmugam G., Mandal A. 2014. 1, 1, 1, 3, 3, 3-Hexafluoro-2-propanol and 2,2,2-trifluoroethanol solvents induce self-assembly with different surface morphology in an aromatic dipeptide. *Org. Biomol. Chem.*, 12: 6181-6189, <https://doi.org/10.1039/C4OB00821A>
 35. Daowtak K., Pompimon W., Salerno M., Udomtanakunchai C. 2023. Decelerate amyloid fibrillation by the alkaloids extracted from *Stephania venosa*. *J Assoc Med Sci.*, 56(3): 52-59, [10.12982/JAMS.2023.053](https://doi.org/10.12982/JAMS.2023.053).
 36. Hanczyc P. and Fita P. 2021. Laser Emission of Thioflavin T Uncovers Protein Aggregation in Amyloid Nucleation Phase. *ACS Photonics.*, 8 (9) : 2598-2609, [10.1021/acsp Photonics.1c00082](https://doi.org/10.1021/acsp Photonics.1c00082)
 37. Fagihi MHA. and Bhattacharjee S. 2022. Amyloid Fibrillation of Insulin: Amelioration Strategies and Implications for Translation., *Acs Pharmacol Transl.*, 5 (11) : 1050-1061, [10.1021/acsp tsci.2c00174](https://doi.org/10.1021/acsp tsci.2c00174)
 38. Ziaunys M., Sakalauskas A., Mikalauskaite K., Smirnovas V. 2021. Exploring the occurrence of thioflavin-T-positive insulin amyloid aggregation intermediates. *PeerJ.*, 9:e10918, [10.7717/peerj.10918](https://doi.org/10.7717/peerj.10918).
 39. Ziaunys M., Sakalauskas A., Smirnovas V. 2020. Identifying Insulin Fibril Conformational Differences by Thioflavin-T Binding Characteristics. *Biomacromolecules*. 21(12):4989-4997, [10.1021/acs.biomac.0c01178](https://doi.org/10.1021/acs.biomac.0c01178)
 40. Chouchane K., Pignot-Paintrand I., Bruckert F., Weidenhaupt M. 2018. Visible light-induced insulin aggregation on surfaces via photoexcitation of bound thioflavin T. *J. Photochem. Photobiol. B.*, 181: 89-97. <https://doi.org/10.1016/j.jphotobiol.2018.02.025>.
 41. Chatani E. and Yamamoto N. 2018. Recent progress on understanding the mechanisms of amyloid nucleation. *Biophys. Rev.*, 10: 527–534, <https://doi.org/10.1007/s12551-017-0353-8>
 42. Nielsen L., Khurana R., Coats A., Frokjaer S., Brange J., Vyas S., Uversky VN., Fink AL. 2001. Effect of Environmental Factors on the Kinetics of Insulin Fibril Formation: Elucidation of the Molecular Mechanism. *Biochemistry*. 40: 6036–6046, <https://doi.org/10.1021/bi002555c>

43. Gancar M., Kurin E., Bednarikova Z., *et al*, 2020.. Amyloid Aggregation of Insulin: An Interaction Study of Green Tea Constituents. *Sci Rep.*, 10: 9115, <https://doi.org/10.1038/s41598-020-66033-6>
44. Qadeer A., Rabbani G., Zaidi N., Ahmad E., Khan JM., Khan RH. 2012. 1-Anilino-8-naphthalene sulfonate (ANS) is not a desirable probe for determining the molten globule state of chymopapain. *PLoS One.*, 7(11): e50633, [10.1371/journal.pone.0050633](https://doi.org/10.1371/journal.pone.0050633).
45. Hawe A., Sutter M., Jiskoot W. 2008. Extrinsic fluorescent dyes as tools for protein characterization. *Pharm Res.*, 25(7):1487-99, [10.1007/s11095-007-9516-9](https://doi.org/10.1007/s11095-007-9516-9)
46. Gast K., Siemer A., Zirwer D. 2001. Fluoroalcohol-induced structural changes of proteins: some aspects of cosolvent-protein interactions. *Eur Biophys J.*, 30: 273–283, <https://doi.org/10.1007/s002490100148>
47. Prusty A. and Sahu S. 2013. Development and Evaluation of Insulin Incorporated Nanoparticles for Oral Administration. *ISRN Nanotechnology*. 2013(6): 591751 [10.1155/2013/591751](https://doi.org/10.1155/2013/591751).
48. Sneideris T., Darguzis D., Botyriute A., Grigaliunas M., Winter R., Smirnovas V. 2015. pH- Driven Polymorphism of Insulin Amyloid-Like Fibrils. *PLoS One*. 10(8): e0136602, [10.1371/journal.pone.0136602](https://doi.org/10.1371/journal.pone.0136602)
49. Charii H., Boussetta A., Benhamou A A., Mennani M., Essifi K., Ablouh El-H., El Zakhem H., Grimi N., Boutoial K., Moubarik A. 2024. Exploring the potential of chitin and chitosan extracted from shrimp shell waste in enhancing urea-formaldehyde wood adhesives. *Int. J. Adhes. Adhes.*, 129: 103599, [10.1016/j.ijadhadh.2023.103599](https://doi.org/10.1016/j.ijadhadh.2023.103599).
50. Akbarian M., Rezaie E., Farjadianb F., Bazyarc Z., Sarvari MH., Arad EM., Mirhosseinid SA., Amanid J. 2020. Inhibitory effect of coumarin and its analogs on insulin fibrillation /cytotoxicity is depend on oligomerization states of the protein. *RSC Adv.*, 10: 38260-38274., [10.1039/D0RA07710K](https://doi.org/10.1039/D0RA07710K)
51. Mukherjee M., Das D., Sarkar J., Banerjee Nilanjan., Jana J., Bhat J., Reddy JG., Bharatam J., Chattopadhyay S., Chatterjee S., Chakrabarti P., 2021. Prion-derived tetrapeptide stabilizes thermolabile insulin via conformational trapping. *iScience*, 24 (6) : 102573, <https://doi.org/10.1016/j.isci.2021.102573>
52. Panda C., Kumar S., Gupta S., Pandey LM. 2023. Structural, kinetic, and thermodynamic aspects of insulin aggregation. *Phys Chem Chem Phys*. 25 (36): 24195-24213. doi: 10.1039/d3cp03103a.

53. Kurouski D. 2016. Supramolecular Organization of Amyloid Fibrils. Exploring New Findings on Amyloidosis. InTech; 2016. <http://dx.doi.org/10.5772/62672>
54. Knowles T.P.J., Waudby C.A., Dobson C.M. 2009. An analytical solution to the kinetics of breakable filament assembly. *Science*. 326:1533–1537, [10.1126/science.1178250](https://doi.org/10.1126/science.1178250).
55. Stine Jr.WB., Dahlgren KN., Krafft GA., LaDu MJ. 2003. In Vitro Characterization of Conditions for Amyloid- β Peptide Oligomerization and Fibrillogenesis. *J. Biol. Chem.*, 278: 11612-11622, <https://doi.org/10.1074/jbc.M210207200>.
56. Khan S., Ansari B., Ansari NK., Naeem A. 2024. Protective role of chlorogenic acid in preserving cytochrome-c stability against HFIP-induced molten globule state at physiological pH. *Int. J. Biol. Macromol.*, 261 (2) : 129845, <https://doi.org/10.1016/j.ijbiomac.2024.129845>
57. Nichols MR., Moss MA., Reed DK., Cratic-McDaniel S., Hoh JH., Rosenberry TL. 2005. Amyloid-beta protofibrils differ from amyloid-beta aggregates induced in dilute hexafluoroisopropanol in stability and morphology. *J Biol Chem.*, 280(4):2471-2480. [10.1074/jbc.M410553200](https://doi.org/10.1074/jbc.M410553200)
58. Colomer I., Chamberlain A., Haughey M. et al. 2017. Hexafluoroisopropanol as a highly versatile solvent. *Nat Rev Chem.*, 1: 0088. <https://doi.org/10.1038/s41570-017-0088>
59. Das A., Shah M., Saraogi I. 2022. Molecular Aspects of Insulin Aggregation and Various Therapeutic Interventions. *ACS Bio & Med Chem Au*. 2 (3) : 205-221, [10.1021/acsbiomedchemau.1c00054](https://doi.org/10.1021/acsbiomedchemau.1c00054)
60. Colomer I., Chamberlain AER., Haughey MB., Donohoe TJ. 2017. 1,1,1,3,3,3-Hexafluoro-2-propanol (HFIP): more than a polar protic solvent. <https://ora.ox.ac.uk/objects/uuid:72dc250a-656e-4367-827d-17835acc28ba/files/m8a4b91e56bb28ad4538cc736a059a873>
61. Muta H., Lee YH., Kardos J., Lin Y., Yagi H., Goto Y. 2014. Supersaturation-limited amyloid fibrillation of insulin revealed by ultrasonication. *J Biol Chem.*, 289(26): 18228-18238, [10.1074/jbc.M114.566950](https://doi.org/10.1074/jbc.M114.566950).
62. Yoshimura Y., Lin Y., Yagi H., Lee Y. H., Kitayama H., Sakurai K., So M., Ogi H., Naiki H., Goto Y. 2012. Distinguishing crystal-like amyloid fibrils and glass-like amorphous aggregates from their kinetics of formation. *Proc. Natl. Acad. Sci. U.S.A.* 109: 14446–14451, <https://doi.org/10.1073/pnas.1208228109>

63. Yoshimura Y., So M., Yagi H., Goto Y. 2013. Ultrasonication: an efficient agitation for accelerating the supersaturation-limited amyloid fibrillation of proteins. *Jpn. J. Appl. Phys.* 52: 07HA01-01-07HA01-08, [10.7567/JJAP.52.07HA01](https://doi.org/10.7567/JJAP.52.07HA01)
64. Yoshida K., Yamaguchi T., Adachi T., Otomo T., Matsuo D., Takamuku T., Nishi N. 2003. Structure and dynamics of hexafluoroisopropanol-water mixtures by x-ray diffraction, small-angle neutron scattering, NMR spectroscopy, and mass spectrometry. *J. Chem. Phys.*, 119 (12): 6132–6142. <https://doi.org/10.1063/1.1602070>
65. Mulla H. R. and Cammers-Goodwin A. 2000. Stability of a Minimalist, Aromatic Cluster in Aqueous Mixtures of Fluoro Alcohol. *J. Am. Chem. Soc.*, 122: 738–739, <https://doi.org/10.1021/ja993363b>
66. Gerig J. T. 2004. Structure and Solvation of Melittin in 1,1,1,3,3,3-Hexafluoro-2-Propanol/Water. *Biophys. J.*, 86: 3166–3175, [10.1016/S0006-3495\(04\)74364-7](https://doi.org/10.1016/S0006-3495(04)74364-7)
67. Buck M. 1998. Trifluoroethanol and colleagues: cosolvents come of age. Recent studies with peptides and proteins. *Q. Rev. Biophys.* 31: 297-355, [10.1017/s003358359800345x](https://doi.org/10.1017/s003358359800345x)
68. Wang L., Wang D. and Li F. 2014. Insight into the structures of the second and fifth transmembrane domains of Slc11a1 in membrane mimics. *J. Pept. Sci.* 20: 165–172, [10.1002/psc.2593](https://doi.org/10.1002/psc.2593)
69. Hong D.-P., Hoshino M. Kuboi R., Goto, Y. 1999. Clustering of Fluorine-Substituted Alcohols as a Factor Responsible for Their Marked Effects on Proteins and Peptides. *J. Am. Chem. Soc.* 121: 8427–8433, <https://doi.org/10.1021/ja990833t>

CHAPTER 4

Effect of sulfur containing amino acids on thermal fibrillation of insulin



7.1 Prologue of the study

In the detail research to find amyloid inhibitory substances, it is equally important to get a protein stabilizing feature in that substance. In solution or during in-vitro applications of protein, the non-covalent interactions comprising electrostatic (including hydrogen bonds) and van der Waals (dipole–dipole, dipole–induced dipole, and induced dipole–induced dipole) are crucial for maintaining the native folds of a protein in a stable way. Besides the aromatic-aromatic, aromatic-aliphatic and/or aliphatic-aliphatic interactions made by different compounds employed for the said purpose, interaction made by sulphur containing amino acid with a protein do have the potential to be a good choice to study with.

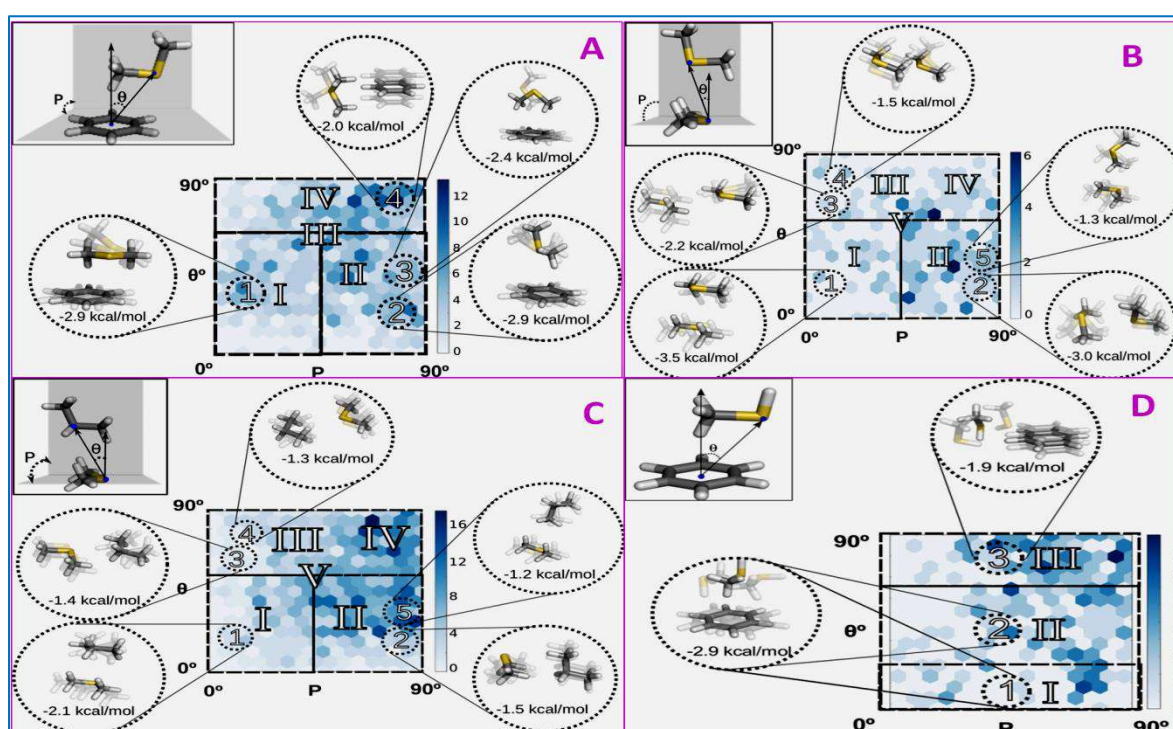


Fig. 7.1. 2D histograms of the frequencies of occurrence of the following interactions, clustered according to the conformational space defined by the distance d and the angles P and θ . The orientation and strength of A. Met–Phe interactions, B. Met–Met interactions, C. Met–Leu interactions and D. Cys–Phe interactions. The position in the 2D histogram of the most representative structure in the cluster and the energy-minimized structures are indicated by Roman and arabic numbers respectively. *Ab initio* geometry optimization and calculated energy of interaction are shown inside dotted circles as solid sticks. Representative structures obtained in the cluster analysis are shown as transparent sticks. *Fig. adapted from Gómez-Tamayo J.C. et. al., 2016, Prot. Sci., 25: 1517-1524. <https://doi.org/10.1002/pro.2955>

The only two biologically prevalent amino acids are Cysteine and Methionine that contain a highly polarizable sulfur atom due to presence of filled 3p and empty 3d orbitals creating a permanent dipole [1]. There found a high frequency of contacts between sulfur-containing residues and aromatic residues in proteins in the research work of Morgan *et al.* observed, and identified large stacked arrangements composed of aromatic and Met or Cys residues [2]. In protein crystal structures, the occurrence of Cys- and Met-aromatic interactions were noted [3-4]. Met–aromatic and Met–Met interactions in the family of G protein-coupled receptors were defined in different literature reports [5-7]. Another similar research outlined that Met and Cys often interact with Leu, Ile, Val, Phe, and other Met or Cys as in their study involving crystal structures of membrane protein [8]. The researchers also claimed that the flexible side-chains of Met and Cys made them extra versatile (Fig. 7.1) and adaptable to conformational changes of the protein.

Besides the said influences of Cys and Met when they are themselves located in the protein's sequences, different notable interactions were traced involving also the free cysteine and methionine residues with protein structures. Among the important discoveries, it was noted that, a hydrogen bond involving the -SH group is more willing to donate its proton to a carbonyl group in spite of accepting the proton. As a ligand, the -SH group performed very poorly while bound to anionic substrates and its interaction with a carboxylate group is rare. It preferably interacts in a non-hydrogen bond forming manner. The most notable thing is that in the S...C=O interaction, the main chain or side chain amide group which is close to the C atom, is faced towards the S atom [9]. While in cases of S...N interaction, the S atom is placed on top of the N atom of another main chain or side chain guanidinium group. Cys residues prefer to place itself nearby the aromatic amino acid residues in a protein interact along its face [9]. A stereo image superimposition done with the structures of SARS 3CLpro showed that cysteine residues favorably positioned in a hydrophobic environment of protein and development of its hunched posture (Fig. 7.2) in the surroundings of aromatic residues was identifiable [10]. So, the said research in literature concluded that, free cysteine interaction with non-membrane proteins is potentially done with hydrophobic residues than with polar/charged residues.

Another significant observation was that, when Cys located in protein's own sequence, the formation of intra-residue S...C=O interaction constrains the main-chain and side-chain torsion angles (psi and chi). But when added externally, free cysteine prefers the inter-residue

interactions which were non-local and were found to stabilize the tertiary structure of the protein. The pKa values of the Cys residues was observed to be get lowered by S...C=O interactions in enzyme active sites [9].

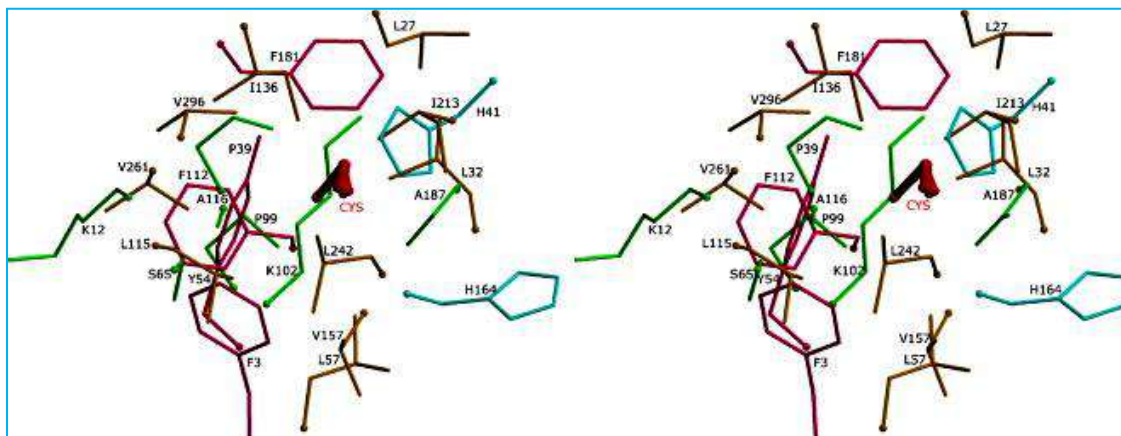


Fig. 7.2. Stereo images of superimposition of cysteines on SARS 3CLpro (PDB code [1UJ1](#)). The neighboring residues of cysteine are Phe, Tyr (in purple/pink color), His (in cyan), Leu, Ile, Val (in gold), Ala, Pro, Ser, Lys (in green) in a sphere of 3.7 Å radius. *Fig. adapted from Ho SL et.al., 2009, J Taiwan Inst Chem Eng., 40 (2): 123-129. [10.1016/j.jtice.2008.07.015](#).

All these observations motivated the selection of the two sulfur-containing amino acids, cysteine and methionine in the present approach of modulating insulin amyloid formation in vitro. The structure of insulin is itself stabilized by two inter-chain disulfide bonds between the A and B chains (A7-B7 and A20-B19), and one intra-chain disulfide linkage in the A chain (A6-A11) [11- 13]. The exposure of hydrophobic grooves is consequential in insulin aggregation and hydrophobic interactions as well as hydrogen bonding to get the access to stabilize insulin monomer are observable feature in aggregation inhibitors [14-15]. The sulfur containing amino acids can be a choice in this study as they are able to interact with proteins.

7.2. Effect of free Cysteine and Methionine on protein stability : Literature evidences

The sulfur containing amino acids preferably Cys were shown to possess thiophilic interaction between the aromatic side chains and in turn reduced the fibrillation of amyloid- β 1-40 (A β 40) and 1-42 (A β 42) [16]. It was also noted that, the aggregates of A β 40 and A β 42 generated in presence of Cys were less cytotoxic. Methionine also proved itself good in making interaction with proteins. The heme in cytochrome c protein is bound by the ligand methionine through its sulfur atom [17]. In another enzyme myeloperoxidase, the methionine generates a sulfonium ionic bond to link with heme [18-19]. In type IV Collagen, a sulfinimine bond (-S=N-) which was the nitrogen analogue of a sulfoxide (-S=O-), was discovered by a combination of high-resolution mass spectrometric and nuclear magnetic resonance studies. The crosslink between hydroxylysine-211 and methionine-93 was established as the sulfinimine group (-S=N-) [20]. Like Cysteine, methionine also preferred to interact with neighboring aromatic residues [21], and confers stability of the protein as revealed by crystallographic studies [22]. The stabilization of protein structure by Met, was due to widespread methionine-aromatic interaction occurring at a distance ~ 6 Å where that of a salt bridge is <4 Å [23]. Cysteine having the sulfur atom possesses numerous oxidation states

[24] as shown in fig.7.3 in proteins.

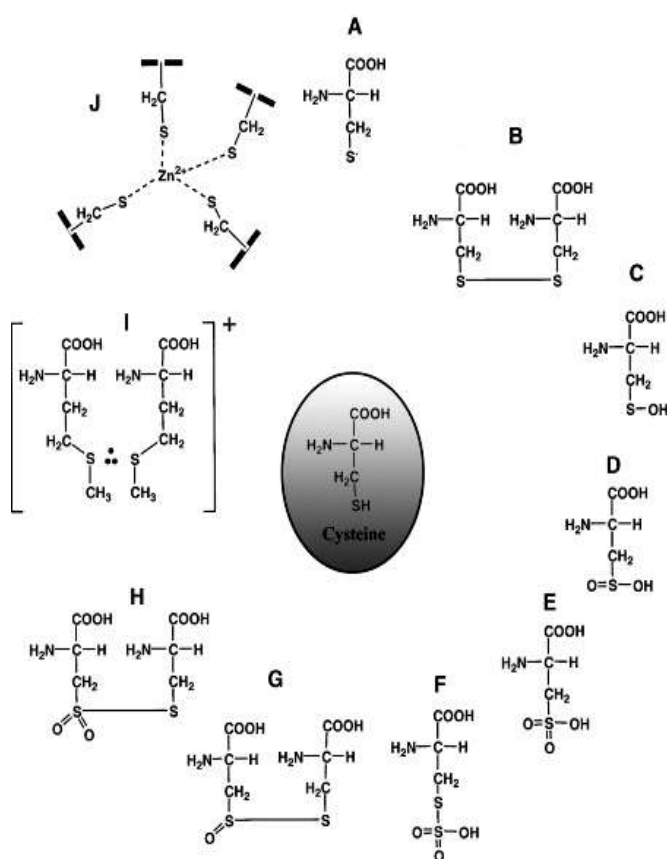


Fig.7.3. Different oxidation states of Cysteine (A) Cysteinyl radical (-1), (B) cystine (i.e., “cysteine disulfide”) (-1), (C) cysteine sulfenic acid (0), (D) cysteine sulfinic acid (+2), (E) cysteine sulfonic acid (+4), (F) cysteine-S-sulfate (+5), (G) cystine-S-monoxide (+1), (H) cystine-S-dioxide (+3), (I) methionine disulfide radical cation with a three electron bond (-3/2), and (J) a tetrahedral ZnCys_4 complex (-2). *Fig. adapted from Giles NM. Et.al., 2003, [10.1016/s1074-5521\(03\)00174-1](https://doi.org/10.1016/s1074-5521(03)00174-1)

Intracellular protein stability was reported to confer by methionine through inclusion of the sulfur atom [22, 23]. The antioxidant activity of Cys is important in protecting protein structure [25]. Methionine was shown to manage the various oxidative stresses on cell to prevent cell damage [26]. Both Cys and Met possessed similar hydrophobicity and ability to form protein stabilizing S-aromatic motifs [27] as depicted in Fig. 7.4.

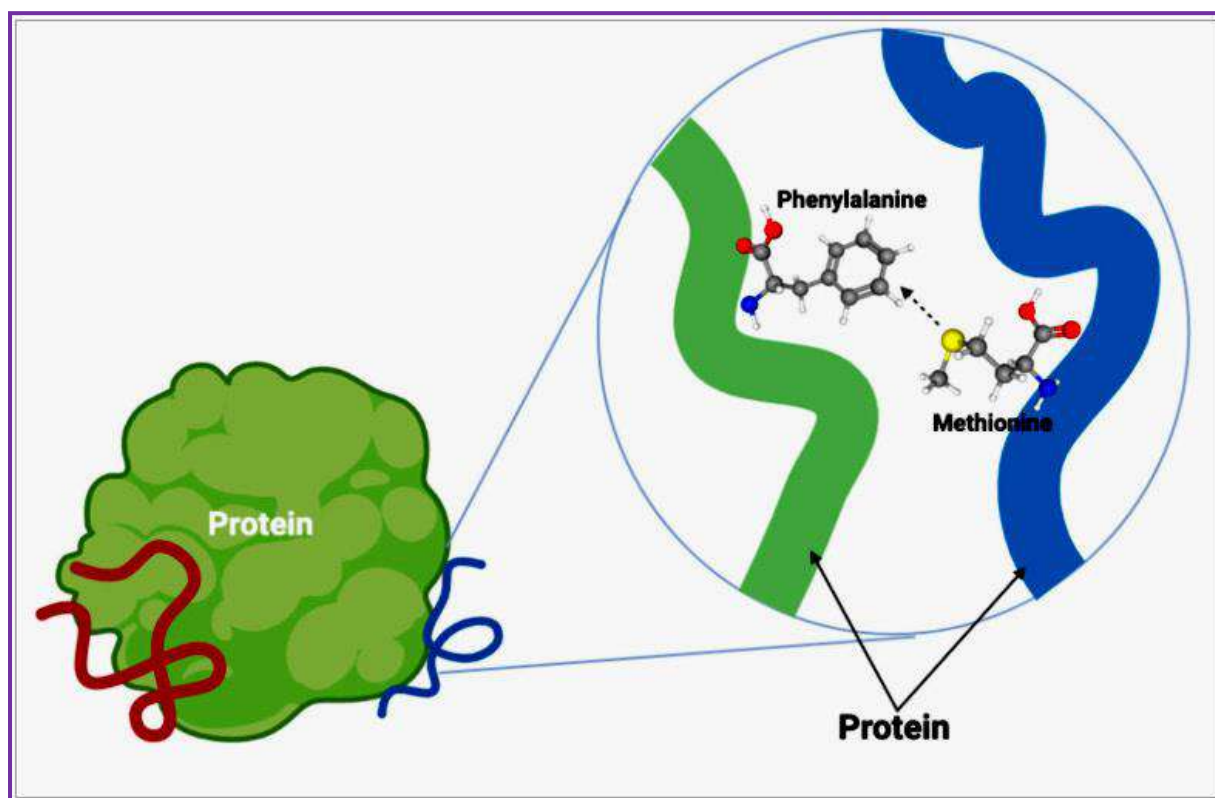


Fig. 7.4. The S-aromatic motif of Methionine. The S-aromatic motif is formed between the sulfur atom (yellow ball) of amino acids such as methionine and an aromatic residue, like phenylalanine, within proteins. These common interactions stabilize protein structure.

**Fig. adapted from Savino RJ., et.al., 2022, Molecules. 27 (12): 3679, [10.3390/molecules27123679](https://doi.org/10.3390/molecules27123679).*

The commonly found S-aromatic motifs formed by sulfur containing amino acids renders the protein dynamic flexibility and in turn stabilizes their structure and functions [28].

Literature evidences inspired the present study on investigation of sulfur containing amino acids, Cys and Met on insulin stability under thermally induced aggregation conditions.

7.3. MATERIALS AND METHODOLOGIES

7.3.1. The reagents and chemicals required in the present study were enlisted in Table 7.1.

Table 7.1. Chemicals and equipments required

ITEMS	OBTAINED FROM
Human insulin (Huminsulin R)100 IU/ml (r-DNA origin)	Eli Lilly and Company India Pvt. Ltd.
HPLC grade 100% Pure Distilled Water,	Sigma-Aldrich
Methanol & Fluorescent probes, viz., 8-Anilinonaphthalene-1-sulfonic acid (ANS), Thioflavin T (Th T)	Sigma Chemical Co. (St. Louis, USA)
KOH, Acetone	Merck (Mumbai, India)
L-Cysteine ($C_3H_7NO_2S$)	Sigma-Aldrich
L-Methionine($C_5H_{11}NO_2S$)	Sigma-Aldrich
Quartz cuvettes and Hellma absorption cuvettes	Sigma-Aldrich
Magnetic beads, Membrane dialysis tubing	Sigma-Aldrich

Different fluorescent probes namely, ANS, Thioflavin T (ThT) were used as received without further purification. The experiments were performed in HPLC water. All other reagents used were of analytical grade.

7.3.2. Methodologies employed

In order to investigate the effects of Cys and Met individually on insulin aggregation, the stock solution of Cys and Met were made as described in section 3.6. The amino acids were allowed to interact with insulin and undergo fibrillation conditions. The aggregates formed in absence and in presence of sulfur containing amino acids were experimented through different spectroscopic, fluorimetric, light scattering approaches as detailed in the sections 3.7-3.17

7.4. RESULTS OF RESEARCH FINDINGS

Intrinsic fluorescence changes in the course of insulin aggregation in presence of Cys and Met

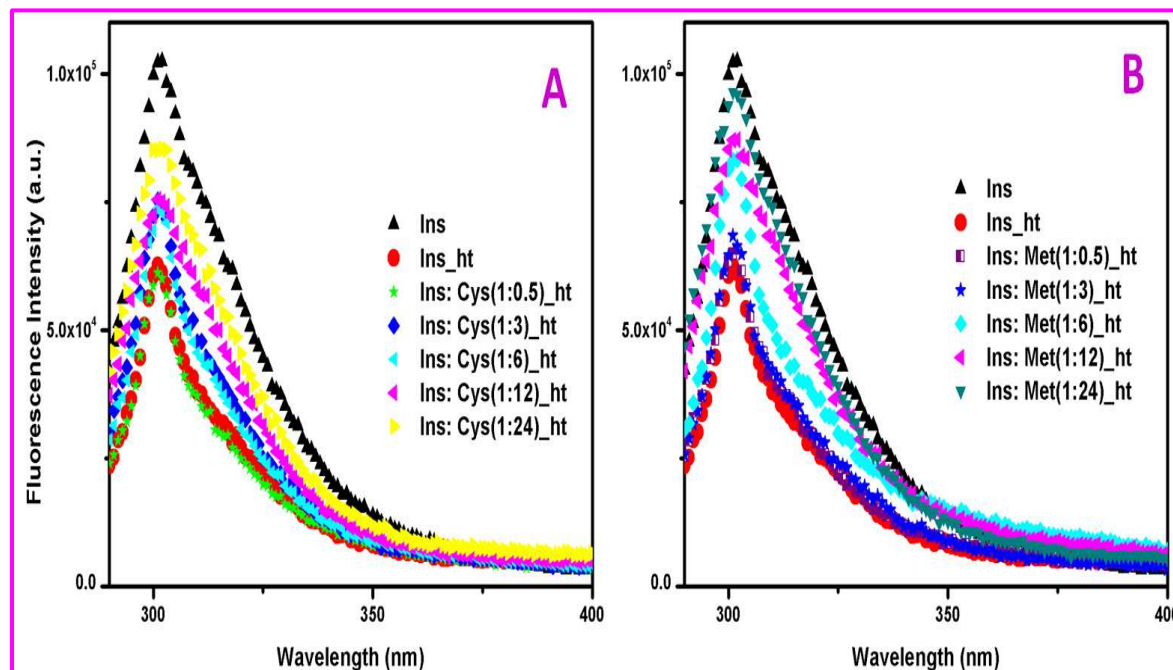


Fig. 7.5. *Intrinsic fluorescence emission intensities of tyrosyl residues of insulin recorded in the excitation wavelength 274 nm. The samples depicted were monomeric human insulin (black triangles, panel A and B), heat treated insulin (red circles, panel A and B), insulin interacted with Cys and Met at different ratio (1:0.5, 1:3, 1:6, 1:12 and 1:24) respectively in panel A and B. The emission was noted in the range of 290-400 nm and intensities peaked at i.e., λ_{max} was at 304 nm. Concentration of protein was kept at 5.5 μM in each cuvette having path length of 1 cm. Each reading is blank corrected and is an average of three different scans.*

The emission fluorescence intensities had reached a peak value at 304 nm (black triangles, fig.7.5 A and B) as expected for Tyr emission of human insulin [29]. The visible quenching of fluorescence emission intensities with the same λ_{max} was observed in case of heat treated insulin (red circles, fig.7.5 A and B) both in absence and presence of sulfur containing amino acids under experimental conditions. The possible reasons of Tyr fluorescence quenching can be : 1), phenol group protolysis of Tyr 2), resonance energy transfer from Tyr to Tyr, Tyr to Phe, 3), excited chromophore interaction with hydrated peptide carbonyl groups; or 4), interactions involving cystine groups with the excited chromophore [30]. At the experimental

pH 1.6, the first two possibilities are not justified. The initial structural reorganization during insulin fibrillation causes aromatic residues to come in close proximity and thus energy transfer is facilitated between donor and acceptor molecules within the protein matrix and in solution. As a result quenching of Tyr fluorescence took place. It actually indicated the emergence of solvent-exposed hydrophobic groups i.e., the partially folded intermediates, in solution during the course of aggregation.

It was also observed that, with increasing concentration of Cys and Met, the quenching of Tyr fluorescence became less. This can be due to availability of more sulfur containing amino acids in solution and diminishing the fatal unfolding of insulin to expose its hydrophobic grooves.

Thioflavin T assay to monitor fibrillation in presence of Cys and Met

ThT getting excited at 440nm, more preferably bind to the amyloid fibrils and possess manifold rise in emission intensity at around 483nm [31]. The occurrence of this phenomenon had observed for heat aggregated insulin depicted in Fig.7.6 A and B in red curves. Thus the generation of amyloid fibrils in solution in absence of any sulfur containing amino acids under experimental condition was prevalent. In order to get a clearer view of the influence of amino acid on insulin fibrillation, the ThT emission intensities of the samples were plotted against the interacting ratio as shown in Fig.7.6 C. Ratio of addition of Insulin and corresponding sulfur containing amino acid was denoted as I: AA in Fig.7.6 C. Cys and Methionine with increasing concentration of interaction with insulin showed different effects on fibrillation. Overall, both the amino acids slightly decreased the amount of generated amyloid fibrils in solution as indicated by lowering of emission intensities (Fig.7.6 C) in presence of the two individually. Methionine was shown to decrease the said fibrillation gradually with increasing concentration. But Cysteine performed in an inconsistent manner i.e., the inhibitory effect of Cys on fibrillation did not follow any concentration dependence and occurred randomly.

The unpredictable effect of Cysteine addition on insulin fibrillation may account for the variety of oxidation states of Cysteine as depicted in Fig.7.3 during making interaction with insulin. However, this also indicated lack of any stable intermediate formation by Cys with insulin during the course of protection of the protein against fibrillation.

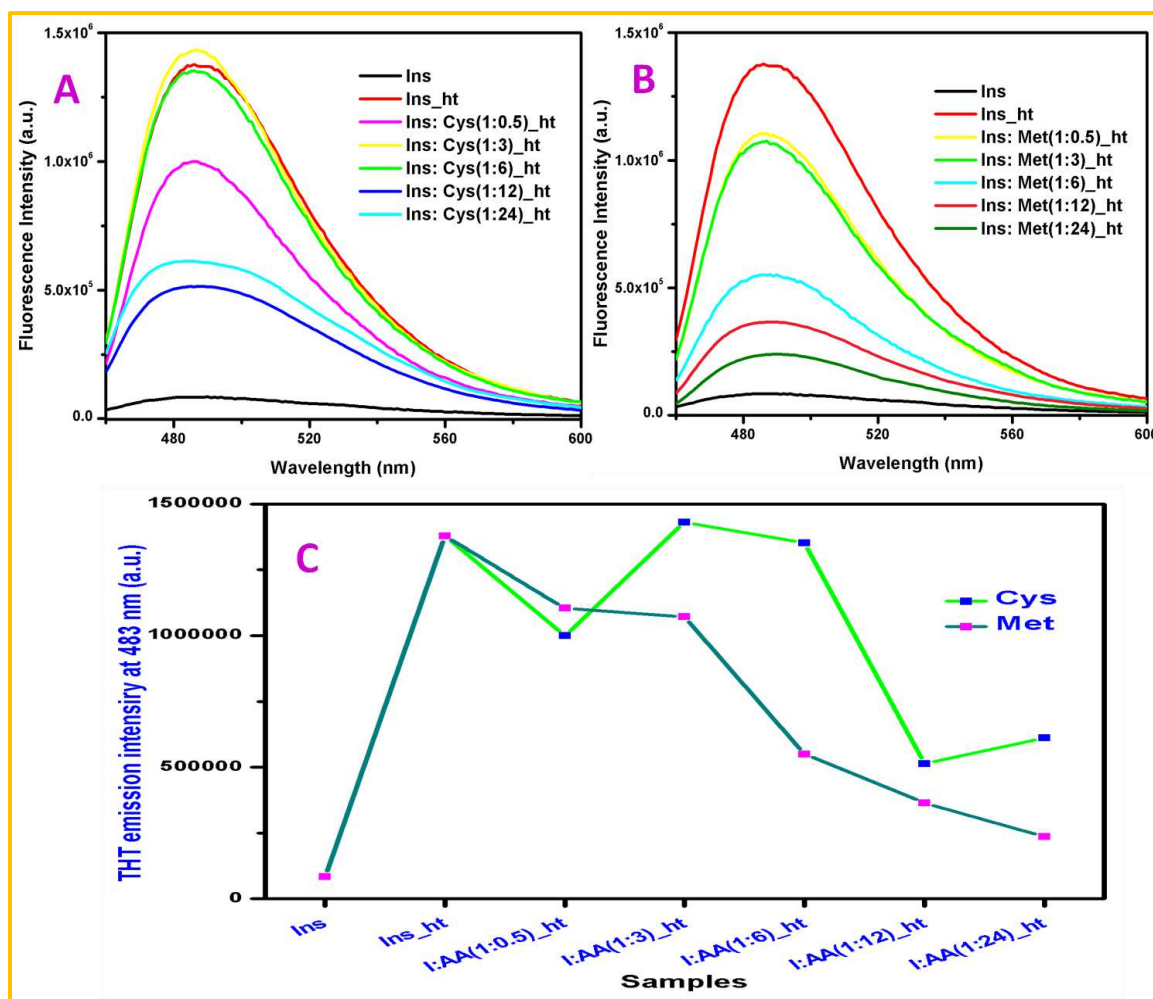


Fig. 7.6. ThT assay results. Heat induced fibrillation of insulin in presence of A. Cysteine and B. Methionine. ThT was excited at 440nm and emission recorded within the range 460-600 nm. 1 cm path-length rectangular quartz cuvette was used. The slits were kept at ex/em slit widths of 3/3 nm. Insulin and ThT conc. in solution were $5.5\mu\text{M}$ and $31.36\mu\text{M}$ respectively. Panel C showing the end-point ThT emission intensity (at 483nm) of insulin, heat treated insulin (I) without amino acid (AA) and in presence of Cys (blue square with green line) and Met (magenta square with olive line) separately at different millimolar ratios (from 1:0.5 up to 1:24).

Spectra determination of insulin aggregation under amino acid influence with 8-Anilidonaphthalene-1-sulfonic acid (ANS)

A hydrophobic fluorescence probe, 8-Anilino-1-naphthalenesulfonic acid (ANS) gives high intensity in hydrophobic environments, and exhibit peak shift and intensity change in response to change in microenvironment of protein [32].

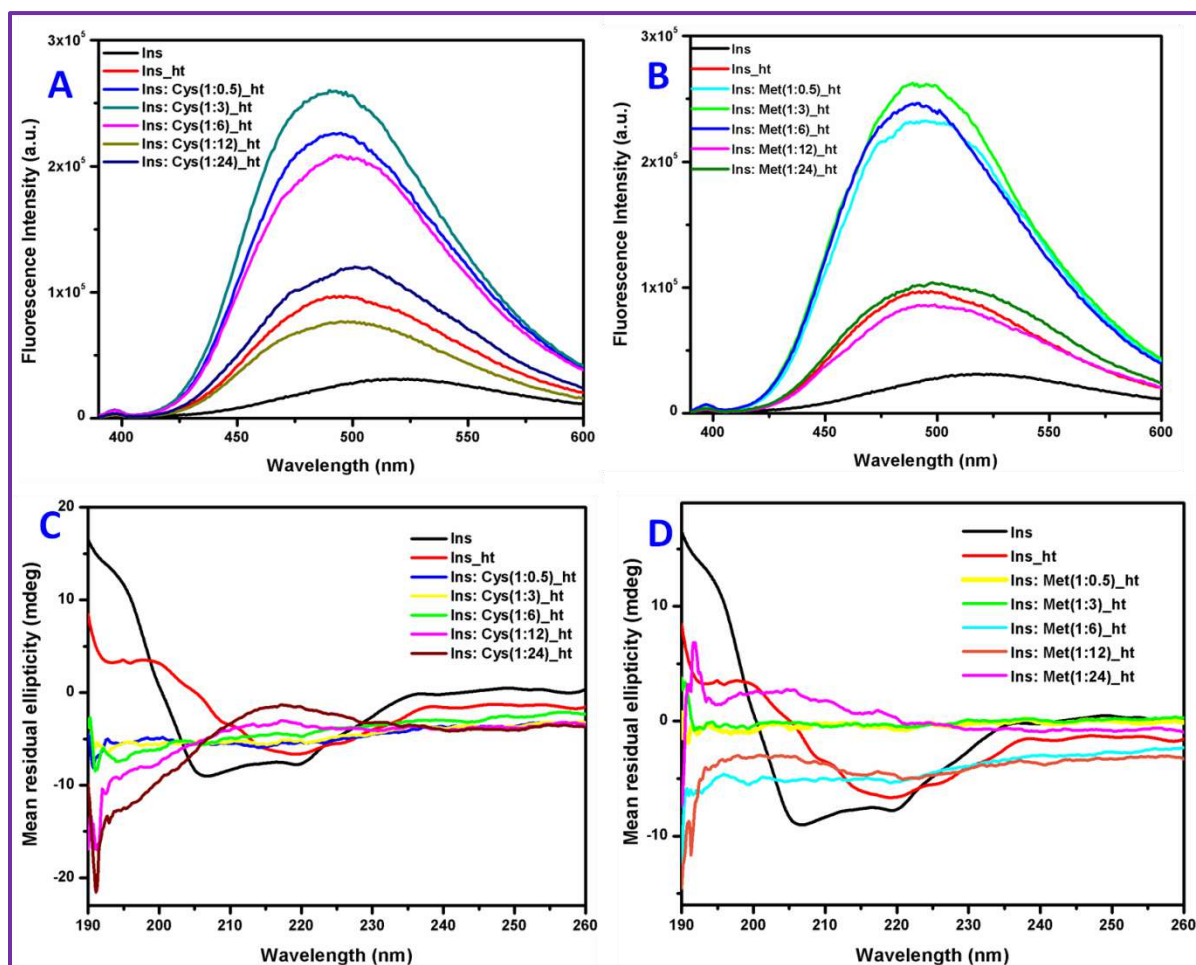


Fig 7.7. The effects of Cys and Met on conformational changes of insulin during aggregation. ANS Fluorescence emission spectra of heat treated insulin in presence of Cys (panel A) and Met (panel B) at different millimolar ratios viz., 1:0.5, 1:3, 1:6, 1:12 and 1:24 depicted in different colors. Excitation was done at 350 nm while emissions range was 400–600 nm. Protein and ANS dye concentrations were $5.5\mu\text{M}$ and $30\mu\text{M}$ respectively. Path length of cuvette was 1 cm. Each scan was performed in triplicates and averaged. Blank values (only $30\mu\text{M}$ ANS) were subtracted before presenting. Panels C and D showed Far-UV CD spectra of monomeric insulin (black, heat treated insulin (red), heat treated insulin in presence of Cys (panel C) and Met (panel D) at different interaction ratio. The protein concentration for CD assay was maintained as $6.5\mu\text{M}$. PerkinElmer quartz cuvette having 2mm path length was used.

The ANS spectra for heat treated insulin in Fig. 7.7 A and B in red curves was different in both band position and intensity from the spectra found for untreated insulin sample (black curve, panel A and B). The visible blue shift with rise in emission intensity was an indication of less polar environment where the energy difference was larger. The hydrophobic clusters

of insulin get exposed during aggregation and converted to a molten globule state as indicated by the said enhancement of ANS fluorescence [33-35]. Under the influence of Cys and Met individually in panels A and B respectively, however, there was prevalent blue shift with increasing intensity occurred with respect to monomeric insulin ANS spectra (black curve, panel A and B). But the shift is comparatively less than that of heat treated insulin itself (red curve, panel A and B). It thus can be said that, insulin gets into molten globule state due to aggregation in presence of Cys and Met under experimental conditions applied but in some lesser amounts.

The mechanism behind the observation was, having two distinct contributing excited states of ANS [36-37] during emission; the first Non-polar (NP) state localized on the naphthalene moiety of ANS is the fluorescent state in hydrophobic solvents. The maximum wavelength of fluorescence emission depends moderately on the polarity. In polar solvents however, relaxation of NP state form the intramolecular charge-transfer state (ICT). ICT is dynamically stabilized through intermolecular electron transfer (ET), ionization and subsequent electron salvation in the aqueous solution. The major quenching mechanism for ANS fluorescence yielding a low quantum yield is mainly done by the ET. Cys and Met thus can be said to favor the changes necessary during the unfolding followed by misfolding of insulin during aggregation leading to the low quantum yield in ANS fluorescence.

Far UV-CD spectral changes in courses of aggregation under sulfur containing amino acid influences

The Far UV-CD spectral curve minima was found at 208nm ($\pi \rightarrow \pi^*$) with a negative shoulder at 222nm ($n \rightarrow \pi^*$) as well as a strong positive band at 191-193nm ($\pi \rightarrow \pi^*$) (black curve, Fig. 7.7 panel C and D) are characteristic to realize the alpha helical dominating structure of insulin monomer [38-40]. The transition of peak minima to around 216 nm ($n \rightarrow \pi^*$) with strong positive band at 195–200 nm ($\pi \rightarrow \pi^*$) had confirmed the generation of beta-sheet during amyloid fibrillation of insulin in heat treated sample (red curve, Fig. 7.7 panel C and D). In the rest curves of both the panel C (Cys treated samples) and D (Met treated samples), there observed no distinct curve minima as in the monomeric form of protein. Here the content of α -helix decreased which indicates that the ordered structure of insulin was destroyed. However, strong negative band was found around 192 nm ($\pi \rightarrow \pi^*$) in Cys treated insulin samples (Fig.7.7, panel C). This majorly indicated the occurrence of random coiling of insulin under heat treatment with Cys co-incubation. Far UV-CD of Met

treated samples (Fig.7.7, panel D) gave close to zero CD signals in the 210–220 nm regions, which is characteristic for an unfolded protein. Random coil conformation was also prevalent here as shown by a weak positive band at ~ 212 nm ($n \rightarrow \pi^*$) and a relatively strong negative band around 193 nm ($\pi \rightarrow \pi^*$). The positive ellipticity found at 200–210 nm for Met treated samples at higher conc. ratio, ins: Met as 1:24 (magenta curve, panel D) was accounted for type II beta-turns. From the results, it can be stated that, the increased content of random coils proved that the insulin tends to be loose and disordered under the experimental conditions and also the fibrillation event of insulin is mediated in presence of the Cys and Met individually.

Dynamic Light Scattering (DLS) assay of experimental insulin aggregates

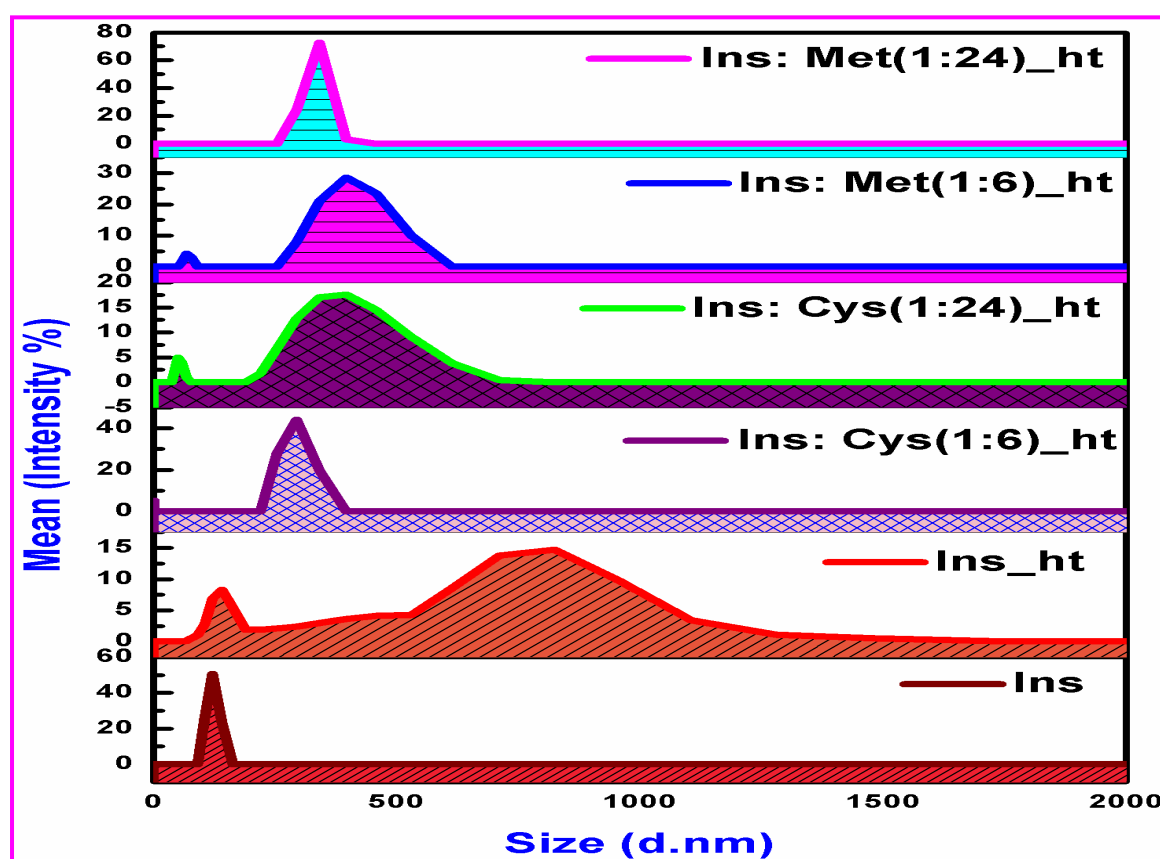


Fig. 7.8. Dynamic Light scattering assay of different insulin aggregates formed under experimental conditions. Changes in the particle size of insulin during heat incubation without or with Cys and Met at different millimolar ratios depicted by different colors. Protein concentration was maintained 20 μ M in each solution

Results of DLS assay showed that monomeric insulin having particle size within 110 nm diameter gave sharp peak (brown curve, Fig.7.8). The heat incubation of insulin results in different sized particle or higher order aggregates ranging upto 2 μ M in diameter (red curve, Fig.7.8). Cys when co-incubated with insulin prior heating also yielded insulin aggregates. At lower interacting ratio of Ins: Cys as 1: 6 (purple curve, Fig.7.8), the aggregate generated gave sharp peak at the diameter range of particle size within 350-400 nm but at higher ratio of Ins: Cys as 1: 24. 7.8), larger particle size obtained upto 710nm diameter indicated more aggregation. Methionine on the other hand, at lower concentrations, yielded higher sized aggregates having around 500nm average diameter as shown in blue curve, Fig.7.8. The incubation at higher Met percentages produced sharp peak at diameter range of 390nm. These data suggested that, Cys and Met individually was aggregation enhancer of insulin upon heating.

7.5. DISCUSSIONS AND MAJOR CONCLUSIONS

The studies on the effect of sulfur containing amino acids on heat induced insulin fibrillation gave an insight into the interactions made by protein and free amino acids. Various ratio of Ins: Cys and Ins: Met starting from 1: 6 to 1: 24 were allowed to interact followed by heat treatment. Insulin alone was also underwent heat treatment to be served as positive control. Various fluorimetric, spectroscopic and scattering assay suggested that, the insulin formed aggregates in spite of the involvement of the sulfur containing amino acids. CD results had shown the occurrence of random coiling of insulin and increased amount of beta-sheet and beta-turn rich species in the amino acid influenced insulin aggregates. DLS results confirmly proved thae higher order of aggregates were formed in presence of Cys and Met in solution. But the sizes of aggregates formed in absence of any modulator varied greatly from that of in presence of the same. At higher interacting ratio, Cys produced higher sized particles than methionine. However, at lower ineracting ratio, the reverse was true.

7.6. REFERENCES

1. Grossfield A., Woolf TB. 2002. Interaction of tryptophan analogs with POPC lipid bilayers investigated by molecular dynamics calculations. *Langmuir*, 18: 198–210, <https://doi.org/10.1021/la0106485>.
2. Morgan RS., Tatsch CE., Gushard RH., McAdon J., Warme PK. 1978. Chains of alternating sulfur and pi-bonded atoms in eight small proteins. *Int J Pept Protein Res.*, 11: 209–217, <https://doi.org/10.1111/j.1399-3011.1978.tb02841.x>
3. Pal D., Chakrabarti P. 2001. Non-hydrogen bond interactions involving the methionine sulfur atom. *J Biomol Struct Dyn.*, 19: 115–128, <https://doi.org/10.1080/07391102.2001.10506725>
4. Zauhar RJ., Colbert CL., Morgan RS., Welsh WJ. 2000. Evidence for a strong sulfur-aromatic interaction derived from crystallographic data. *Biopolymers*, 53: 233–248, [https://doi.org/10.1002/\(SICI\)1097-0282\(200003\)53:3<233::AID-BIP3>3.0.CO;2-4](https://doi.org/10.1002/(SICI)1097-0282(200003)53:3<233::AID-BIP3>3.0.CO;2-4)
5. Cordomi A., Gomez-Tamayo JC., Gigoux V., Fourmy D. 2013. Sulfur-containing amino acids in 7TMRs: molecular gears for pharmacology and function. *Trends Pharmacol Sci.*, 34: 320–331, <https://doi.org/10.1016/j.tips.2013.03.008>
6. Nygaard R., Zou Y., Dror RO., Mildorf TJ., Arlow DH., Manglik A., Pan AC., Liu CW., Fung JJ., Bokoch MP., Thian FS., Kobilka TS., Shaw DE., Mueller L., Prosser RS., Kobilka BK. 2013. The dynamic process of beta(2)-adrenergic receptor activation. *Cell*. 152: 532–542, <https://doi.org/10.1016/j.cell.2013.01.008>
7. Magnan R., Escrieut C., Gigoux V., De K., Clerc P., Niu F., Azema J., Masri B., Cordomi A., Baltas M., Tikhonova IG., Fourmy D. 2013. Distinct CCK-2 receptor conformations associated with beta-arrestin-2 recruitment or phospholipase-C activation revealed by a biased antagonist. *J Am Chem Soc.*, 135: 2560–2573, <https://doi.org/10.1021/ja308784w>
8. Gómez-Tamayo J.C., Cordomí A., Olivella M., Mayol E., Fourmy D. and Pardo L. 2016. Analysis of the interactions of sulfur-containing amino acids in membrane proteins. *Prot. Sci.*, 25: 1517-1524. <https://doi.org/10.1002/pro.2955>
9. Pal D., Chakrabarti P. 1998. Different types of interactions involving cysteine sulfhydryl group in proteins. *J Biomol Struct Dyn.*, 15 (6): 1059-1072, [10.1080/07391102.1998.10509001](https://doi.org/10.1080/07391102.1998.10509001).

10. Ho SL., Wang AH. 2009. Structural bioinformatics analysis of free cysteines in protein environments. *J Taiwan Inst Chem Eng.*, 40 (2): 123-129. [10.1016/j.jtice.2008.07.015](https://doi.org/10.1016/j.jtice.2008.07.015).
11. Lawrence MC. 2021. Understanding insulin and its receptor from their three-dimensional structures. *Mol Metab.*, 52:101255, [10.1016/j.molmet.2021.101255](https://doi.org/10.1016/j.molmet.2021.101255).
12. van Lierop B., Ong S.C., Belgi A. *et al.* 2017. Insulin in motion: The A6-A11 disulfide bond allosterically modulates structural transitions required for insulin activity. *Sci Rep.*, 7: 17239, <https://doi.org/10.1038/s41598-017-16876-3>
13. Chang SG., Choi KD., Jang SH., Shin HC. 2003. Role of disulfide bonds in the structure and activity of human insulin. *Mol Cells.*, 16(3):323-330, [https://doi.org/10.1016/S1016-8478\(23\)13808-8](https://doi.org/10.1016/S1016-8478(23)13808-8)
14. Das A., Shah M., Saraogi I. 2022. Molecular Aspects of Insulin Aggregation and Various Therapeutic Interventions. *ACS Bio Med Chem Au.*, 2(3):205-221, [10.1021/acsbioimedchemau.1c00054](https://doi.org/10.1021/acsbioimedchemau.1c00054).
15. Rosetti B., Marchesan S. 2023. Peptide Inhibitors of Insulin Fibrillation: Current and Future Challenges. *Int. J. Mol. Sci.*, 24: 1306. <https://doi.org/10.3390/ijms24021306>
16. Takai E., Uda K., Yoshida T., Zako T., Maeda M., Shiraki K. 2014. Cysteine inhibits the fibrillisation and cytotoxicity of amyloid- β 40 and 42: implications for the contribution of the thiophilic interaction. *Phys Chem Chem Phys.*, 16 (8): 3566-3572, [10.1039/c3cp54245a](https://doi.org/10.1039/c3cp54245a).
17. Senn H., Wüthrich K. 1985. Amino acid sequence, haem-iron co-ordination geometry and functional properties of mitochondrial and bacterial c-type cytochromes. *Q. Rev. Biophys.*, 18:111–134, [10.1017/S0033583500005151](https://doi.org/10.1017/S0033583500005151)
18. Taylor KL., Pohl J., Kinkade JM. 1992. Unique autolytic cleavage of human myeloperoxidase. Implications for the involvement of active site MET409. *J Biol Chem.*, 267:25282–25288, [https://doi.org/10.1016/S0021-9258\(19\)74037-X](https://doi.org/10.1016/S0021-9258(19)74037-X)
19. Kooter IM., Moguilevsky N., Bollen A., van der Veen LA., Otto C., Dekker HL., Wever R. 1999. The Sulfonium Ion Linkage in Myeloperoxidase: Direct Spectroscopic Detection by Isotopic Labeling and Effect of Mutation. *J Biol Chem* 274:26794–26802, <https://doi.org/10.1074/jbc.274.38.26794>
20. Vanacore R., Ham AJ., Voehler M., Sanders CR., Conrads TP., Veenstra TD., Sharpless KB., Dawson PE., Hudson BG. 2009. A sulfilimine bond identified in collagen IV. *Science*. 325:1230–1234, [10.1126/science.1176811](https://doi.org/10.1126/science.1176811)

21. Reid KSC., Lindley PF., Thornton JM. 1985. Sulfur-aromatic interactions in proteins. *FEBS Lett.*, 190: 209–213, [https://doi.org/10.1016/0014-5793\(85\)81285-0](https://doi.org/10.1016/0014-5793(85)81285-0)
22. Zauhar RJ., Colbert CL., Morgan RS., Welsh WJ. 2000. Evidence for a strong sulfur-aromatic interaction derived from crystallographic data. *Biopolymers*. 53:233–248, [https://doi.org/10.1002/\(SICI\)1097-0282\(200003\)53:3<233::AID-BIP3>3.0.CO;2-4](https://doi.org/10.1002/(SICI)1097-0282(200003)53:3<233::AID-BIP3>3.0.CO;2-4)
23. Valley CC., Cembran A., Perlmutter JD., Lewis AK., Labello NP., Gao J., Sachs JN. 2012. The Methionine-aromatic Motif Plays a Unique Role in Stabilizing Protein Structure. *J Biol Chem.*, (<4 Å) 287:34979–34991, <https://doi.org/10.1074/jbc.M112.374504>
24. Giles NM., Watts AB., Giles GI., Fry FH., Littlechild JA., Jacob C. 2003. Metal and redox modulation of cysteine protein function. *Chem Biol.*, 10 (8) : 677–693, [10.1016/s1074-5521\(03\)00174-1](https://doi.org/10.1016/s1074-5521(03)00174-1)
25. Levine R.L., Mosoni L., Berlett B.S., Stadtman E.R. 1996. Methionine residues as endogenous antioxidants in proteins. *Proc. Natl. Acad. Sci. USA.*, 93:15036–15040, [10.1073/pnas.93.26.15036](https://doi.org/10.1073/pnas.93.26.15036).
26. Vogt W. 1995. Oxidation of methionyl residues in proteins: Tools, targets, and reversal. *Free Radic. Biol. Med.*, 18: 93–105, [10.1016/0891-5849\(94\)00158-G](https://doi.org/10.1016/0891-5849(94)00158-G).
27. Savino RJ., Kempisty B., Mozdziak P. 2022. The Potential of a Protein Model Synthesized Absent of Methionine. *Molecules*. 27 (12): 3679, [10.3390/molecules27123679](https://doi.org/10.3390/molecules27123679).
28. Orabi E.A., English A.M. 2018. Modeling Protein S–Aromatic Motifs Reveals Their Structural and Redox Flexibility. *J. Phys. Chem. B.*, 122: 3760–3770, [10.1021/acs.jpcb.8b00089](https://doi.org/10.1021/acs.jpcb.8b00089).
29. Bekard IB., Dunstan DE. 2009. Tyrosine autofluorescence as a measure of bovine insulin fibrillation. *Biophys J.*, 97(9): 2521–31, [10.1016/j.bpj.2009.07.064](https://doi.org/10.1016/j.bpj.2009.07.064).
30. Cowgill R.W. 1976. Tyrosyl fluorescence in proteins and model peptides. In: Chen R.F., Edelhoch H., editors. *Biochemical Fluorescence: Concepts 2*. Marcel Dekker; New York, 441–486.
31. Sulatskaya AI., Rychkov GN., Sulatsky MI., Mikhailova EV., Melnikova NM., Andozhskaya VS., Kuznetsova IM., Turoverov KK. 2022. New Evidence on a Distinction between A β 40 and A β 42 Amyloids: Thioflavin T Binding Modes, Clustering Tendency, Degradation Resistance, and Cross-Seeding. *Int. J. Mol. Sci.*, 23(10):5513, <https://doi.org/10.3390/ijms23105513>

32. Ota C., Tanaka S-i., Takano K. 2021. Revisiting the Rate-Limiting Step of the ANS–Protein Binding at the Protein Surface and Inside the Hydrophobic Cavity. *Molecules*. 26(2):420, <https://doi.org/10.3390/molecules26020420>
33. Gasymov O.K., Abduragimov A.R., Glasgow B.J. 2007. Molten globule state of tear lipocalin: ANS binding restores tertiary interactions. *Biochem. Biophys. Res. Commun.*, 357: 499–504, [10.1016/j.bbrc.2007.03.186](https://doi.org/10.1016/j.bbrc.2007.03.186).
34. Gonzalez W.G., Miksovska J. 2014. Application of ANS fluorescent probes to identify hydrophobic sites on the surface of DREAM. *Biochim. Biophys. Acta Protein Proteonomics*. 1844: 1472–1480, [10.1016/j.bbapap.2014.05.004](https://doi.org/10.1016/j.bbapap.2014.05.004).
35. Singh K., Hussain I., Mishra V., Akhtar M.S. 2019. New insight on 8-anilino-1-naphthalene sulfonic acid interaction with TgFNR for hydrophobic exposure analysis. *Int. J. Biol. Macromol.*, 122: 636–643, [10.1016/j.ijbiomac.2018.10.208](https://doi.org/10.1016/j.ijbiomac.2018.10.208).
36. Gasymov O.K., Glasgow B.J. 2007. ANS fluorescence: potential to augment the identification of the external binding sites of proteins. *Biochim. Biophys. Acta Protein Proteonomics*. 1774: 403–411, [10.1016/j.bbapap.2007.01.002](https://doi.org/10.1016/j.bbapap.2007.01.002).
37. Kosower E.M., Huppert D. 1986. Excited state electron and proton transfers. *Annu. Rev. Phys. Chem.*, 37:127–156, [10.1146/annurev.pc.37.100186.001015](https://doi.org/10.1146/annurev.pc.37.100186.001015).
38. Yanti S., Wu ZW., Agrawal D.C. 2021. Interaction between phloretin and insulin: a spectroscopic study. *J Anal Sci Technol.*, 12: 34, <https://doi.org/10.1186/s40543-021-00284-4>
39. Ke C., Li L. 2023. Influence mechanism of polysaccharides induced Maillard reaction on plant proteins structure and functional properties: A review. *Carbohydr Polym.*, 302: 120430, [10.1016/j.carbpol.2022.120430](https://doi.org/10.1016/j.carbpol.2022.120430)
40. Li S., Peng Z., Leblanc RM. 2015. Method To Determine Protein Concentration in the Protein-Nanoparticle Conjugates Aqueous Solution Using Circular Dichroism Spectroscopy. *Anal Chem.*, 87(13): 6455-6459, [10.1021/acs.analchem.5b01451](https://doi.org/10.1021/acs.analchem.5b01451).

SUMMARY

Protein aggregation or amyloid formation is a common problem in different fields. In vivo aggregation of therapeutic proteins at injection sites or in-vitro aggregation during storage, transport or delivery is of major concern. Cases of amyloid plaque deposition from injected insulin as well as during its storage and delivery are major threat to diabetic patients. Such amyloid plaques generated from other proteins are the origin of a number of neurodegenerative disorders. The proteins showing marginal stability are susceptible to such pathogenic amyloid deposition. The approach to prevent such fatal aggregation needs to develop the stabilization procedure of the native folds of the protein under study. In order to stabilize the necessary conformations of protein, different small interacting molecules can be employed. In this thesis work, the significant therapeutic protein human insulin was selected to study its amyloid generation in vitro. The reason to choose the said protein lies in the fact that, the amyloid generated from insulin shares common structural features with other protein aggregates related to fatal disorders. Besides this, the availability of human insulin due to recombinant DNA technologies and its solubility in water made it to study as a model protein in this vast field. The knowledge on its beta-sheet rich amyloid structure transition from alpha-helix rich native monomeric state, direct the study in search of helix stabilizers to inhibit the said process. While doing investigations on the stabilization of insulin even in aggregating conditions, natural molecules like micronutrients, vitamins and amino acids were chosen to interact with. These molecules are generally considered essential in our diets and are nearly devoid of any ill-effects at lower concentrations of application. Another approach was taken to encounter the stability of insulin in aqueous-alcohol mixtures. Fluorinated co-solvents like HFIP and TFE were employed in this purpose. The literature findings on the protein interaction ability and alpha-helix inducing capabilities of the two co-solvents inspired the said study.

Firstly the insulin monomer was allowed to form irreversible amyloid fibrils under laboratory conditions. In the process of generating amyloid fibrils, pH played a critical role. The most aggregated fibrillar form for insulin was found at pH 1.6. The kinetics study on the temperature driven insulin fibrillation at highly acidic pH derived its three stages of amyloid formation that was in agreement with previous findings. The initiation of fibrillation arrived through a Lag phase in which the seed or nucleus for amyloid had been generated. The Log

phase involved rapid elongation of fibrils where the Stationary phase maintained a constant rate of fibrillation without any acceleration.

In the first approach to inhibit insulin aggregation with micronutrients in the form of metal ions, Fe^{3+} and Cu^{2+} were employed. Through detail investigation with multispectroscopic, fluorimetric, light scattering and imaging assays, the two metal ions proved effective at low interacting concentrations against the said fibrillation. Fe^{3+} delayed the nucleation or lag phase and also shortened the log phase of insulin fibrillation kinetics. So it was effective in preventing fibril maturation and elongation event. Cu^{2+} on the other hand had affected the log phase and noticeably shortened the lag phase fibrillation. It had been shown to moderately prevent insulin oligomerization and reduced the amount of mature fibril in aggregation favoring condition. The necessary structural unfolding and corresponding misfolding of insulin during thermal incubation promote it to expose the abundant buried hydrophobic amino acid residues. Fe^{3+} and Cu^{2+} both effectively maintained the hydrophobic patches of the native monomer but in this endeavor, the former was most effective in protecting the percentages of alpha-helix in insulin secondary conformation. The fewer aggregates formed in presence of Fe^{3+} co-incubated insulin were in lesser diameter than that of Cu^{2+} co-incubated sample. Overall, the two metal ions individually prevented the generation of higher diameter aggregates in experimental conditions. The very few aggregates generated in presence of Fe^{3+} revealed small spherule and 'worm-like' globular morphology but Cu^{2+} generated 'needle shaped' fibrillar morphology of protein aggregates. Thus it can be concluded that, individually Fe^{3+} and Cu^{2+} effectively slowed down the process of insulin fibrillation, among which Fe^{3+} mediated prevention was more potent. As Fe^{3+} did not totally prevent the generation of aggregates upon heating but reduced their affinity to form clusters of aggregate. The binding affinity for Fe^{3+} with insulin was also found greater than that of Cu^{2+} . ΔG° value for binding of Fe^{3+} with protein was found to be -7.02 kcal/ mol where for that for Cu^{2+} was -6.31 kcal/ mol.

The mechanism for the observable inhibition posed by the two metal ions was also proposed. Being transition metal ions, both of them possessed d-electrons. In the experimental aqueous media, both the metal ions favorably formed either octa or hexa-conjugated complex with water with the formation of respective hydroxides. In that condition, they made access with protein side chains easily with surface hydrogen bonding. Besides this, being very good heat and electrical conductors, they somehow neutralized the thermal incubation effect on protein structure. The metal coordination sites preferably located in the protein metal interfaces were

similar for the two as found in the molecular docking studies. The four amino acid residues aspartate/asparagine, glutamate, histidine and cysteine of insulin were assumed to coordinate with the two said transition metal ions. At low pH the Cu^+ ions disproportionate into Cu and Cu^{2+} . Here also the greater hydration energy of Cu^{2+} compared to Cu^+ , had favored the binding of it with protein interfaces. Cu^{2+} was also more efficient in making self association of insulin at a faster rate than Fe^{3+} as revealed by the shortening of lag phase of fibrillation kinetic study by it. The accelerated nucleation rate/self aggregation of insulin as well as quick nucleation (within 90 min) was observed in the presence of Cu^{2+} compared to Fe^{3+} (around 150 min). As the study revealed Cu^{2+} moderately inhibited the following process of fibril elongation and mature fibril generation. Thus it can be stated that Cu^{2+} favorably binds to the self-aggregated structure of insulin through accessible surface interactions with Tyr, Glu and Asn side chains thus preventing the elongation event of insulin aggregation and also inhibiting the formation of the higher molecular weight irreversible aggregated form of the said protein i.e., the amyloid structure. It was also assumed that, Cu^{2+} can access only limited surface residues of insulin assembly and prevent further clusterization of it. This was also the reason behind requirements of lower interacting concentration of Cu^{2+} compared to Fe^{3+} .

The following study employing water soluble B vitamins, Vitamin B₁, B₆ and B₁₂ in the approach to protect monomeric conformation of insulin under aggregation inducing conditions, also produced promising outcomes. Vitamin B₁ was much stable at acidic pH and effective in inhibition of the pathogenic amyloid fibrillation of insulin whereas vit.B₆ mediated inhibition was feeble. Vit.B₁₂ aggravates the aggregation process. The thiazolium ring of Vit.B₁ was very prone to interact with protein structure according to literature reports. The interaction of vitamin B₁ with insulin structure was proposed to mediate by H-bond and electrostatic interactions. The sulfur group present in vit.B₁ may form inter molecular disulphide bond within two or more vit.B₁. This in turn served as a shield to prevent more insulin molecules to come closer during aggregation. The best inhibitory activity was observed at interacting ratio of 1:5 (Insulin: Vit.B₁). Here the ratio clearly defined that five times multiplied concentration than insulin was needed to give optimum shielding activity of Vitamin B₁ against fibrillation. The proposed stabilizing forces behind the Insulin–Vit.B₁ interaction were H-bond between insulin and vit.B₁, disulfide bond within adjacent vitamin molecules, electrostatic interactions, van der waal forces etc. The resulting polar environment created in presence of Vitamin B₁ disfavored the hydrophobic association and burying event of non-polar residues of insulin. This in turn inhibited the misfolding and self-

aggregation of insulin. Vit.B₆ in pyridoxal form was able to maintain similar polar environment because of presence of three exposed hydroxyl groups in it. It also was assumed to make connection with insulin through the polar side chains. The interaction of insulin with Vit.B₆ did not satisfactorily prevent the fibrillation process. Vit.B₁₂ induced the said aggregation of insulin. Because of poor accommodation bulky structure of Vit.B₁₂ within the folds of insulin, it could not fit itself. The inner stability of Vit.B₁₂ and decrease in sphere of solvation had made Vit.B₁₂ poor ligand for insulin. Moreover, the stability of monomeric insulin in the aqueous solvent was greatly hampered in presence of Vitamin B₁₂. The vitamin B₁ was also shown to mediate the initial alpha-helical percentages regardless of the aggregating conditions. The morphology of aggregates in presence of vitamin B₁ was very slender comparatively to other cases. Longer fibrils with blunt stems were produced in presence of vitamin B₆ and Vitamin B₁₂ separately. The amount of fibrils was markedly less in presence of vitamin B₆. As a concluding remark it can be stated that the inhibitory effect of vitamin B₁ on insulin fibrillation was considerable at an interacting ratio of 1:5 for insulin: vitamin.

Investigation on the interactions of insulin with fluorinated co-solvents, HFIP and TFE during the course of aggregation was also informative. Maintenance of hydrophobicity of protein is critical in the inhibition of its amyloidogenic behavior. Insulin amyloid structure is dominated by the species of cross- β -sheet instead of the alpha-helix in monomer form. Effect of HFIP on the progress of insulin fibrillation was found negligible as it shortened the lag phase of fibrillation slightly without changing the duration of elongation phase. Whereas, TFE greatly lengthened the Lag phase up to 150 minutes and thus assumed to delay the onset of fibrillation. In spite of the fact, HFIP at 10% v/v interaction ratio provided better protection to insulin monomeric form against the fibrillation than TFE at pH1.6. HFIP being a volatile solvent disrupts assembly of unfolded monomers to generate amyloid fibrils. Additionally, in aqueous solution the acidity of HFIP was enhanced which in turn maintained the monomer predominating form of insulin due to the protonation of His residues at acidic pH. Before getting supersaturated, HFIP and TFE interact with protein interfaces to maintain its solubility in monomeric form. The possible formation of HFIP micro droplets at the amphoteric protein-alcohol interfaces in the aqueous medium can explain the results of the present study. Micro droplet structure was identified already in literature reports. HFIP as well as TFE were found to induce the alpha helical state of protein and thus stabilize the alpha helix dominated monomeric form of insulin. However, above 10% v/v interaction ratio

of fluorinated alcohol, the aggregation of insulin may take place. The HFIP mediated insulin fibrils were of needle shaped crystal-like morphologies whereas TFE mediated were of branched higher aggregated structure of insulin.

Sulfur containing amino acids, Cys and Met on the other hand interacted with insulin freely but could not protect it against heat induced fibrillation in a significant manner. In the process of mature fibril formation, insulin first unfolds itself followed by refolded in an erroneous manner to generate the seed of nucleation. Here the data suggested, the unfolding of insulin was followed by a random coiling under the influence of Cys and Met. On the other hand increased amount of beta-sheet and beta-turn rich species had found in the aggregates. At higher interacting ratio, Cys produced higher sized particles than methionine. However, at lower interacting ratio, the reverse was followed.

FUTURE SCOPES

Initially, the biochemical parameters involving the effects of different natural modulators as well as co-solvents on insulin fibrillation were verified *in vitro*. Various fluorescent probe based assays were employed to get the results. Besides this, CD spectroscopic and Infra-Red assays helped to determine the relevant secondary structural conformation changes of insulin aggregates under modulator influences. The study of kinetics of fibril generation had delved the hints of mechanism of modulator exhibited effects. Light scattering assays were inevitable in this respect. The sizes of particle generated thus revealed to compare the effects of different modulators on insulin under aggregating conditions. It was also proved that different protein modulators had some commonality while making interaction with insulin. Morphological imaging assays were to confirm the assumptions made by previous experimental results. *In silico* prediction method had determined the efficiencies of modulator binding with insulin. The study under the thesis heading had been utilized its scopes maximally. This study results can enlighten and be referred in future studies on protein aggregation and inhibition. The study even can be extended in the following ways.

All the said experiments were performed *in vitro* and *in silico*. In order to delve more information about the modulators effect on insulin in native conditions within living system, the study can be extended on *in vivo* models. Therapeutic efficiencies of the insulin amyloid inhibitors found among the experimented modulators also have to be determined implying their relevant toxicity levels in cellular systems.

LIST OF PUBLICATIONS

1. **Paul S.**, Begum S., Parvej H., Dalui R., Sardar S., Mondal F., Sepay N. and Halder U.C. **2024**. *In vitro* retardation and modulation of human insulin amyloid fibrillation by Fe^{3+} and Cu^{2+} ions, *New J. Chem.*, 48: 3120–3135, <https://doi.org/10.1039/D3NJ04431A>
2. Begum S., **Paul S.**, Parvej H., Mondal F., Dalui R., Pradhan A., Sepay N. and Halder U.C., **2024**. Anion-Induced Amyloid Fibrillation of Human Insulin *In vitro*, *ChemistrySelect*, 9: e202303699, <https://doi.org/10.1002/slct.202303699>
3. Parvej H., Dalui R., Begum S., **Paul S.**, Mondal F., Maity S., Sepay N. and Halder U.C. **2024**. Promotion and modulation of amyloid fibrillation of bovine beta-lactoglobulin by hydroxychalcones, *J. Mol. Struct.*, 139164, ISSN 0022-2860, <https://doi.org/10.1016/j.molstruc.2024.139164>.
4. Begum S., Parvej H., Dalui R., **Paul S.**, Maity S., Sepay N., Afzal M and Halder U.C. **2023**. Structural modulation of insulin by hydrophobic and hydrophilic molecules, *RSC Adv.*, 13: 34097–34106, <https://doi.org/10.1039/D3RA06647A>
5. Parvej H., Begum S., Dalui R., **Paul S.**, Mandal B., Sardar S., Sepay N., Maiti G., Halder U.C. **2022**. Coumarin derivatives inhibit the aggregation of β -lactoglobulin. *RSC Adv.*, 12: 17020–17028, <https://doi.org/10.1039/D2RA01029A>
6. Pal S., Maity S., Sardar S., Begum S., Dalui R., Parvej H., Bera K., Pradhan A., Sepay N., **Paul S.**, Halder U.C. **2020**. Antioxidant ferulic acid prevents the aggregation of bovine β -lactoglobulin *in vitro*, *J. Chem. Sci.*, 132: 103, <https://doi.org/10.1007/s12039-020-01796-z>
7. Maity S., Sepay N., Pal S., Sardar S., Parvej H., **Paul S.**, Chakraborty J., Pradhan A., Halder U.C. **2021**. Modulation of amyloid fibrillation of bovine β -lactoglobulin by selective methionine oxidation, *RSC Adv.*, 2021, 11, 11192–1120, [10.1039/d0ra09060c](https://doi.org/10.1039/d0ra09060c)

PROCEEDINGS AND WORKSHOPS

1. *Presentation of Poster entitled 'Inhibition of amyloid fibrillation of human insulin by effective metal ions' in an **International Seminar** on Recent Advances in Chemistry and Material Science [RACMS-2022] organized by the Indian Chemical Society in association with Bangladesh Chemical Society and Department of Chemistry, Jadavpur University held during 30th-31st July and 2nd-3rd August, 2022.*
2. *Presentation of Poster on 'Effect of metal ions on insulin aggregation in vitro' in a **National Seminar** on Emerging Trends in Chemical Sciences [CAS II PROGRAM] organized by Department of Chemistry, Jadavpur University held on 7th January, 2020.*
3. *Participated in National Seminar on 'Chemical Sciences: Today and Tomorrow', CSTT-2019 [CAS II PROGRAM] organized by the Department of Chemistry, Jadavpur University on 14th March, 2019.*
4. *Participated in a 2-day workshop on 'Introduction to Fractal Geometry and it's application in Condensed Matter Physics' organized by CMPRC, Jadavpur University on 13th -14th December, 2018.*
5. *Participation of 2-days National seminar on 'Twist and Turns of Physics research', TTPR-2017 held on 21st - 22nd February, 2017 at the Department of Department of physics, Jadavpur University.*

ANNEXURES



JADAVPUR UNIVERSITY
KOLKATA-700 032
MARK SHEET

NO.: CW/16052/ 000790

(For Ph.D/M. Phil. Course Work)

Results of the	PH.D. COURSE WORK EXAMINATION, 2020		
In	LIFE SCIENCE & BIO-TECHNOLOGY	held in	DECEMBER, 2019 - JANUARY, 2020
Name	SWARNALI PAUL	Class Roll No.	201920502001
Examination Roll No.	PHDLSBT2001	Registration No.	of

Subject Code / Name	Credit Hr.(c _i)	Marks
COMPULSORY UNITS:: EX/LSBT/PHD/1.1 REVIEW OF LITERATURE & RESEARCH METHODOLOGY	4	60
ELECTIVE UNITS :: EX/LSBT/PHD/1.2A :: TISSUE CULTURE TECHNIQUES EX/LSBT/PHD/1.2B :: MICROBIOLOGY EX/LSBT/PHD/1.2C :: PRINCIPLE OF MOLECULAR BIOLOGY TECHNIQUES EX/LSBT/PHD/1.2D :: INTRODUCTION TO MOLECULAR BIOLOGY TECHNIQUES	4	72

Total Marks : 132 (out of 200)

Remarks: P

Prepared by :

Checked by :

Date of issue : 16 - 09 - 2020

Controller of Examinations